NATURAL ORGANIC MATTER (NOM) IN SOUTH AFRICAN WATERS

VOLUME I: NOM FRACTIONATION, CHARACTERISATION AND FORMATION OF DISINFECTION BY-PRODUCTS

A Report
to the Water Research Commission

by

SS Marais[1,2], NG Ndlangamandla[2], DA Bopape[2], WF Strydom[2,3],
W Moyo[2], N Chaukura[2], AT Kuvarega[2], L de Kock[2], BB Mamba[2],
TAM Msagati[2] and TI Nkambule[2]

[1] Process Technology Department, Rand Water, Vereeniging, 1930, South Africa.
[2] Nanotechnology and Water Sustainability (NanoWS) Research Unit, University of South Africa, College of Science Engineering and Technology (CSET), UNISA Science Campus, Roodepoort, Johannesburg, 1710, South Africa.
[3] Water Services Division, Vaalkop WTW, Magalies Water, 38 Heysteck Street, Rustenburg, South Africa

WATER
RESEARCH
COMMISSION

EXECUTIVE SUMMARY

Background and motivation

Human activities and natural disasters have constrained the quantity and quality of water usable for human needs. These problems are worsened by the inability of water treatment facilities to meet the demand for quality water for potable use. Moreover, rapid industrialisation, agricultural activities, and population growth have caused a rise in the variety of pollutants in aquatic systems. Organic pollutants are broadly classified as natural or synthetic. Natural organic matter (NOM) is an intricate diverse mix of humic acids (HA) and non-humic substances (NHS) widely found in aquatic systems like rivers and lakes, and their removal is challenging because they are resistant to biodegradation. NOM is from soils, decomposing organic matter residues like lignin or charcoal from plants and animals, microbial waste and anthropogenic faecal load, agricultural activities and urban landscapes. The composition of NOM depends on the biogeochemical interactions in the surrounding environment. Because of the different origins of the material and the degree of transformation it has undergone, the composition of NOM in different water bodies is not uniform. Natural phenomena such as floods and droughts affect NOM levels and consequently influence the quantity in water bodies. These variations in the quantity and quality of NOM determine the choice, design and operation of water treatment processes. Despite being harmless to biota or humans, the occurrence of NOM in raw water is a challenge for the efficient operation of water treatment processes. It is essential that NOM be removed from drinking water because besides imparting repulsive organoleptic properties, it reacts with disinfectants like chlorine to produce disinfection by-products (DBP) such as halogenated organics like trihalomethanes (THM) and haloacetic acid (HAA). At high temperatures NOM breaks down to form organic acids, which corrode piping material of the water distribution system. To completely remove NOM, its character must be determined so that rapid approaches and protocols are devised and implemented for its abatement. Conventional removal approaches, including coagulation, adsorption, ion exchange, and oxidation have been used to remove NOM from aqueous systems.

Objectives

The specific objectives of the project were:

1. To investigate the nature of natural organic matter (NOM) occurring in source water in the relevant parts of the country (this was done via extensive sampling of various water sources indicated in the methodology section).
2. To characterise NOM at various stages of the water treatment plants using combined NOM characterisation techniques.
3. To investigate the use of suitable existing and novel techniques and processes to remove the problematic NOM fractions. Various NOM removal methods were explored by investigating enzymatic degradation, nanomaterials, advanced oxidation processes. The use of chlorine dioxide as a pre-treatment step, preparation and application of macroporous hybrid silica material for size exclusion/ gel permission chromatography and innovation in characterisation measurement and monitoring of NOM in SA water systems were also explored.
4. Ultimately the project aims to recommend solutions for practical and rapid strategies for the removal of NOM.

Major results and conclusions

The character of NOM is non-uniform in different locations due to geology and human activities in the various regions and NOM in the same location may differ seasonally due to issues of rainfall events, drought, floods

or run-off. Samples from selected South African water treatment plants collected in the period from September 2015 to September 2016 were characterised using conventional methods such as DOC, UV_{254} and SUVA, and advanced methods such as FEEM in order to determine the character of NOM. Owing to the size and complexity of NOM, which limits its removal efficiency from water by the available water treatment technologies, we developed novel nanomaterials for photodegradation of NOM into smaller molecules prior to its removal. Another approach involved developing polystyrene-based polymeric stationary phase extraction materials for NOM fractionation. The effect of disinfection using ClO_2 on NOM removal and plant throughput was also investigated.

Characteristics such as pH, turbidity and conductivity measurements were found to be different across the different treatment plants and sampling rounds, proving the variation in the water quality at these plants. DOC, UV-Vis and SUVA data enabled us to demonstrate both the quantitative and qualitative variation of the NOM across the different seasons and geographical locations of the treatment plants. In order to effectively remove NOM from water, its composition needs to be well understood. However, conventional NOM characterisation methods such as DOC, UV analysis, SUVA, turbidity, conductivity and pH, do not provide adequate information about the chemical character or composition of the NOM. Instead they are limited to providing information about the quantity (DOC) and the quality (SUVA) of NOM. Advanced techniques such as FEEM, which provide such information are therefore required. FEEM data seem to indicate high aromatic NOM removal percentages, indicating that water sources with high levels of NOM can be effectively treated. Overall, FEEM provided information on the treatability of NOM throughout the water treatment process.

Effective characterisation of NOM in water is essential for the improvement of its removal from water treatment systems. Most importantly, when monitoring NOM at the water treatment plant, the size, fluorescence and polarity of NOM should be investigated.

A study of the effect of seasonal variations on the quantity, quality and treatability of NOM has revealed that the DOC and UV_{254} removal peaked during the autumn season. This is due to the aromatic soluble compounds found in leaves, which leach into water sources. No notable correlation between UV_{254}, DOC and SUVA to percentage DOC and UV_{254} removal from water was noted.

The water treatment process at Rand Water was found to be more successful than others in the survey in the removal of high molecular weight (HMW) aromatic organic matter compared to low molecular weight (LMW) and aromatic NOM. During the study period the median NOM removal at the Rand Water Zuikerbosch and Vereeniging plants was 43% and 57%, respectively. This concurred with the average raw water SUVA value of 3.3 ℓ/mg.m and 4.2 ℓ/mg.m for the Zuikerbosch and Vereeniging plants, respectively. Reduced NOM removal was observed during the summer season.

SUVA correlated well to the removal of disinfectant by-product (DBP) precursors but could not be used as an indicator for NOM reactivity with chlorine. Higher aromatic NOM levels in summer indicated seasonal influence on organic loading and NOM removal, which resulted in increased TTHM formation. Seasonal NOM variation was indicated by the size distribution of the organic matter as well as the quantity of NOM. The seasonal variation in NOM character points to the need to continuously characterise and monitor NOM removal. In this regard, advanced NOM characterisation techniques ensure an in-depth understanding of NOM character and reactivity that the different NOM fractions have on the disinfectant used.

The strong positive correlation observed between the HMW NOM fraction of the raw water and actual measured TTHM formation in the drinking water indicates the aromatic NOM fraction was responsible for the THM formation, especially during summer. During winter the LMW NOM fraction was mostly responsible for the THMs formed. The HMW NOM fraction was found to be the main precursor to TTHM and chloroform formation, specifically during summer months. The positive correlation between SUVA and UV_{254} suggests

SUVA can be used as an indicator of NOM removal. Owing to the weak regression between SUVA and measured TTHM formation in the final drinking water, there is a need to incorporate THM formation potential (THMFP) on the individual NOM fractions to determine confidently the likelihood of the specific fraction to form THMs.

The use of chlorine dioxide as a pre-treatment step led to the complete removal of bacterial indicator organisms. Generally, NOM removal was higher when ClO_2 (instead of Cl_2) was used a as pre-oxidant, and this led to an improvement in the taste and odour of the final water. Whereas some THM levels were out of range when using Cl_2, results that were consistently within specification were obtained with ClO_2 dosing. In addition, coagulant demand reduced when ClO_2 was used as pre-oxidant. As a result of longer filter run times, throughput increased by 5%. The recycling of process waste water in combination with ClO_2 as pre-oxidant achieved a plant water loss below 4%. Therefore, it was concluded that ClO_2 was an appropriate technology that effectively deals with treatment challenges caused by the presence of NOM in the raw water source.

The synthesised nanomaterials for photolysis of NOM were found to be thermally stable, porous and amorphous, and they degraded NOM significantly. Various column performance tests showed (1) minimum silanol activity of the stationary phases; (2) successful hydrophobic retention (HR); (3) the column can selectively elute molecules based on their molecular weight - this proved that the column can separate NOM according to its different molecular weight fractions; and (4) the stationary phase was stable at basic pH.

The major findings were:
- NOM levels showed seasonal variations.
- Raw and final water samples from Olifantspoort (LO) results showed more NOM fractions in the final water compared to the raw water, this shows that the current water treatment procedure does not remediate NOM, instead it adds more NOM in the water. Therefore, more improvements towards NOM removal should be carried out in the current water treatment processes.
- Samples from the Mtwalume (MT) water treatment plant indicated the presence of trace amounts of fulvic acid (FA) and humic acids (HA), while samples from the Mid-Vaal (MV) water treatment plant, showed a decrease in HA and FA in final water as compared to raw water. The Preekstoel (VP) plant showed no HA in final water samples indicating successful treatment by the treatment plant.
- Plettenberg Bay (P) raw water was found to contain high aromatic NOM content compared to other raw water sources.
- Generally, water samples with high humic substances (e.g. in HL, P and VP treatment plants) were effectively treated. The final water after filtration process showed very little or no traces of humic fractions, proving the effectiveness of the filters used at P treatment plant in removing NOM.
- Various raw water samples from the various water treatment plants revealed that the treatability of NOM using nanomaterials was not uniform.
- The use of ClO_2 as a pre-treatment disinfectant reduced coagulant dosage, enhanced NOM removal, and increased process throughput.

Recommendations for further research

In order to develop a better understanding of NOM character and its removal, there is need to carry further investigations. Seasonal variations of different NOM fractions should inform the correct NOM removal methods to enhance effectiveness of removal. Extensive sampling that will account for all the geographic locations in SA is required. Further development and refining of nanomaterials for NOM photolysis could also increase treatability of the various fractions of NOM.

ACKNOWLEDGEMENTS

The project team wishes to thank the following people for their contributions to the project.

Reference Group	Affiliation
Dr N Kalebaila	Water Research Commission
Prof B Opeolu	Cape Peninsula University of Technology
Dr M Thwala	Council for Scientific and Industrial Research
Dr B Moodley	University of KwaZulu-Natal
Mr R Rajagopaul	Umgeni Water
Ms L Coetzee	CSV Water
Ms M Kruger	Midvaal Water
Dr E Ncube	Rand Water
Ms N Basson	Sedibeng Water
Others	
Dr T Nkambule	University of South Africa (project leader)
Prof B Mamba	University of South Africa
Prof T Msagati	University of South Africa
Dr L de Kock	University of South Africa
Dr A Kuvarega	University of South Africa
Ms S Marais	University of South Africa / Rand Water (student)
Ms N Ndlangamandla	University of South Africa (student)
Ms D Bopape	University of South Africa (student)
Mr B Strydom	University of South Africa / Magalies Water (student)
Mr W Moyo	University of South Africa (student)
Dr N Chaukura	University of South Africa (student)

CONTENTS

LIST OF FIGURES

LIST OF TABLES

ACRONYMS & ABBREVIATIONS

AC	Activated Carbon
AFM	Atomic Force Microscopy
AG-MP-50	Cation resin
AOPs	Advanced Oxidation Processes
AU	Arbitrary Units
BAC	Biologically Activated Carbon
BDOC	Biodegradable Dissolved Organic Carbon
BET	Brunauer-Emmett-Teller
C18	Non polar cartridge
CN	Polar catridge
$CHCl_3$	Chloroform
$CHCl_2Br$	Dichlorobromomethane
$CHBr_2Cl$	Dibromochloromethane
C/N 53	Carbon / Nitrogen medium
CO_2	Carbon dioxide
ClO_2	Chlorine dioxide
DBP	Disinfection By-product
DAF	Dissolved Air Flotation
DPN	N, N-diethyl-p-phenylenediamine
DBCM	Dibromochloromethane
DOM	Dissolved Organic Matter
DOC	Dissolved Organic Carbon
DVB	Divinylbenzene
ECD	Electron Capture Detector
EDS	Energy Dispersive Spectrometer
EEM	Excitation Emission Matrix
FEEM	Fluorescence Excitation Emission Matrix
E-PSQ	End-capped Polysilsesquioxane
FA	Fulvic Acid
FTIR	Fourier Transform Infrared
GAC	Granular Activated Carbon
GPC	Gel Permission Chromatography
GC-MS	Gas Chromatography-Mass Spectrometry
H_2O	Water
H_2O_2	Hydrogen Peroxide
HA	Humic Acid
HAAs	Haloacetic Acids
HBC	Hydrogen Bonding Capacity

HCl	Hydrochloric Acid
HMDS	Hexamethyldisilazane
HMW	High Molecular Weight
HPI	Hydrophilic
HpiA	Hydrophilic Acid
HPLC	High Performance Liquid Chromatography
HPO	Hydrophobic
HpoA	Hydrophobic Acid
HPSEC	High Performance Size Exclusion Chromatography
HR	Hydrophobic Retention
HS	Humic Substance
ICP	Inductively Coupled Plasma
KHP	Potassium Hydrogen Phthalate
LiP	Lignin Peroxidase
LC-MS	Liquid Chromatography-Mass Spectrometry
Lac	Laccase
LC-OCD	Liquid Chromatography Organic Carbon Detection
LMW	Low Molecular Weight
MnO_2	Manganese dioxide
MSD	Molecular Size Distribution
NH_2	Amine
MIEX	Magnetic Ion Exchange Resin
M_W	Molecular Weight
MnP	Manganese-dependent Peroxidase
mPRAM	Modified Polarity Rapid Assessment Method
NOM	Natural Organic Matter
NaOH	Sodium Hydroxide
NPT	N, Pd co-doped TiO_2 nanomaterial
NTU	Nephelometric Turbidity
NEU	Neutral Hydrophilics
O_3/UV	Ozone Based Applications
PCA	Principal Component Analysis
ParaFac	Parallel Factor Analysis
PAC	Powdered Activated Carbon
PRAM	Polarity Rapid Assessment Method
SPME	Solid Phase Microextraction
PS-DVB	Poly Styrene-Divinyl Benzene
PSQ	Polysilsesquioxane
SANS	South African National Standard
SEM	Scanning Electron Microscope
SEC	Size Exclusion Chromatography

SDS	Sodium Dodecyl Sulphate
SHA	Slightly Hydrophobic Acids
SPE	Solid Phase Extraction
S	Styrene
SS	Steric Selectivity
SUVA	Specific Ultraviolet Absorbance
TEM	Transmission Electron Microscope
TGA	Thermogravimetric Analysis
THF	Tetrahydrofuran
THMs	Trihalomethanes
TiO_2	Titanium Dioxide
TiO_2/UV	Photocatalysis Processes
TOC	Total Organic Carbon
TPI	Transphilic
UV/H_2O_2	Photo Assisted Fenton
USEPA	United States Environmental Protection Agency
UV-Vis	Ultraviolet and Visible Absorption Spectroscopy
UV_{254nm}	Ultraviolet Absorbance measurement at 254 nm
VHA	Very Hydrophobic Acids
WA-10	Weak Anionic Resin
WTP	Water Treatment Plant
WTW	Water Treatment Works
XPS	X-ray Photoelectron Spectroscopy
XRD	X-ray Diffraction

CHAPTER 1: BACKGROUND

_____

1.1 INTRODUCTION

The continued increase of worldwide human populations coupled with the scarcity of clean water implies that alternative water sources must be made available to meet the increased demand for fresh water. Fresh water drinking sources are a precious commodity and, in many arid regions of the world, can be scarce or completely unavailable. In areas where freshwater sources are available, the biological and/or chemical pollutant load may make the water unsuitable for conventional drinking water treatment, adding to the scramble for potable water sources. As such, many water treatment companies in the world (South Africa included) are now turning to the reuse of municipal waste water, either directly or indirectly, to help meet various water supply challenges. New methods of increasing drinking water supply such as desalination have their immediate drawbacks. They are, for example, inherently expensive and consume high amounts of energy. The preservation and understanding of local water sources, therefore, remains a priority for all countries. This often includes the studying of the local water sources to determine pollutant composition so as to ensure a better design of the water treatment system based on the localised raw water quality.

An emerging environmental concern is the presence of natural organic matter (NOM) in water systems. The prevalence of NOM in water remains a huge challenge for water supplying companies and municipalities responsible for its distribution. Major drawbacks associated with NOM include the inhibition of precipitation precursors, which form the backbone of drinking water treatment (for example, the reaction of components of NOM with disinfectants to form DBPs resulting in health issues amongst consumers) (Lozovik _et al._, 2007). NOM is also responsible for the yellow-brownish colour, undesirable taste and odour of natural waters (Kim and Yu, 2005). As a source of nutrients for heterotrophic bacteria, NOM promotes bacterial regrowth in the distribution system, which compromises water quality. All these individual or combined effects negatively affect human and aquatic life. The complex and heterogenic nature of the structure of NOM, coupled with its non-uniform composition in different water types presents a huge challenge in its effective characterisation before even attempting to reduce its levels from drinking water.

The composition of NOM throughout water systems remains a huge challenge for understanding its influence in drinking and cooling water or waste water treatment. NOM is a mixture of organic compounds having diverse chemical properties, which occur in all natural water sources as a result of decaying animal and plant material (Listiarini _et al._, 2010). Organic matter of natural waters is divided into two large groups – allochthonous and autochthonous. Allochthonous organic matter is a mixture of organic matter of humic nature and terrigenous origin, the sources of which are products of incomplete decomposition of plant and animal remains (Imai and Nagai, 2003). Autochthonous organic matter forms in water bodies as a result of photosynthesis and the destruction of detritus (dead bacteria, phytoplankton, and animal bodies) (Lozovik _et al._, 2007).

The re-occurrence of organic compounds in water sources also poses a challenge to the South African water treatment industry, especially since their occurrence is yet to be fully understood. An understanding of the occurrence of NOM in water is important in order to determine their prevalence in South African water sources for potable water supply. The efficiency of the South African water treatment plants to remove NOM-based contaminants needs to be determined due to the ever increasing raw water quality.

Nkambule _et al._ (2012) studied eight different water treatment plants, across the various water types in South Africa; a combination of conventional and advanced NOM characterisation techniques was studied. The conventional techniques used included dissolved organic carbon (DOC) analysis, ultraviolet analysis, specific ultraviolet absorbance (SUVA), turbidity, colour and conductivity. The conventional techniques employed in

_____

the characterisation of NOM have many disadvantages. For example, the DOC gives the amount of NOM present in the sample but does not indicate its composition. The SUVA gives an indication of the aromaticity but not the molecular composition of the NOM. Thus, pinning down the composition of NOM before attempting to remove it has proven to be a difficult task. This has since led to the development of a rapid protocol for NOM characterisation, which enables changes in NOM character to be traced as the NOM goes through the various water treatment processes (Nkambule *et al*., 2012). The advanced characterisation protocol developed and employed by the researchers involved an analysis of the biodegradable dissolved organic carbon (BDOC), NOM fractionation using the polarity rapid assessment method (PRAM) and the fluorescence excitation emission matrices (FEEM) analysis. The complex signals obtained from FEEM analysis could then be separated into their individual underlying fluorescent phenomena using parallel factor analysis (ParaFac) on Mat-lab. The results obtained through the combined advanced NOM characterisation techniques gave a more in-depth insight into the composition of NOM. Not only did the techniques give a qualitative estimation of the NOM composition, but they also provided a quantitative perspective to the characterisation of NOM.

The fluorescence excitation emission matrices (FEEM) provide the structural information of NOM based on the excitation and emission wavelengths of the molecular group. Usually, the absorption/emission wavelength pair is different for different groups of molecules, and hence aromatics can be distinguished from carbohydrates, for example. The biodegradable dissolved organic carbon (BDOC) is used as an indicator of bacterial regrowth potential in the distribution network. This method of analysis is based on measuring the reduction of DOC over a six-day period by bacteria fixed on biologically active sand (BAS). Fractionation techniques are often introduced to reduce the molecular heterogeneity of NOM. The characterisation techniques based on fractionation isolate the group of compounds present in the NOM, based on their physical properties. These fractionation techniques may be used in combination with spectroscopic methods. A recently developed NOM fractionation method is the polarity rapid assessment method (PRAM). The characterisation of NOM with PRAM is based on preferential adsorption of dissolved organic matter (DOM) fractions onto the solid-phase extraction (SPE) sorbents. Each fraction exhibits different properties in terms of molecular weight, for example, where the higher molecular weight hydrophobic NOM fractions would be less soluble in water and could be removed efficiently by coagulation while the lower molecular weight hydrophilic fractions would be soluble and therefore difficult to remove (Matilainen and Sillanpaa, 2010).

In this study, liquid chromatography equipped with organic carbon detection (LC-OCD) was used as a characterisation method for the size and character of NOM. LC-OCD consists of three size exclusion chromatography (SEC) columns that separate the organic carbon into fractions of different sizes while taking into account the hydrophobic and ionogenic character (Uyguner and Bekbolet, 2005). LC-OCD characterises the organic fractions in the low concentration permeates and hence gives insight into the rejection of low molecular weight (LMW) organics. The technique does not require any sample pre-treatment and is also very sensitive. Using LC-OCD is advantageous in the sense that it gives information on the amount of NOM as well as the type of compound involved (Huber and Frimmel, 1992a, b). Using LC-OCD, it is also possible to evaluate the content of high molecular weight (HMW) polysaccharides and biopolymers in the sample, which are not generally visible or traceable by UV-detectors (Marhaba and Van, 2000).

The knowledge of the NOM composition of the local water source is an important prerequisite for efficient design of water treatment plants that will achieve its optimal removal. With these NOM characterisation techniques developed, research into the influence of NOM in the treatment of water – for example, for the cooling water at Eskom – can now be taken to greater heights, resulting in an in-depth understanding of the influence of natural organic matter throughout the water treatment process.

1.2 PROJECT AIMS

The following are the aims of the project:

1. To investigate the nature of natural organic matter (NOM) occurring in source water in selected parts of the country (this was done via extensive sampling of various water sources indicated in the methodology section).

2. To characterise NOM at various stages of the water treatment plants using combined NOM characterisation techniques.

3. To investigate the use of suitable existing and novel techniques and processes to remove the problematic NOM fractions. Various NOM removal methods were explored by investigating enzymatic degradation, nanomaterials, advanced oxidation processes. The use of chlorine dioxide as a pre-treatment step, preparation and application of macroporous hybrid silica material for size exclusion/ gel permission chromatography and innovation in characterization measurement and monitoring of NOM in SA water systems were also explored.

4. To recommend solutions for practical and rapid strategies for the removal of NOM.

CHAPTER 2: LITERATURE REVIEW

_____

2.1 OCCURRENCE AND FATE OF NOM DURING POTABLE WATER TREATMENT

The continuous occurrence of natural organic matter (NOM) in surface water is primarily from the decay and leaching processes of organic materials from plants, animals and micro-organisms and their transportation in water (Page *et al*., 2002b). NOM is described as an intricate mixture of organic components and although their composition differs within water bodies, they occur naturally in all surface waters. The major component of NOM is humic substances (derived from soil or produced by chemical and biological processes) (Page *et al*., 2002b) of low to moderate molecular weight and consisting of both aromatic and aliphatic components (Letterman *et al*., 1999).

Natural organic matter (NOM) (**Figure 2-1**) is composed of different organic compounds, from highly aliphatic to highly coloured aromatic compounds (Matilainen *et al*., 2010). It can be derived both from sources within the aquatic environment (autochthonous) and from external sources (allochthonous) (Nkambule *et al.,* 2012b). In addition to being negatively charged, NOM has a variety of molecular sizes and chemical compositions. NOM also has both hydrophilic and hydrophobic components (Matilainen *et al*., 2010).
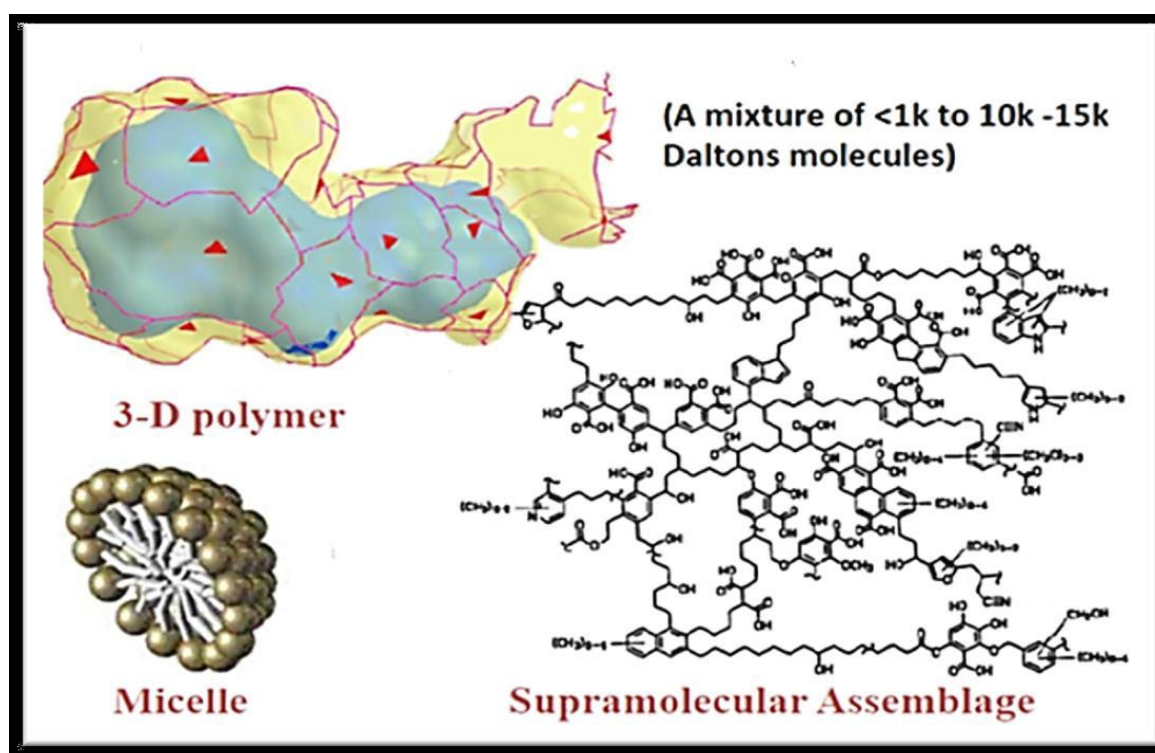
Figure 2-1 Illustration of different representations of the NOM structure (Nkambule *et al*., 2012b)

The hydrophobic component of NOM is largely aromatic and consists of fulvic and humic acids.(Matilainen *et al.*, 2010). The difference between fulvic and humic acids is their solubility under different pH conditions. Humic acid is insoluble under acidic conditions but soluble at higher pH values; fulvic acids, on the other hand, are soluble under all pH conditions (Chen *et al.,* 2002). Humic substances constitute about 70% of the total organic carbon (TOC) (Matilainen *et al*., 2010; Nkambule *et al*., 2012b).

The hydrophilic component is mainly composed of aliphatic carbons and nitrogenous compounds, such as amino acids, carbohydrates and sugars (Matilainen *et al*., 2010). The hydrophobicity of NOM can be

_____

determined using Specific Ultra-violet Absorbance (SUVA) spectroscopy. High values of SUVA (> 4) indicate a presence of a high molecular weight and hydrophobic organic matter. Low SUVA values on the other hand indicate the presence of mainly hydrophilic and low molecular weight organic compounds (Matilainen *et al*., 2010).

In its natural environment NOM is not necessarily problematic. However; during water treatment (especially during the disinfection process) NOM may react with the disinfectant (i.e. chlorine) and thus result in the quality of the treated water being compromised by the disinfection by-products (DBPs) that are produced (Özdemır, 2014). Impaired water quality due to insufficient removal of NOM during water treatment includes odour, taste and colour problems in the final treated water as well as microbial regrowth in the water distribution system (LeChevallier *et al*., 1991). The easily biodegradable NOM fractions are used by bacteria as a food source and thus enhance and sustain bacterial regrowth in the distribution system (Page *et al*., 2002a; Baghoth *et al*., 2009). So not only will biofilm growth within the distribution pipelines be increased, the quality of the final water that is supplied to the consumer will be hugely compromised (Van der Kooij, 1992).

2.2 NOM AS DISINFECTION BY-PRODUCT (DBP) PRECURSOR

In 1974 J.J. Rook discovered that insufficient removal of NOM from surface water during potable water treatment can result in the formation of DBPs when residual NOM reacts with chlorine during the disinfection process (Howe *et al*., 2012). Throughout the world, the DBPs that are of most concern, due to their high concentrations and prevalence in chlorinated drinking water, are trihalomethanes (THMs) and haloacetic acids (HAAs) (Frimmel and Jahnel, 2003; Fabris *et al.,* 2008; Matilainen and Sillanpää, 2010; Kristiana *et al*., 2011).

Recently, levels of THMs that do not comply with the new SANS: 241 standard have been detected in South African drinking waters. According to the new standard (SANS: 241, 2011), total THM should now be reported according to the following four main constituents (concentration limits indicated in brackets):

- Bromoform (≤ 0.100 mg/ℓ);
- Chloroform (≤ 0.300 mg/ℓ);
- Dibromochloromethane (≤ 0.100 mg/ℓ); and
- Bromodichloromethane (≤ 0.060 mg/ℓ).

Although chlorinated/chloraminated water generally has lower THM and HAA concentrations than chlorinated waters (Knight *et al*., 2011), they still pose a risk of forming the by-product N-nitrosodimethylamine (NDMA), which is also a significant health concern (Mitch *et al*., 2003; Howe *et al*., 2012).

Considerable research efforts have recently been directed towards determining the influence on DBP formation of NOM character based on molecular weight (Chowdhury, 2013; Özdemır, 2014) and polarity (Lu *et al*., 2009; Roe *et al*., 2008; Tubić *et al*., 2013). It is known that certain NOM fractions that increase the formation of DBPs (Marhaba *et al*., 2003) can result in the formation of specific chlorinated by-products (Özdemır, 2014). Furthermore, it has been established that the amount of DBPs formed is affected by different properties of the organic precursors (Chang *et al*., 2001).

In addition, iodine and bromine are highly reactive with the hydrophilic fraction of NOM and thus generate DBPs that are considered to be more hazardous than their chlorinated precursors (Matilainen and Sillanpää, 2010). Lastly, it has been revealed that the hydrophilic fraction of NOM is a major contributor of biodegradable organic carbon, which promotes microbiological regrowth in the distribution system (Świetlik and Sikorska 2006; Matilainen and Sillanpää, 2010).

2.3 CHARACTERISATION AND QUANTIFICATION OF NOM

Water from the Vaal Dam is abstracted by a bulk potable water utility (Rand Water) providing an average 3 653 million litres of water per day to more than 12 million people in South Africa (Ncube *et al.*, 2012) however, little is known regarding the nature, occurrence and concentration of NOM in the Vaal Dam surface water. Different NOM fractions have been reported to be responsible for the formation of a specific DBP (Hassouna *et al.*, 2014, Özdemır, 2014). Since the amount and composition of NOM in source water affects the efficiency of water treatment plants (Sharp *et al.*, 2006) and different chemical properties of NOM are removed by different treatment processes (Parsons *et al.*, 2004), it will be practical to first characterise NOM in the source water of Rand Water. This will allow for optimal removal of the problematic NOM fractions and thus permit the optimisation for improved DBP precursor removal.

The difficulty in NOM characterisation lies in the fact that organic matter does not have a homogeneous organic matrix, but is a mixture of divergent size, structure and functionality. To overcome this limitation various measurements and characterisation techniques are required to allow for reliable identification. The characteristics and amount of NOM depend on the climate, topography and geology of the particular area (Nkambule *et al.,* 2012c). Other authors reported that the character of NOM also depends on the type of agricultural and industrial activities practised in that location (Nkambule *et al.,* 2012c). Thus, it is important to first understand the composition of the NOM in the water source, also taking into consideration the local NOM conditions. Once these aspects have been understood, NOM removal technologies/methods can then be developed (Nkambule *et al.,* 2012c).

NOM is usually characterised by Total Organic Carbon (TOC), adsorption of UV at 254 nm and dissolved organic carbon (DOC) (Matilainen *et al.,* 2011). Since NOM is the main cause of colour in NOM-contaminated water, the amount of colour present can be used to determine the amount of NOM in water. All these methods only provide information regarding the amount of NOM present in water; however, they provide limited information on the character of NOM (Matilainen *et al.,* 2011).

Characterisation of NOM also entails the isolation and fractionation of NOM into minor fractions using various characterisation techniques. Due to NOM being a composite mixture having a polydisperse and irregular structure (Hertkorn, 2006), separation of NOM based on hydrophobicity has been the subject of several investigations (Leenheer, 1981; Rosario-Ortiz *et al.*, 2007; Piper *et al.*, 2010). The minor NOM fractions are classified as hydrophobic (HPO), hydrophilic (HPI) or transphilic (TPI). Hydrophobic NOM fractions refer to humic substances that have a higher aromaticity (Edzwald and Van Benschoten, 2010). Advanced characterisation methods available to fractionate organic matter include the polarity rapid assessment method (PRAM), the modified PRAM (mPRAM), high performance size exclusion chromatography (HPSEC), fluorescence excitation-emission matrices (FEEM), parallel factor (ParaFac) and biodegradable dissolved organic carbon (BDOC) analysis.

It is worth noting that there is no single tool that can provide all the information required for the characterisation of NOM. Therefore combined application of different tools is often utilised (Chen *et al.*, 2002).

2.3.1   Organic carbon as parameter

2.3.1.1   *Total organic carbon (TOC)/ dissolved organic carbon (DOC)*

Dissolved organic carbon (DOC) is defined as the organic carbon present in water after it has been filtered through a 0.45 µm filter, whereas total organic carbon (TOC) represents all non-purgeable organic carbon present in a water sample (Matilainen *et al.,* 2011). Both the TOC and DOC method involve oxidation (either

with UV persulfate or high thermal combustion) of the organic carbon present in the water to form carbon dioxide. The resulting CO_2 is then measured by Fourier transform infrared (FTIR) spectroscopy (Matilainen *et al.*, 2011).

2.3.1.2 *Ultraviolet and visible absorption spectroscopy (UV-Vis)*

Research has shown that any wavelength ranging from 220 to 280 nm is appropriate for the measurement of NOM (Matilainen *et al.,* 2011). However, the molar absorptivity values vary due to the range of chromophores present in NOM. Specifically, 220 nm corresponds to both aromatic and carboxylic chromophores, whereas 254 nm is associated with the aromatic character of the molecule (Matilainen *et al.*, 2011). Other molar absorptivity values such as 214 nm (associated with nitrites and nitrates), 272 nm (the best predictor for trihalomethane formation) and 300 nm (used as measure of DOC by Rand Water and other treatment plants) have been used for NOM measurement (Nkambule *et al.*, 2012c).The UV absorbance at a wavelength of 254 nm (UV_{254}) is a rapid and accessible measurement to water treatment plant personnel (Lobanga *et al.,* 2014) and is an indication of the presence of aromatic organics, due to the double bonds in aromatic rings that absorb UV light at this wavelength.

2.3.1.3 *Specific ultraviolet absorbance (SUVA) spectroscopy*

SUVA is defined as the UV absorbance of the sample of interest at 254 nm divided by DOC concentration of that sample (Matilainen *et al.*, 2011). SUVA is an indicator of the chemical composition of organic carbon and it gives an indication of the amount of humic substances relative to the non-humic substances in a water sample (Weishaar *et al.*, 2003; Edzwald and Van Benschoten, 2010). A high SUVA value (> 4 ℓ/mg.m) indicates the presence of high molecular weight NOM, which gives rise to high oxidant demand and high percentage removal (60 – 80%) of TOC by coagulation. Conversely, a low SUVA value (< 2 ℓ/mg.m) indicates the presence of low molecular weight NOM that requires low oxidant demand but low percentage removal (< 20 – 40%) of TOC by coagulation. There is a good correlation between high SUVA values and the treatability of NOM by coagulation (Matilainen *et al.,* 2011). Also, SUVA values > 4 ℓ/mg.m suggest the presence of mostly hydrophobic and aromatic organic material in the water, whereas SUVA < 2 ℓ/mg.m indicates the presence of mainly hydrophilic material (Matilainen *et al.*, 2011).

2.3.2 NOM polarity

2.3.2.1 *Resin fractionation*

Fractionation selectively separates different groups of organic molecules based on their chemical and physical properties (Chen *et al.*, 2002). One of the most commonly used approaches for differentiating between hydrophilic and hydrophobic NOM is to characterise them as organic materials that are either absorbed or not absorbed on the Amberlite XAD resins (Matilainen *et al.*, 2011). This method is therefore used for the isolation of humic fractions from water (Matilainen *et al.*, 2011). The material that is utilised for the fractionation of NOM is usually composed of Amberlite XAD-8 and XAD-4 resins. Whereas the XAD-4 resin adsorbs transphilic NOM (weakly hydrophobic acid fractions), the XAD-8 resin isolates hydrophobic NOM consisting of NOM of high molecular weight and aromatic character (Matilainen *et al.*, 2011).

The hydrophilic fractions are not adsorbed by either of the above-mentioned resins. However, they can be separated using WA-10 (weak anionic resin) and AG-MP-50 (cation resin) (Matilainen *et al.*, 2011). The rapid resin fractionation method, which is based on XADs, separates dissolved organic carbons into four portions based on molecular weight and character. These fractions are: slightly hydrophobic acids (SHA), very hydrophobic acids (VHA), neutral hydrophilics (NEU), and charged hydrophilics (Chow *et al.*, 2004).

2.3.2.2 Modified polarity rapid assessment method (mPRAM)

The change in polarity of NOM in a water sample can be determined through the use of polar-, non-polar and anion-exchange solid phase extraction (SPE) cartridges. This is achieved by evaluating the amount of material adsorbed onto each cartridge using ultraviolet absorbance measurement at 254 nm (UV_{254}) (Rosario-Ortiz *et al.*, 2004). The polarity rapid assessment method (PRAM), which can be used to characterise the change in NOM polarity throughout the water treatment process, is a very useful tool to evaluate and thus optimise treatment efficiency and removal of NOM. The original PRAM technique was modified by Nkambule *et al.* (2011) producing three NOM fractions instead of the original six fractions, thus resulting in a less time-consuming method. The modified PRAM is a form of series PRAM; in contrast, the published method is a parallel PRAM procedure. Three different types of sorbents (hydrophobic, hydrophilic sorbents and anion exchange resins) are used as SPE cartridges to fractionate NOM into a hydrophobic, hydrophilic and transphilic fractions. All three fractions that are eluted provide good information for the characterisation of the NOM based on its composition, as these three fractions best represent the composition of the NOM with respect to its aromaticity.

2.3.3 NOM size

2.3.3.1 High performance size exclusion chromatography (HPSEC)

The HPSEC method, which is a reproducible, relatively fast technique, divides NOM graphically into six peaks representing the humic fractions ranging from high to low molecular weight and the percentage of each fraction (Pelekani *et al.*, 1999; Nissinen *et al.*, 2001). The high molecular weight (HMW) fraction represents the humic and fulvic type compounds that leach from the soil, and the low molecular weight (LMW) fraction represents the non-humic fractions (Szabó and Tuhkanen, 2007). The change in the molecular weight distribution throughout the water treatment process can also be used to indicate NOM removal after each treatment step (Vuorio *et al.,* 1998; Matilainen *et al.*, 2002).

2.3.3.2 Gel permeation chromatography (GPC)

This fractionation method involves a continuous flow of analyte through the stationary phase via molecular diffusion (Amy *et al.*, 2015). It separates compounds based on their molecular size; very large molecules have a short retention time because they do not pass through the gel pores of the stationary phase and are thus eluted first (Amy *et al.*, 2015). Some of the properties that may influence the GPC results are the type and grade of the gel, the composition of the eluent used, the method and degree of the organic material being used as well as the standard synthetic chemicals used for the calibration of the gel column (Amy *et al.*, 2015). Since NOM is heterogeneous in terms of size, this method can differentiate different components based on weight and size distribution (Nkambule *et al.*, 2012b).

2.3.3.3 Liquid chromatography with organic carbon detection (LC-OCD)

Liquid chromatography coupled with organic carbon detection (LC-OCD) consists of three size exclusion chromatography (SEC) columns that separate the organic carbon into fractions of different sizes while taking into account their hydrophobic and ionogenic character (Uyguner and Bekbolet, 2005). The principle of the LC-OCD is based on the separation of the organic mixture by liquid chromatography (LC) followed by their detection by organic carbon detector (OCD). The organic carbon detection principle is similar to those of classical TOC analysers, which are; acidification, purging of "inorganic" carbon, oxidation of TOC to carbon dioxide and detection of carbon dioxide by a Non-Dispersive Infra-red (NDIR) detector (Humbert *et al.*, 2005). Conventional LC-OCD uses GPC and does not use an organic solvent as a gradient. It employs the principle of separation based on size without taking into account the polarity of the NOM.

2.3.4 NOM fluorescence

Fluorescence is a technique used to determine the presence of biodegradable NOM in water (Matilainen *et al.,* 2011). A sample is excited with a light source usually at a particular wavelength and the emitted light is at a different wavelength (Baghoth, 2012).

2.3.4.1 Fluorescence excitation emission matrix (FEEM) spectroscopy

Another advanced NOM characterisation tool, the FEEM, can predict the type and amount of organic matter in a sample (Roe, 2011; Baghoth, 2012), as the composition and concentration of organic matter influences the intensity and shape of the fluorescence spectra (Coble, 1996). FEEM spectroscopy is used to determine various forms of humic substances. Research has shown that by gathering all the emission spectra at different excitation wavelengths the excitation emission matrix (EEM) is obtained (Baghoth, 2012). The location and size of the EEM peaks depends on the composition of NOM present in water. The importance of this method lies on its ability to sense changes in properties of the species of interest. Fluorescence and absorbance can provide highly correlated results in seconds to minutes, even continuously. Optical absorbance and fluorescence EEMs provide rapid (sec to min), sensitive (ppb to ppm) information on dissolved organic matter for drinking and waste water treatment. FEEM is also readily adaptable to a variety of treatment processes for research, pilot and direct applications. Finally FEEM offers robust correlations with DBP formation and oxygen demand parameters, can facilitate real-time process control, and can reduce chemical consumption, violation issues and labour costs (Rosario-Ortiz *et al.,* 2007).

2.3.4.2 Parallel factor (ParaFac) analysis

ParaFac is basically for identifying specific components of the sample that can fluoresce. It is used to model data of EEMs into individual components of fluorophores (Pifer and Fairey, 2012), and can differentiate components into protein-like and humic-like forms (Nkambule *et al*., 2012a). Moreover, ParaFac can be used as a tool to predict DBP formation by using fluorophore component scores in the evaluation of DBPs (Johnstone, 2009). Peak picking methods were previously used to identify the fluorescent components of the sample (Pifer and Fairey, 2012). However, ParaFac is more efficient because it allows individual components of NOM to be extracted for further analysis (Nkambule *et al*., 2012a).

2.3.5 Bacterial degradation of NOM and biological tests

Results from a study performed by Young (2005) indicate that bacterial degradation of intermediate to LMW NOM components cause the M_w of NOM in solution to increase. These results also indicate that NOM bioavailability is not solely dominated by molecular weight; other factors in conjunction with microbial community structure also affect the bioavailability. Various studies have also suggested that the LMW organic matter fractions are more biologically reactive (more rapidly utilised) and yield higher bacterial efficiencies than HMW dissolved organic matter (Axmanová *et al*., 2006; Khodse and Bhosle, 2011). These LMW and HPI NOM fractions are the NOM components that are not easily removed by conventional water treatment (Van Leeuwen *et al.,* 2005) and are more prone to form DBPs when they remain after treatment (Hwang *et al*., 1999; Marhaba and Van, 2000).

Biological tests are developed to assess the biodegradable organic matter level in water and are based on two concepts, namely: the biodegradable dissolved organic carbon (BDOC) and assimilable organic carbon (AOC) (Matilainen *et al.,* 2011). BDOC determines the fraction of DOC assimilated and mineralised by heterotrophic microbes, whereas AOC determines the bacterial regrowth based on the amount of nutrients present in water. AOC is believed to represent low molecular weight molecules. The idea is to decrease or reduce BDOC as

much as possible since its availability in the treated water enhances bacterial regrowth in the distribution system (Matilainen *et al.*, 2011).

The BDOC method was used by Nkambule *et al.* (2011) as a NOM characterisation tool for measuring the availability of NOM to be utilised by bacteria. This method is however time consuming (6 days). Part of this study is focus-ed on providing an additional NOM characterisation tool through the use of the BDOC method. Specifically, an attempt has been made to incorporate the bacterial degradation of the LMW and HPI NOM fraction so as to provide a more rapid technique. Not only will this study allow a better understanding of the effect of chemical composition of NOM (specifically polarity) on bioavailability, it will also provide an insight into the relationship between polar NOM fractions and bacterial utilisation.

According to Haarhoff *et al.* (2010), organic pollution (of which NOM is a major contributor) creates significant problems during water treatment. One of these is the proliferation of micro-organisms and subsequent deterioration of microbiological quality in the distribution system. When the removal of BDOC was tracked in the treatment train in a water treatment plant in Namibia, it was found that 47% of the BDOC was removed during the sand filtration process. Whilst pre-ozonation was utilised in the Namibian case study, the ability of ClO_2 to remove DOC will be investigated in this study.

2.3.6   Elemental composition of NOM

Measuring the conformation and the size of NOM material under various local conditions can be another way of doing the structural analysis; this can be done using photon correlation spectroscopy or atomic force microscopy (AFM). AFM however gives better chemical and structural data on NOM in relation to bacteria-NOM adhesion forces (Matilainen *et al.*, 2011).

2.3.6.1   Fourier transform infrared (FTIR) spectroscopy

FTIR spectrum can provide a unique fingerprint of a specific molecule (Matilainen *et al.*, 2011). However, the interpretation of the results may be too difficult and complicated due to the fact that NOM is a complex molecule. In this study, DOC analysis, UV_{254} nm, SUVA, mPRAM, HPSEC, FEEM, BDOC, LC-OCD and gel permeation chromatography were employed for the effective characterisation of NOM. It was envisaged that these methods would assist in addressing the characterisation and treatability objectives of the study.

2.4 NOM REMOVAL TECHNOLOGY

Surface water generally contains higher concentrations of NOM with a different composition compared to groundwater. Therefore, more effective treatment processes are required to remove NOM prior to the disinfection step when surface water is treated for potable use (Gallard and Von Gunten, 2002; Howe *et al.*, 2012).

Research has shown that water availability problem is expected to increase in the coming years, and this is expected even in those regions that are currently recognised as water rich (Nkambule *et al.*, 2009b). This challenge requires intensive research for identifying more effective, robust and new methods for water treatment. Other than the capability to minimise the use of chemicals that could have negative impacts on the environment, the desired methods should be low-cost and less energy intensive.

2.4.1 Coagulation

For the past years, coagulation has been used to reduce colour, turbidity and to eliminate pathogens during water treatment (Matilainen *et al.*, 2010). However, the conditions used for colour removal and turbidity are not exactly the same for those of NOM removal and this has necessitated the adoption of enhanced coagulation methods. In enhanced coagulation, significantly higher amounts of the coagulant that allows the removal of NOM from the water source are used (Matilainen *et al.*, 2010). Recent work has shown that the hydrophilic fraction of NOM is not effectively removed by normal coagulation as compared to the hydrophobic fraction (Matilainen *et al.,* 2010). This is because the hydrophilic fraction consists of a higher content of acidic functional groups, which are more difficult to destabilise by the coagulation process (Matilainen, 2007).

2.4.2 Oxidation

Pre-oxidation has been proven to remove organic matter much more efficiently, thus leading to an improvement of the coagulation process (Matilainen *et al.*, 2010). Ozonation is the preferred form of pre-oxidation and its influence is closely related to the characteristics of NOM, as it deals with odour, colour and taste in water (Matilainen *et al.*, 2010). Ozonation is commonly attained through post-ozonation and pre-ozonation (Pei *et al.*, 2007). Pre-ozonation increases the biodegradability of organic matter in water, thus enhancing the removal of NOM by increasing the biological activity in the filter of a biologically activated carbon (BAC) filtration system (Matilainen *et al.*, 2010). Post ozonation on the other hand is generally used instead of pre-chlorination, and some studies showed that it could increase the reduction of TOC in the coagulation step of the water treatment (Pei *et al.*, 2007).

Pre-chlorination is not recommended when high concentrations of cyanobacteria are present in the source water as this can cause cell lyses and subsequent release of toxins and taste and odour compounds (Bezuidenhout *et al.,* 2013). The presence of NOM causes the formation of DBPs when chlorine is used as a disinfectant or oxidant (AWWA, 2011).

2.4.2.1 Chlorine dioxide

Chlorine dioxide is effective in destroying phenols and other constituents of industrial effluents that form tastes and odours when treated with chlorine (Denysschen, 2000). AWWA (2011) reported that chlorine dioxide is not effective in the inactivation of cyanotoxins. Rodriquez *et al.* (2007) compared the reaction of different oxidants with the cyanotoxins microcystin LR, cylindrospermopsin and anatoxin-a. They found that chlorine dioxide is not a suitable oxidant for inactivation of cyanotoxins due to the low rate constant for reaction of chlorine dioxide with these toxins.

Metcalf and Eddy (2003) reported that chlorine dioxide is an effective disinfectant and is in fact more effective than chlorine in the inactivation of most viruses, spores, cysts and oocysts. An advantage of using chlorine is that its biocidal properties are not affected by the pH. According to Faust and Aly (1999), chlorine enhances coagulation, but it promotes formation of THMs. Chlorine dioxide also improves the coagulation process (Faust and Aly, 1999), and it does not form THMs (AWWA, 2011).

The most significant contaminants present in the raw water source of the Vaalkop water treatment works (WTW) are iron, manganese, colour, chlorophyll-a, DOC, *E. coli*, *Cryptosporidium* oocysts, *Giardia* cysts as well as taste and odour compounds (Van der Walt *et al.,* 2009). According to AWWA (2011), taste and odour control has been one of the primary applications of chlorine dioxide in the past. Van der Walt *et al.* (2009) reported that chlorine dioxide is effective in the removal of swampy, grassy and fishy odours, but that is ineffective against the removal of odours caused by Geosmin and 2-MIB.

Clogging of filters is a common problem at Vaalkop WTW during times when algal blooms are experienced. A study was conducted by Huang *et al*. (1997) where the inactivation effect of chlorine dioxide and liquid chlorine on algae and animal planktons were compared. It was found that the destructive effect of chlorine dioxide on algae was better than that of chlorine on certain species. It was also found that chlorine dioxide possessed a better inactivation effect on viruses and animal planktons than chlorine. According to tests conducted by Zamir *et al*. (2008), pre-treatment with chlorine dioxide also improves the turbidity at the outlet of the sedimentation tank when compared to treatment train without ClO_2.

The current pre-treatment options available at Vaalkop WTW are oxidation with chlorine or adsorption with powder activated carbon (PAC). Oxidation plays a very important role in the potable water treatment train and it is usually employed at the head of the treatment plant. The purpose of oxidation is to remove inorganic and organic compounds (AWWA, 2011). One of the problems experienced during the pre-treatment step at the Vaalkop WTW is that manganese is present in high concentrations during specific times of the year. Studies conducted on the oxidation of manganese with chlorine dioxide showed rapid oxidation of manganese to colloidal particulate MnO_2 (Van der Walt *et al*., 2009).

Raczyk-Stanislawaik *et al.* (2003) found that chlorine dioxide, upon reaction with natural organic matter (NOM), forms BDOC such as aldehydes and short chain carboxylic acids. The BDOC is then consumed by bacteria and can cause bacterial regrowth in the water distribution systems if the oxidation of the NOM takes place after sand filtration. In this study, it was envisaged that an introduction of the ClO_2 pre-treatment step at Vaalkop will result in the reduction of DOC, thus allowing bacteria to be eliminated during the final disinfecting step.

In anticipation and in response to possible changes in the macro environment, specifically raw water quality, it is recommended that chlorine dioxide be tested to determine whether it will be more effective than chlorine gas in the pre-treatment process during times of adverse raw water quality.

2.4.3   Activated carbon filtration

When NOM is removed during the filtration process it decreases the chances of removing other pollutants. This is due to NOM competing for the adsorption sites with other target pollutants. In order to overcome this problem, powdered or granular AC is used, since molecules with lower molecular weight are more adsorbable on activated carbon filtration (Matilainen *et al.,* 2010). This can be attributed due to the fact that the smaller the size of the molecule, the easier it will be for it to enter the nanopores (Matilainen, 2007).

2.4.4   Membrane filtration

Reverse osmosis, ultrafiltration, microfiltration and nanofiltration are pressure driven membrane methods with various NOM removal potentials (Matilainen *et al.,* 2010). Some of the disadvantages of membranes include membrane fouling and decline of flux, of which NOM is the major cause (Matilainen *et al.,* 2010). In order to overcome this adverse effect, pre-treatment coupled with coagulation is practised.

2.4.5   Degradation of NOM

Most conventional methods used for NOM removal in almost all the available water treatment plants involve the use of chemicals that result in the generation of sludge. Sludge consists of concentrated NOM which often pose serious disposal problems (Solarska *et al*., 2009; Lee, 2005). Conventional processes for the removal of

NOM include coagulation, membrane filtration, magnetic ion exchange resin (MIEX) and alum precipitation (Lee, 2005). The development of alternative methods that degrade NOM to harmless products is receiving a lot of attention from researchers. In this study, a three-step degradation approach was employed for the effective degradation of NOM to smaller and harmless molecules by incorporating enzymes, nanomaterials and UV based advanced oxidation processes.

2.4.5.1 Enzymatic degradation of NOM

Bioremediation technology, which involves the use of micro-organisms such as fungi and bacteria, or isolated enzymes to degrade organic pollutants into harmless products, has been given much attention because it is environmentally friendly, cost-effective, and limits by-product formation (Lee, 2005). This method has been reported to remove biodegradable organic matter, and reduce chlorine demand during the disinfection step as there will be no or very little NOM available to react with free chlorine (Lee, 2005). Not only has this technology been applied in the treatment of water to potable standards, it has also been used in the treatment of concentrated NOM wastes from other water treatment processes.

Examples of the application of this technology include the use of saprotrophic fungi and white-rot fungi (WRF) (Lee, 2005) to degrade humic substances (Grinhut *et al.,* 2007). White rot fungi have been reported to efficiently degrade lignin and a wide range of recalcitrant organic pollutants. The action or activity of WRF is due to their non-specific extracellular oxidative enzyme system, which may include lignin peroxidase (LiP), laccase (Lac) and manganese-dependent peroxidase (MnP) that completely mineralises lignin to CO_2 and H_2O. Non-specificity allows WRF to oxidize a variety of xenobiotic compounds with some structural similarity to the lignin substructures. These enzymes were found to degrade the humic substances resulting from the formation of carboxyl and phenoxy radicals (Solarska *et al.*, 2009). According to Solarska *et al.* (2009), biodegradation of NOM apparently leads to the formation of low molecular weight compounds such as organic acids, fulvic acids and low molecular weight humics.

Phanerochaete chrysosporium is the most extensively studied ligninolytic white rot fungus that mineralises NOM. ATCC 34541 removed 40 – 50% NOM from solution; however, this was due to adsorption and to a partially metabolically linked activity (Lee, 2005). It was reported that the activity of this fungus to remove colour was affected by environmental conditions such as pH, carbon and nitrogen content, as well as NOM concentration. In addition, it was reported that a combination of yeast contaminants isolated from a MIEX concentrate with the *P. chrysosporium* gave NOM removals of 70 – 80% (Lee, 2005).

Enzymes are generally substrate-specific and each enzyme normally only catalyses a single type of reaction, such as esterification (Solarska *et al.*, 2009). By binding to the specific substrate in the NOM molecule, the enzyme can then start degrading that part of the molecule into smaller pieces, which are easy to remove from the water source using specific treatment processes (Solarska *et al,.* 2009). Enzymes break certain bonds in the NOM structure, something which other methods fail to do. The amino acids, carbohydrates, proteins and carboxylic acids found in source water vary in their susceptibility to microbial biodegradability (Solarska *et al.,* 2009).

2.4.5.2 Photodegradation of NOM using nanomaterials

TiO_2 is the semiconductor photocatalyst that has received a lot of attention because of its chemical and biological stability, non-toxicity, insolubility in water, high photocatalytic activity, high stability in acidic and basic media, availability and low cost (Matilainen and Sillanpää, 2010). TiO_2 has been used in the removal of NOM whereby its photocatalytic ability was monitored using different analytical methods (Matilainen and Sillanpää, 2010).

However, photolysis based on TiO_2 has a wide band gap and there is thus a very small portion of the solar spectrum that can be used in sensitising TiO_2 (Nkambule *et al*., 2012c). Research has shown that doping of TiO_2 with noble metals such as palladium has a significant photocatalytic activity (Nkambule *et al.*, 2012c). These metals decrease the TiO_2 band making electron transfer between the bands more efficient, thereby resulting in the formation of oxidative species like hydroxyl radicals (Nkambule *et al*., 2012c). These radicals are strong oxidising agents and can oxidise organic pollutants found in water into mineralised products i.e. water and carbon dioxide (Nkambule *et al*., 2012c).

Nkambule *et al.* (2012c) reported on the use of nanocatalysts in the efficient degradation of NOM when compared to conventional NOM treatment methods. The improved photocatalytic effect was due to the co-doping of TiO_2. It has been shown that, for example, a 96% degradation efficiency of hydrophobic fractions of NOM brought about by the increased interaction with nanoparticles was achieved; on the other hand, a degradation efficiency of 35% was observed when the UV based method used (Nkambule *et al*., 2012c).

2.4.5.3   *UV based advanced oxidation processes*

Advanced oxidation processes (AOPs) are a combination of methods used for the oxidation of NOM from waters and they include TiO_2/UV, UV/H_2O_2, O_3/H_2O_2, O_3/UV, $H_2O_2/catalyst$, Fenton and photo-Fenton processes, and ultrasound. AOPs basically include all the processes where hydroxyl radicals are being formed as an intermediate through different methods (Matilainen and Sillanpää, 2010). In AOP processes, the H_2O_2 molecule is divided into two hydroxyl radicals via absorbing photons and these radicals can attack organic molecules under proper operating conditions to produce end-products such as water, CO_2 and inorganic acids (Matilainen and Sillanpää, 2010). However, it must be noted that these radicals can react with carbonate and bicarbonate ions, which are commonly available in raw water, thus reducing the amount of hydroxyl radicals to react with NOM (Lamsal *et al.,* 2011).

2.4.5.3.1   *Photo assisted Fenton (UV/H_2O_2)*

During treatment with UV, NOM molecules are oxidized and aromatic fractions are reduced. Moreover, high molecular NOM molecules are converted into low biodegradable compounds (Matilainen and Sillanpää, 2010). Generated hydroxyl radicals, reduce both total organic carbon and disinfection by-product formation potential in raw water. At the appropriate hydrogen peroxide concentration and right UV dose, NOM can be completely mineralised into inorganic molecules (Matilainen and Sillanpää, 2010). Studies conducted based on direct measurement of rate constants for reactions between hydroxyl radicals and several dissolved organic matter (DOM) that were isolated from various sources showed that hydroxyl radicals were three to four magnitudes more reactive than those of chlorine and ozone (Lamsal *et al.*, 2011).

2.4.5.3.2   *Photocatalysis processes (TiO$_2$/UV)*

These processes use oxygen as oxidising agent and semiconductor metal oxide as catalyst (Andreozzi *et al.*, 1999). The first step involves the absorption of UV irradiation of the TiO_2 followed by the formation of electron-hole pairs (Andreozzi *et al.*, 1999). This results in the excitement of electrons from the valence band to the conduction band, which in turn leads to the formation of hydroxyl radicals and the creation of highly oxidative holes on the valence band (Nkambule *et al.,* 2012c). Organic compounds like NOM are then degraded by hydroxyl radicals in the solution and by holes on the TiO_2 surface (Matilainen and Sillanpää, 2010). Oxidation reaction can be affected by these parameters: water matrix, solution pH, catalyst concentration, light wavelength and intensity (Matilainen and Sillanpää, 2010).

2.4.5.3.3 Ozone based applications (O_3/UV)

Ozone is primarily used as a disinfectant and for management of taste and odour in water treatment (Matilainen and Sillanpää, 2010). Ozone selectively reacts with NOM via an electrophilic addition to double bonds, which eventually leads to the degradation of NOM. This process also leads to the formation of oxidation by-products as well as possible release of entrapped compounds. These by-products may results in biological regrowth in the water conveyance system (Matilainen, 2007). Moreover, hydroxyl radicals that are formed when ozone decomposes in water also react with NOM via a direct, fast and non-selective reaction (Matilainen and Sillanpää, 2010).The hydroxyl formation potential in this case is much lower as compared to AOPs.

CHAPTER 3: METHODOLOGY

3.1 STUDY SITES: SAMPLING AREA AND FREQUENCY

Water samples were collected according to the previous WRC project on NOM (Haarhoff *et al.*, 2012). The selected sampling sites included at least five different sites and samples were collected from the following sources: surface waters, municipal water treatment plants and industrial water treatment plants. It was envisaged that this comprehensive sampling would give a broad narrative on the character and composition of NOM throughout South Africa. The treatment plants of interest are broadly located within the five water types of South Africa, which includes oligotrophic, hypertrophic and highly coloured water. Water sources located within sites prone to acid mine drainage (AMD) were also be sampled.

The surface water samples were collected from Vaal Dam and Vaalkop Dam. Samples from water treatment plants were collected prior to and after entering the filtration system of the treatment plants of Rand Water, Magalies Water, Sedibeng Water, Midvaal Water and Eskom. Sampling was carried out five times to ensure that any variability in NOM composition due to change in season or rainfall would also be accounted for. Permission to participate in the study was sought and granted by these water treatment plants. Sampling at each site was carried out in August 2015, November 2015, February 2016, May 2016, and August 2016 to incorporate seasonal variation. The NOM characterisation analyses that were undertaken are listed in Sections 3.2 and 3.3 of this chapter. Temperature, pH, alkalinity and turbidity measurement of the samples were conducted on site at each of the sampling points.

3.1.1 Sampling at the WTPs

Samples were collected from the eight of the following water treatment plants, which utilise various water treatment processes: Magalies Water (MP 1–3), Rietvlei plant (RV), Lepelle Northern Water (Ebenezer (LE), Olifantspoort (LO) and Flag Boshielo plant (LF)), Midvaal (MV) plant, Plettenberg Bay (P) plant, Preekstoel (VS and VB) plant, Amanzimtoti (AM), Hazelmere (HL), Mtwalume (MT) and Umzinto (UM) water treatment plant. **Figure 3-1** shows the map of South Africa with the sampling sites marked with a star symbol. Data relating to the water samples, which includes sampling sites, codes and dates is summarised in **Table 3-1.**
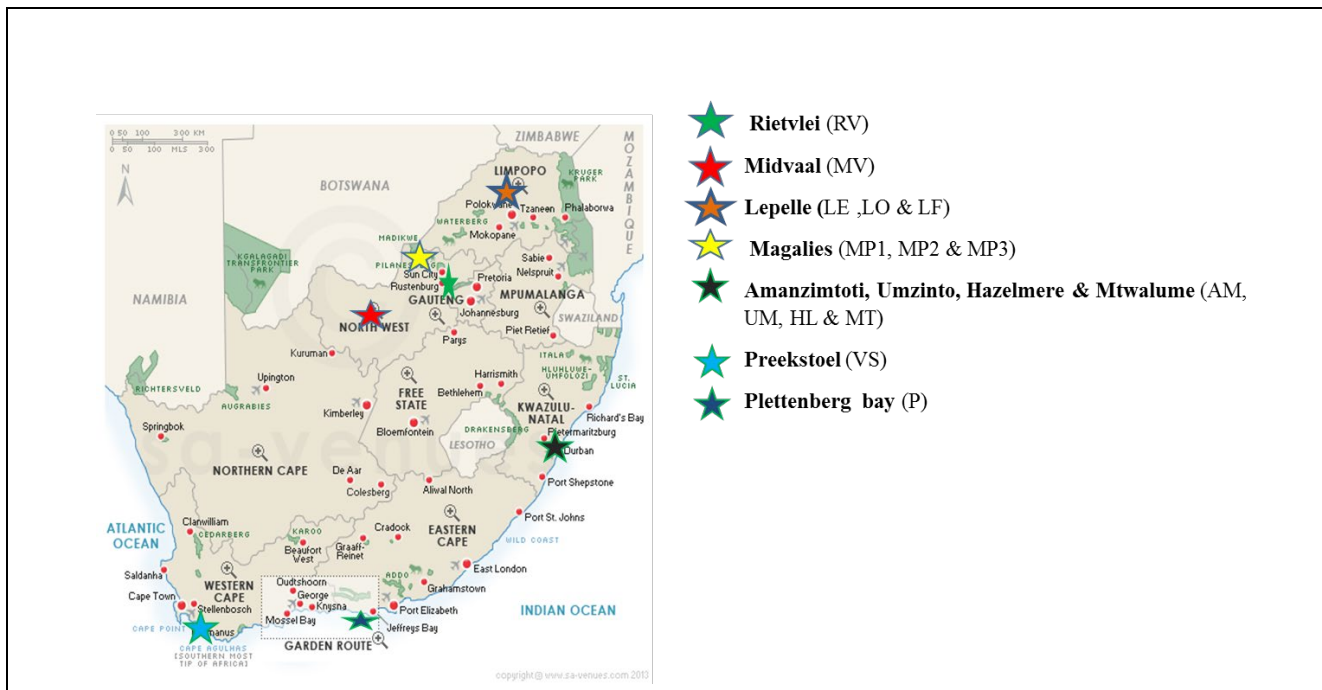
Figure 3-1 Locations of the different sampling points (Google maps)

Table 3-1 Description of sampling codes from various water treatment plants

Water treatment plant	Code description/treatment stage	Sample Code	Sampling dates
Magalies plant 1	Raw water	MP1-1	
	After dissolved air flotation	MP1-2	
	After filtration	MP1-3	
	After granular activated carbon	MP1-4	
	After disinfection	MP1-5	
Magalies plant 2	After pre-treatment	MP2-1B	11.11.2015; 06.05.2016; & 22.07.2016
	After dissolved air flotation	MP2-2	
	After sedimentation	MP2-3	
	After filtration	MP2-4	
	After disinfection	MP2-5	
Magalies plant 3	After sedimentation	MP3-2	
	After COCO dissolved air flotation	MP3-3	
	After disinfection	MP3-5	

Table 3-1 Description of sampling codes from various water treatment plants (cont'd)

Water treatment plant	Code description/treatment stage	Sample Code	Sampling dates
Rietvlei plant	Raw water	RV-1	23 November 2015, 26 February 2016, 30 April 2016, 5 July 2016 and 27 September 2016
	After coagulation/flocculation	RV-2	
	After granular activated carbon	RV-3	
	After dissolved air flotation/filtration	RV-4	
	After disinfection	RV-5	
Lepelle Northern Water - Ebenezer plant	Raw water	LE-1	24 February 2016, 5 May 2016, 30 June 2016 and 29 September 2016
	After aeration	LE-2	
	After coagulation/flocculation	LE-3	
	After filtration	LE-4	
	After disinfection	LE-5	
Lepelle Northern Water- Olifantspoort plant	Raw water	LO-1	
	After settling (coagulation/ flocculation)	LO-2	
	After filtration	LO-3	
	After disinfection	LO-4	
Lepelle Northern Water - Flag Boshielo plant	Raw water	LF-1	
	After settling (coagulation/ flocculation)	LF-2	
	After filtration	LF-3	
	After disinfection	LF-4	
Midvaal Water	Raw water	MV-1	2 March 2016, 3 May 2016, 28 June 2016 and 26 September 2016
	After pre-ozonation	MV-2	
	Before flotation	MV-3	
	After chemical dosing	MV-4	
	After flotation	MV-5	
	Before settling	MV-6	
	After settling	MV-7	
	After filtration	MV-8	
	After disinfection	MV-9	

Table 3-1 Description of sampling codes from various water treatment plants (cont'd)

Water treatment plant	Code description/treatment stage	Sample Code	Sampling dates
Plettenberg Bay plant	Raw water	P-1	20 June 2016 and 20 September 2016
	After flocculation	P-2	
	After sedimentation	P-3	
	After filtration	P-4	
	After disinfection	P-5	
Veolia Water - Preekstoel (Surface water)	Raw water	VP-1	21 June 2016 and 19 September 2016
	After mixing	VP-2	
	After sedimentation	VP-3	
	After filtration	VP-4	
	After disinfection	VP-5	
Veolia Water - Hermanus plant (Borehole water)	Raw water	VH-1	
	After filtration (Manganese)	VH-4 (Mn)	
	After filtration (Iron)	VH-4 (Fe)	
Amanzimtoti plant	Raw water	AM-1	24 June 2016 and 22 September 2016
	After coagulation	AM-2	
	After clarification	AM-3	
	After filtration	AM-4	
	After disinfection	AM-5	
Hazelmere plant	Raw water	HL-1	
	After coagulation	HL-2	
	After clarification	HL-3	
	After filtration	HL-4	
	After disinfection	HL-5	
Umzinto plant	Raw water	UM-1	
	After coagulation	UM-2	
	After clarification	UM-3	
	After filtration	UM-4	
	After disinfection	UM-5	
Mtwalume plant	Raw water	MT-1	
	After coagulation	MT-2	
	After clarification	MT-3	
	After filtration	MT-4	
	After disinfection	MT-5	

3.1.2   Rand Water sampling

For the Rand Water treatment plant, sampling was carried out on a monthly basis over a period of 24 months; NOM characterisation data from the raw water sources in Rand Water's catchment area was collected.

Samples were collected from the full-scale plant after the coagulation and filtration stages (**Figure 3-2**). This is to enable the assessment of NOM treatability as well as calculation of the removal of the various fractions after these treatment steps.
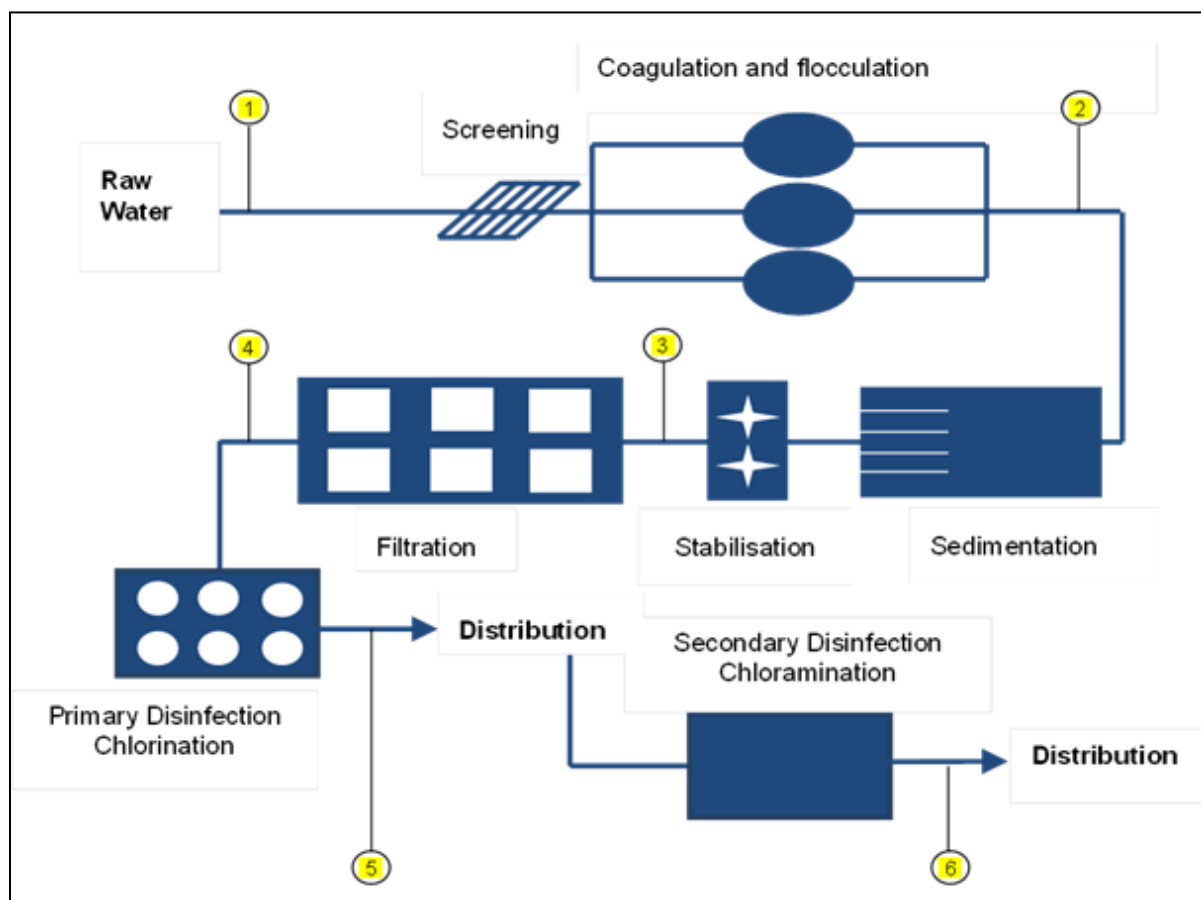
Figure 3-2 Process flow diagram of the sampling points within Rand Water's conventional water treatment process

3.2 PART A: NOM CHARACTERISATION, TREATABILITY AND DBP FORMATION

3.2.1 Characterisation and quantification of NOM

The following NOM characterisation techniques were used: DOC, UV_{254}, SUVA, BDOC, mPRAM, FEEM and HPSEC. These methods allowed the establishment of the character of NOM, its composition and the amount of NOM in each of the sampling points mentioned in **Table 3-1**. A comparative analysis was undertaken of the strength and accessibility of these analytical techniques as well as their contribution towards the understanding of the composition and character of NOM in the water samples that were collected in each of the sampling points. The 24 month characterisation study took into account the effect of seasonal variation on the composition and character of NOM. These results were used to evaluate the efficiency of current treatment processes in the removal of DBP precursors (NOM).

3.2.1.1 *DOC, UV_{254} and SUVA*

Bulk organic loading of the water was determined by filtering the samples through a 0.45 µm membrane filter. DOC and UV absorbance were measured at a wavelength of 254 nm (UV_{254}) in order to determine the organic

carbon during the various seasons as well as the aromatic character of NOM. UV_{254} and DOC measurements were taken using a spectrophotometer (Agilent Technologies Cary 60 UV-Vis) and a Shimadzu TOC-L analyser, respectively. Standard carbon solutions of 1 mg/ℓ, 5 mg/ℓ, 10 mg/ℓ, 20 mg/ℓ and 30 mg/ℓ were prepared using potassium hydrogen phthalate (KHP) and de-ionised water. The standard solutions were used to calibrate the instrument. Measurements were carried out in triplicate and the resulting values were averaged out with any significant outliers being discarded. To determine the presence of humic and non-humic substances in the sample, specific ultraviolet absorbance (SUVA) values in ℓ/mg.m were calculated according to **equation 3.1** (Weishaar *et al.,* 2003).

$$SUVA = \frac{UV_{254}\left(cm^{-1}\right) \times 100\,\dfrac{cm}{m}}{DOC\left(\dfrac{mg}{\ell}\right)}$$

[Equation 3.1]

Also, the percentage UV_{254} and DOC removal after each treatment step were calculated to indicate the NOM removal efficiency by the water treatment plant.

3.2.1.2 *Bacterial degradation of NOM: BDOC method*

Biodegradable Dissolved Organic Carbon (BODC) represents the fraction of dissolved organic carbon (DOC) that can be mineralised by bacteria. The BODC method measures the amount of organic matter that is biodegradable by a bacterial inoculum. The inoculum is biologically active sand (sand colonised by bacteria) originating from a water treatment plant filter. Typically a water sample is inoculated with sand and aerated for the duration of the experiment. DOC measured at the beginning and then at specific time intervals (e.g. every day or second day) until a minimum is reached after several days. BDOC concentration is derived from the difference between the initial concentration and minimum DOC values. Although the BDOC method is a simple way of determining the fraction of NOM (DOC) available for growth stimulation, it is a fairly lengthy analysis as the readings are collected over a period of 6 days (Nkambule, 2012). In an attempt to provide a more rapid NOM characterisation tool that will provide insight on the biodegradability of HPO and low molecular weight (LMW) NOM fractions, an amended BDOC technique was investigated. This amended BDOC method measured the decrease in DOC while simultaneously monitoring the bacterial biomass production.

This method was researched by collecting surface water samples from the Vaal Dam over a 12 month period, taking into account a change of NOM during various seasons. Raw water was filtered through 0.45 µm membrane filters, thereafter after six NOM fractions were isolated using PRAM. The same experiment was repeated using water sampled after the coagulation/flocculation step in a full-scale conventional water treatment plant. These collected samples, a control sample as well as a bulk water sample (without fractionation) were then inoculated with heterotrophic bacteria. The introduction of bacteria in the BDOC method is to allow the simultaneous measurement of organic carbon available to the bacteria and the monitoring of bacterial growth in the different samples.

Phylogenetic identification of bacteria using 16S rDNA sequence analysis has indicated that the bacterial community growing off the LMW NOM fraction was dominated by the γ-Proteobacteria (*Pseudomonas sp.)* phylotype (Covert and Moran, 2001; Axmanová *et al*., 2006). Bacteria belonging to the γ-Proteobacteria phylogenic group has previously been identified in Rand Water's distribution system. Other studies have also demonstrated the preponderance of proteobacteria in drinking water distribution systems, even though chlorine and chloramines are used as disinfectants (Santo Domingo *et al*., 2003; Williams *et al*., 2004; Tian *et al*., 2014). Therefore, the collected NOM-containing water samples were inoculated with concentrated heterotrophic bacteria laced water samples and suspended growth bacteria. Whereas the heterotrophic bacteria laced water samples were obtained from the pre-chlorination stage of the full-scale plant, the

suspended growth bacteria were isolated from the distribution system of Rand Water. The bacteria were first concentrated by filtering a water sample through a 1 µm nuclepore filter (to remove possible protozoa). After centrifuging the filtrate, the resulting pellet was re-suspended in sterilised water and used as an inoculum.

Samples were then inoculated and incubated in amber bottles at room temperature on a shaker table at 50 rpm. Amber bottles and room temperature conditions were used mimic bacterial environmental conditions in the distribution pipelines. Sample bottles were glass wool stoppered to prevent contamination by bacteria in the laboratory, and to allow the flow of air and maintain an aerobic system. Aliquots of inoculated incubated samples were removed and analysed at various time intervals (0 to 72 hours). Young (2005) performed a 308 hour pilot experiment and discovered that bacterial growth peaked at 24 hours, declined at 72 hours and therefore only studied the first growth cycle (i.e. 0 to 72 hour time period).

Preliminary experiments were performed in order to establish the incubation period for achieving maximum bacterial biomass. The heterotrophic bacterial biomass production was determined by taking aliquot samples of 10 mℓ at various time intervals and measuring bacterial growth. According to CHANG (2011), the measurement of optical density at 600 nm is a simple assay to measure the extent of bacterial growth, and immediate results are obtainable.

At each selected time interval a sample was collected for UV_{254}, DOC analysis (BDOC) and to measure the resulting biomass production. DOC and biomass production were monitored as two complementary parameters. The major difference in the case of the amended BDOC method is that DOC was not monitored at the point where no further decrease in DOC was observed, but instead up to the time interval where maximum biomass production was observed. This provided some insight into the relationship between the bacteria and their utilisation of NOM in water containing the different NOM fractions (HPO, HPI and TPI). The same experiment was repeated with added nutrients (C:N:P ratio) to the culture media to optimise bacterial growth. This ensures a rapid, but accurate method that will be appropriate for monitoring bacterial utilisation of the various fractions based on their polarity and molecular weight.

A comparative analysis of the biodegradability of the bulk NOM and the biodegradability of the respective NOM fractions provides insight into the mechanism involved in biodegradable organic matter consumption (Labanowski and Feuillade, 2009). This method gives an indication of how the removal of the HPI fraction from the final drinking water will reduce the BDOC, identifies the problematic NOM fraction and sheds light on the bacterial degradation of the HPI NOM fraction. The problematic NOM fraction will be identified as the fraction that shows abundant bacterial growth compared to bacterial growth within the other NOM fractions. Also, the deterioration of water quality within samples due to the presence of specific NOM fractions, the influence of bacterial growth and the amount of DBPs formed can be evaluated in one experimental set-up.

3.2.1.3 *Modified polarity rapid assessment method (mPRAM)*

The PRAM fractionation procedure generates three NOM fractions and is a very rapid method of NOM characterisation by quantifying the amount of material adsorbed onto three different solid-phase extraction (SPE) cartridges. After filtering the samples through a 0.45 µℓ membrane filter, 20 mℓ of the sample was passed through each cartridge at a flow rate of 1.2 mℓ /min within a vacuum manifold connected to a vacuum pump. The hydrophobic and hydrophilic analytes were extracted from the non-polar (C18) and polar (CN) SPE cartridge by eluting them with 0.1M NaOH (approximately 10 mℓ). The TPI fraction is thus collected as the fraction that passes through the NH2 and CN cartridge. The supernatant from the three SPE cartridges was then analysed by UV_{254} to evaluate the amount of material adsorbed onto each cartridge.

3.2.1.4 Fluorescence excitation emission matrix (FEEM) characterisation

Fluorescence EEM measurements were conducted using a Horiba AquaLog Spectrometer. The spectrometer displayed a maximum emission intensity of 1000 arbitrary units (AU). The spectrometer uses a xenon excitation source and excitation and emission slits were set at 10 nm band pass. To obtain FEEMs, excitation wavelengths were slowly increased from 200 nm to 600 nm at 5 nm band pass for each excitation wavelength; the emission at longer wavelengths is often detected at 0.3 nm steps. To partially account for Raleigh scattering, the fluorometer's response to a blank solution was subtracted from the fluorescence spectra of the sample to be analysed. De-ionised water, with known concentrations of DOC, was used as a blank solution. Absorbance of light from the lamp by DOC molecules in the sample was accounted for by using an inner-filter correction applied to the data by using UV-Vis spectral data from the blank. The AquaLog is equipped with a reference detector to monitor and ratiometrically correct both the excitation source's spectrum for the emission detector and the absorbance signals. A transmission detector is attached to the AquaLog's sample compartment to record the transmission/absorbance spectrum of the sample under the same spectral-band pass and resolution conditions as the fluorescence EEM data. The corrected EEMs were then plotted using Origins Lab (supplied with the instrument) using 20 contour lines, with each contour interval representing 1/20th of the maximum fluorescence intensity.

3.2.1.5 High performance size exclusion chromatography (HPSEC)

The change in molecular size distribution (MSD) of organic matter is a fast and consistent method to demonstrate performance of the treatment process with regards to NOM removal (Pelekani *et al*., 1999; Myllykangas *et al.,* 2002). The MSD was determined by means of HPSEC as described by Nissinen *et al*. (2001). A water sample was first filtered through a 0.45 µm syringe filter. Thereafter, a 20 µl sample was injected into a Hewlett Packard 1100 HPLC system. Humic molecular fractions were separated on a TSK G3000SW column (7.5 mm x 300 mm) at a flow rate of 0.7 mℓ/min and using 0.01 M sodium acetate as a mobile phase. A 70 mm guard column of the same phase was used to protect the analytical column. The peak area of each fraction was measured after detection at 254 nm.

3.2.2 NOM treatability

Figure 3-2 is a schematic illustration of the NOM fractionation, characterisation procedures and subsequent DBP formation, which will aid in determining NOM treatability of the water. The procedure of fractionation and characterisation were performed on the source water samples, water sampled after stabilisation as well as on water that has gone through the filtration process of the full-scale plant. For the DBP study, water samples collected after the filtration step were chlorinated to determine the DBPs formed in each of the NOM fractions. Both raw data (i.e. data from the full-scale plant) and live data (i.e. data generated data from laboratory scale experiments) were used throughout the study.
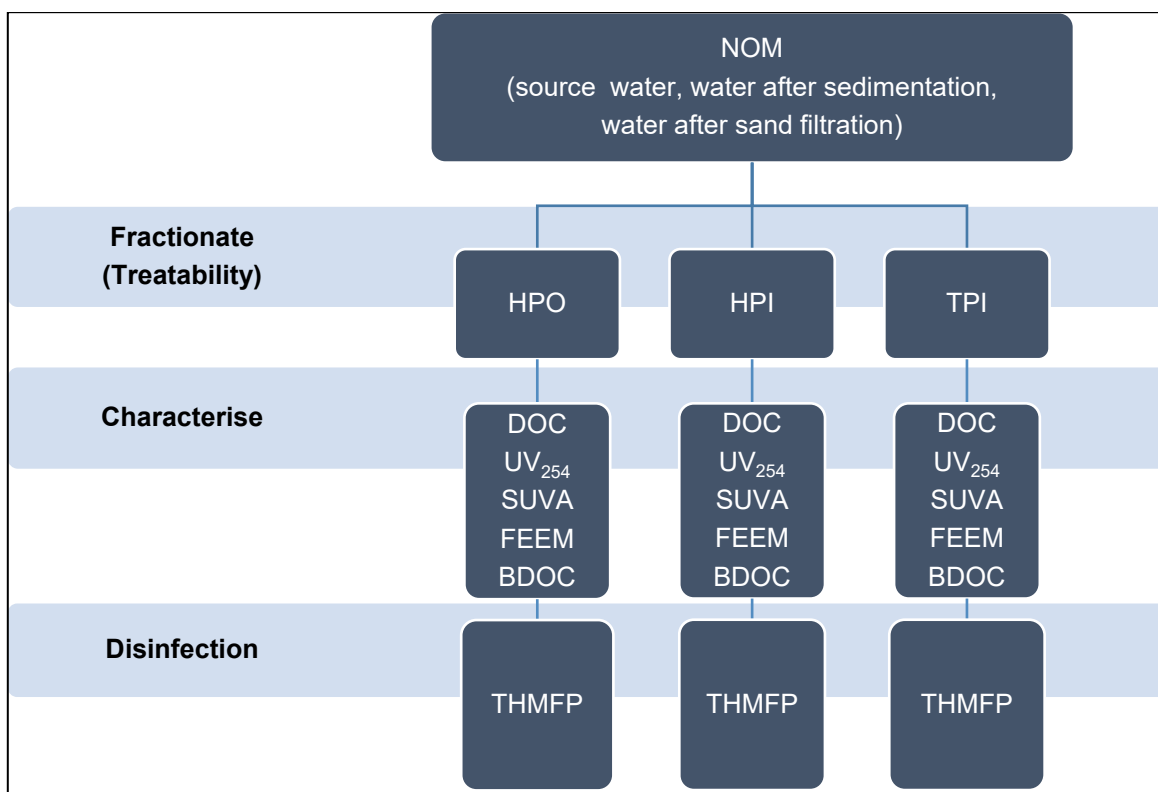
Figure 3-3 Schematic illustration of the NOM fractionation, characterisation and DBP formation studies performed on bench scale using samples from the full-scale plant

3.2.3   DBP formation and NOM fractionation

It was envisaged that the question of whether removal of HPI NOM will reduce DBP formation would be answered by coupling the DBPs formed with PRAM fractionation. The effect of NOM polarity on the formation of the disinfection by-products was thus determined. This was achieved mainly by fractionating the NOM into three fractions using the mPRAM method, which involved undertaking DBP formation potential studies by chlorinating the individual NOM fractions and measuring the THMs that were formed. **Figure 3-3** illustrates the process that was followed. Fractionation was achieved through mPRAM as described by Nkambule *et al*. (2011), this involved the use of an SPE method that utilises non-polar sorbent (C18), polar sorbent (CN) as well as anion exchange (NH2) cartridges. Furthermore, FEEM analyses of the respective NOM fractions were undertaken to determine the components responsible for the DBPs that were formed.

The selected DBPs included the following THMs: $CHCl_3$, $CHBr_3$, $CHCl_2Br$, and $CHBr_2Cl$.

3.2.3.1   DBP analysis

After sampling the chlorinated water for THM analysis, ascorbic acid was immediately added to quench the residual disinfectant. Samples were analysed using a Headspace Sampler (Agilent 7697A) coupled to a Gas Chromatograph (Agilent 6890N). After the separation of the THMs on the capillary gas chromatography column (J & W Scientific, 30 mm x 0.530 mm x 0.5 µm), detection was carried out with an electron capture detector (ECD). The four THMs determined in the final water samples were: bromoform, chloroform, dibromochloromethane and bromodichloromethane. As well as their individual concentrations, their sum was also reported as TTHM in µg/ℓ. The detection limits are as follows: bromoform 0.36 µg/ℓ, chloroform 0.21 µg/ℓ, dibromochloromethane (DBCM) 0.33 µg/ℓ and bromodichloromethane (BDCM) 0.27 µg/ℓ.

3.3 PART B: DEVELOPMENT OF NOM SEPARATION AND REMOVAL TECHNIQUES

This section of the study was focused on the development of materials for SEC/GPC stationary phases. The novelty of this study was to synthesise a new polymer matrix to be used as a stationary phase that can retain larger particles in the SEC/GPC for a longer period of time, and thus release smaller particles (low molecular weight compounds) first. The two macro porous stationary phases, which were used in the study, are macro porous poly(styrene-divinylbenzene) and macro porous polysilsesquioxane. It was predicted that the developed material would be better suited for NOM separation due to its ability to be stable over a wide pH range (Hosoya and Frechet, 1993), achieve no column efficiency degradation and having very good adsorbent properties (Burleigh *et al*., 2002).

3.3.1 Synthesis of hybrid silica materials for NOM separation

3.3.1.1 *Preparation of polysilsesquioxane*

3.5.1.1.1 *Chemicals*

1,2-Bis (triethoxysilyl) ethane, 1,4-bis (trimethoxysilylethyl) benzene, NaOH, HCl, CTAC, EtOH and deionised water were purchased and used without further purification.

3.5.1.1.2 *Synthesis*

Polysilsesquioxane was prepared by base catalysed hydrolysis and condensation of the alkoxysilyl precursors around supramolecular assemblies of CTAC. In a typical synthesis, 6 mℓ of CTAC (25 weight %) and 2.6 mℓ of 25% NaOH were added under stirring conditions to 100 mℓ of deionised water. To this mixture, 9.4 mℓ of 1,4-bis-(trimethoxysilylethyl)benzene were added. The reaction flask was then covered and the mixture continued stirring at room temperature until gelation (about 2 h).

3.5.1.1.3 *Post synthetic treatment*

The synthesis gels were heated at 70°C for 48 h. The resulting as-synthesised materials were then placed in excess (350 mℓ/g) acidified ethanol (1M HCl) and refluxed for 6 h to extract the surfactant templates. The isolation of the products was carried out by filtration and washing with absolute ethanol. The extraction procedure was repeated and the samples dried under vacuum at 60°C (Burleigh *et al*., 2002).

3.3.1.2 *Preparation of poly(styrene-divinylbenzene)*

Following a modified procedure by Hosoya and Frechet (1993), 7 mℓ (7.2 weight % in water, particle size = 1.5 pn) of the monomer was swelled with a solution of 0.3 g of benzoyl peroxide in 3.2 mℓ of dibutyl phthalate. A mixture of 20 mℓ of water containing 0.15 g of sodium dodecyl sulfate (SDS) was emulsified using a sonicator. The second swelling step started after the total disappearance of the droplets from the previous emulsion. In the second swelling step, 16.5 mℓ of the emulsified monomers (7 mℓ of styrene and 9.5 mℓ of commercial divinylbenzene (55% DVB)), and 25 mℓ of toluene (porogen) in 170 mℓ of water containing 3.4 g of poly(vinyl alcohol) (MW 85,000-1 46,000, 88% hydrolysed) were added to the dispersion resulting from the first swelling step. The polymerisation was carried out in a 500 mℓ round-bottomed glass reactor (Buchi BEP 280) under continuous stirring (100 rpm) at 70 ºC for 10 hours. After polymerisation, the beads were transferred to a beaker containing 200 mℓ of methanol, washed twice and respectively with methanol and THF. The yield of 95%of the uniformly sized particles calculated with respect to the weight of added monomers was achieved.

For comparison of pore size formation purposes, similar porous styrene-divinylbenzene particles were prepared by a standard suspension polymerisation technique. The organic phase consisting of 7 mℓ styrene, 9.5 mℓ divinylbenzene, 3.2 mℓ dibutyl phthalate and 0.16 g benzoyl peroxide was stirred in a 2 wt.% aqueous solution of the poly(vinyl alcohol) at 70ºC for 10 hours. The work-up procedure of the beads was done as described above. The efficiency of the synthesised material was compared to a commercially available stationary phase.

3.3.2 NOM separation and removal by GPC

Characterisation of samples obtained from the study area described in Part A was done by DOC (Section 3.2.1.1) and FEEM (Section 3.2.1.4) analyses. Thereafter, GPC characterisation was performed using the newly synthesised polymer matrix.

CHAPTER 4:   EVALUATING THE CHARACTER OF NOM AND ITS REMOVAL BY SOUTH AFRICAN WATER TREATMENT PLANTS

4.1 INTRODUCTION

NOM in water compromises water quality. This in turn poses a threat to the effectiveness of the available water treatment processes in the removal of NOM and other micro-pollutants present in water. Based on this information, most water treatment plants have now added NOM to their list of priority pollutants to be removed during the water treatment processes (Dlamini and Haarhoff, 2012). Most of the treatment plants are dependent on surface water as their feed, and this type of water is often compromised due to high agricultural run-offs, floods and droughts and other water reuse processes that negatively affect its supply (Haarhoff *et al.,* 2009).

This chapter reviews the character of NOM occurring in South African waters and evaluates the effectiveness of various water treatment processes used by specific South African water treatment plants for the removal of NOM. The first step towards the removal of NOM from water is its characterisation, since the character of NOM is not uniform across different water sources. Conventional methods such as DOC, UV_{254} and SUVA are typically used for the characterisation of NOM, however, these methods do not provide enough information about the composition of the NOM in water. Therefore, advanced characterisation methods such as FEEM are required to close this information gap. Once the character of NOM is defined or understood then various NOM removal methods can be employed.

The South African National Standards (SANS) and the World Health Organisation (WHO) have set the maximum allowable DOC levels at 10 mg/ℓ and 5 mg/ℓ, respectively (Nkambule *et al*., 2011). In principle, the readily available water treatment processes should be able to reduce NOM in water to below the acceptable standards (Mamba *et al*., 2009).

4.2 CONVENTIONAL METHODS FOR CHARACTERISATION OF NOM

4.2.1   pH, turbidity and conductivity of the water

In the water industry, pH is used to determine the alkalinity or the acidity of the water (Ashery *et al.,* 2010). The measured pH values of the water treatment plants (WTPs) under investigation ranged from 2.32 to 9.33 (**Appendix A**). The pH values of the raw and final water are generally alkaline, with the most alkaline value recorded for Midvaal (Ashery *et al.,* 2010). The raw water from the Preekstoel (VP-1) treatment plant is the most acidic water, and this could be because this water is very high in ion content (**Figure 4-1 (a)**). In principle, processes such as biofiltration also depend on pH for their proper functioning (Funes *et al.,* 2014). Thus, the high pH levels of VP and Hermanus (VH) treatment plant final water could be due to the Fe and Mn not being effectively removed from the raw water source of the VH plant. This could be due to the presence of NOM in the water, which has been reported to compromise the removal of Fe and Mn (Ashery *et al.,* 2010). If Fe and Mn ions are not effectively removed from the solution, they tend to compete with H^+ ions for the active site on the biofilter or biosorbent surface (Zhang *et al*., 2014). This affects the pH of the water of both the VH and VP due to the fact that the treated water from VH is then blended with the treated water from VP.

Similarly, the effectiveness of the coagulation process is also reliant on the pH of the water (Nkambule *et al.,* 2011). The pH levels of the water before the coagulation process can affect the removal of NOM from that particular water source (Mamba *et al.*, 2009). The higher the pH the lower the efficiency of NOM removal, and vice versa. This is because at low pH levels, NOM can easily aggregate, which promotes an efficient removal of NOM from water (Mamba *et al.,* 2009). Furthermore, the effect of pH on NOM removal was also studied by Ashery *et al.* (2010), and it was shown that the optimum removal was obtained when the water pH was adjusted to 5-6 before the addition of alum coagulant. This raises another important point; it is also important for the pH of the feed water to be determined prior to the coagulation step. In addition, according to the South African Target Water Quality, the allowable no risk pH should is between 6 and 9; and it can be concluded from the results of the pH measurements that all the final water samples meet the allowable operational limits.

The turbidity of the water (**Figure 4-1 (b)**) can, on the other hand, be used as an indicator of the total amount of clay particles and colloids present in water (Nkambule *et al.,* 2012b). Ashery *et al.* (2010) studied the effect of pH on turbid water and observed that the optimum turbidity removal was at around pH 5-6 when using the alum coagulant. In instances where the turbidity of water is higher than the accepted standards, processes such as flocculation and filtration could be affected during the water treatment (Obi *et al.,* 2009). Turbidity can also affect the effectiveness of chlorine during the disinfection step (Mamba *et al.,* 2009). The acceptable values of turbidity in water are between 0 to 1 NTU, as water with higher turbidity values may cause problems such as the ones mentioned above.

In this study, the turbidity of all the water samples at their final stages of the treatment process was found to be in the range 0.0 – 3.0 NTU, with the Flag Boshielo Water plant (LF) having the highest turbidity value and the Magalies Water (MP1) having the lowest turbidity (**Figure 4-1 (b)**). The turbidity levels were found to decrease as the water passed through various treatment steps (**Tables A1-11** (**Appendix A**)). The standard error of the mean values proves that the quality of raw water kept on changing for various sampling rounds. This can be attributed to natural causes such as floods, droughts and human activities performed near the raw water sources, which end up polluting the water sources.

Lastly, **Figure 4-1 (c)** shows the water conductivity measurement for the various WTPs. The conductivity of the water is highly dependent on the concentration of ions with the ability to transfer electrical current (Obi *et al.,* 2009). When the ion content in water is high, it increases the chances of bursting of pipes and may also affect the health of the consumer by causing skin problems (Obi *et al.,* 2009). The allowable conductivity level for no risk is < 700 mS/cm. The measured levels of conductivity (**Figure 4-1 (c)**) of water samples was found to be in the range of 135.3–781.3 mS/cm, with the Plettenberg Bay plant (P) having the lowest conductivity and Olifantspoort plant (LO) having the highest conductivity. Moreover, the measured conductivity values of the water samples varied from plant to plant. An increase in conductivity measurements was however observed as the water was being taken through the various treatment processes (**Tables A1-11** (**Appendix A**)), mostly because of an introduction of various ions through the chemicals that were being used in the water treatment stages (Mamba *et al.,* 2009).
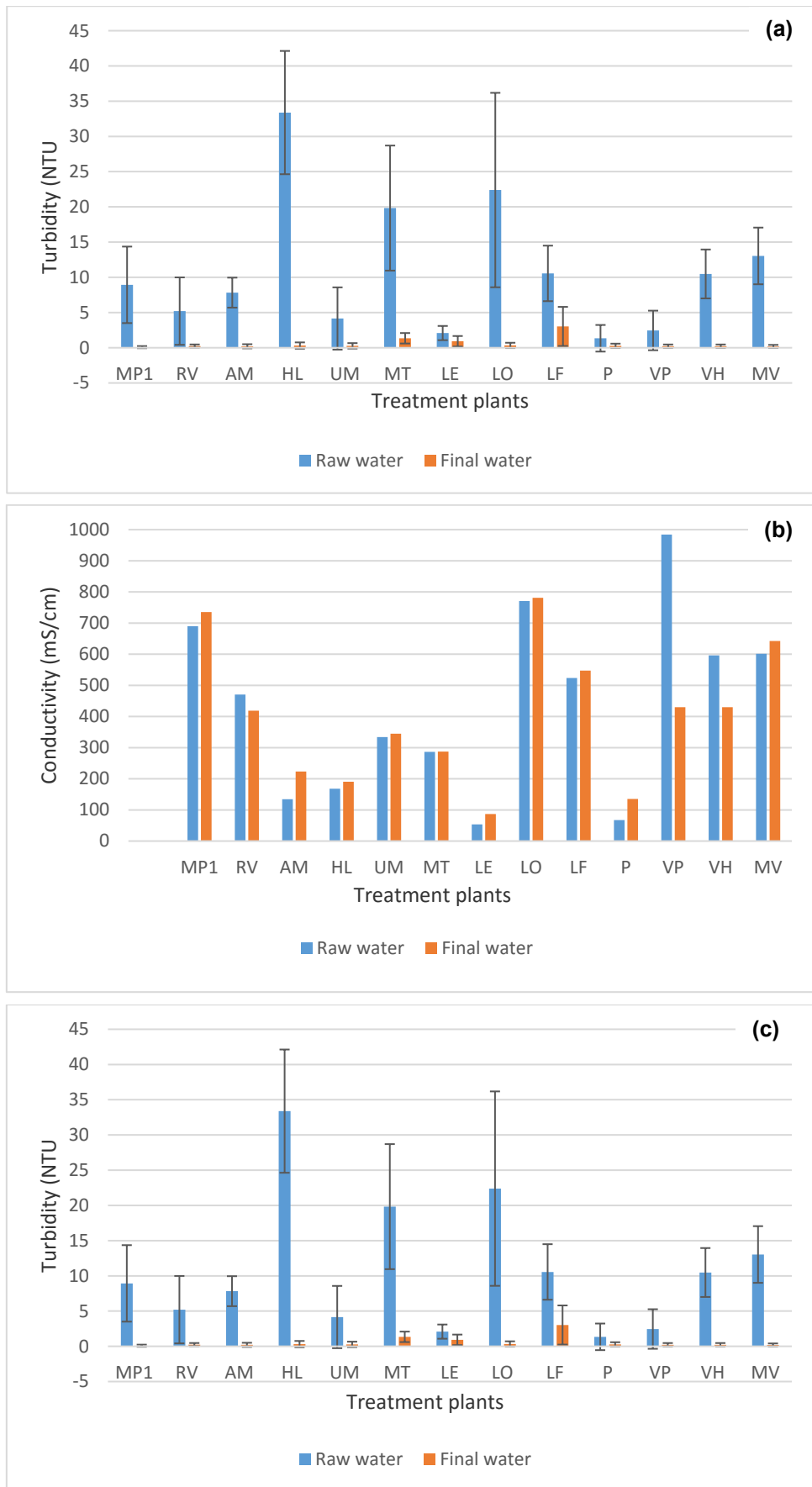
Figure 4-1 pH (a), turbidity (b) and conductivity (c) measurements for the various WTPs

4.2.2   Removal of DOC

DOC levels varied throughout the water treatment process (**Tables A1-11** (**Appendix A**)) for the various treatment plants. Secondly, it must be noted that the final water from most of the water treatment plants has DOC values that are below the allowable standards recommended by both WHO and SANS (**Figure 4-2 (a)**), with Mtwalume (MT) plant and VH having the highest and lowest DOC values, respectively. In addition, these results also show that plants from Umgeni (Durban, KwaZulu-Natal) have the highest levels of NOM. This is concordant with literature reports that this water is montaigne water consisting of high NOM content and low colour (Dlamini *et al.,* 2012).

The removal efficiency of DOC from water by the various water treatment plants differs, with P having the highest and HL having the lowest NOM removal (**Figure 4-2 (b)**). This is because the various treatment plants use different treatment processes and chemical dosages to treat the water. However, some plants with similar treatment processes still showed different NOM removal efficiencies (e.g. UM and MT). The observed differences in DOC removal could be due to the different chemical dosages that are applied by these two plants. The non-uniform character of NOM present in the raw waters of the two plants (**Appendix D**) also contributes to the observed differences in NOM removal. The character of the NOM of the raw water from the two plants was found to be different even though both plants are located within an hour of each other in Kwazulu-Natal. This significant difference is attributed to the different geology, topography and human activities (industrial and agricultural) being practised around the two raw water sources (Nkambule *et al.* 2009). The raw water for UM is located in an area with high industrial, farming and other human-related activities, which occur upstream of the raw water source. MT on the other hand has its water quality impacted by sand mining, which increases the water turbidity. These activities could be the core factor for the observed difference in DOC removal efficiency. Some studies have proven that the character of NOM can become non-uniform over the years due to natural causes such as increase in temperatures and decrease in acid deposition, and other human related activities such as industrial and agricultural activities (Evans *et al.*, 2005).

When compared with LE-1 and LE-2, a slight increase in the amount of DOC was observed for LE-3 (after sedimentation) in all the rounds of sampling (**Table A5** (**Appendix A**)). Degradation occurring on the edges of the sedimentation tank is often responsible for increased amounts of DOC levels (Mamba *et al.*, 2009).
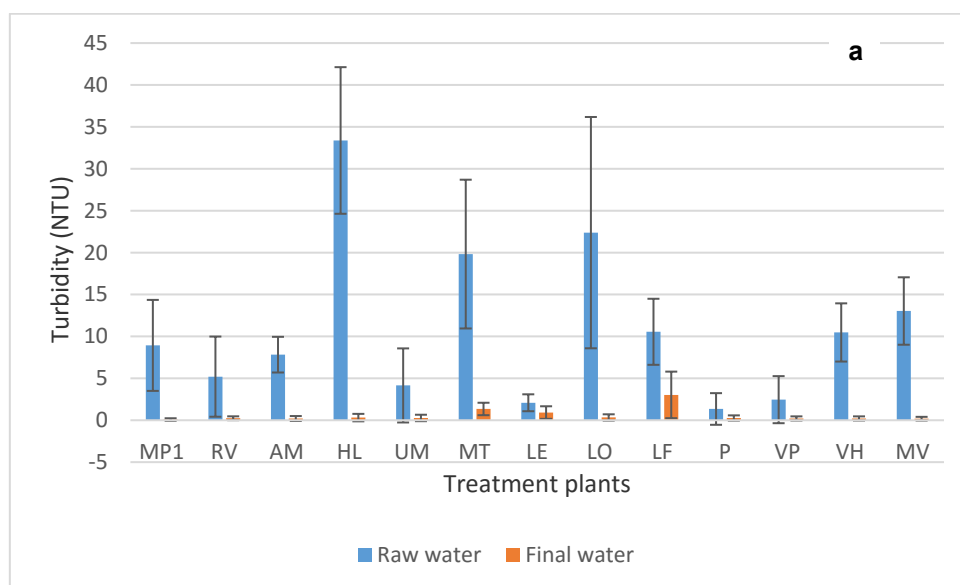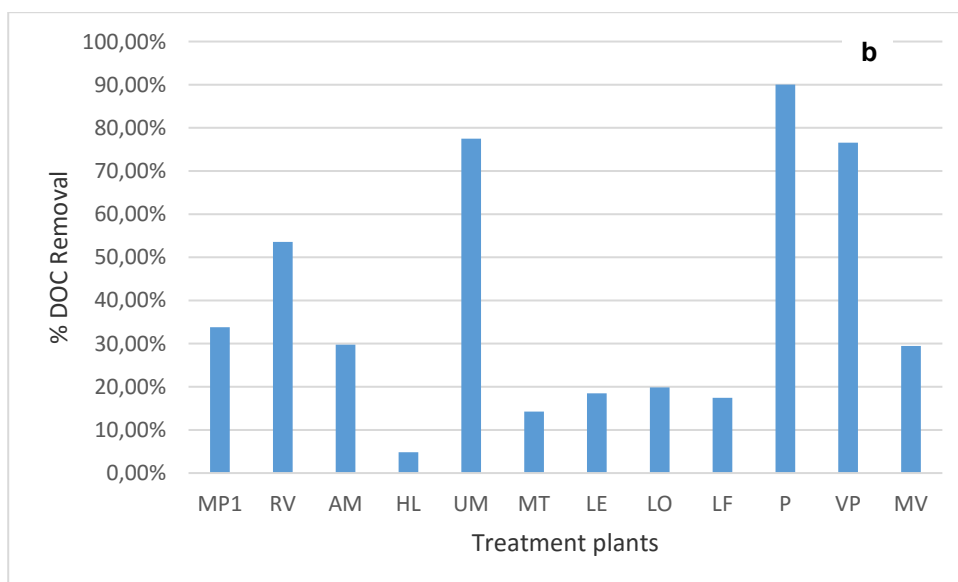
Figure 4-2 DOC (a) and % DOC removal (b) for various WTPs

4.2.3 UV-Vis analysis of various WTPs

Any wavelength ranging from 220 to 280 nm is appropriate for the measurements of NOM (Nkambule *et al.,* 2012a). However, the molar absorptivity values vary due to the range of chromophores present in NOM. Specifically, the wavelength of 254 nm is associated with the aromatic character of the molecule and is also used in industries for the maximum absorption of NOM molecule (Nkambule *et al.,* 2009b). Furthermore, 214 nm is associated with nitrites and nitrates; 272 nm on the other hand is the best predictor for the formation of trihalomethanes (Nkambule *et al.,* 2012b).

A decrease in the absorbance values of UV_{254} from raw water to final water was observed for all the treatment plants (**Figure 4-3 (a)**), suggesting that the aromatic character of NOM decreased. Moreover, the raw water of all the plants under investigation generally had high UV_{214} values, with the raw water of the VP plant having the highest UV_{214} absorbance value. This means that the raw water of the VP plant consists of a high nitrate and nitrite content. However, it should be noted that the UV_{214} absorbance values decreases after the subsequent treatment steps. Also, the UV_{272} absorbance values were found to be high, which means that the water has a great potential to form trihalomethanes (THM). As with the UV_{214} absorbance values, the UV_{272} absorbance values also decreased after the subsequent treatment steps.

Overall, the raw water from the Preekstoel (VP) and Plettenburg Bay (P) plants consists of NOM with high aromatic content and THM formation potential compared to the other water treatment plants. The water from these plants was also brownish relative to the water of all the other plants. These observations are in line with a study undertaken by Thebe *et al.* (2000), which showed that the surface waters located along the coastal belt of the southern Cape consists of high NOM concentrations with high colour content.

In addition, the obtained results show that the HL plant has the highest percentage removal of the aromatic content of NOM (as measured by the decrease of the UV_{254}) and LE the lowest removal of aromatics (**Figure 4-3 (b)**). From these findings it can be concluded that most of the NOM in the water was removed by coagulation, which targets mainly the hydrophobic fraction (and by extension the aromatic character) of NOM. Similar findings, which were reported by Thebe *et al.* (2000), attribute this to the ease of removal associated with the presence of humic substances (i.e. compared to non-humic substances). Moreover, the observed difference in the removal efficiency of aromatic content of NOM (UV_{254}) could be due to the different types of coagulants being used by these plants. Equally important, the type of water (including its pH) being treated

needs to be compatible with the type of coagulant being used in order to achieve optimum removal of the targeted pollutant (Mamba *et al.,* 2009).
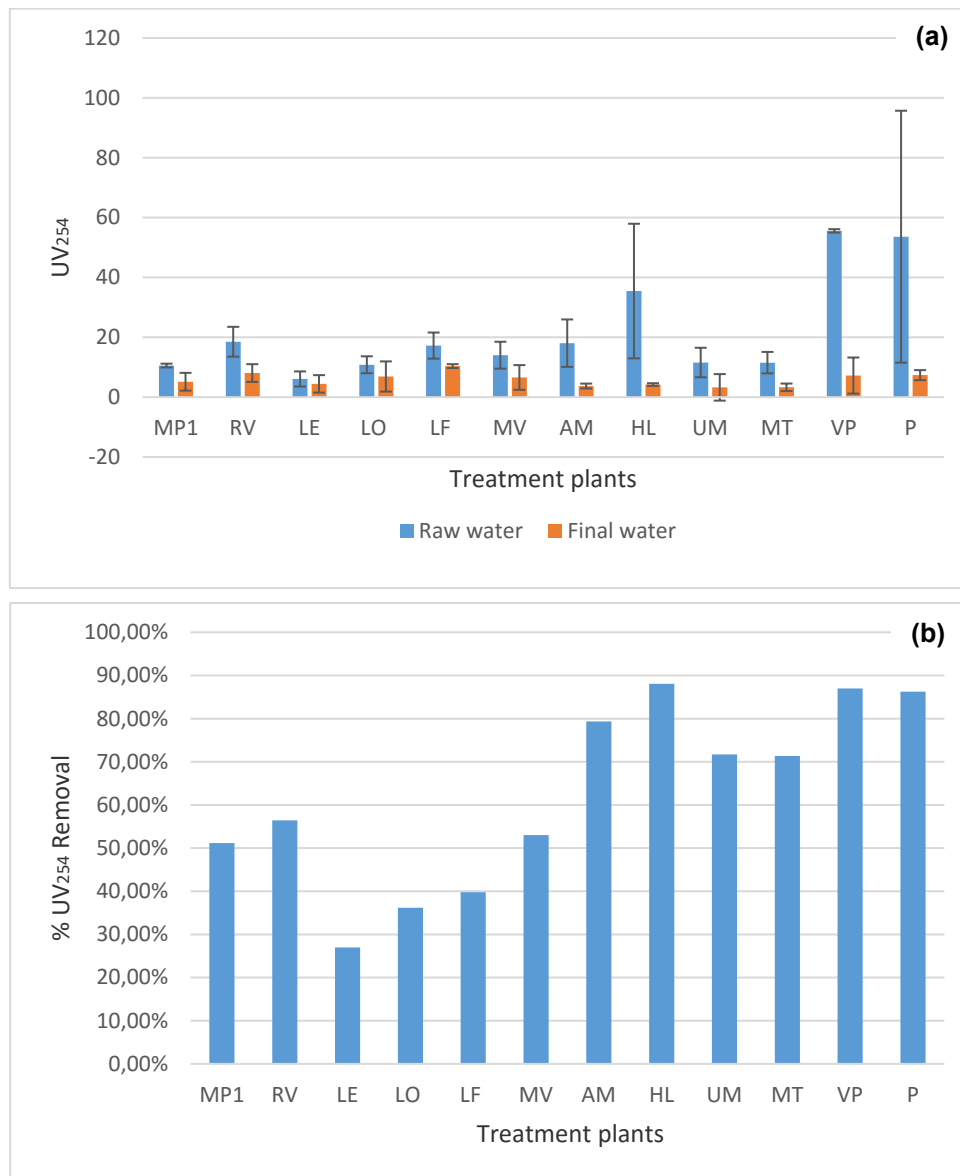
Figure 4-3 UV$_{254}$ (a) and % UV$_{254}$ removal (b) for various WTPs

The raw water in most of the WTPs showed relatively high absorbance compared to the water that was collected from the other treatment steps (**Figure 4-4**). This was expected since the raw water consists of all the suspended particles and colloids that might also absorb some UV light (Nkambule *et al*., 2012c). Moreover, there was a decrease in the UV absorbance after every treatment step in most plants, proving the effectiveness of the treatment plants in removing NOM; these results were consistent with what was observed by Nkambule *et al.* (2012a). RV-4 (after dissolved air filtration) absorbs higher than RV-3 (after GAC) and it also has a higher DOC (**Figure 4-4 (a)**). This could be due to the filters not being properly cleaned (thus leading to overloading) or some defects in the filtration unit itself (Obi *et al.,* 2009). This possibly indicates that the filters need to be backwashed properly.

(a)

(b)

(c)
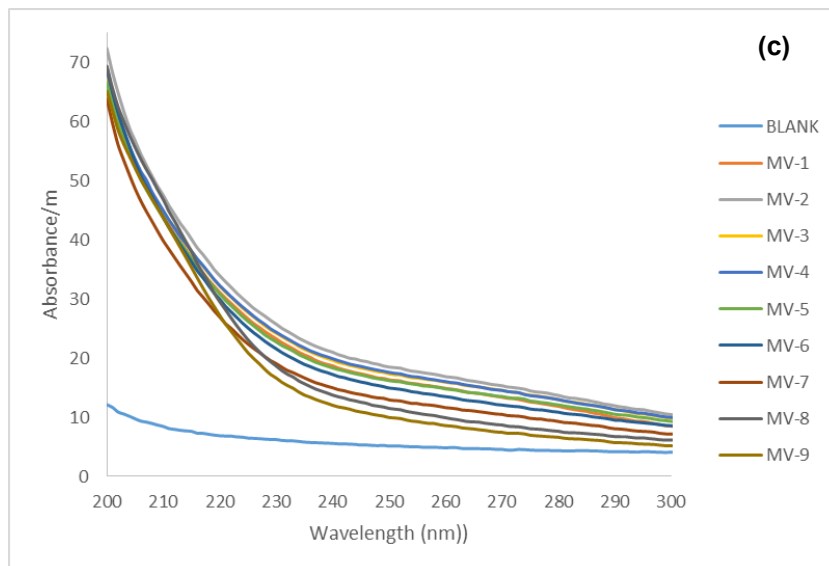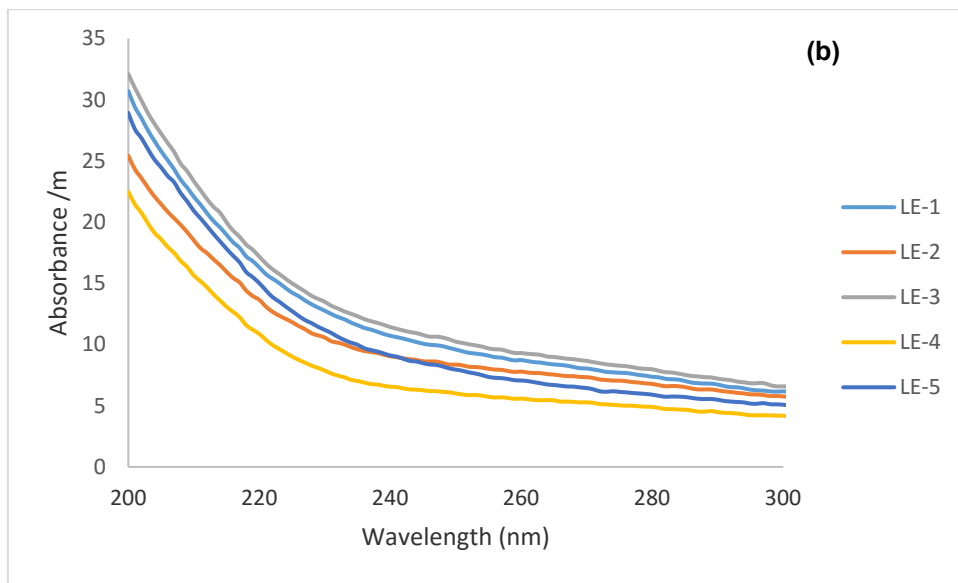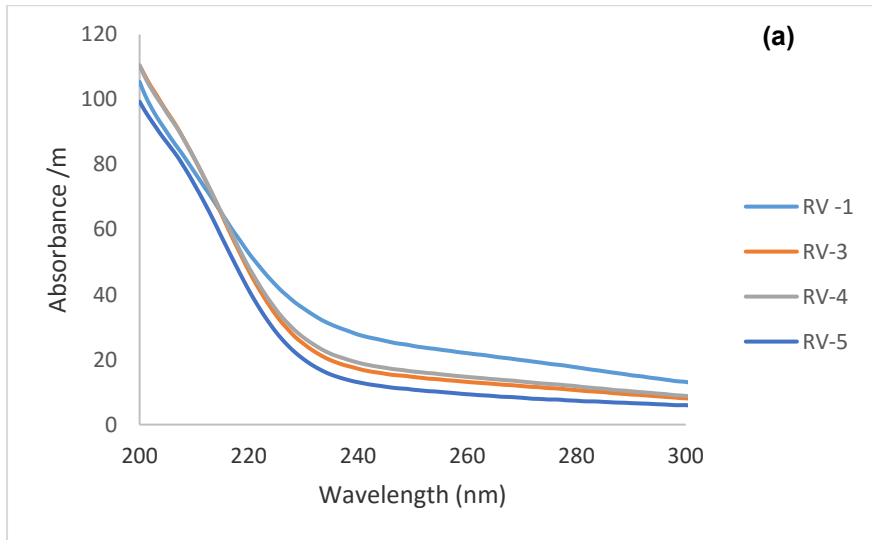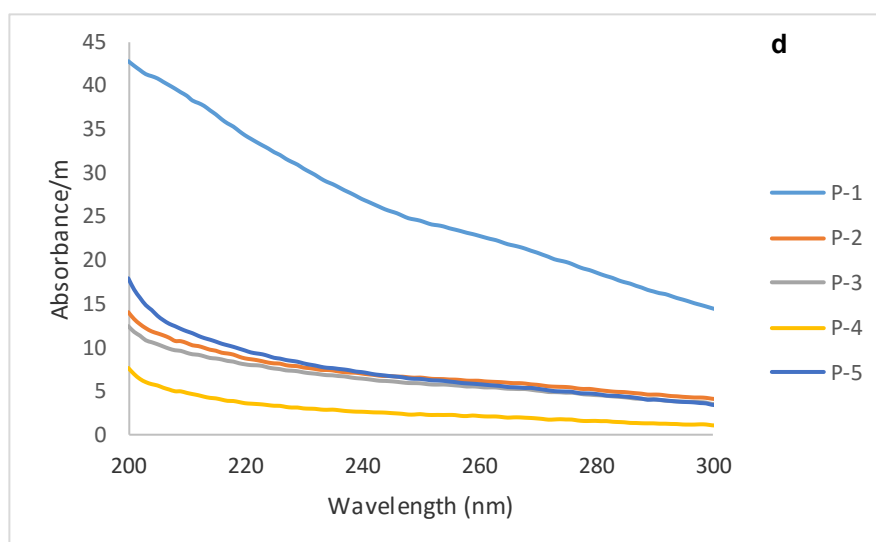
Figure 4-4 UV scan for the Rietvlei plant (a), Ebenezer plant (b), Midvaal plant (s) and Plettenberg Bay treatment plant (d)

In addition, MV-2 (after pre-ozonation) and MV-4 (after chemical dosing) have higher absorbance values compared to MV-1 (**Figure 4-4 (c)**), and this might be due to the addition of chemicals (ozone during ozonation and ferric chloride with cationic polymer during chemical dosing) which could have reacted with the pollutants that were initially present in water. Accordingly, by-products (especially in the case of MV-2 which is the pre-ozonation process) can be formed and might absorb high UV compared to raw water sample (**Figure 4-4 (c)**). The same was observed for the LE plant (**Figure 4-4 (b)**), with LE-5 having the highest DOC, UV$_{254}$ and turbidity compared to the water from the former treatment step and this could be for the same reason as explained above. As expected from the brownish colour, the raw water sample for Plettenberg Bay absorbed higher than the other samples (**Figure 4-4 (d)**). It can also be observed that P-4 absorbs lower than P-5; this could be due to the sand filters being used in this plant, thus proving the effectiveness of the filters in the removal of pollutants present in water. This allows the effective removal of most of the NOM present in water before the disinfection step, thus limiting the formation of disinfectant by-products (DBPs), which are carcinogenic to humans.

4.2.4   SUVA analysis of various WTPs

The raw water for Magalies (MP1, 2 and 3) and Umzinto (UM) plants has SUVA values that are less than 2 (1.76 and 1.16, respectively) (**Figure 4-5**), meaning that the NOM is made up of non-humic substances and is hydrophilic in nature with their final water being more hydrophilic than the corresponding raw water (1.42 and 0.87 ℓ/mg.m respectively) (Świetlik and Sikorska 2006; Mamba *et al*., 2009). For the RV, LE, LO, MV, AM and MT plants, the nature of NOM in the respective raw water is transphilic (3.87, 3.06, 2.38, 2.45, 2.26 and 2.02 ℓ/mg.m respectively) and it remained in that form (2.77, 2.38, 2.46, 1.40, 0.87 and 0.90 ℓ/mg.m respectively) throughout the treatment process for most of the plants, except for AM and MT plants which became hydrophilic. Lastly, the raw water for Plettenberg Bay (P), Preekstoel (VP) and Hazelmere (HL) was found to be hydrophobic in nature (26.7, 7.74 and 5.91 ℓ/mg.m respectively), with the P plant being the most hydrophobic (i.e. highly aromatic) (Haarhoff *et al*., 2009; Nkambule *et al*., 2009b; Matilainen *et al*., 2011). Furthermore, the brownish colour is evidence of the high amount of humic substances in the raw water (Thebe *et al*., 2000). Previous findings have shown that water with high SUVA has high DOC removal potential (Nkambule *et al*., 2012a). Similar findings were obtained in this study with respect to the P and VP plants. This trend was, however, not observed for all treatment plants under investigation; the UM plant, which has the lowest SUVA value did not have the lowest UV$_{254}$ percentage removal. Furthermore, the results indicate that the character of NOM kept on changing throughout the treatment process (**Tables C1 – C18 (Appendix C)**).

The results also show that the SUVA increases in the order LE-2 (after aeration) > LE-1 (raw) and LE-5 (final) > LE-4 (after filtration) (**Table C5** (**Appendix C**)). From these findings, it is clear that addition of the coagulants and disinfectants to the water containing this type of NOM results in increased SUVA values (i.e. NOM becoming more transphilic in nature). Similar findings were observed for SUVA increasing in the order, LO-4 (final) > LO-3 (after filtration) and LF-4 (final) > LF-3 (after filtration) (**Tables C6** and **C7** (**Appendix C**)) and this could be for a similar reason. Overall, the types of NOM present in the raw water sources for LE, LO and LF were not the same, even though all of these plants are located in the Limpopo Province. The difference in the SUVA values is probably due to the different industrial and agricultural activities being practised near the raw water sources. Similar results were observed for HL, AM, UM and MT plants which are located in KwaZulu-Natal.
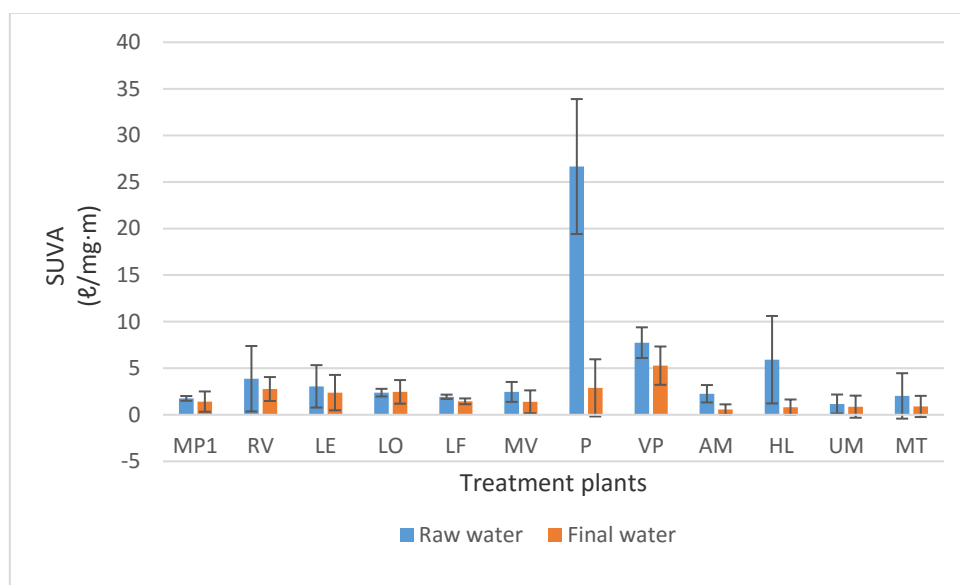
Figure 4-5 SUVA values for samples from various WTPs

4.3 ADVANCED CHARACTERISATION TECHNIQUES

4.3.1   Fluorescence excitation emission matrices (FEEM)

The principle behind FEEM is based on the fact that after a sample has been excited at a particular wavelength, a number of emission scans over various wavelengths are obtained and are used to define the composition of NOM. This technique is very useful as it has the ability to determine the amount and the nature of fluorophores being analysed. A FEEM label description graph, which shows the regional distribution of NOM fractions in water samples, is shown in **Figure 4-6**.
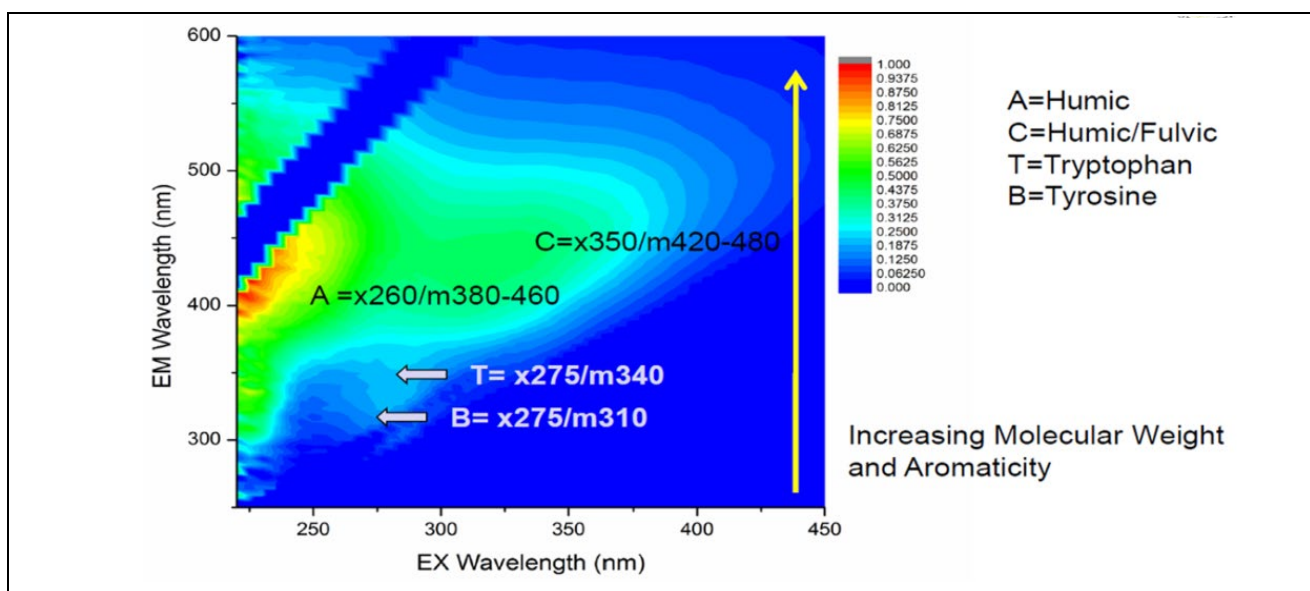
Figure 4-6 An example of FEEM spectra for the classification of the EEM region of a raw water sample (Nkambule *et al*., 2012a)

The fluorescence EEM spectra of the raw water samples for the RV and MV treatment plants showed a similar regional distribution of the NOM fractions. To this end, the FEEM spectra for the raw water samples of the RV (**Figure 4-7 (a)**) and MV (**Figure 4-7 (b)**) treatment plants indicate the presence of humic (A), tryptophan (T) and tyrosine (B) fractions. Over and above the occurrence of these compounds, the RV water sample was found to contain the humic/fulvic-like fraction (C).

NOM fractions (humic and fulvic) were also observed, albeit in different quantities, in raw waters of VP, HL and P treatment plants (see **Figures 4.7 (e)** – **(f)**). From these results, it can be concluded that the high UV_{254} removal efficiency that was observed for these plants (VP, HL and P) was due to the presence of high amounts of humic substances in these treatment plants. The higher the amount of aromatics (shown by high UV_{254}) in water, the easier it will be to treat the water by coagulation.

All the raw water samples (**Figures 4.7** and **4.8**) were found to contain, amongst others, the aromatic protein fraction, which has excitation (EX) and emission (EM) wavelength boundaries of 200–250 nm and 280–320 nm, respectively. Furthermore, the NOM of the raw water samples for the Lepelle treatment plant was found to be composed exclusively of the aromatic protein fraction (**Figures 4.7 (c)** - **(d)**). These results once again emphasise the notion of the varying character of NOM that is found in various water sources. Most importantly, it highlights how the FEEM can be used to determine the NOM (humic substance) removal efficiency during the various stages of the water treatment process (Nkambule *et al*., 2012a). **Figure 4-8 (b)** indicates that after the coagulation process, most of the humic and fluvic components had already been removed. This proves that coagulation deals mostly with those molecules that are hydrophobic in nature (Matilainen *et al*., 2010; Lobanga *et al*., 2013; Bello *et al*., 2014). Moreover, water that has gone through the filtration process has very little or no traces of humic fractions (**Figure 4-8**). This is a good indication that the filters being used by the Plettenberg Bay (P) plant effectively remove organic pollutants (humic substances) from water.
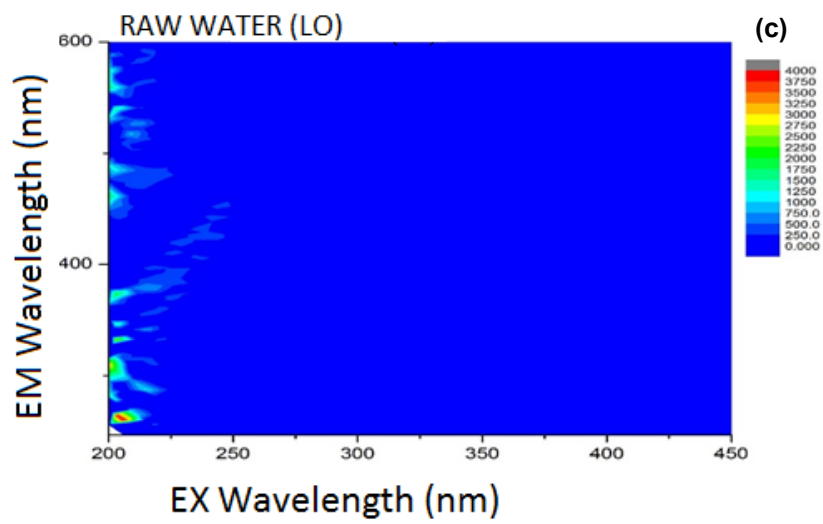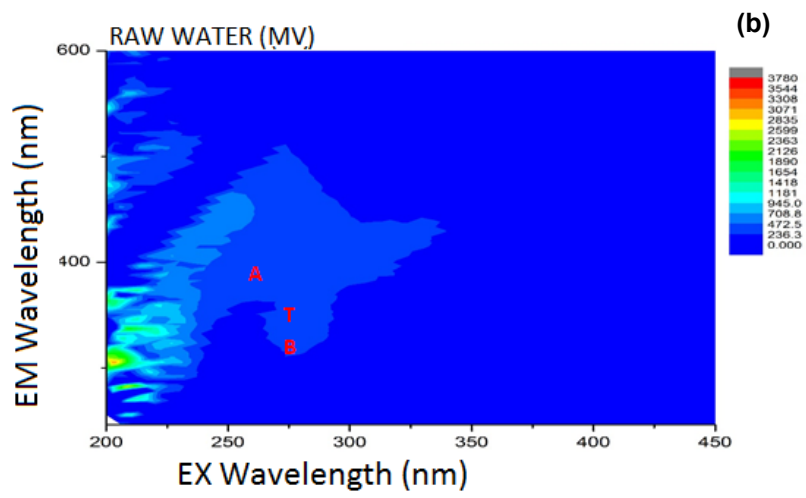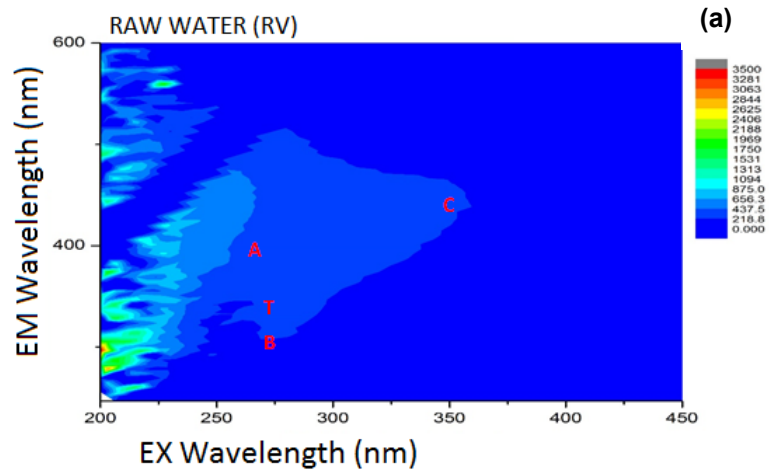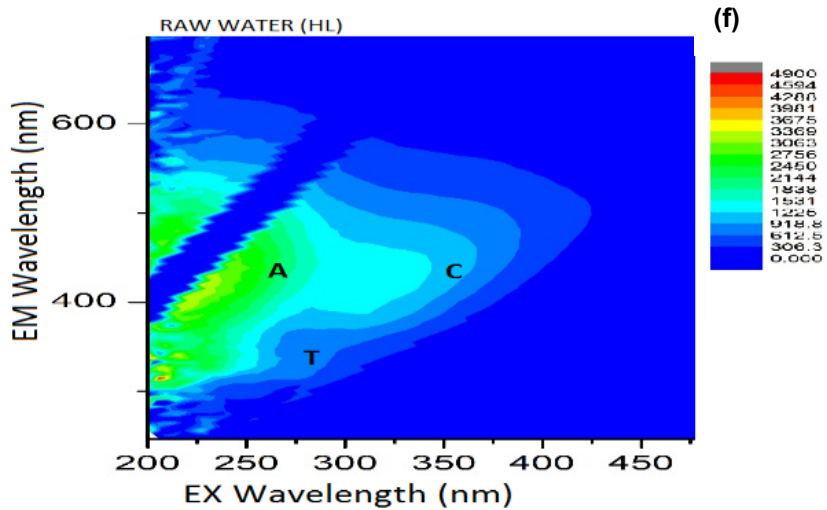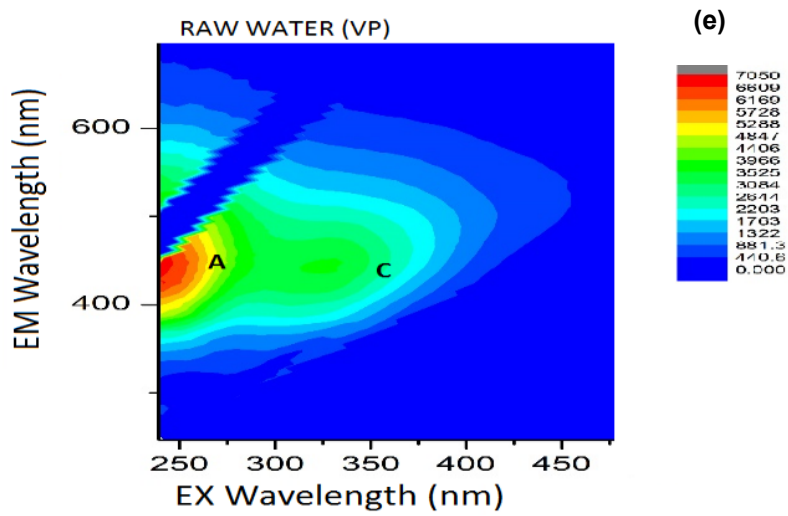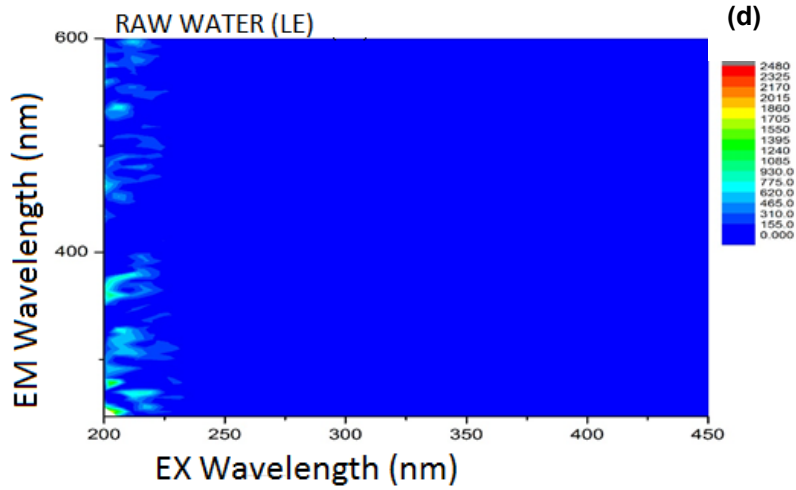
Figure 4-7 FEEM spectra of the RV (a), MV (b), LO (c), LE (d), VP (e), HL (f) raw water
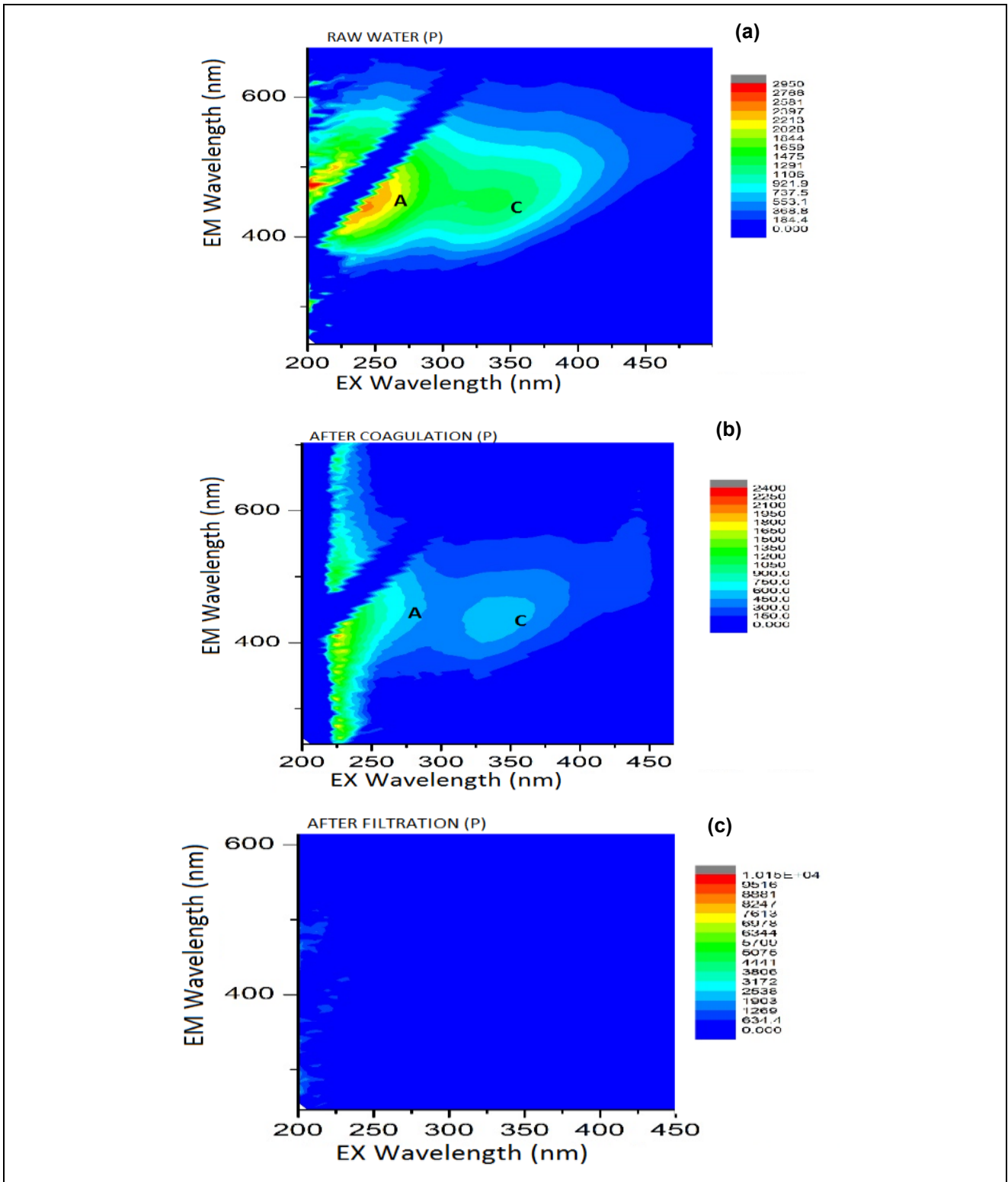
Figure 4-8 FEEM spectra of the (a) raw water sample of the P treatment plant prior to treatment; (b) water sample of the P treatment plant after coagulation; and (c) water sample of the P treatment plant after filtration

4.4 EFFECT OF SEASONAL VARIATIONS ON NOM TREATABILITY

The effect of seasonal variations on the treatability of the NOM of the RV treatment plant was studied (**Figure 4-9**). RV treatment plant was selected based on the fact that the sampling rounds performed for this plant covered all the seasons, while other plants show two to three seasons (interchangeably) only. The seasonal variation with regard to UV_{254}, which defines the aromatic character of NOM, was autumn>winter>spring>summer, whereas for DOC it was autumn>summer>winter>spring. These results show that highest levels of aromatic content of NOM (as evidenced by UV_{254} measurements) and DOC were found during the autumn (R2) season.

NOM is derived both from internal (autochthonous) and external (allochthonous) sources. During windy and rainy seasons, allochthonous NOM becomes dominant. The source of allochthonous NOM is mainly plant and animal remains that often find their way into the water resources (Wershaw *et al*., 2005). Thus, the observed high levels of DOC and UV_{254} in autumn can be attributed to the leaves from the trees that become deposited into the water sources. Leaves consist of aromatic components, which are the main contributor of the enhanced aromatic (UV_{254}) readings of NOM in water. Additionally, literature shows that increased levels of DOC over a period of years most likely result from the addition of hydrophobic NOM fractions into the water sources (Sharp *et al*., 2006).

Observed high levels of DOC during the summer compared to spring and winter could be due to issues of high run-offs, which tend to introduce various forms of pollutants (plants and animal remains) into the raw water sources. The observed trend could also be due to microbial effect, as microbes are usually more active during the warm summer months and autumn season (drier times). Microbes facilitate the release of DOC from the soil, which then finds its way to the raw water sources when there is enough rainfall (Sharp *et al*., 2006). The activity of some microbes towards the degradation of NOM is also temperature dependent (Ritson *et al*., 2014). Uyak *et al.,* (2008) observed that there were high levels of DOC in spring and autumn due to issues of run-offs and precipitations, which release various forms of NOM from the soil's upper layer into the water sources (Uyak *et al.*, 2008). The main point, which was confirmed in this study, is that the chemical character of NOM is highly influenced by changes in climatic conditions.
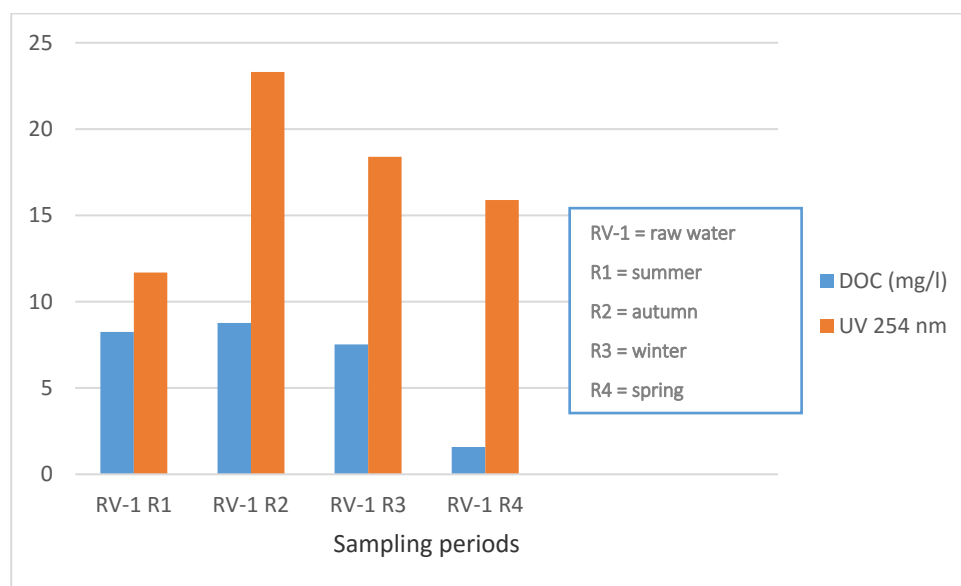
Figure 4-9 Effect of seasonal variation on UV_{254} and DOC for RV treatment plant.

The results in **Figure 4-10** show that high SUVA was observed in spring and autumn for the RV treatment plant; low SUVA values (NB: SUVA < 2 indicates presence of hydrophilic material) were experienced during

summer. Since DOC is inversely proportional to SUVA, the high spring SUVA levels are attributable to low DOC levels. The high autumn SUVA levels (NB: SUVA between 2 and 4 indicates presence of transphilic organic material) could be due to the aromatic fractions that are found in leaves, which find their way into water resources thus increasing the hydrophobicity of the NOM. Teixeira and Nunes (2016) observed that the hydrophobicity of NOM was high in summer and spring, which are hot seasons, compared to winter and autumn which are cold seasons. Summer and spring were also shown to have high UV_{254} (aromatic content of NOM) (Teixeira and Nunes, 2016).
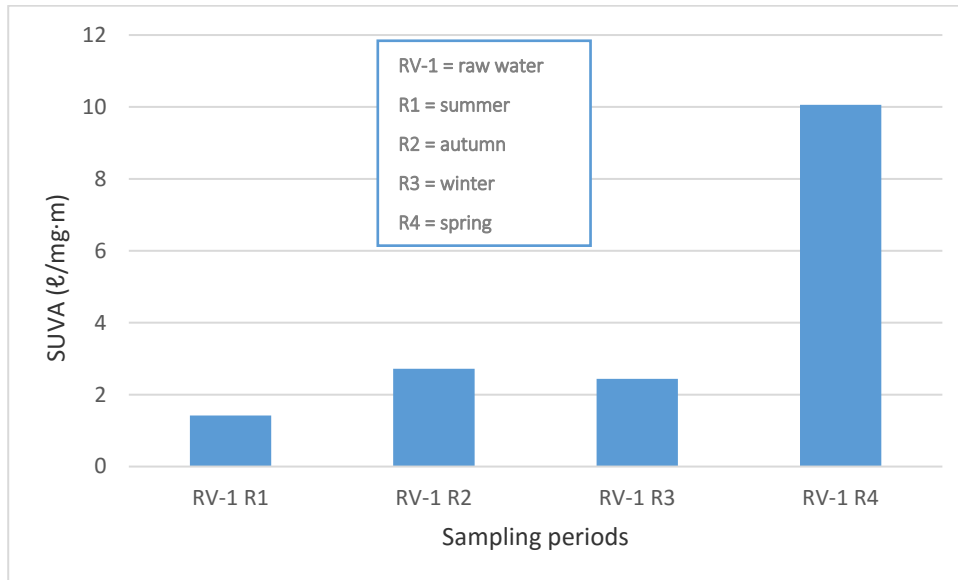
Figure 4-10 SUVA measurements for the RV treatment plant

It was expected that the raw water with the high UV_{254} and SUVA will experience a high removal of aromatic content of NOM (Teixeira and Nunes, 2016). This is due to the fact that the highly aromatic hydrophobic fractions (which are determined by UV_{254}) are more amenable to their removal using the coagulation process (Matilainen *et al.,* 2010; Ritson *et al.,* 2014). The results obtained in this study however, do not seem to indicate any direct correlation between the high UV_{254} and SUVA levels and high DOC removal rates (**Figure 4-11**).
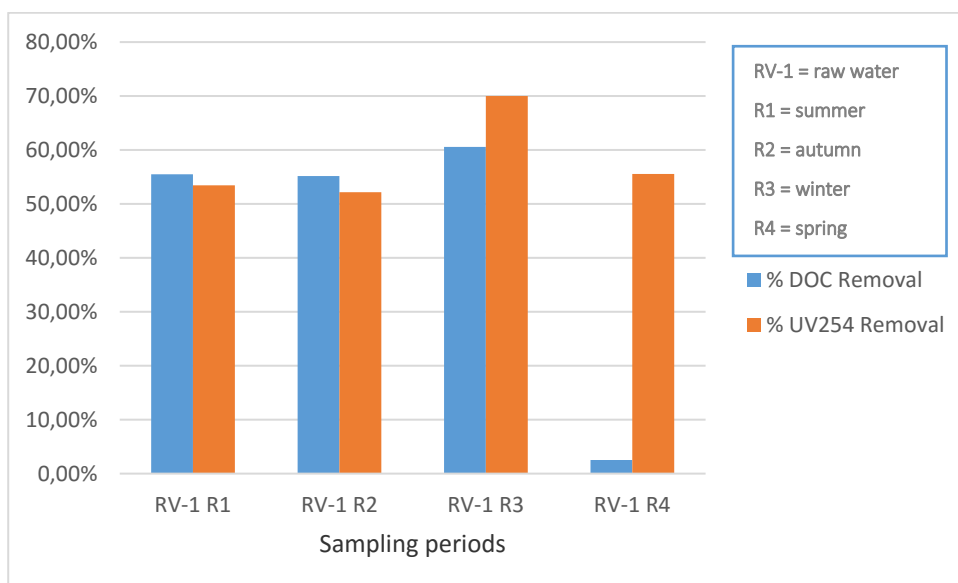
Figure 4-11 Percentage UV_{254} and DOC removal for the RV treatment plant

4.5 CONCLUSION

For every sampling round, the pH, turbidity and conductivity measurements were different across the different treatment plants, thus proving the variation in the water quality at these plants. We were able to demonstrate, using the DOC, UV-Vis and SUVA results, both the quantitative and qualitative variation of the NOM quantities across the different seasons and locations of the treatment plants. As expected, conventional methods (DOC, UV analysis, SUVA, turbidity, conductivity and pH) that were employed for the characterisation of NOM did not give enough information about the chemical character or composition of the NOM but are instead limited to providing information about the quantity (DOC) and the quality (SUVA) of NOM in the water. However, in order to effectively remove NOM from water, its composition needs to be well understood. Therefore, advanced characterisation methods (such as FEEM), which provide such information are required. To this end, the FEEM results have shown that NOM samples with high humic substances (e.g. in HL, P and VP treatment plants) were effectively treated, as they showed high UV_{254} (aromatic character of NOM) removal percentages. FEEM also provided information regarding the treatability of NOM throughout the water treatment train.

Effective characterisation of NOM in water can lead towards the improvement of its removal efficiency. The observed differences in the treatability of NOM can be due to the fact that the character and the amount of NOM in various regions is not the same and this can affect its removal efficiency in water. Moreover, due to the fact that various treatment plants use various treatment processes it is expected that the removal efficiencies of pollutants in water could be different. Conversely, even though some treatment plants may have similar treatment steps, the chemical dose used by each treatment plant might not be the same. All these factors play a role on the removal efficiency of NOM in water.

Lastly, the effect of seasonal variations on NOM quantity, quality and treatability was studied. It was shown that the DOC and UV_{254} were high in autumn compared to other seasons. This was due the aromatic nature of the soluble compounds found in leaves, which end up deposited into water sources. It was also concluded that there was no correlation between UV_{254}, DOC and SUVA to % DOC and UV_{254} (aromatic content of NOM) removal in water.

CHAPTER 5: SEASONAL NOM QUANTITY AND QUALITY: THE INFLUENCE OF NOM CHARACTER ON DBP FORMATION

5.1 INTRODUCTION

The quantity and quality of NOM in South African water sources in the different regions is not uniform and differs from source to source, implying that there is no single NOM identifying/ removal technique that can be prescribed for all water sources. NOM quality refers to the total composition of the organic matter and NOM quantity to the amount of organic matter, as measured by dissolved organic carbon (DOC). Seasonal variation in NOM quantity and quality is also questionable, as studies have shown (Goslan, 2003; Sharp *et al*., 2006). Once the character of NOM is defined, various NOM removal methods can be considered to treat specific source water. Both conventional (such as specific UV-absorbance, UV-Vis (at 254 nm), DOC, and advanced characterisation methods such as fluorescence excitation-emission matrices (FEEM), polarity rapid assessment method (PRAM), pyrolysis gas chromatography-mass spectrometry, biodegradable dissolved organic carbon (BDOC) techniques have been previously employed for NOM characterisation in water (Matilainen *et al.,* 2011; Nkambule *et al*., 2012). Conventional methods do not give sufficient information about the character (composition) of NOM in water as they only inform the researcher about the quantity (DOC) or the hydrophobicity of NOM. Advanced characterisation methods, on the other hand, provide more qualitative information about the character of NOM which then leads to a more advanced understanding of how the organic matter will possibly react during the water treatment process (NOM treatability). Not only is the variable NOM character throughout source waters a concern in terms of quantification, but the differing NOM composition also affects water sources that are more prone to form a specific DBP during the oxidation step of drinking water treatment.

5.2 POLARITY, SIZE AND FLUORESCENCE AS PARAMETER FOR NOM QUANTITY AND QUALITY

Identifying the composition of NOM during water treatment for potable use is essential as it depicts the type of NOM that is dealt with and provides insight with regards to the treatability of the organic matter. The difficulty when studying NOM is that organic matter is a mixture of organic compounds of divergent size, irregular structure and functionality (Hertkorn, 2006), keeping in mind that the character of NOM greatly influences its removal (Nkambule *et al*., 2012). The objective of this chapter is therefore to identify the combination of NOM characterisation techniques to use in order to successfully determine NOM quantity and quality. The characterisation of NOM will also provide knowledge on the influence that NOM character has on the formation of DBPs (specifically THMs). The focus of this study was on trihalomethanes (THMs) due to THMs being currently the only DBP regulated by SANS: 241. In addition, THMs are mainly formed during chlorination, occurring in high concentration levels in the final treated water (Kristiana *et al*., 2011; Knight *et al*., 2011). This research is essential for providing a protocol to determine the quality and quantity of NOM by studying the polarity, size and structure of the organic matter within a water source both before and after treatment.

5.2.1 Bulk raw water characteristics

The selected water treatment plant for this section is the bulk water service provider Rand Water treatment plant, which abstracts water from the Vaal Dam and supplies on average 4000 Mℓ/d to various provinces (mainly Gauteng). The sampling sites for this section were located at the intake of the water treatment plant and throughout the water treatment steps as previously described in Section 3.1. To monitor seasonal variation

within the source water, sampling was scheduled for the months of June–August (winter), September–November (spring), December–February (summer) and March–May (autumn). Fortnightly sampling was carried out at the Rand Water treatment plants during these months and during the period 2014–2016. Bulk raw water parameters that were determined included temperature, pH, conductivity, colour, alkalinity and turbidity and analysis of these were conducted after transportation to the laboratory. NOM characterisation analyses are described in the sections hereafter.

The average seasonal surface water characteristics of the Vaal Dam between January 2014 and July 2016 are displayed in **Table 5-1**. Water from the Vaal Dam (Rand Water's intake source) typically has a medium colour (31 CU – 117 CU), high turbidity (29 NTU – 80 NTU), high pH (7.7 – 8.7) and a conductivity between 16 mS/m and 25 mS/m.

Table 5-1 Rand Water source water characteristics from January 2014 – July 2016

Sampling	Parameters								
	Turb. NTU	Colour CU	Cond. mS/m	pH	Alk. mg/ℓ CaCO$_3$	Temp. °C	DOC mg/ℓ	UV$_{254}$ m^{-1}	SUVA ℓ/mg.m
March – May autumn, n=18	48.9	61.5	17.5	7.30	62.3	20.6	4.60	17.7	3.70
Jun – Aug winter, n=18	48.1	68.0	19.5	8.20	71.3	21.5	4.80	17.2	3.80
Sept – Nov spring, n=12	55.7	73.3	18.1	8.10	66.0	24.9	4.70	22.5	4.70
Dec – Feb summer, n=18	48.4	52.9	18.9	8.20	68.5	25.9	4.80	14.7	3.60

5.2.2 DOC, UV$_{254}$, SUVA

The seasonal average of DOC in the Vaal Dam (source water to Zuikerbosch and Vereeniging water treatment plants) ranged between 4.6 and 4.8 mg/ℓ (**Table 5-1**). A decrease in the UV$_{254}$ was observed (decreased from 17.2 ℓ/mg.m in the winter to 14.7 ℓ/mg.m in the summer). The SUVA value of a water sample can be used to indicate whether the composition of NOM in a water sample is mainly humic matter, non-humic matter or a mixture of the two (Edzwald and Tobiason, 2010). The source water from the Vaal Dam was found to have a median SUVA value of 3.4 ℓ/mg.m during the study period and was the lowest during summer (averaged 3.6 ℓ/mg.m). A SUVA value within the range 2 - 4 ℓ/mg.m similar to the one observed at the Vaal Dam surface water is an indication that the source water is a mixture of humic and non-humic matter, and it contains NOM of low and high molecular weights and has both a HPO and HPI character (Edzwald and Tobiason, 2010). Not only is SUVA an indication of the amount of humic substances within a sample but it can also be used to predict NOM removal by the coagulation process (Parsons *et al.,* 2004; Edzwald and Tobiason, 2010). SUVA is a measure of the aromaticity of NOM in a sample and low SUVA values are indicative of NOM having low aromaticity and HPO (Kitis *et al*., 2002). This therefore poses a challenge with respect to the removal of NOM by the treatment process (Matilainen *et al*., 2005). Values observed in **Figure 5-1**, indicate increased UV$_{254}$ removal percentages at higher SUVA values. Source water having larger UV$_{254}$ absorbing properties and being more aromatic in nature also appears to be more easily treated, resulting in increased NOM removal as indicated by higher UV$_{254}$ removal percentages (**Figure 5-1**). **Table 5-2** gives details of the sample codes and their descriptions sampled at the Rand Water plants during November 2015.

Table 5-2 Description of sampling codes from the Rand Water treatment plants

Water treatment plant	Code description	Sampling Code
Rand Water - Zuikerbosch plant	Raw water	ZB-1
	After coagulation/flocculation	ZB-2
	After sedimentation	ZB-3
	After carbonation	ZB-4
	After filtration	ZB-5
	After primary disinfection	ZB-6
Rand Water- Vereeniging plant	Raw water	VG-1
	Raw water	VG-2
	After sedimentation	VG-3
	After filtration	VG-4
	After primary disinfection	VG-5

Tables 5-3 and **5-4** show low UV_{254} absorbance values for the raw water for ZB and VG during the various treatment steps; this indicates successful NOM removal by the coagulation process. Not only is the aromatic character of NOM lower, the UV_{272} values, which are known as a predictor for trihalomethane formation, also decreased after the coagulation process.

Table 5-3 UV values at different wavelengths for Zuikerbosch water treatment plant (in m^{-1}) sampled during November 2015

Sample Codes	UV Absorbance			
	214	254	272	300
ZB1	55.91	43.30	42.35	47.19
ZB2	36.03	32.69	22.73	26.08
ZB3	16.04	3.43	2.47	3.46
ZB4	17.61	5.00	4.05	4.92
ZB5	18.49	5.88	4.93	3.38
ZB6	16.47	3.86	2.91	2.51

Table 5-4 UV values at different wavelengths for Vereeniging water treatment plant (in m^{-1}) sampled during November 2015

Sample Codes	UV Absorbance			
	214	254	272	300
VG-1	55.19	42.57	41.62	46.49
VG-2	59.92	47.31	46.35	49.71
VG-3	17.34	4.73	3.78	3.77
VG-4	20.33	7.72	6.76	6.59

| VG-5 | 15.72 | 3.11 | 2.16 | 2.37 |

Figures 5-1 and **5-2** also indicate high absorbance values of the raw water and that the absorbance tended to decrease after the coagulation step. The UV scan indicated the wavelengths between 250 to 280 nm as being the most suitable for the measurements of NOM activity, as previously documented by Nkambule *et al*., (2012b).
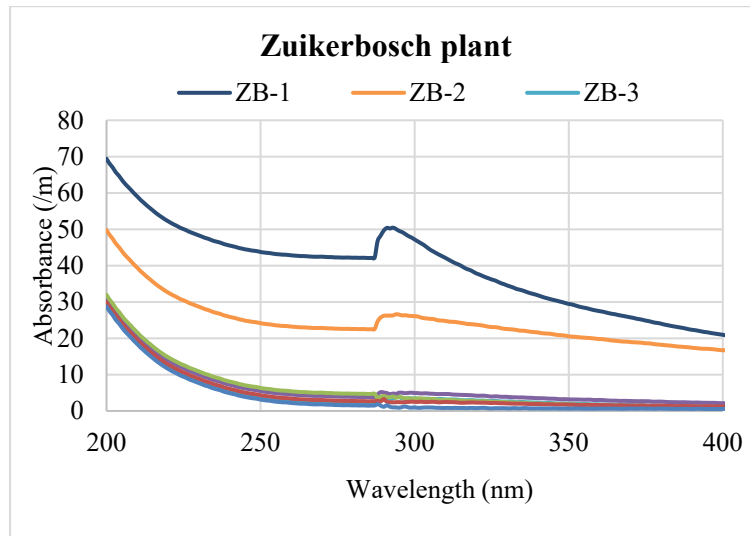
Figure 5-1 UV scan for Zuikerbosch plant
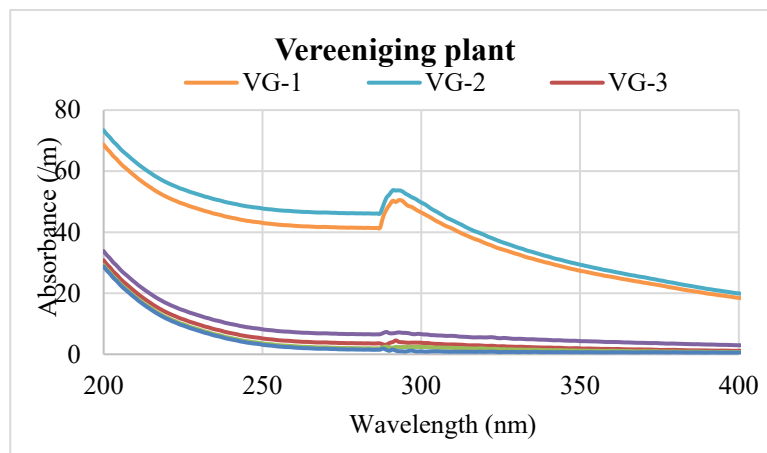
Figure 5-2 UV scan for Vereeniging plant

High SUVA values imply that the NOM is dominated by humic substances and high DOC removal efficiency can simply be carried out by coagulation (Edzwald and Tobiason, 2010). This notion is supported by the data shown in **Figure 5-3**.The data indicated positive (but not so strong) correlations between raw water UV_{254} and UV_{254} removal as well as between raw water SUVA and UV_{254} removal ($R^2 = 0.7176$, $p < 0.05$). It can therefore be predicted that high SUVA values in the raw water will result in high UV_{254} removal, something that was observed in other water treatment plants (White *et al.,* 1997; Parsons *et al*., 2004). High UV_{254} values are indicative of NOM that is more aromatic and more HPO in nature (Kitis *et al.,* 2002). This was confirmed in White *et al*. (1997) where HPO NOM was found to have high SUVA values, indicated by a positive correlation ($R^2 = 0.72$) between SUVA and HPO NOM. The prediction that NOM (UV_{254}) removal will increase when high UV_{254} levels are observed in the raw water, indicates that the coagulation process shows preference for removal of the HPO NOM fractions compared to the HPI fractions.
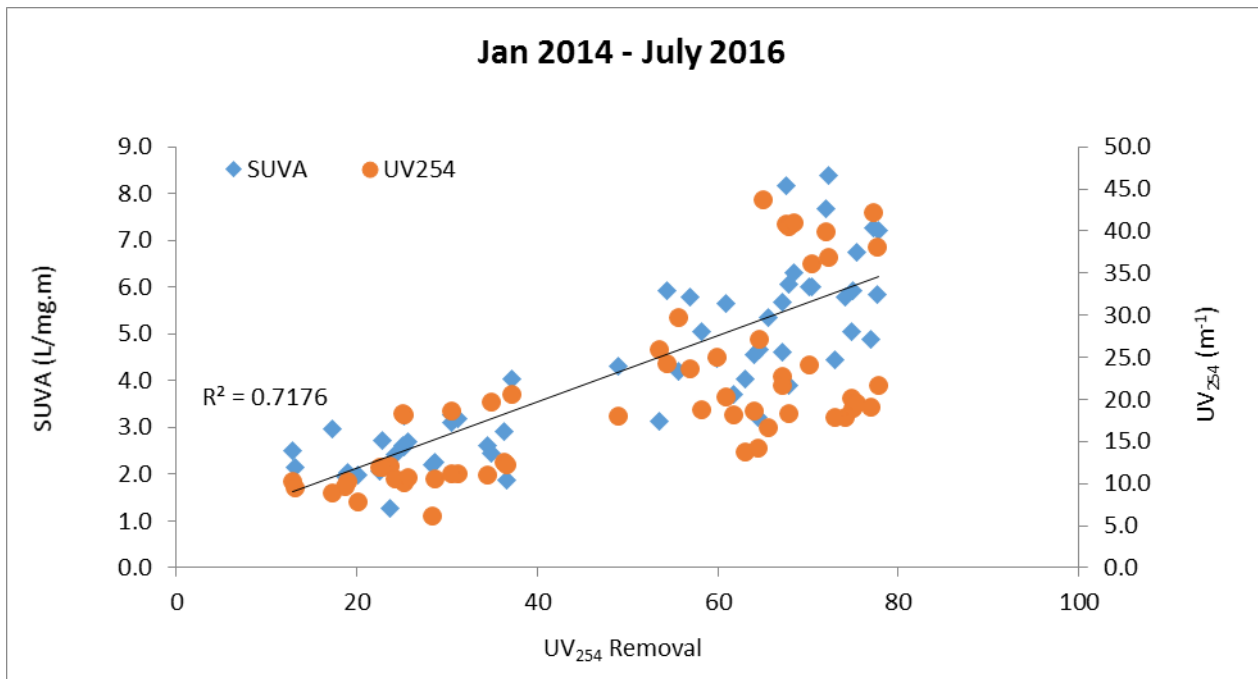
Figure 5-3 Correlation between SUVA and UV$_{254}$ percentage removal

5.2.3 Polarity - mPRAM

NOM was fractionated in the source water and water sampled after coagulation/flocculation and sand filtration to monitor the change in polarity during treatment. This technique splits the NOM in three fractions based on polarity into a HPO, HPI and TPI fraction. The modified PRAM technique allowed NOM removal, measured by the C18, CN and NH2 sorbents, representing NOM removal of the HPO, HPI and TPI fractions after full-scale treatment at the Rand Water plant. The fractionation performed on the Vaal Dam source water resulted in an equal distribution of the HPO and HPI as indicated in **Figure 5-4**. At the Rand Water treatment plants typical removal of the HPO fraction was observed after settling and sand filtration processes (**Figure 5-5**).
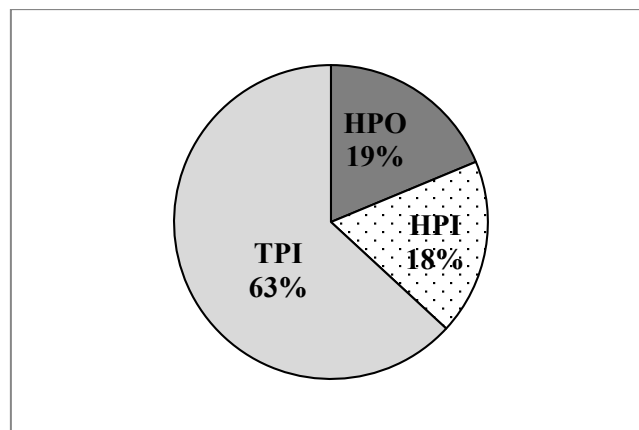
Figure 5-4 Average distribution of the fractions in the raw water using the modified PRAM
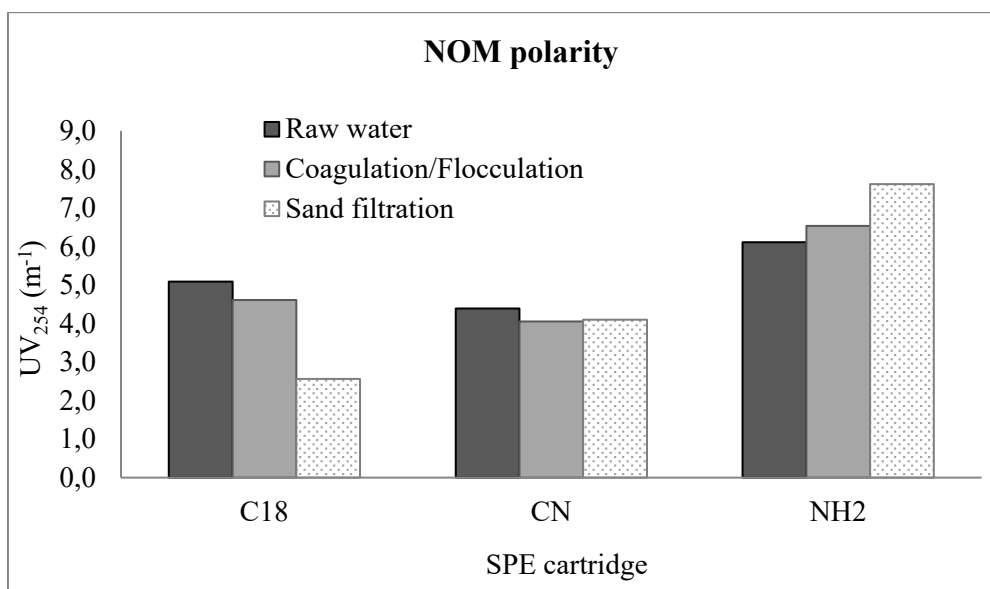
Figure 5-5 NOM removal measured by modified PRAM technique

5.2.4   Size - HPSEC

NOM characterisation by HPSEC is based on the differential separation of molecules of different molecular sizes flowing through a porous matrix. During this separation technique, molecules that are larger than the gel pores are eluted first due to rapid movement through the column, while smaller molecules penetrate through the gel pores (Pelekani *et al*., 1999; Nissinen *et al*., 2001). HPSEC analyses have been used extensively to determine the removal efficiency of NOM by water treatment plant specifically after the various treatment steps when comparing the MSD before and after treatment (Nissinen *et al*., 2001; Matilainen *et al*., 2002). Generally, five NOM fractions (five peaks) were eluted by HPSEC, with   peaks I – II being the high molecular weight fraction and peaks III – IV being the intermediate molecular weight fraction. Peaks V and VI represent the low molecular weight fraction (Vuorio *et al*., 1998, Nissinen *et al*., 2001).

Figure 5-6 is a typical example of the chromatographs produced by HPSEC, which represents the molecular weight fractions eluted in each sample. The peak height of each fraction was measured in milli-absorbance units (mAU) and retention time ranged between 0 and 20 minutes. On average the HMW fraction accounted for up to 51% of the total NOM fractions. However, during the period July 2014 to February 2015 the HMW fraction on average constituted 35% of the total NOM (**Figure 5-7**).
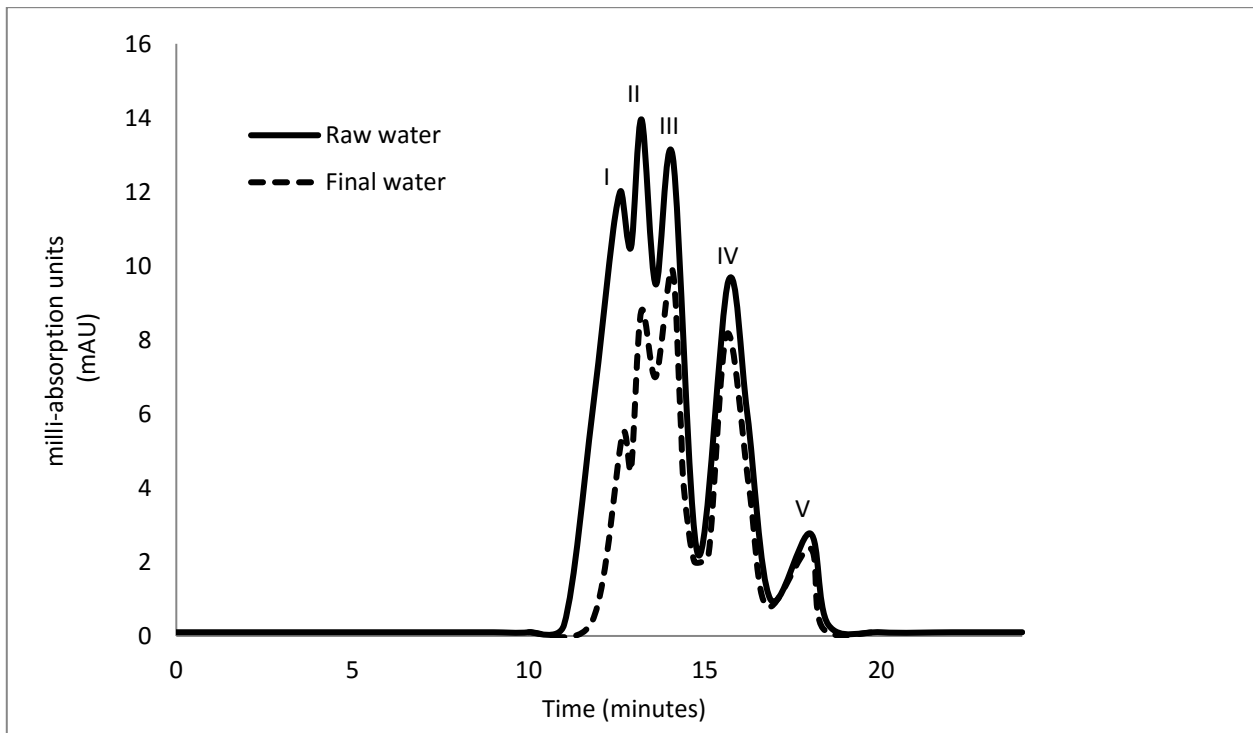
Figure 5-6 Typical HPSEC chromatograph of humic fractions of the raw and final water, indicating change in molecular size after treatment
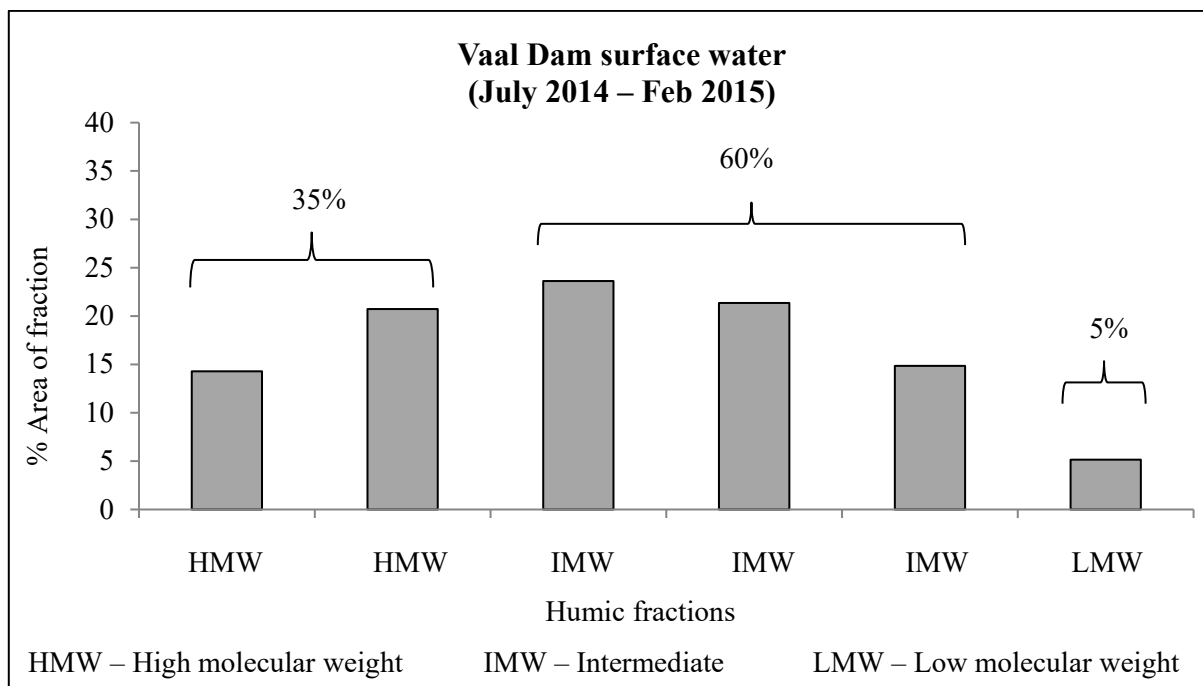
Figure 5-7 Percentage area of each humic fraction in the raw water

5.3 NOM SEASONAL VARIABILITY AND NOM TREATABILITY

Figures 5-8 to **5-12** indicate the seasonal variability of NOM within the Vaal Dam source water. **Figure 5-8** indicates that the distribution of the molecular sizes of NOM differed slightly during the various seasons. A decrease in the humic fractions was observed during summer season when high temperatures and rainfall

occurred. This suggests that the total organic content decreased in summer during this specific year, as evidenced by a decrease in the DOC values from winter 2014 to summer 2015 (**Figure 5-9).** It should also be noted that the removal of the LMW fraction (peaks V and VI) proved to be more difficult during the summer period (**Figure 5-8**). In general, the seasons that had high raw water SUVA values showed high NOM removal percentages in the full-scale treatment plant (**Figures 5-10, 5-11** and **5-12**). However, high raw water SUVA values did not always lead to the prediction of low TTHM formation as the SUVA values only indicates the ease of NOM removal due to the higher aromatic character and the more hydrophobic nature of NOM as seen in autumn (**Figure 5-9)** and summer 2014 (**Figure 5-11**). On average the TTHM formation peaked during the summer season when the raw water had lower UV_{254} absorbance values (**Figure 5-10)**. High SUVA values which were accompanied high NOM removal (reduction in UV_{254} percentage) were observed during spring (**Figure 5-10)**. As soon as the rain period started in early summer the SUVA value of the raw water decreased, and aromaticity (UV absorbance) decreased, resulting in reduced NOM removal when comparing summer to autumn and winter (**Figure 5-10)**.

Seasonal variation in NOM composition in the raw water source is not surprising as this was observed in other studies (Goslan, 2003; Sharp *et al.,* 2006). NOM quantity and TTHM formation vary seasonally but are not exactly the same each spring or each summer; they are therefore difficult to foresee due to rainfall that most probably influences the total NOM composition. Therefore, more information regarding the quality or composition of NOM within the source water is required when monitoring NOM, especially how the character of NOM influences the TTHM formation.
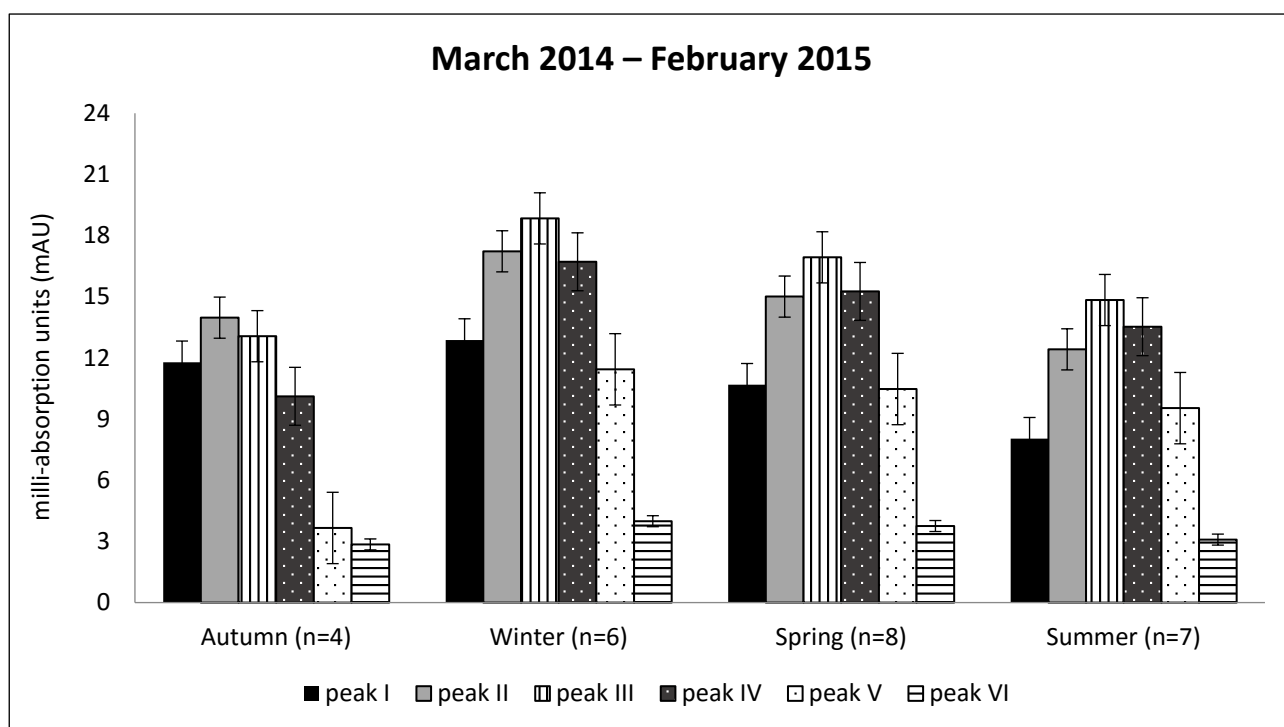
Figure 5-8 Seasonal humic fractions in the Vaal Dam raw water from March 2014 to February 2016
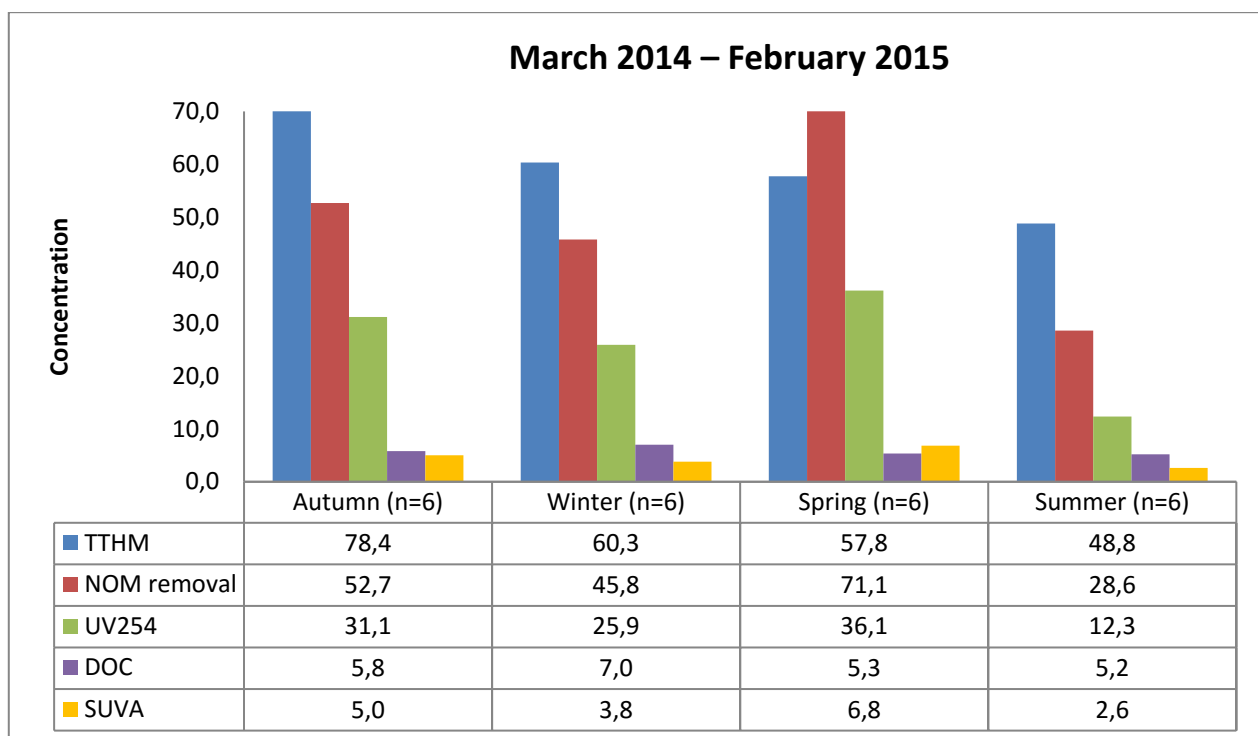
Figure 5-9 Organic content in the source water, NOM removal and TTHM formation in the final water during March 2014 – February 2015

	Autumn (n=6)	Winter (n=6)	Spring (n=6)	Summer (n=6)
TTHM	78,4	60,3	57,8	48,8
NOM removal	52,7	45,8	71,1	28,6
UV254	31,1	25,9	36,1	12,3
DOC	5,8	7,0	5,3	5,2
SUVA	5,0	3,8	6,8	2,6
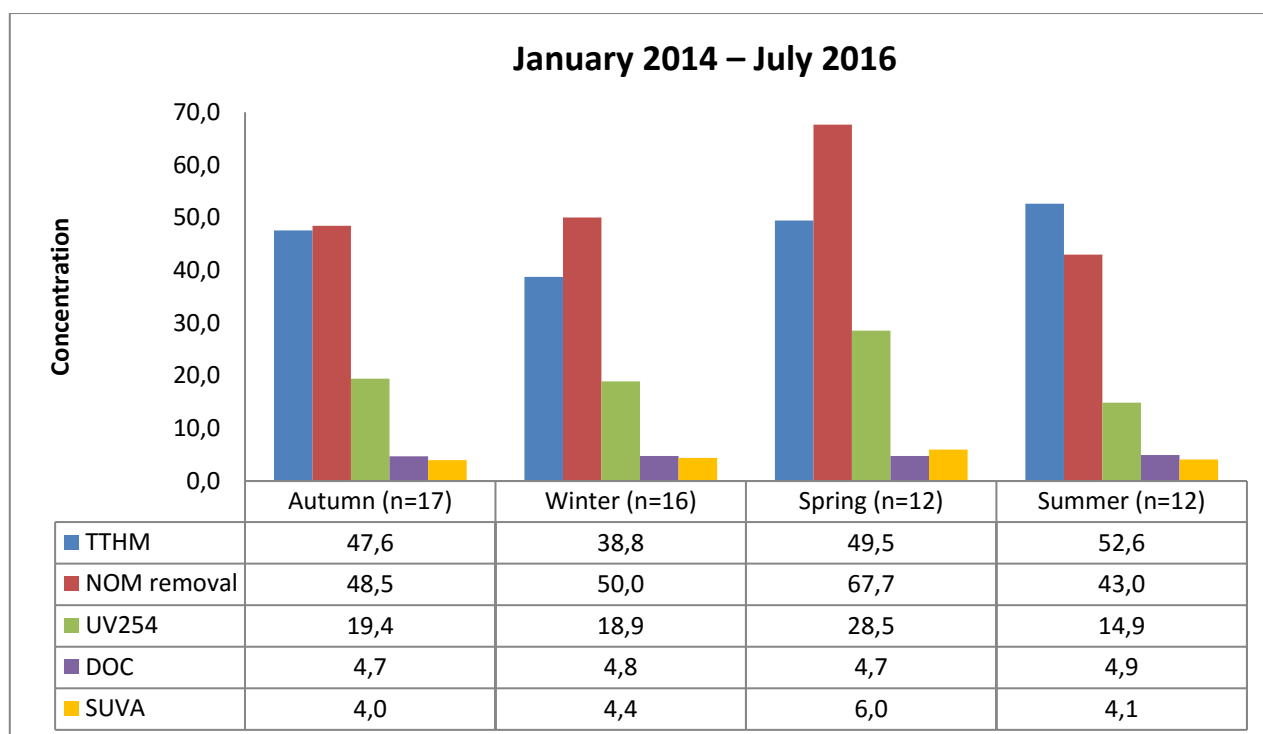
Figure 5-10 Average seasonal variability in the source water, NOM removal and TTHM formation in the final water

	Autumn (n=17)	Winter (n=16)	Spring (n=12)	Summer (n=12)
TTHM	47,6	38,8	49,5	52,6
NOM removal	48,5	50,0	67,7	43,0
UV254	19,4	18,9	28,5	14,9
DOC	4,7	4,8	4,7	4,9
SUVA	4,0	4,4	6,0	4,1
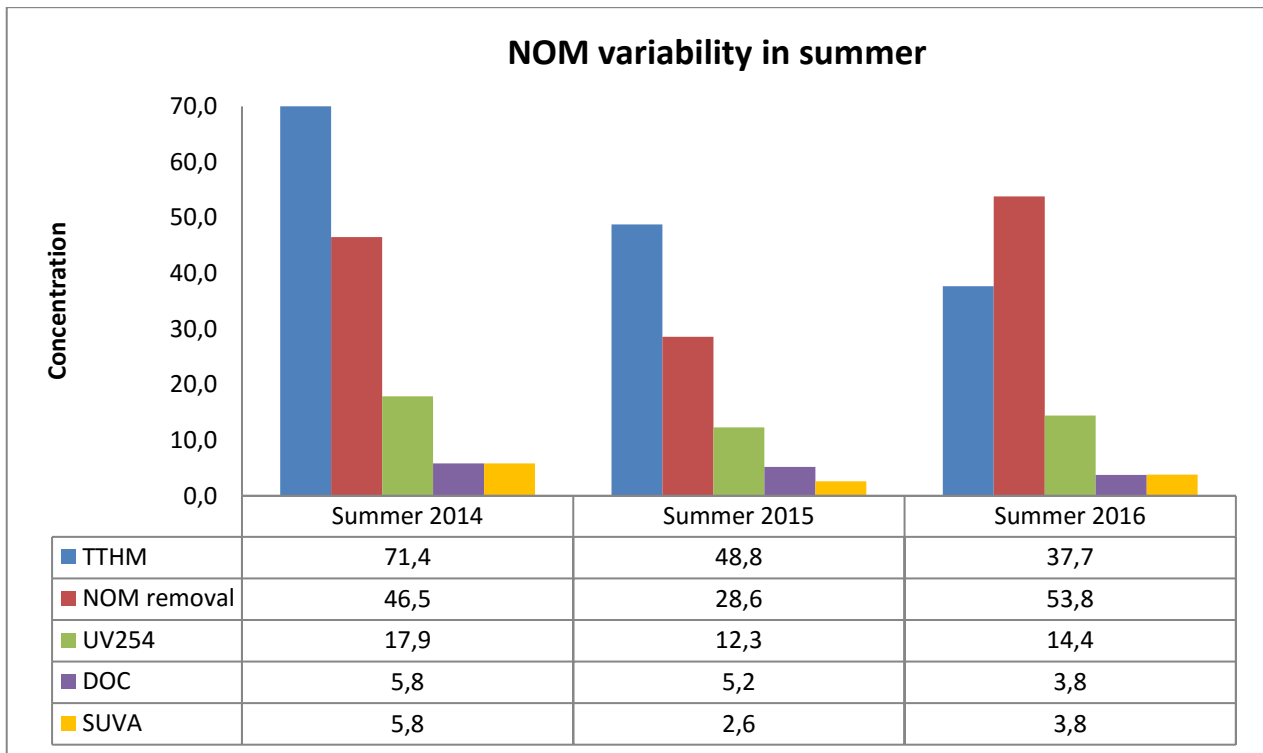
Figure 5-11 NOM variability in summer 2014 – 2016

	Summer 2014	Summer 2015	Summer 2016
TTHM	71,4	48,8	37,7
NOM removal	46,5	28,6	53,8
UV254	17,9	12,3	14,4
DOC	5,8	5,2	3,8
SUVA	5,8	2,6	3,8
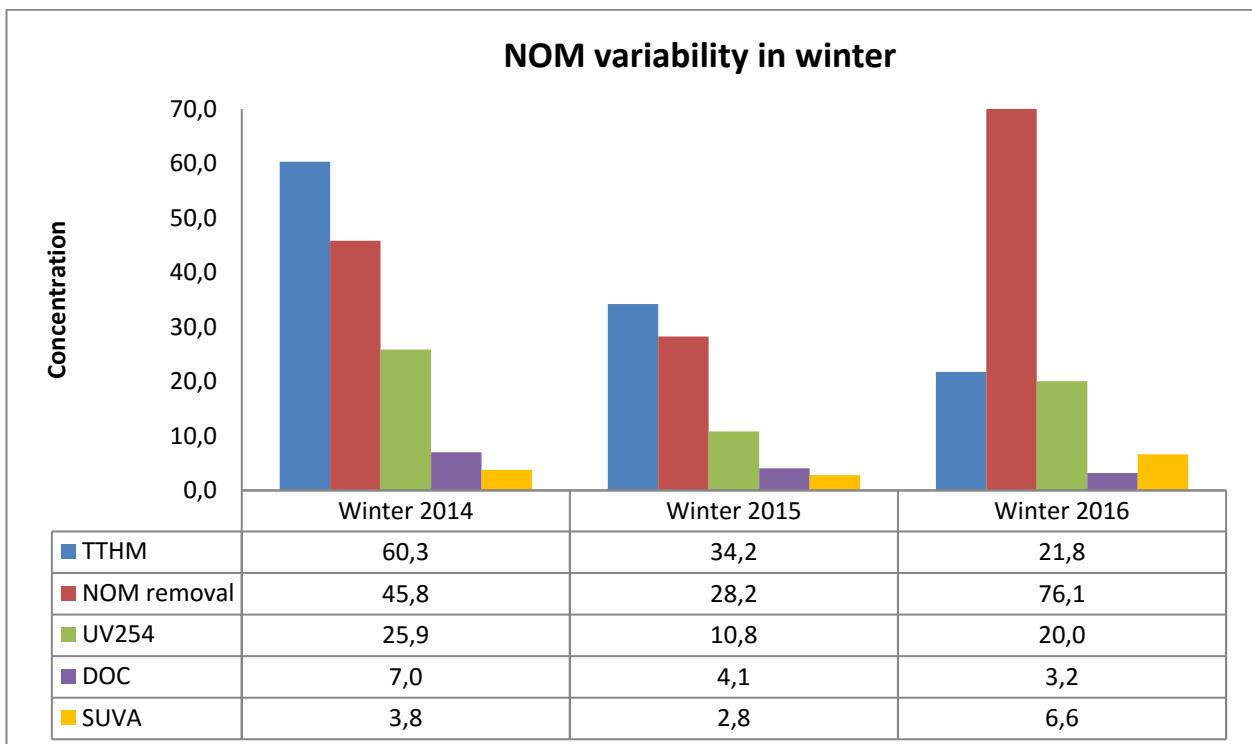
Figure 5-12 NOM variability in winter 2014 – 2016

	Winter 2014	Winter 2015	Winter 2016
TTHM	60,3	34,2	21,8
NOM removal	45,8	28,2	76,1
UV254	25,9	10,8	20,0
DOC	7,0	4,1	3,2
SUVA	3,8	2,8	6,6

During summer a strong positive correlation exists between SUVA and UV_{254} percentage removal, as indicated by R^2 = 0.9369 ($p < 0.05$) (**Figure 5-13**). This correlation between SUVA and UV_{254} percentage removal was stronger during summer (Dec.2014 – Feb.2015), indicating that higher SUVA values correlate to high rates of NOM removal. This was also observed in **Figure 5-10**, where NOM removal was higher during spring when the raw water had a high SUVA value. UV absorbance in the source water in both winter and summer months correlated well to UV_{254} removal by the full-scale plant. This indicates that the aromatic nature of the NOM in

the source water resulted in higher NOM removal after treatment (**Figure 5-13**). However, no significant relationship was observed between SUVA (or UV_{254}) and THMs. This indicates that UV absorbing fractions are not the only indicators of THMs in the final water. Therefore, this suggests that the use of SUVA and UV_{254} to predict formation of THMs requires further investigation. Other studies have documented similar findings where SUVA appeared to be a weak collective indicator for THMs (Fram *et al*., 1999; Weishaar *et al*., 2003). However, positive correlations between DOC and trihalomethane formation potential (THMFP) (Van Leeuwen *et al*., 2005) and also between SUVA and THMFP were observed (Gallard and Von Gunten, 2002; Parsons *et al*., 2004).
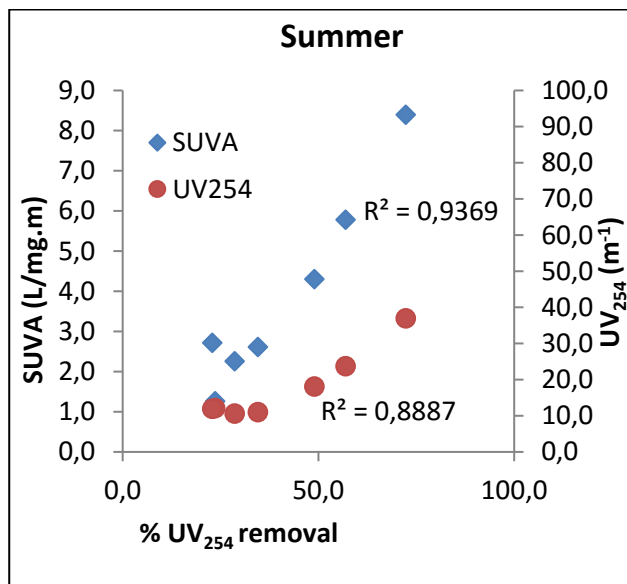
Figure 5-13 Correlations between raw water SUVA and UV_{254} against UV_{254} percentage removal by the full-scale plant in summer
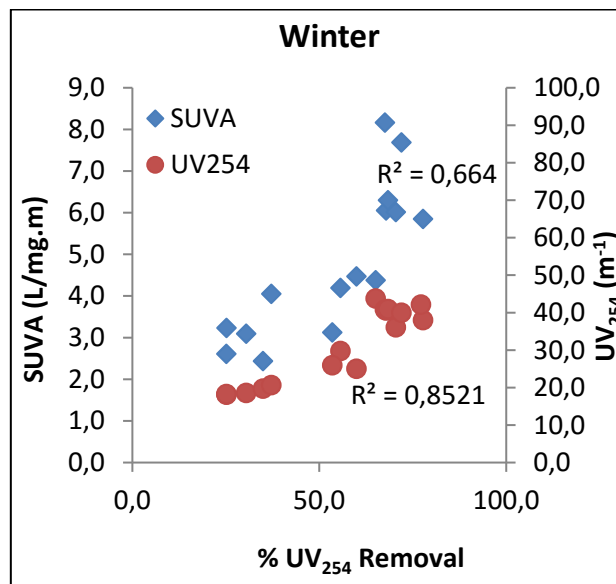
Figure 5-14 Correlations between raw water SUVA and UV_{254} against UV_{254} percentage removal by the full-scale plant in winter

These results concurred with other studies indicating that conventional water treatment removes mostly the HMW NOM and that the LMW are not easily removed (White *et al*., 1997; Matilainen *et al.,* 2005). It is known that the HMW fraction represents the humic and fulvic type compounds that leach from the soil and the LMW fraction represents the non-humic fractions (Szabó and Tuhkanen, 2007). Chowdhury (2013) demonstrated that HMW NOM strongly correlates to SUVA and UV_{254} (more aromatic compounds of NOM).

Figure 5-15 compares the removal of the NOM molecular sizes after sedimentation, filtration, primary and secondary disinfection by the Rand Water full-scale water treatment plants. These results showed that on average 45% of the HMW fraction was removed by the Rand Water treatment process; however, the low molecular weight (LMW) fraction (peak V) remained unchanged in the final water, indicating that this fraction was not removed by conventional water treatment (**Figure 5-15**). The change in MSD throughout the water treatment process is also clearly evident after the various treatment steps. A high reduction of the HMW NOM (peak I and II) and IMW (peak III) in the water after sedimentation was observed in this and other studies (Vuorio *et al.,* 1998; Matilainen *et al.* 2002). Additional removal of the fractions after filtration (rapid gravity sand filtration) was not observed, indicating that coagulation primarily removes the HMW NOM. After primary disinfection (chlorination) further removal of the HMW and IMW NOM is evident (**Figure 5-15**).
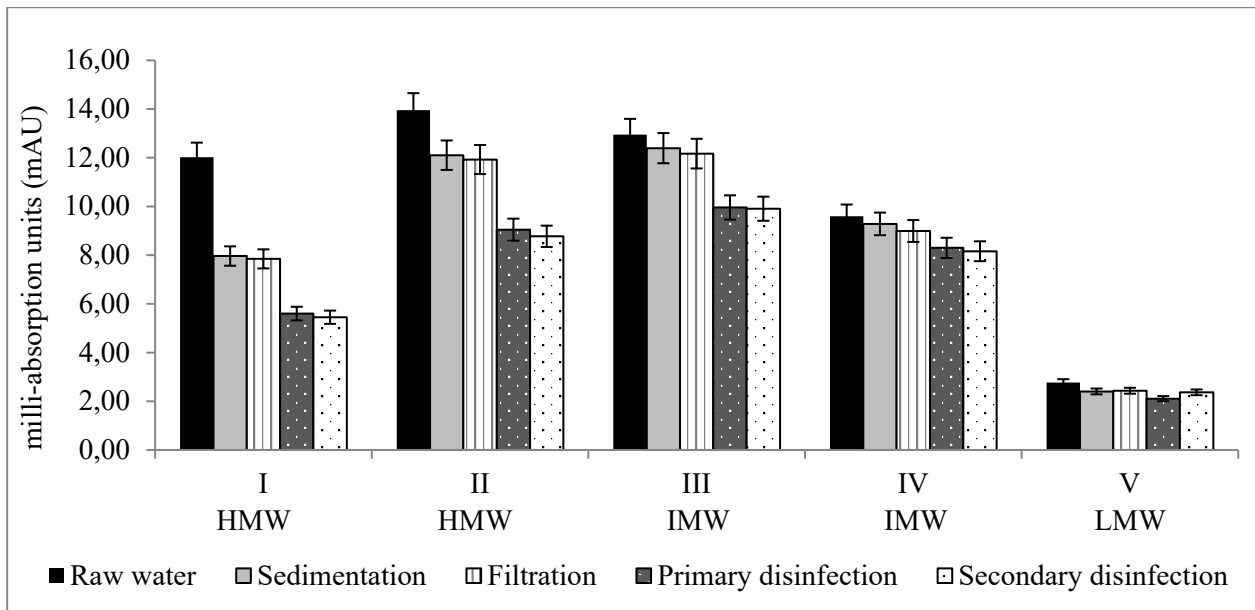
Figure 5-15 Molecular size distribution (MSD) of the humic fractions indicated by the average peak heights after the various treatment steps at Rand Water

5.4 INFLUENCE OF NOM CHARACTER ON TRIHALOMETHANE FORMATION

Not only can the transformation of the molecular size through the water treatment train be used to indicate NOM removal and efficiency of the treatment option adopted (Vuorio *et al*., 1998; Matilainen *et al*., 2002), it can also be utilised to determine the molecular weight fraction that is responsible for the DBP formed. MSD results (peaks I and II) displayed in **Figures 5-16** and **5-17** showed significant correlations between NOM of high molecular sizes (peaks I and II) and chloroform formation, as indicated by $R^2 = 0.9633$ (p < 0.05) and $R^2 = 0.9501$ (p < 0.05), respectively. Similar results were observed where HMW organic matter was associated with increased reaction of chloroform formation during chlorination (Chowdhury, 2013). During winter and spring, moderate correlations between HMW NOM (peaks I and II) and chloroform formation were observed, as indicated by regression coefficients of 0.5872 (p < 0.05) and 0.6930 (p < 0.05), respectively (**Figures 5-16** and **5-17**). A strong and positive correlation between NOM of larger molecular size was only evident during the summer. This indicates that during summer the formation of TTHM and more specifically chloroform was primarily due to HMW NOM (**Figures 5-16 to 5-19**). Various studies have shown that the HMW hydrophobic NOM fraction is a precursor to chloroform formation (Roe *et al.,* 2008, Lu *et al*., 2009, Yee *et al*., 2009).
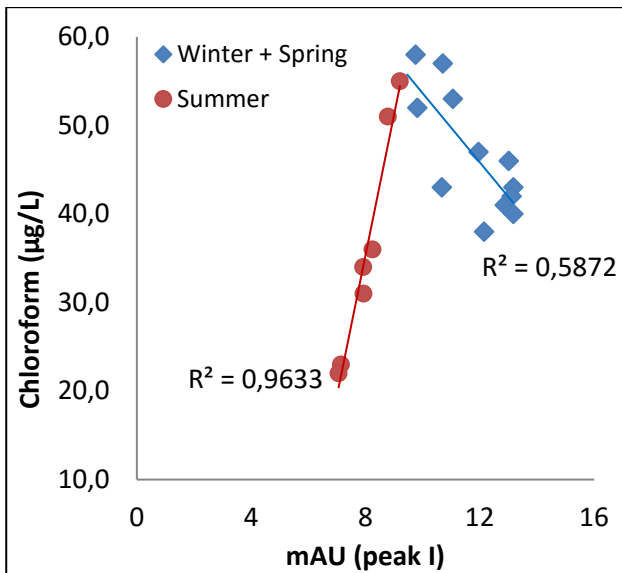
Figure 5-16 Seasonal correlation between peak I (HMW) and chloroform formation
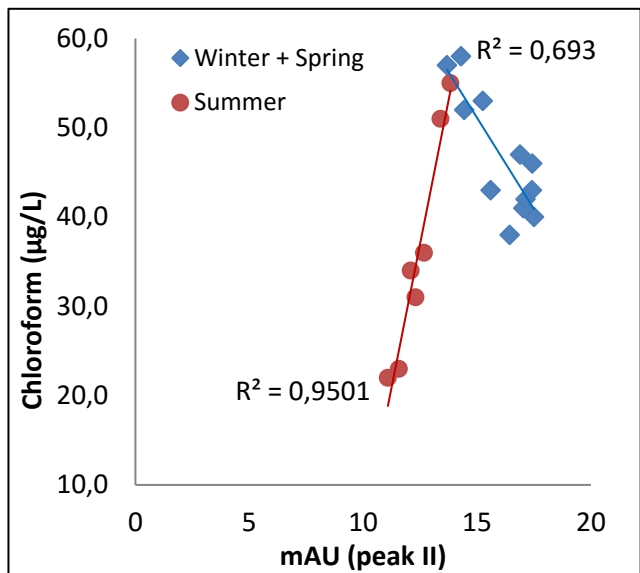
Figure 5-17 Seasonal correlation between peak II (HMW) and chloroform formation

Figure 5-18 indicates that during summer the formation of TTHM was primarily due to the HMW NOM fraction, and this is indicated by strong positive correlations with R^2 regression coefficients above 0.9427 ($p < 0.05$). During winter, the TTHM formed in the final treated water was not due to the presence of the HMW NOM fractions, and is indicated by a fairly low correlation coefficient value (**Figure 5-19**).
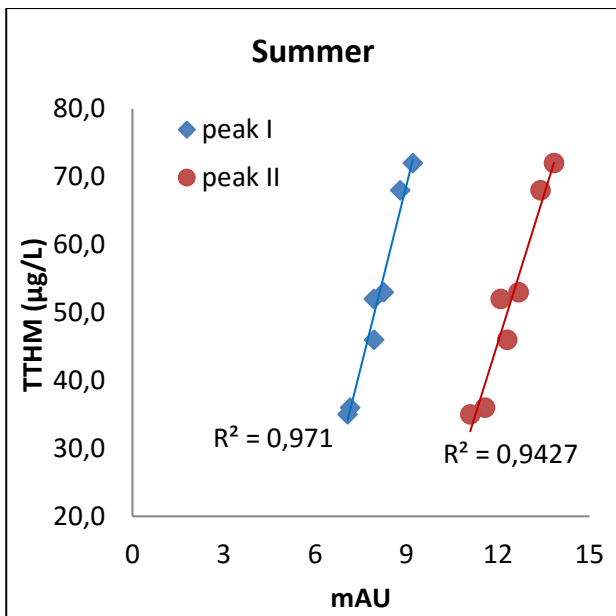
Figure 5-18 Positive correlation between HMW NOM and TTHM during summer
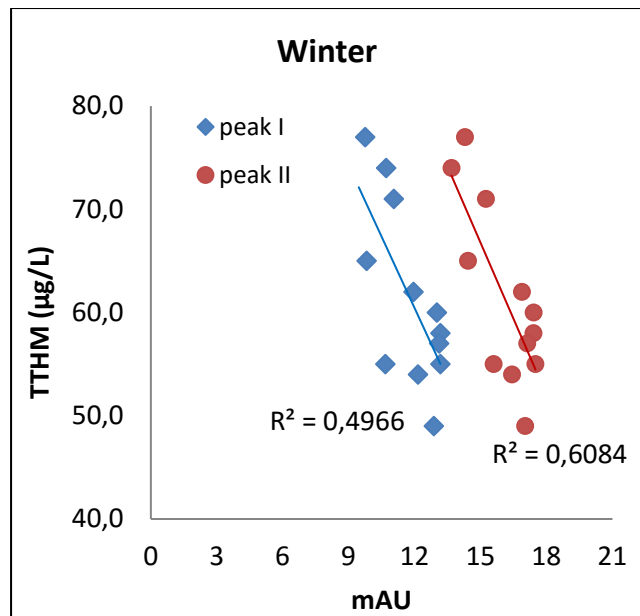
Figure 5-19 Moderate correlation between HMW NOM and TTHM during winter

Looking at **Figure 5-20**, it is evident that the LMW fraction (peak V) is poorly correlated to chloroform in summer and shows a moderate relationship towards chloroform in winter ($R^2 = 0.5887$, $p < 0.05$). A moderate correlation exists between the intermediate molecular weight (IMW) NOM (peak IV) and the DBP in winter (**Figure 5-21**), indicated by a $R^2 = 0.656$ ($p < 0.05$). Unlike LMW NOM, the bigger molecular size organics are positively associated with both UV_{254} and SUVA (Chowdhury, 2013). A study performed by Ozdemir *et al*. (2014) suggests that smaller molecular weight fractions are associated with low SUVA values (<2 ℓ/mg.m).
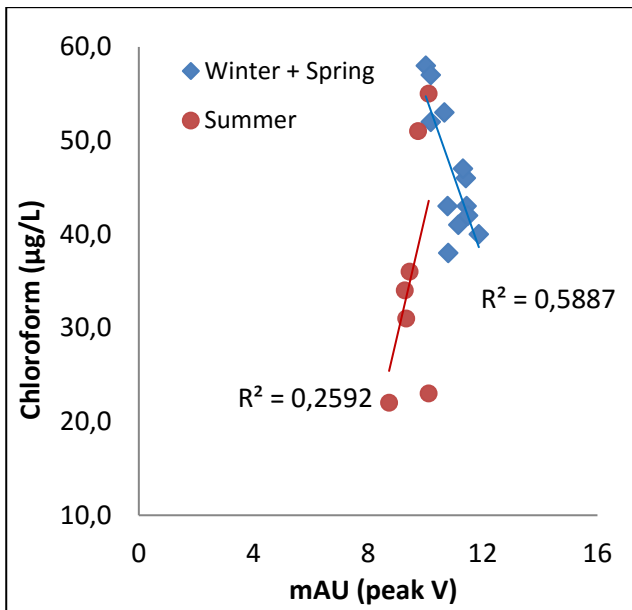
Figure 5-20 Seasonal correlation between peak V (LMW) and chloroform formation
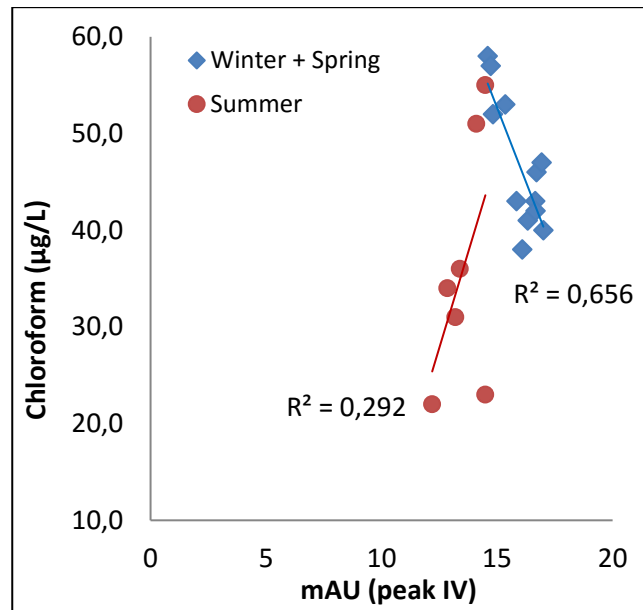
Figure 5-21 Seasonal correlation between peak V (LMW) and chloroform formation

It can be concluded from **Figure 5-22** that during the 12 month study period TTHM formation was at its lowest during the winter. Autumn and spring showed the highest TTHM and chloroform formation but the raw water during these months possessed high UV$_{254}$ values, as indicated in **Figure 5-9**. Although water with high SUVA values is more easily treatable by coagulation and results in superior NOM removal (**Figures 4-10 – 4-12**), the TTHM formation during autumn and spring having high SUVA values also had the highest chloroform formation. This indicates that source water that is hydrophobic and more aromatic in nature has higher UV$_{254}$ removal percentages. However, the character of NOM is different during winter and summer, as indicated in **Figures 5-18** and **5-19**. The chloroform that is the major component of the THM species was mostly attributable to the HMW hydrophobic NOM fraction occurring in summer (**Figure 5-18**) and the LMW less hydrophobic fraction correlated better to chloroform formation during winter (**Figure 5-21**).
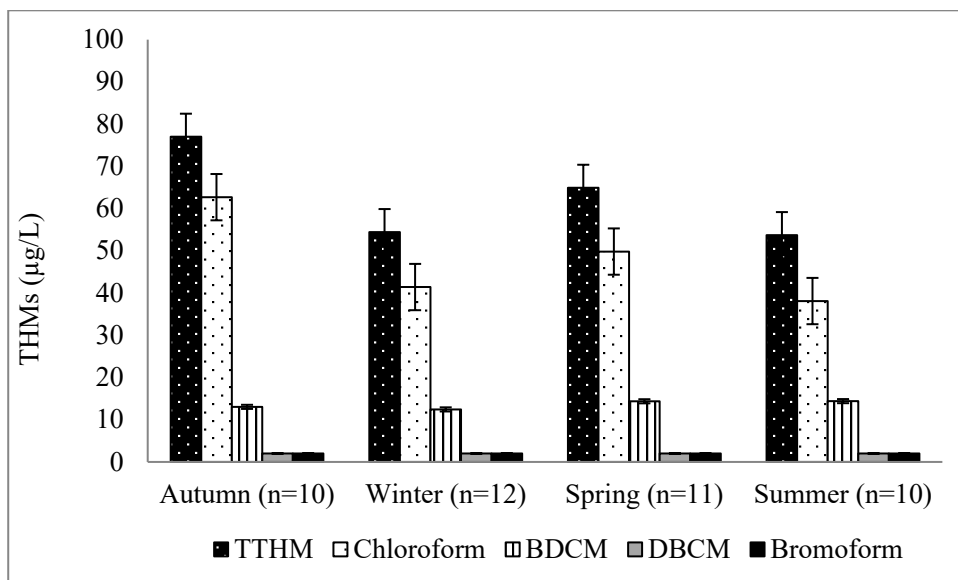
Figure 5-22 Seasonal THMs formation during March 2014 to February 2015 with standard error bars

In **Figure 5-23** the upper and lower points of the whiskers in the box-and-whisker plots indicate the maxima and minima of the different THMs at each sampling point and the line across the box represents the mean value. **Figure 5-23** clearly indicates an increase in BDCM, chloroform and TTHM concentrations between the various sampling points in the distribution system after primary and secondary disinfection. The THM

concentrations after chlorination and chloramination showed concentrations increasing in the sequence bromoform < DBCM < BDCM < chloroform. The mean TTHM concentration after primary disinfection was 17.0 µg/ℓ, 39.2 µg/ℓ at the 5 km point (after primary disinfection) and 67.1 µg/ℓ after secondary disinfection. These values are well below the maximum allowable THM drinking water guideline values in South Africa, regulated by SANS: 241 and indicates satisfactory removal of organic matter by the Rand Water treatment process.
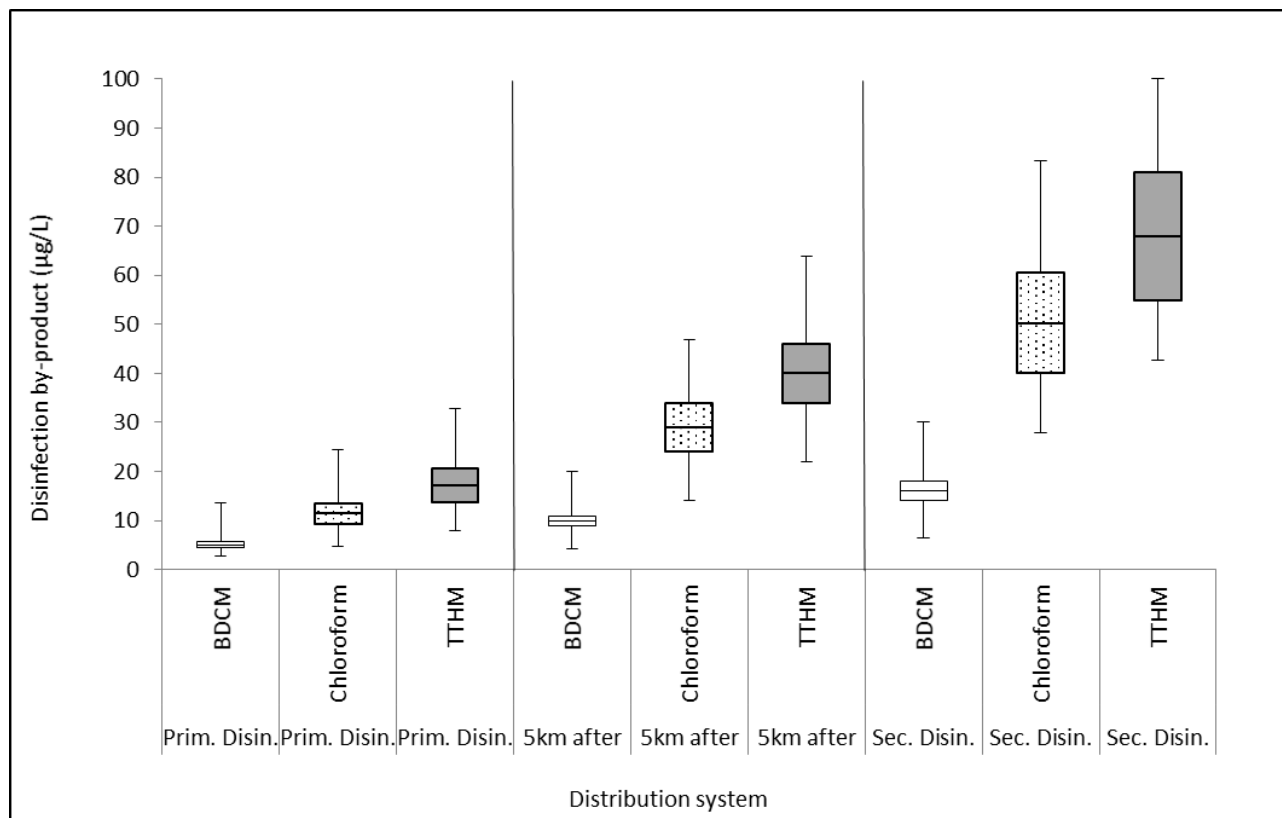
Figure 5-23 Spatial variability of THM formation in the distribution system during the study period

Prim. Disin.	-	Primary disinfection	BDCM	-	Bromodichloromethane
5km after	-	5 km after primary disinfection	TTHM	-	Total trihalomethane
Sec. Disin.	-	Secondary disinfection			

5.5   NOM FRACTIONATION AND TREATABILITY OF THE INDIVIDUAL FRACTIONS

5.5.1   m-PRAM (modified polarity rapid assessment method)

Fractionation of the organic matter was achieved by making use of NOM polarity using a solid phase extraction method specifically adapted to divide the NOM into a hydrophobic, hydrophilic and transphilic fractions. The main aim was focused on keeping this method rapid, as NOM needs to be monitored on a continuous basis due to seasonal influences, which are known not only to affect NOM character but also to influence the total NOM removal and amount of THMs formed.

Fractionation was initially performed using mPRAM as described by Nkambule *et al.* (2011), which uses a non-polar sorbent (C18), polar sorbent (CN) as well as anion exchange (NH2) cartridges. The procedure is described in **Section 3.2.1.3**.

5.5.2 Trihalomethane formation potential on the fractioned NOM

After obtaining the three NOM fractions based on the polarity method, the potential for these individual fractions to form the various trihalomethane species was determined. The methodology thereof is described in Section 3.2.3.

5.5.3 BDOC (biodegradable dissolved organic carbon) – bacterial degradation of NOM

The BDOC method used by Nkambule *et al*. (2011) as a NOM characterisation tool measures the availability of NOM to be utilised by bacteria. In this section, the bacterial degradation of the LMW and HPI NOM fraction was established. Not only did this provide a better understanding of how the chemical composition of NOM (polarity) affects the bioavailability, it also provided an insight on the relationship between polar NOM fractions and bacterial utilisation. Reduction of BDOC was also be determined throughout the Rand Water treatment train. DOC and biomass production was monitored as two complementary parameters. In the amended BDOC method, the DOC was not monitored at the point where no further decrease in DOC was observed, but rather up to the time interval where maximum biomass production was observed. This proved useful in providing some insight into the relationship between the bacteria and its utilisation of NOM within water containing the different NOM fractions (HPO, HPI and TPI). Such a BDOC technique ensured a rapid, but accurate method that is appropriate for monitoring bacterial utilisation of the various fractions based on its polarity and molecular weight. The methodology of the BDOC technique is described in Section 3.2.1.2.

5.6 CONCLUSION

The conventional water treatment process (coagulation, flocculation, rapid gravity sand filtration) utilised at Rand Water does not efficiently remove the HMW aromatic organic matter, compared to the LMW less aromatic NOM with a smaller UV_{254} absorbance value. During the study period, the median NOM removal (measured as percentage UV_{254}) by the Rand Water Zuikerbosch and Vereeniging water treatment plants were found to be 43% and 57%, respectively. This correlated well with the treatability prediction that was made based on the raw water SUVA average values of 3.3 ℓ/mg.m and 4.2 ℓ/mg.m for the Zuikerbosch and Vereeniging plants, respectively. Lower raw water SUVA values predicted an inefficient removal of NOM, and this was confirmed by the UV_{254} removal achieved by the full-scale plants. During the 24 month study period, reduced UV_{254} removal percentages were observed when raw water SUVA decreased during the summer/ high flow season (rain).

SUVA correlated well with the removal of DBP precursors (UV_{254}) but could not be used as an indicator of NOM reactivity with chlorine as indicated by a weak correlation between SUVA and TTHM. Also, aromatic humic compounds were found not to be the only precursors for the TTHMs formed. Seasonal influences on organic loading and NOM removal were observed, as indicated by less aromatic NOM (decreased UV_{254}) in summer which resulted in an increase in TTHM formation during high flow seasons. TTHM formation during summer months increased when the source water had lower UV_{254} values, thus indicating the less aromatic nature of NOM. Seasonal NOM variability was indicated by the size distribution of the organic matter as well as the amount (quantity) of NOM. The change in NOM character during the various seasons indicates a need for the characterisation of NOM as well as the monitoring of NOM removal on a continuous basis. Results from this work have indicated a need to implement advanced NOM characterisation techniques during NOM monitoring to ensure an in-depth understanding of NOM character and reactivity that the different NOM fractions will have on the disinfectant used.

In this chapter, the effect of NOM character on the formation of THMs during disinfection (chlorination) was investigated. The strong positive correlation observed between the high molecular weight NOM fraction of the

source water and actual measured TTHM formation in the drinking water indicates that the aromatic and more hydrophobic NOM fraction were responsible for the THM formation, especially during summer. During winter, the lower molecular weight NOM fraction being more hydrophilic in nature was mostly responsible for the THMs formed in the drinking water. The HMW NOM fraction was the main precursor to TTHM and chloroform formation, specifically during summer months. The positive correlation existing between SUVA and UV_{254} percentage removal indicates the use of SUVA as an indicator to average percentage removal of NOM, which has an aromatic character. Weak regression between SUVA and actual measured TTHM formation in the final drinking water indicates the need to incorporate THMFP (trihalomethane formation potential) on the individual NOM fractions so as to confidently determine the likelihood of the specific fraction to form THMs.

This study suggests that when monitoring NOM at the water treatment plant the size, fluorescence and polarity of NOM should be investigated when determining NOM quantity and quality. Conventional methods (e.g. DOC) only provide information on the quantity or amount of NOM in the source water, whereas advanced characterisation techniques based on the polarity and size of the NOM provides the WTP with more conclusive information regarding the character of NOM. This could also be helpful when predicting whether the organic matter will be removed by the coagulation process during a specific season as well as determining the influence that seasonal NOM variability has on the THMs formed after disinfection.

CHAPTER 6: CHARACTERISATION OF POLYSILSESQUIOXANE (PSQ) AND POLY (STYRENE-DIVINYL BENZENE) (PS-DVB)

6.1 INTRODUCTION

This chapter presents the results and discussions of the synthesised polymeric materials (i.e. polysilsesquioxane and poly(styrene-divinyl benzene). In particular, the characterisation results from Fourier Transform Infrared (FTIR) spectroscopy, Scanning Electron Microscopy (SEM)/ Energy Dispersive Spectrometer (EDS), X-ray Diffractometer (XRD), Transmission Electron Microscopy (TEM), Raman Spectroscopy, Thermogravimetric Analysis (TGA) and Brunauer-Emmett-Teller (BET) are presented.

6.2 FOURIER TRANSFORM INFRARED (FTIR) SPECTROSCOPY MEASUREMENTS FOR E-PSQ AND PS-DVB

6.2.1   Blending of styrene and divinyl benzene

Poly(styrene-divinylbenzene) (PS-DVB) is a product of co-polymerisation of styrene (S) and divinylbenzene (DVB) monomers (Wiley, 1975; Klingenberg and Seubert, 1998; Garcia-Diego and Cuellar, 2005). The FTIR spectra of S and DVB were analysed first, in order to determine the success of polymerisation for the three PS-DVB polymers with ratio 1:1, 1.5:1 and 10:1. The FTIR spectra (**Figure 6-1**) indicated the presence of the functional groups present in both the monomers and the polymeric materials and are summarised in **Table 6-1**.

The FTIR spectra of styrene (S) and (DVB) show. The spectra shows multiple weak to medium peaks appearing at 1400–1600 cm^{-1}, which indicate the existence of the C=C aromatic (from the aromatic ring) on the S and DVB compounds. At around 3000–3100 cm^{-1}, there exists a medium peak, indicating a C-H aromatic from the aromatic ring. The strong peaks appearing at 3010–3100 cm^{-1} are attributable to the =C-H aliphatic bending bands. At around 1620–1680 cm^{-1} there are multiple peaks, which indicate the presence of the C=C stretch bands (aliphatic) from S and DVB.

The FTIR spectra of DVB and S indicate flexural vibrations from benzene rings (δC−H) of the divinylbenzene (Zhang *et al*., 2015) at around 600–800 cm^{-1}. Medium to weak multiple peaks that appear at 1400–1600 cm^{-1} indicate the existence of the C=C aromatic of the S and DVB (Păcurariu *et al*., 2013). Peaks at 1400–1700 cm^{-1} are due to benzene ring vibrations (vC−C) of S and DVB (Zhang *et al*., 2015). At around 2800–3200 cm^{1}, there exists a medium peak indicating a CH aromatic from the aromatic ring (Li *et al*., 2011; Zhang *et al*., 2015). The strong peaks appearing at 694-988 cm^{-1} indicate the =CH bending, from the two vinyl groups attached on the benzene ring (DVB), and one vinyl group of the S. At around 1620–1680 cm^{-1}, there are mutiple peaks which represent the C=C stretch (aliphatic) from the DVB.
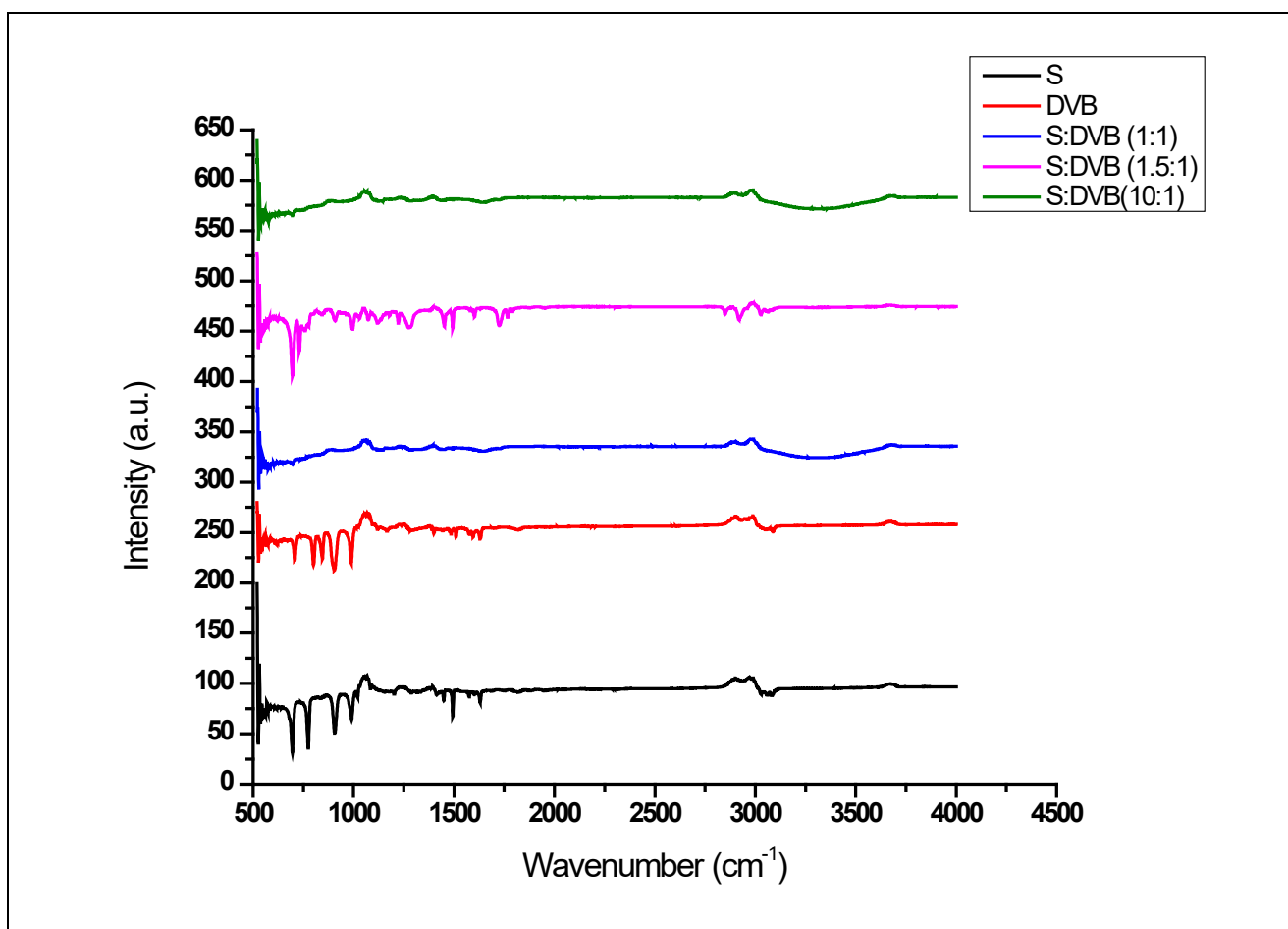
Figure 6-1 FTIR spectra of styrene, divinyl benzene and the styrene-divinyl benzene polymers

The FTIR spectra of PS-DVB (S: DVB, 1:1, v/v), (S: DVB, 1.5:1) and (S: DVB, 10:1) showed weak peaks as compared to the peaks that were observed from the two monomers (S and DVB). There were multiple peaks around 3010-3100 cm^{-1} (=CH) from S and DVB, peaks at 600-800 cm^{-1} (δC−H) of the polymers (PS-DVB). (Li *et al*., 2011; Zhang *et al*., 2015). At around 1400–1700 cm^{-1} there are multiple peaks (νC−C) of the polymeric material PS-DVB (benzene rings) (Zhang *et al*., 2015). At around 2800–3200 cm^{-1} there exist multiple peaks (C-H aromatic) from the aromatic rings on the S and DVB (Chaiyasat *et al*., 2011; Li *et al*., 2011; Zhang *et al*., 2015). At around 1620–1680 cm^{-1} multiple weak peaks occur, indicating the C=C stretch (aliphatic) monomers. At around 1400–1600 cm^{-1} there are multiple peaks indicating the vibrations of C=C stretching from benzene rings, which are present in both the S and DVB (Chaiyasat *et al*., 2011). Peaks observed from PS-DVB 1.5:1 (S: DVB 1.5:1, v/v) are stronger than the peaks for PS-DVB 1:1 and 10:1.

There exists a strong and broad O-H peak at around 3000–3500 cm^{-1} from the FTIR spectra of PS-DVB 1:1 and 10:1 indicating the presence of O-H group in the samples. The O-H group was a residue from solvents used (such as ethanol and methanol) in the synthesis of the polymers. The decrease of number of peaks on all three polymeric materials proved that polymerisation was successful. A decrease in peak intensity between S and DVB was observed as the peaks decreased with the introduction of vinyl groups.

Table 6-1 Functional groups observed from the FTIR spectra of compounds

Compound	Functional groups	Adsorption (cm^{-1})	Peak(s) type
Styrene (S)	C=C (aromatic)	1415–1577	medium-weak
	C-H (aromatic)	3030–3057	Medium
	=C-H (aromatic)	694–1084	strong (multiple)
	C=C (aliphatic)	1415–1627	Medium
	=C-H (aliphatic)	2957–3116	Medium
Divinylbenzene (DVB)	δC−H (aromatic)	617 and 802	medium-weak
	C=C (aromatic)	1402–1593	medium (multiple)
	vC−C (aromatic)	1402,1593 and 1631	Strong
	C-H (aromatic)	3048–3090	Medium
	=C-H (aliphatic)	694–988	Strong
	C=C (aliphatic)	1415–1627	medium (multiple)
	=C-H stretch (aliphatic)	2933–3110	Medium
Poly (styrene-divinyl benzene) PS-DVB (1:1)	=C-H (aliphatic)	695–1073	weak-multiple
	δC−H (aromatic)	695 and 748	Weak
	vC−C (aromatic)	1455, 1582 and 1602	Weak
	C-H (aromatic)	3030–3085	Weak
	C=C (aliphatic)	1602–1719	weak (multiple)
	C=C (aromatic)	1402–1631	Weak
	O-H	3320	Broad
Poly (styrene-divinyl benzene) PS-DVB (1.5:1)	=C-H (aliphatic)	697–1119	weak-multiple
	δC−H (aromatic)	2925 and 2851–2925	Weak
	vC−C (aromatic)	697, 1428 and 1628	Weak
	C-H aromatic	3303	Weak
	C=C (aliphatic)	1658	weak (multiple)
	C=C (aromatic)	1428–1628	Weak
Poly (styrene-divinyl benzene) PS-DVB (10:1)	=C-H (aliphatic)	693–1118	weak-multiple
	δC−H (aromatic)	693, 729 and 753	Weak
	vC−C (aromatic)	1450 and 1601	Weak
	C-H aromatic	3025–3086	Weak
	C=C (aliphatic)	1601–1764	weak (multiple)
	C=C (aromatic)	1314–1658	Weak
	O-H	3303	Broad
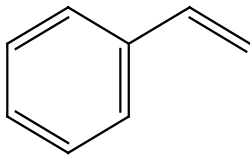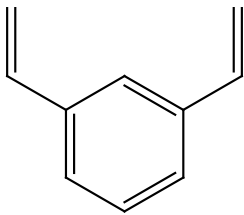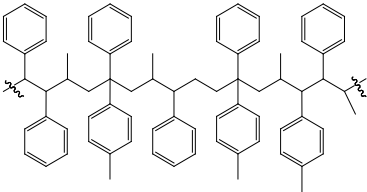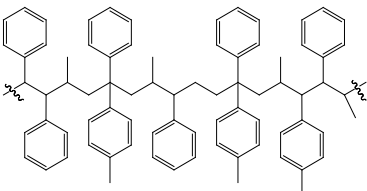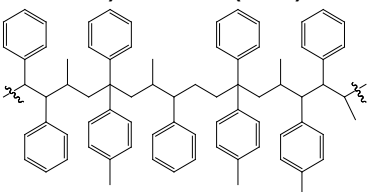
6.2.2 Synthesis of end-capped polysilsesquioxane (E-PSQ)

An FTIR analysis of both the PSQ and E-PSQ (see **Figure 6-2**) revealed an existence of a broad peak at 800–1200 cm^{-1}, which is characteristic of the Si-O-Si stretching band associated with a silica functional group (Hasegawa *et al*., 2009; He *et al*., 2016). Furthermore, a peak appearing at 895 cm^{-1} indicates the existence of Si-C bonds in both PSQ and E-PSQ (Hasegawa *et al*., 2009). The Si-C and Si-O-Si peaks are known to be - characteristic peaks for silica functional groups.
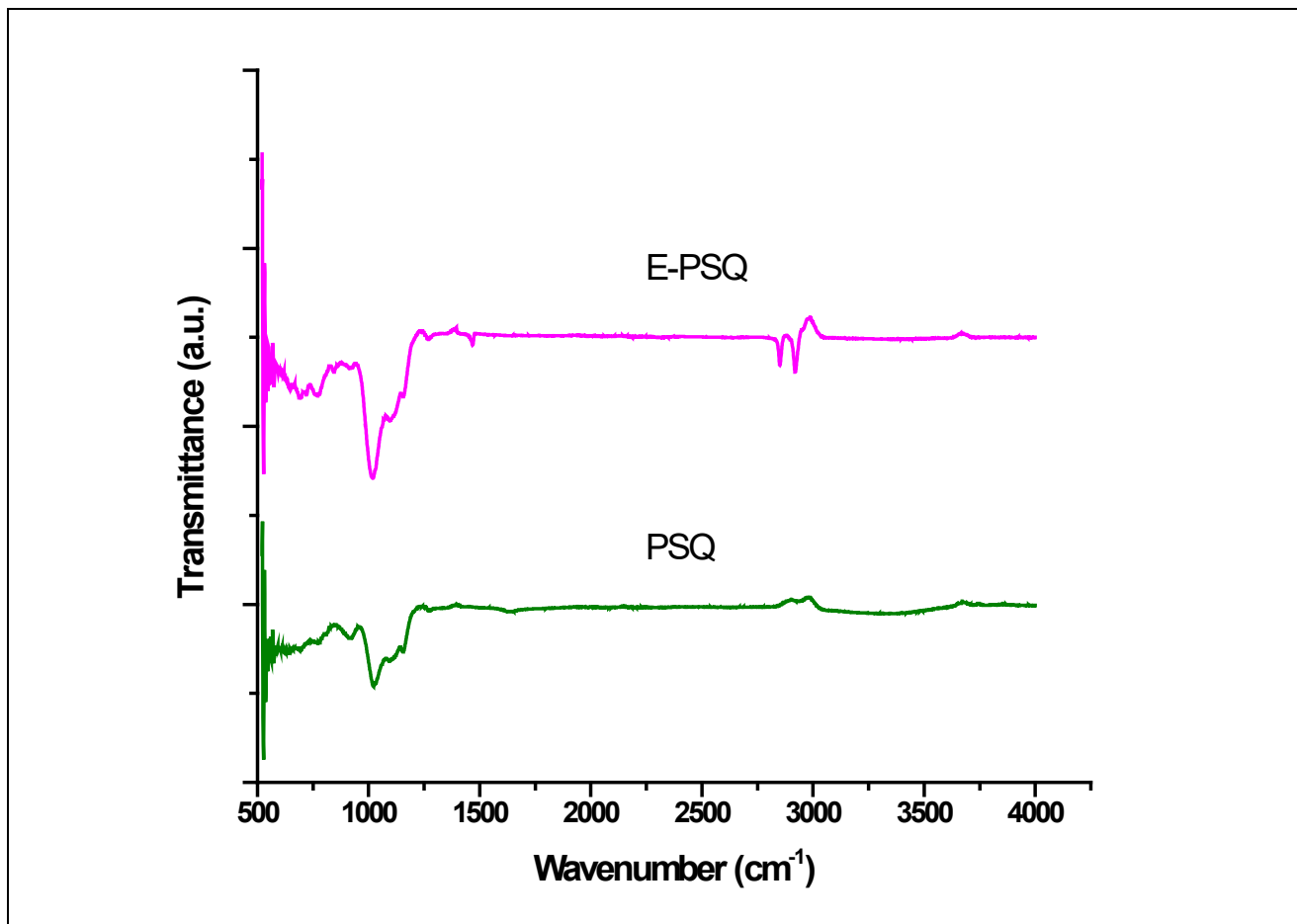
Figure 6-2 FTIR spectra of PSQ and E-PSQ

The end-capped spectrum of PSQ shows the existence of strong peaks appearing at 2845–3000 cm^{-1}, which signifies the C-H stretching band of the new alkyl functional group (Maiga *et al*., 2014). At 1282–1467 cm^{-1}, weak peaks were observed, which indicates the -C-H bending of the new alkyl functional group. The existence of the C-H stretching peaks indicates that a reaction had occurred between hexamethyldisilazane (HMDS) and silanol groups on the active sites of the synthesised silica materials. Therefore, the end-capping of the silanols from PSQ proved to be a success (Maiga *et al*., 2014).

6.3 SCANNING ELECTRON MICROSCOPY (SEM) AND ENERGY DISPERSIVE SPECTROMETER (EDS)

6.3.1   SEM and EDS analysis of PS-DVD

The SEM image of PS-DVB (1:1) **Figure 6-3 (a)** shows a spherical particle with pores of various sizes and shapes. The corresponding EDS **Figure 6-3 (b)** graph shows the presence of both carbon and oxygen as the main element in the sample of PS-DVB, and thus confirms the elemental composition of the resulting PS-DVB polymer (Rao *et al*., 2004). The pores of the PS-DVB are not well defined as compared to those of PS-DVB (1.5:1) and are much more visible as compared to those of PS: DVB (10:1).
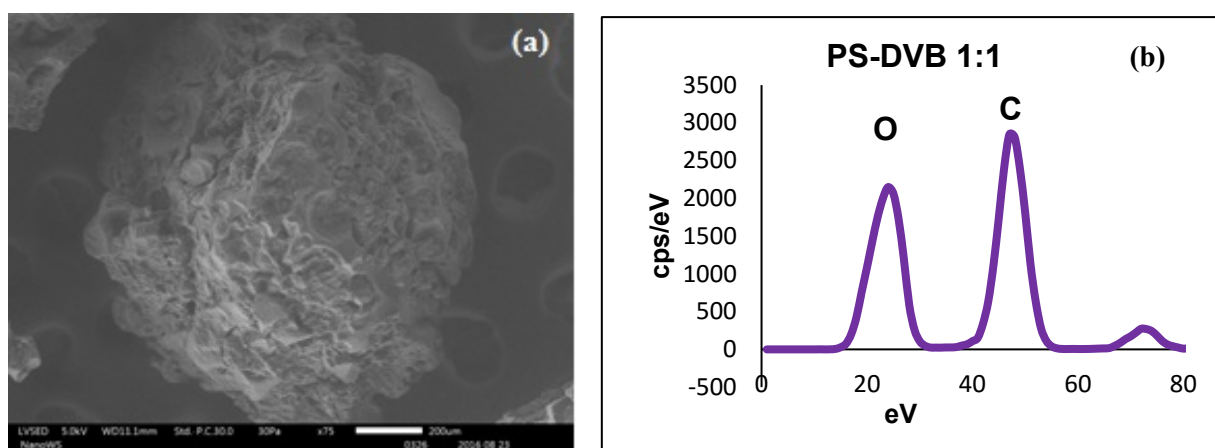
Figure 6-3 SEM (a) and EDS (b) results of PS-DVB (1:1 v/v)

The SEM image of PS-DVB with a ratio (S:DVB,1.5:1, v/v) (see **Figure 6-4 (a)**) shows particles with pores of various sizes and shapes and the corresponding EDS graph shown in **Figure 6-4 (b)** shows carbon and oxygen being the main element in the sample of PS-DVB. The SEM and EDS results confirm the structural morphology, porosity and elemental composition of the resulting polymer as PS-DVB 1.5:1. Further studies regarding the pore sizes and pore volumes were undertaken using other instruments e.g. BET.
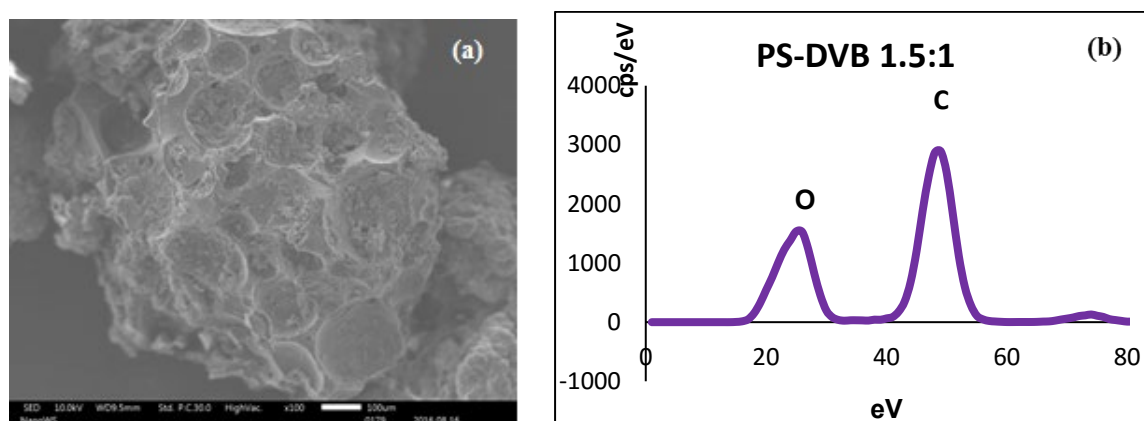
Figure 6-4 SEM (a) and EDS (b) results of PS-DVB (1.5:1 v/v)

The SEM image of PS-DVB (10:1) (see **Figure 6-5 (a)**) shows a spherical particle with no visible pores. Styrene competes with toluene (porogen) during the polymerisation and thus prevents pores from forming. According

to the EDS results (**Figure 6-5 (b)**), both carbon and oxygen are present as main elements; this provides evidence for the elemental composition of the PS-DVB polymer.
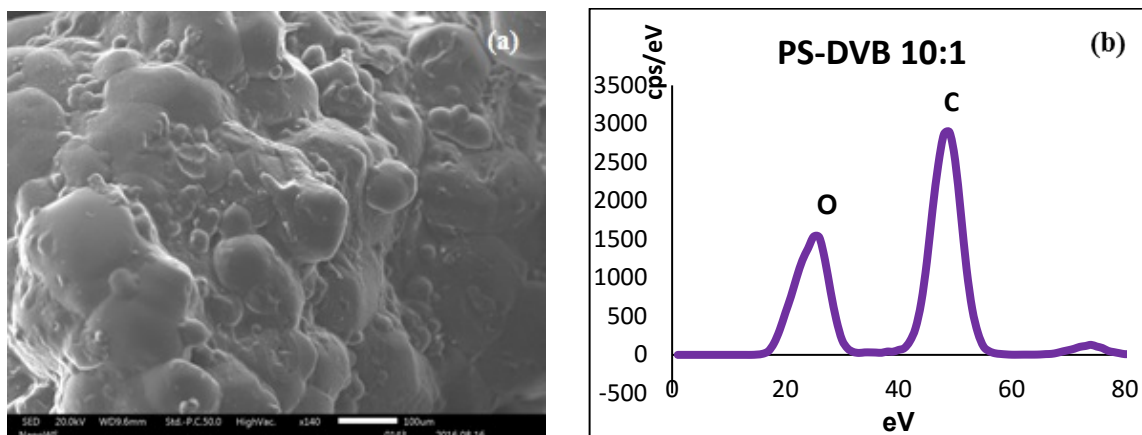
Figure 6-5 SEM (a) and EDS (b) results of PS-DVB (10:1 v/v)

6.3.2. SEM and EDS analysis of PSQ and E-PSQ

The SEM image of PSQ in **Figure 6-6 (a)** shows particles with pores of various shapes and sizes, which are smaller than those of the PS-DVB (1:1 and 1.5:1) but with more visible pores compared to PS-DVB (10:1). The EDS graph (**Figure 6-6 (b)**) shows the presence of carbon, oxygen and silicon as the main elements in the PSQ sample as well as remains of sodium emanating from the salts that were used during the synthesis. The EDS results confirm the elemental composition of the resulting polymer as being PSQ.
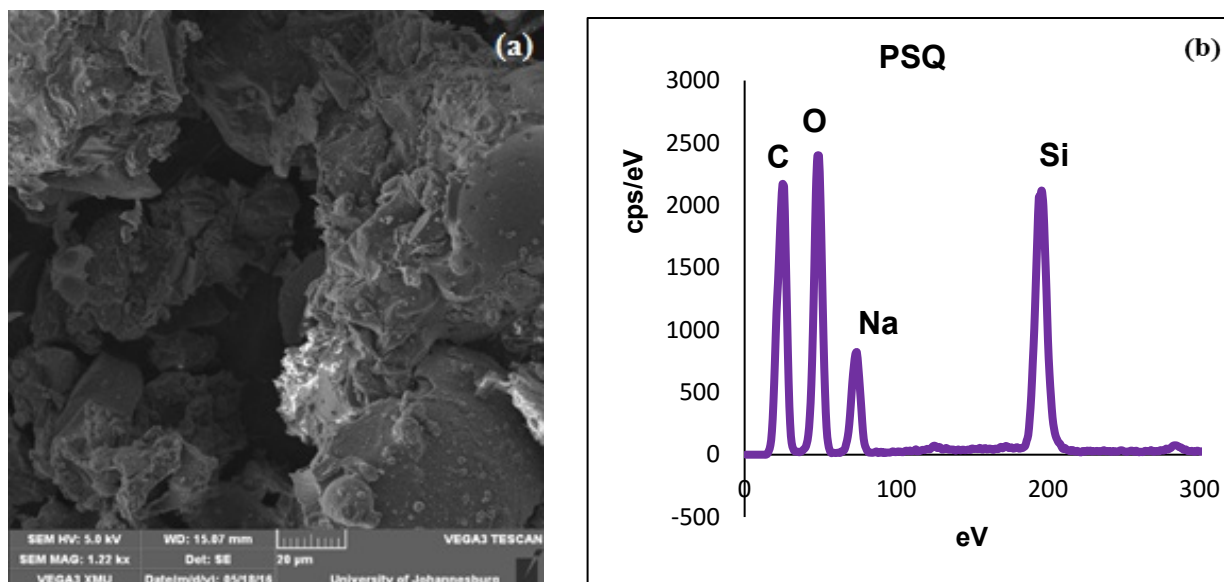
Figure 6-6 SEM (a) and EDS (b) results of PSQ

The SEM image of E-PSQ **Figure 6-7 (a)** shows a particle with pores of various shapes and sizes. EDS results according to **Figure 6-7 (b)** show the presence of carbon, oxygen and silicon as main elements in the sample of PSQ as well as remains of sodium from the salts which were used during the synthesis. The pores of the polymer have decreased and the quantity of silicon was smaller, which confirms the addition of alkyl groups

that resulted from end-capping. The E-PSQ has smaller pores as compared to the PSQ, and PS-DVB (1:1 and 1.5). The results confirm the elemental composition of the resulting polymer as being PSQ.
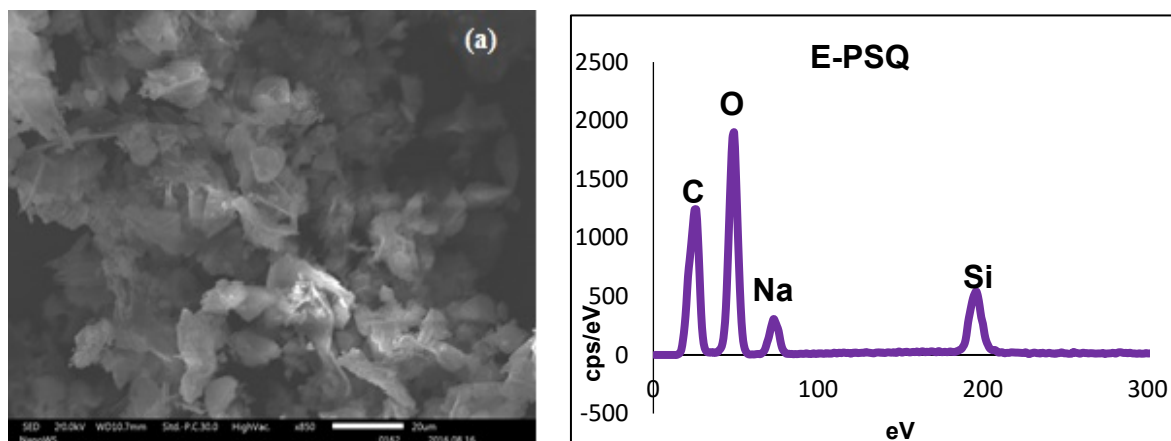
Figure 6-7 SEM (a) and EDS (b) results of E-PSQ

6.4 X-RAY DIFFRACTION (XRD)

6.4.1 XRD analysis of PS-DVB

The two PS-DVB materials PS-DVB (10:1) (**Figure 6-8 (b)**) and PS-DVB (1:1) (**Figure 6-8 (a)**) have no peaks appearing on the theta angle and the X-ray light is non-directional and non-continuous (Li *et al*., 2011). No visible oscillation and deep minima were observed. Therefore, the polymeric materials were found to be amorphous thus indicating the polydispersity of the particles. As shown in **Figure 6-8 (c)**, the PS-DVB (1.5:1) polymeric materials show two visible peaks at 19.78° and 41.11°; these peaks are not sharp and do not form a continuous pattern, instead they are broad. This might be due to the chemical species in the PS-DVB (1.5:1) polymer. These results suggest an amorphous texture of the product and the polydispersed particles.
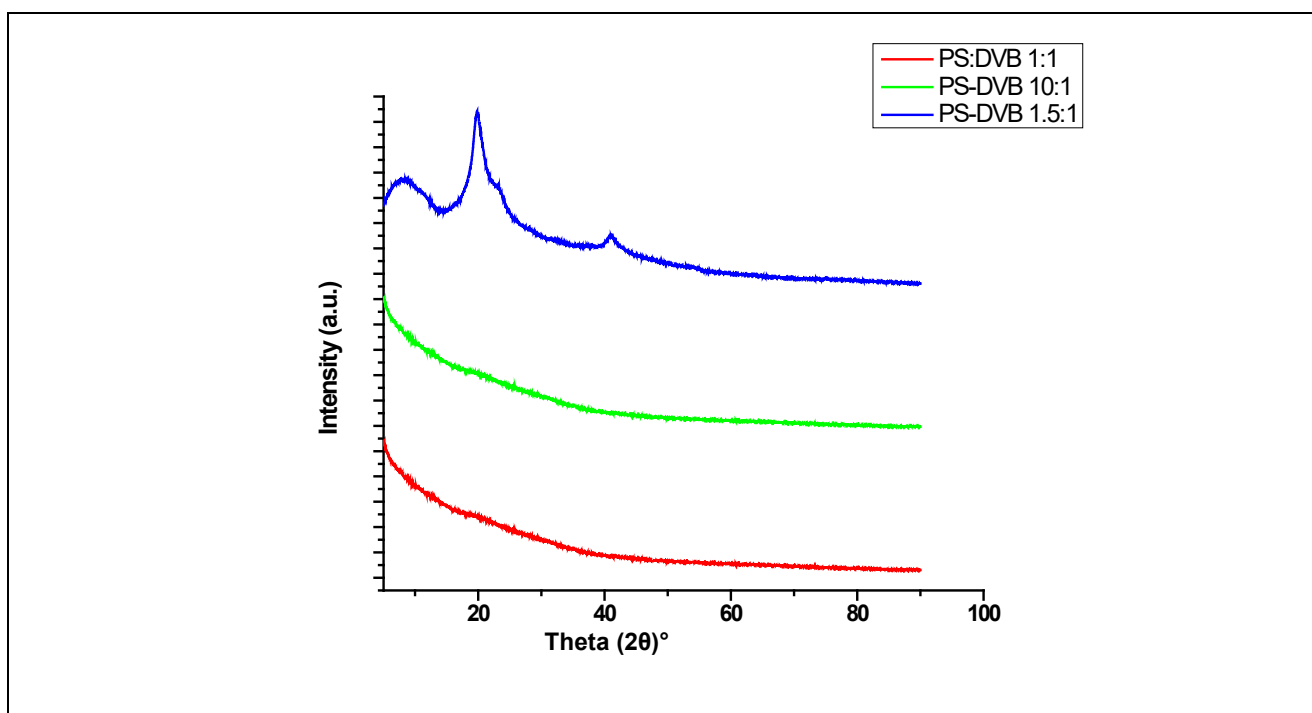
Figure 6-8 XRD spectra of PS-DVB (a) 1.5:1 (b) 10:1 and (c) 1:1

6.4.2   XRD analysis of PSQ and E-PSQ

The XRD spectra show the nature of the polymeric materials to either be amorphous or crystalline, monodisperse or polydisperse (Rao *et al*., 2004; Nakanishi and Kanamori, 2005). The XRD spectra of the two polymeric materials (poly(styrene-divinyl benzene) and polysilsesquioxane) and their modifications are shown in **Figure 6-9**. No 3D arrangement of atoms for the PSQ was observed (**Figure 6-9 (a)**), which means that the diffraction of the X-ray light is non-directional and non-continuous (Burleigh *et al*., 2002). There is no visible oscillation and deep minima; therefore, the sample is amorphous and the particles are polydispersed. The theta angle of the E-PSQ (**Figure 6-9 (b)**) is showing a peak intensity at around 20° (corresponding to the end-capping material), which suggests that the nature of the polymer is amorphous and the particles are polydispersed as no visible oscillation and deep minima were observed.
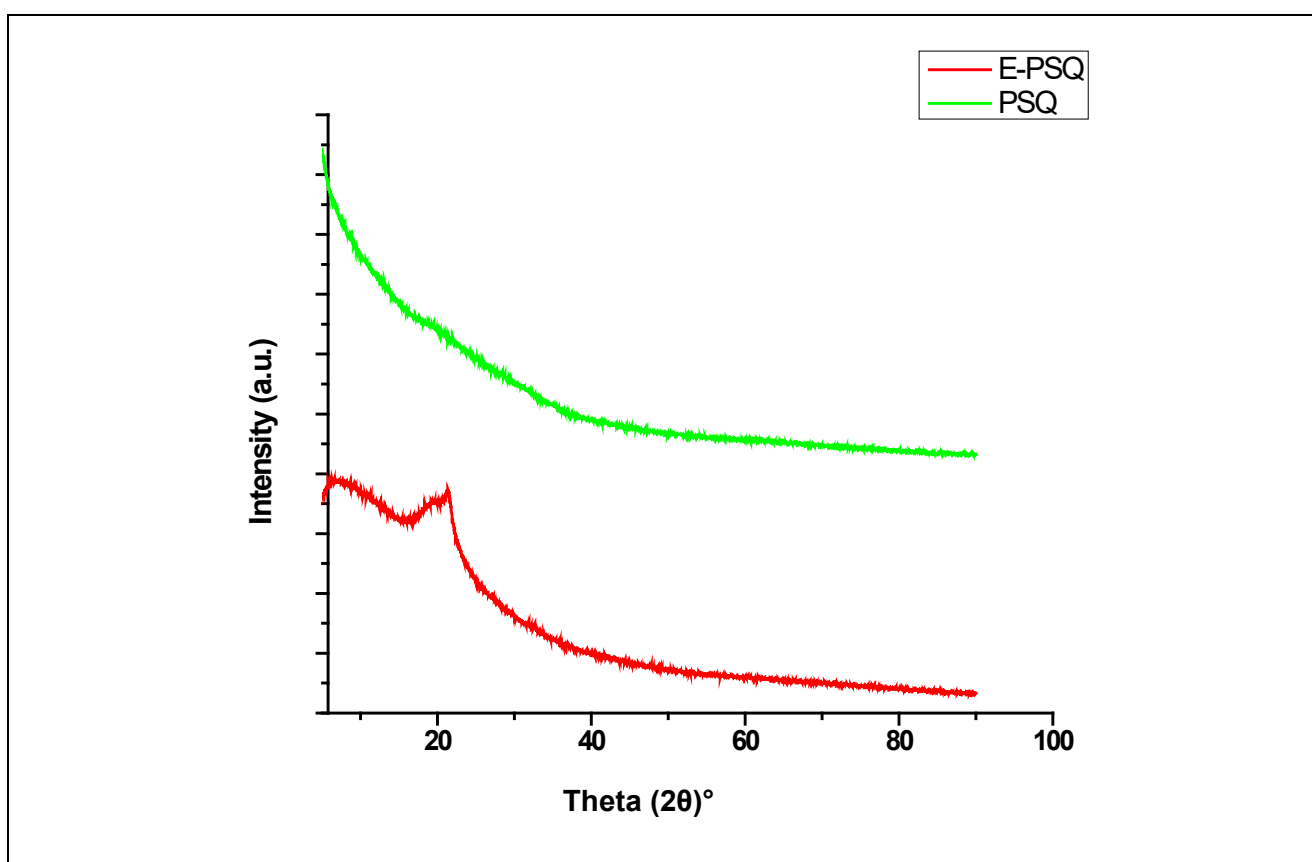
Figure 6-9 XRD spectra of PSQ (a) and E-PSQ (b)

6.5 RAMAN SPECTROSCOPY

6.5.1   Raman analysis of PS-DVB

The Raman spectra revealed the presence of the additional groups that were not detected by FTIR. It also revealed the nature of carbon in the polymeric materials. The Raman spectroscopy for PS-DVB (**Figures 6-10 (a)** – **(c)**) was studied extensively and the vibrational and structural properties of the sp-sp^2 for amorphous carbon have been characterised by G and D bands. Raman spectroscopy was used to investigate the structural characteristics of the PS-DVB and PSQ materials. As shown in **Figure 6-10**, the three PS-DVB

polymers revealed three broad peaks appearing at ~1340 cm^{-1}, 1585 cm^{-1}, ~2675 cm^{-1} and specific peaks corresponding to the polymer structure. The peak at ~1346–1347 cm^{-1} corresponds to the D-band (represents the defects of C-C bond), and the G-band at ~1570–1586 cm^{-1} corresponds to the sp^2 graphitic carbon (C=C) (Zhong *et al.*, 2010; Altava *et al.*, 2011). In addition, the spectra also revealed another D-band peak at ~2685 cm^{-1}, which is characteristic of the 2D-band. In general, the intensity ratio of D-band over G-band (I_D/I_G) is used to determine the degree of disorder of the materials, all summarised in **Table 6-1** (Zhong *et al.*, 2010). The higher the value of I_D/I_G, the more the abundant degree of defects is experienced in the sample. The calculated I_D/I_G ratio was found to be 0.84, 0.86 and 0.78 for PS-DVB 1:1, PS-DVB 1:1.5 and PS-DVB 1:10, respectively. Furthermore, it was found that the I_D/I_G values increased from 0.84 to 0.86 when the amount of S increased within the PS-DVB polymer from 1:1 to 1.5:1 ratio relative to DVB, respectively. This increase may be due to the transformation of the sp^2- C-C domain of polymers to sp^3-domain, which result from the strong covalent bonding interaction between the S and DVB polymer networks at low loading of S, thus leading to a rise or shift to the D-band peak. However, further increase of the amount of S to a PS-DVB ratio of up to 10:1 resulted in the decrease in the I_D/I_G ratio of about 0.74. The reason for this decrease is that 1 wt% amount of DVB polymer was able to chemically interact with specific content of S polymer to a certain extent, hence at high loading of S the effect is reduced.
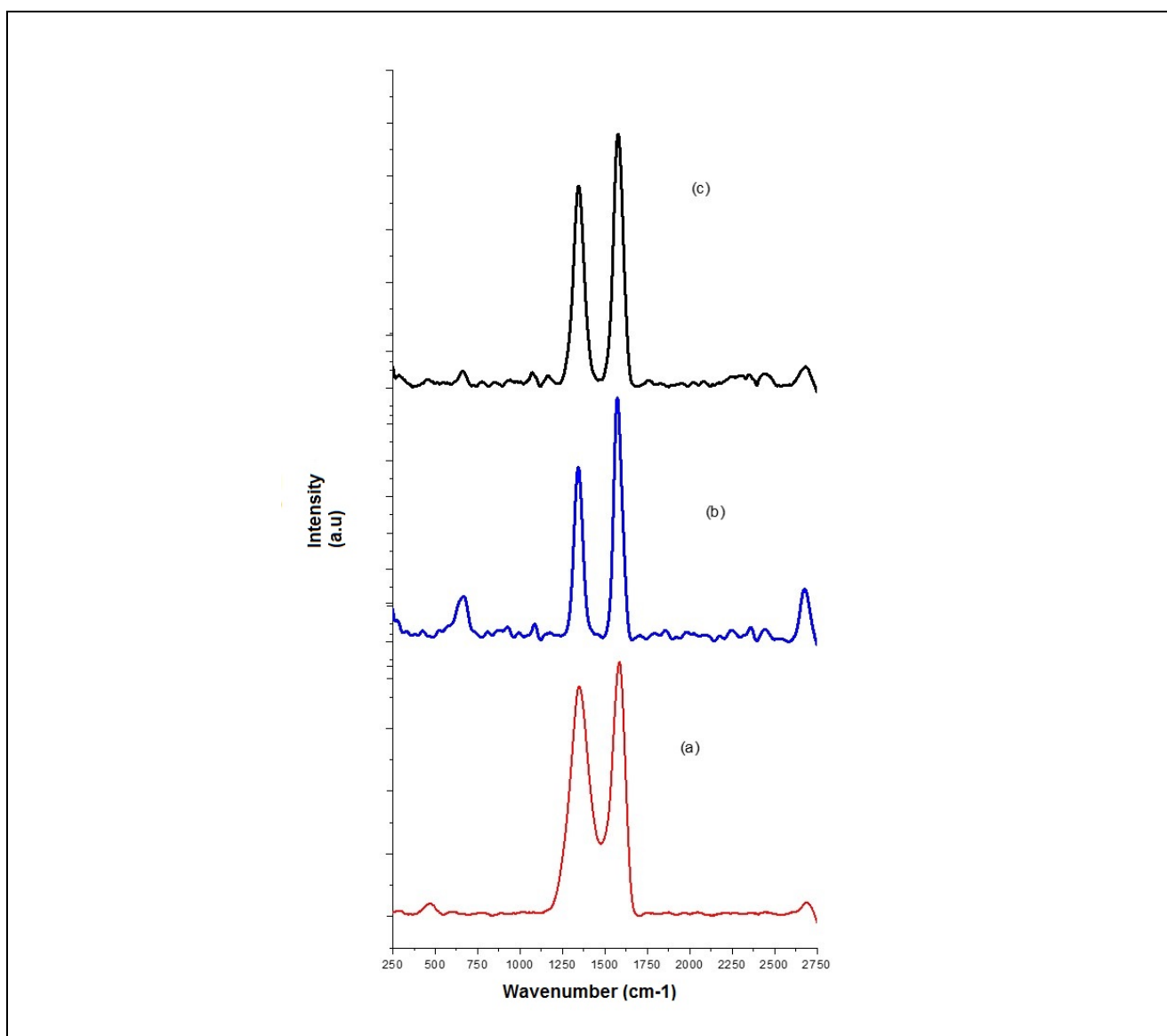
Figure 6-10 Raman spectra for PS-DVB (a) 1:1, (b) 1.5:1 and (c) 10:1

Table 6-2 The intensity ratio of the D and G bands for polymeric materials

Sample	I_D	I_G	I_{2D}	I_D/I_G
PS-DVB 1:1	1346	1586	-	0.84
PS-DVB 1:1.5	1344	1570	2676	0.86
PS-DVB 1:10	1347	1580	2686	0.78
PSQ	1356	1586	-	0.85
E-PSQ	1351	1585	-	0.85

6.5.2 Raman analysis of PSQ AND E-PSQ

The results of a Raman analysis of PSQ and E-PSQ are indicated in **Figure 6-11** (**(a)** and **(b)**). The intensity ratio of the D-band to G-band for both PSQ and E-PSQ polymers was found to be 0.85 for both polymeric materials. The peak at 560 cm^{-1} serves as an indication that during the end-capping of PSQ with hexamethyldisilazane (HMDS), the HMDS was able to react with the OH–(hydroxyl group) from Si-OH. The reaction resulted in the formation of methyl siloxy (Si-C) group, which can produce SiO_2 at high temperatures (Ma *et al*., 2002; He *et al*., 2016). However, the structure of the PSQ was not transformed or destroyed by incorporation of the E polymer, hence no change was observed in the sp^3 hybridised carbon and the I_D/I_G intensity ratio.
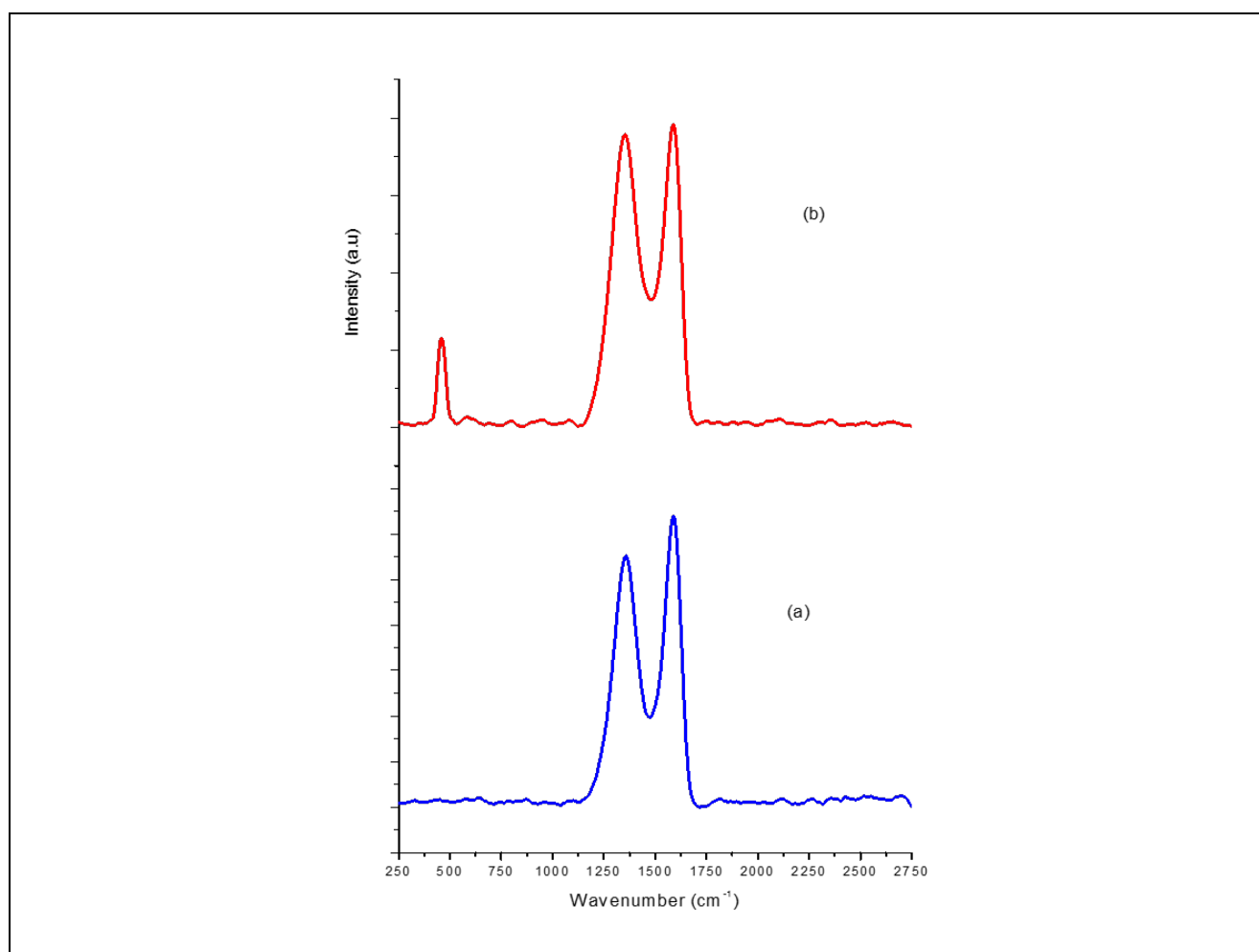
Figure 6-11 Raman spectra for (a) PSQ (b) E-PSQ

6.6 THERMOGRAVIMETRIC ANALYSIS (TGA)

6.6.1 TGA analysis of PS-DVB

The TGA measurements of the polymeric materials were carried out to confirm the stability of the materials over high temperatures (Rao *et al*., 2004; Chaiyasat *et al*., 2011; Li *et al*., 2011; Păcurariu *et al*., 2013). For the three PS-DVB materials, **Figure 6-12 (b)** shows that there was about 5% mass loss due to evaporation at 0–100 °C for PS-DVB (1.5:1). About 20% mass loss due to evaporation 0–200 °C was recorded for PS-DVB (1:1) (**Figure 6.12 (a)**) and about 25% mass loss due to evaporation at 0–150 °C for PS-DVB (10:1) was recorded (**Figure 6.12 (c)**). The weight loss of about 70% was observed at 300–450 °C for the PS-DVB 1.5:1, about 60 weight loss from 150–450 °C for PS-DVB (1:1) and about 65% weight loss from 100–450 °C for PS-DVB (1:1). The most stable PS-DVB was found to be the PS-DVB (1.5:1). Weight loss associated with evaporation was the lowest, and the overall weight loss was observed from higher temperatures of 200 °C.
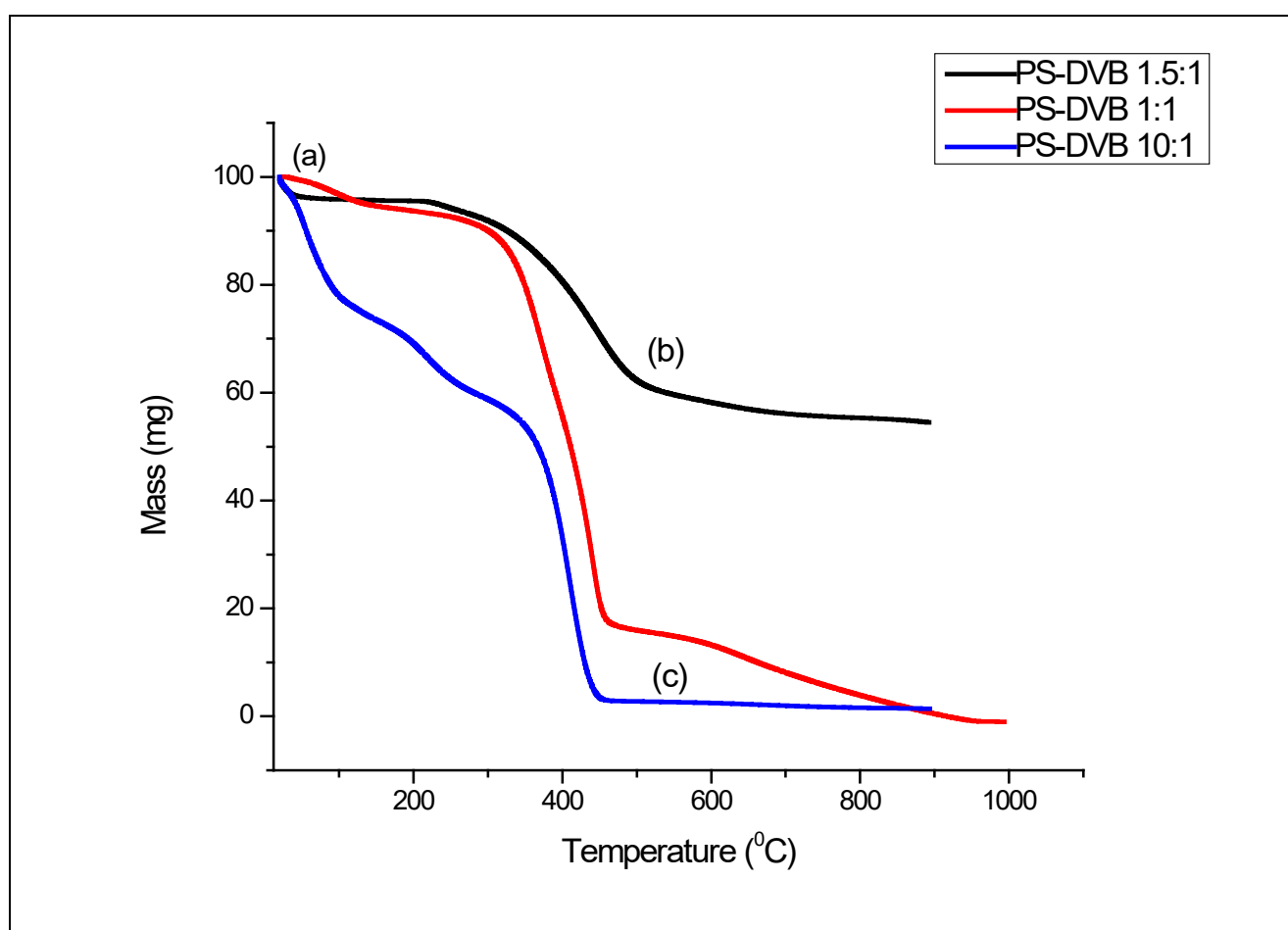
Figure 6-12 TGA graphs for PS-DVB (a) 1:1, (b) 1.5:1 and (c) 10:1

6.6.2 TGA analysis of PSQ and E-PSQ

The TGA measurements of the silica polymeric materials was undertaken to study the thermal stability properties of the materials (Rao *et al*., 2004; Păcurariu *et al*., 2013). A 5% mass loss due to evaporation of moisture at 0–5 °C was observed for PSQ (1.5:1) (see **Figure 6.13 (a)**); a 10% mass loss due to evaporation 0–100 °C was observed for E-PSQ (**Figure 6.13 (b)**). The weight loss of about 40% was observed at 50–500 °C for the PSQ; for E-PSQ about 15% weight loss was observed at 100–250 °C. The addition of the HMDS (end-capping) material decreased the stability of the material at high temperatures because the material

showed a constant continuation of mass degradation from 250–900 °C. Both materials were able to withstand temperatures of up to 900 °C.
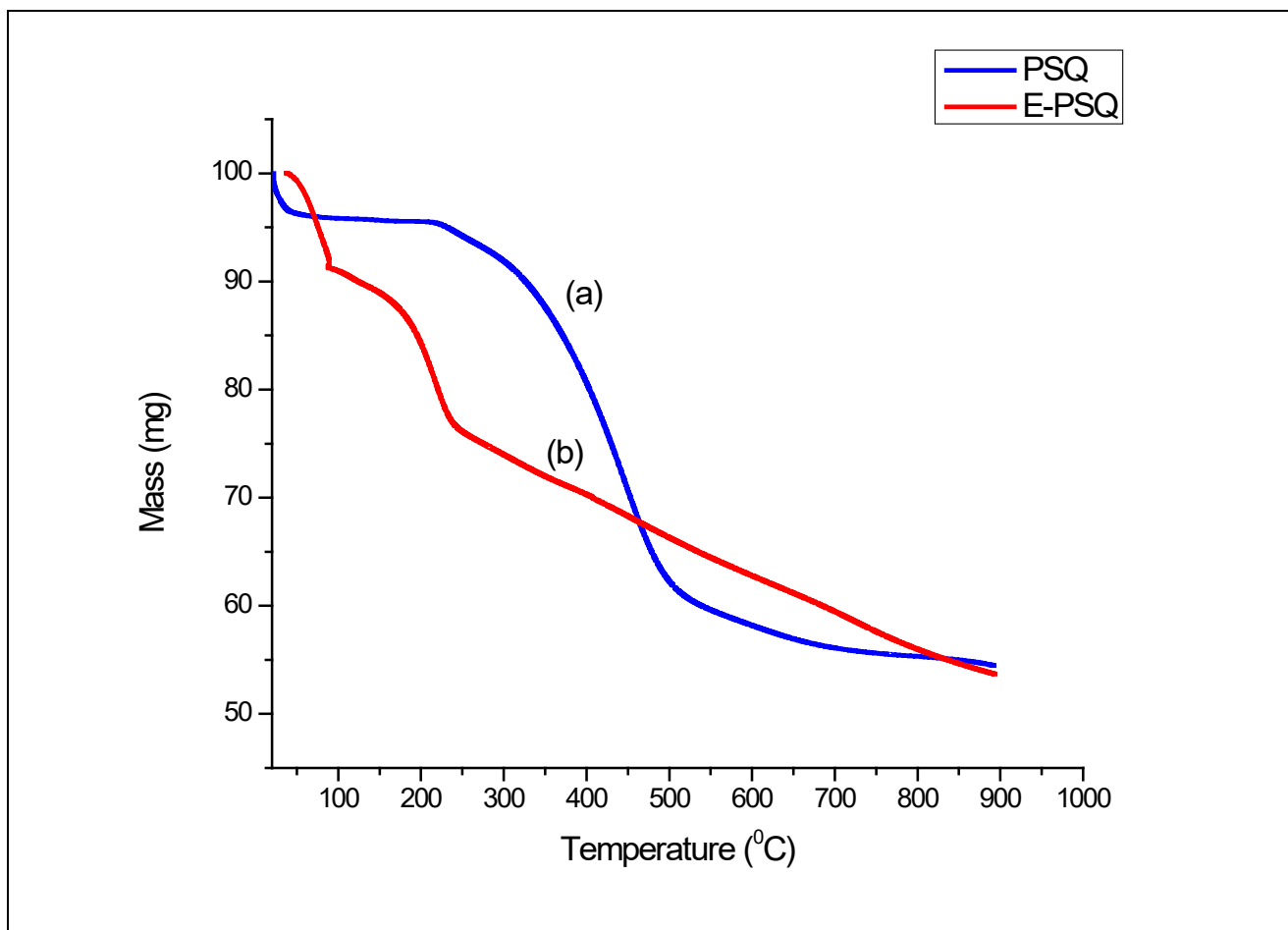
Figure 6-13 TGA graphs for PSQ (a) and E-PSQ (b)

6.7 BRUNAUER-EMMET-TELLER (BET)

The BET results from **Table 6-3** showed that the average pore sizes and surface areas recorded for PS-DVB particles were 18.7 and 2.9 nm, 0.035 and 84.67 m^2/g for 1.5:1 and 1:1, respectively. The average pore volumes were 0.000391, 0.003609 and 0.062123 cm^3/g for PS-DVB 1.5:1, 1:1 and 10:1, respectively. No pore size and surface area were recorded for PS-DVB 10:1 because it was not stable under instrument temperatures.

Table 6-3 BET results on all polymeric materials

Sample	Surface area (m^2/g)	Pore size (nm)	Pore volume (cm^3/g)
PS-DVB (1.5:1)	0.0835	18.72692	0.000391
PSQ	1.0414	6.69712	0.001744
PS-DVB (10:1)	Not available	Not available	0.003609
PS-DVB 1:1	84.6761	2.93462	0.062123
E-PSQ	1038.0202	2.94361	0.763882

The pore size, surface area and pore sizes of PS-DVB 1.5:1 were found to be better and more suitable for SEC/GPC as compared to PS-DVB 1:1 and 1:1. A decrease in the pore size from 6.69 to 2.9 nm as the PSQ material was end-capped was observed. An increase in both the surface area and pore volume was observed when the PSQ was end-capped (E-PSQ). The pore volume increased from 0.001744 (PSQ) to 0.763882 cm^3/g (E-PSQ) and surface area increased from 1.0414 (PSQ) to 1038.02 m^2/g (E-PSQ). The end-capped PSQ (E-PSQ) material was found to be more suitable for SEC/GPC as compared to the PSQ.

6.8 CONCLUSION

Successful blending of the S and DVB monomer to PS-DVB as well as the successful end-capping of PSQ to E-PSQ was confirmed by the FTIR spectroscopy. SEM analysis of PS-DVB (1:1, 1.5:1 and 10:1), PSQ and E-PS material showed the porous nature of all the polymeric materials. The EDS of PS-DVB polymeric materials proved dominant elements to be carbon and oxygen. Both the XRD and Raman spectroscopy proved that the PS-DVB, PSQ and E-PSQ are amorphous in nature. The TGA results showed that the PSQ and E-PSQ were more stable to high temperatures compared to all PS-DVB. The materials decomposed at temperatures higher than 50 °C, which is higher than the oven temperature of the HPLC. Pore sizes and volumes for PS-DVB were 2–18 nm and 0.0003–0.06 cm^3/g, respectively; for the PSQ the pore sizes were found to be 2–6 nm with pore volumes of 0.001–0.7 cm^3/g. The FTIR, SEM, XRD, Raman and BET show that E-PSQ and PS-DVB (1.5:1) were the most stable and suitable polymeric materials to be chosen as SEC stationary phases.

CHAPTER 7: APPLICATION OF POLYSILSESQUIOXANE AND POLY (STYRENEDIVINYL BENZENE) COMPOSITE MATERIAL AS SOLID-PHASE EXTRACTION (SPE) AND GEL PERMEATION (GPC) STATIONARY PHASES

7.1 INTRODUCTION

This chapter provides the details of the application of a composite of polysilsesquioxane (E-PSQ) and poly(styrene-divinyl benzene) (PS-DVB) as solid-phase extraction (SPE) and also as gel permeation chromatography (GPC) stationary phases. The optimal ratio of the two polymeric materials was obtained through optimising experiments performed by packing the materials at various ratios (w/w) on empty SPE cartridges and eluting a known compound, then measuring the efficiency in terms of recoveries. Thereafter, the polymeric material with the optimised ratio was packed on an empty column of SEC/GPC.

7.2 EFFICIENCY OF E-PSQ/PS-DVB AS COMPOSITE ONTO SOLID PHASE EXTRACTION (SPE) CARTRIDGES

7.2.1 Sorbent quantity optimisation

To determine the optimal ratio of the two polymeric materials (PS-DVB and E-PSQ) as GPC stationary phases, empty SPE cartridges were used to pack the materials at different ratios. Samples of humic acid (HA) were prepared at concentrations of 1, 3, 5 and 10 mg/ℓ to represent NOM. Humic acid forms part of the humic substances (HSs) of NOM, which are known to be a major part of NOM, as HSs constitute about 70% of the total organic carbon (TOC) (Matilainen *et al*., 2010; Nkambule *et al*., 2012b). Since the concentration of NOM can be measured as TOC, the TOC of HAs were first investigated using TOC (Teledyne Tekmar TOC Fusion, USA) (**Table 7-1**). Prior to the elution on all the packed SPE cartridges, TOC was measured for the samples after they were eluted from packed SPE columns (**Table 7-2**).

7.2.2 Total organic carbon measurements

The results of TOC measurements before and after elution with SPE are presented in **Tables 7-1** and **7-2**, respectively. **Table 7-1** reports on the TOC concentration of HA before elution through the packed SPE cartridges. From the results presented in **Table 7-2**, there was either an increase or decrease of the TOC value in each cartridge. The compositions of the stationary phases (1:1, 4:1 etc.) were chosen to in order to determine the best sorbent quantity for the fractionation of NOM. The E-PSQ:PS-DVB ratio of 4:1 showed an increase in the TOC values after fractionation as compared to the initial TOC values (**Table 7-1**). This was attributed to organic carbon leaching from the stationary phase materials. However, the 3 mg/ℓ sample of HA showed the least increase in TOC, with a value of 7.35 mg/ℓ as compared to other values which were above 9 mg/ℓ. This indicates that the organic carbon leaching was kept at a minimum.

Both the 1:1 PS-DVB:E-PSQ and E-PSQ: PS-DVB ratio registered organic carbon leaching and retention by the stationary phases, since there is a decrease in TOC up to 0.00 mg/ℓ and an increase of TOC up to a concentration of 24 mg/ℓ. When 3 mg/ℓ of HA was eluted through the PS-DVB: E-PSQ ratio of 1:1 the stationary phase retained all the organic carbon such that no organic carbon was detected by the instrument (**Table 7-**

2). The same trend was observed with the 1 mg/ℓ HA, which was retained by the E-PSQ: PS-DVB (1:1) stationary phase. The carbon cartridge showed the maximum leaching, while the C-18 cartridge overall had the least carbon leaching. The C-18 and carbon cartridges were commercially bought while all other cartridges were hand-packed. Organic carbon leaching from hand-packed cartridges is due to the inaccuracy of the packing process, while the leaching from the carbon and C-18 cartridge is due to excess organic carbon available as the stationary phase.

From data shown in **Table 7-2**, it is clear that both the sorbent ratios, PS-DVB:E-PSQ ratio (1:1, w/w) and the E-PSQ: PS-DVB (1:1, w/w)) had the lowest TOC leaching as compared to other composition of PS-DVB: E-PSQ and E-PSQ: PS-DVB as well as commercial carbon and C-18 SPE cartridges. However, the E-PSQ: PS-DVB (1:1, w/w) proved to have less TOC leaching than the PS-DVB:E-PSQ ratio (1:1, w/w) and was therefore selected (as the best sorbent quantity) for the GPC column packings.

Table 7-1 TOC values for all samples before SPE elution

Aliquot	TOC (mg/ℓ)
HA-1	0.95
HA-2	3.04
HA-3	5.3
HA-4	10.36

Table 7-2 TOC values for samples after SPE elution

E-PSQ/PS-DVB ratio	HA-1 (TOC) at 1 mg/ℓ	HA-2 (TOC) at 3 mg/ℓ	HA-3 (TOC) at 5 mg/ℓ	HA-4 (TOC) at 10 mg/ℓ
1. PS-DVB:E-PSQ (0.8:0.2)	7.49	16.32	25.31	16.30
2. PS-DVB:E-PSQ (0.2:0.8)	22.76	13.58	21.51	21.90
3. E-PSQ:PS-DVB (0.2:0.8)	27.15	23.22	15.26	15.32
4. E-PSQ:PS-DVB(0.8:0.2)	11.82	7.35	18.06	26.85
5. PS-DVB:E-PSQ (0.5:0.5)	12.00	0.00	20.27	22.89
6. E-PSQ:PS-DVB (0.5:0.5)	0.00	18.80	16.3068	24.01
7. E-PSQ	25.92	12.58	10.19	6.19
8. PS-DVB	6.19	24.40	17.18	14.48
9. Carbon	16.62	24.99	26.09	28.08
10. C-18	9.80	10.24	9.55	12.92

7.2.3   Fluorescence excitation emission matrices (FEEM) analysis

The eluents from the ratio selected were then further characterised using FEEM, in order to confirm the organic leaching and to further identify the NOM types remaining from HA eluents. The FEEM method normally provides information about the types of NOM present in different fractions (Penru *et al*., 2013). This method classifies NOM by giving a unique absorption and excitation pattern of NOM at a specific region (Chen *et al*.,

2003). The regions of interest are fulvic-like (Ex 325 nm, Em 425 nm), humic-like (Ex 350 nm, Em 475 nm) and the tryptophan-like (225 nm ≤ Ex≤ 450 nm, Em 450) acids (Nkambule *et al*., 2013).

The NOM that was selected is known to be a hydrophobic NOM (Matilainen *et al*., 2002; Penru *et al*., 2013; Yunos *et al*., 2014). The FEEM results shown below indicate the type of NOM to be humic-like (**Figure 7-1 (a)**) and tryptophan-like (**Figures 7-1 (b)** – **(d)**). The FEEM results also show the leaching of TOC from the selected E-PSQ:PS-DVB (1:1, w/w), which affect the nature and morphology of NOM. The hand-packing SPE procedure was inaccurate, since the pressure was not controlled and flow of solvents was not constant during the fractionation/separation of HA. The vacuum pump had a pressure adjustable knob, hence non-constant pressure.
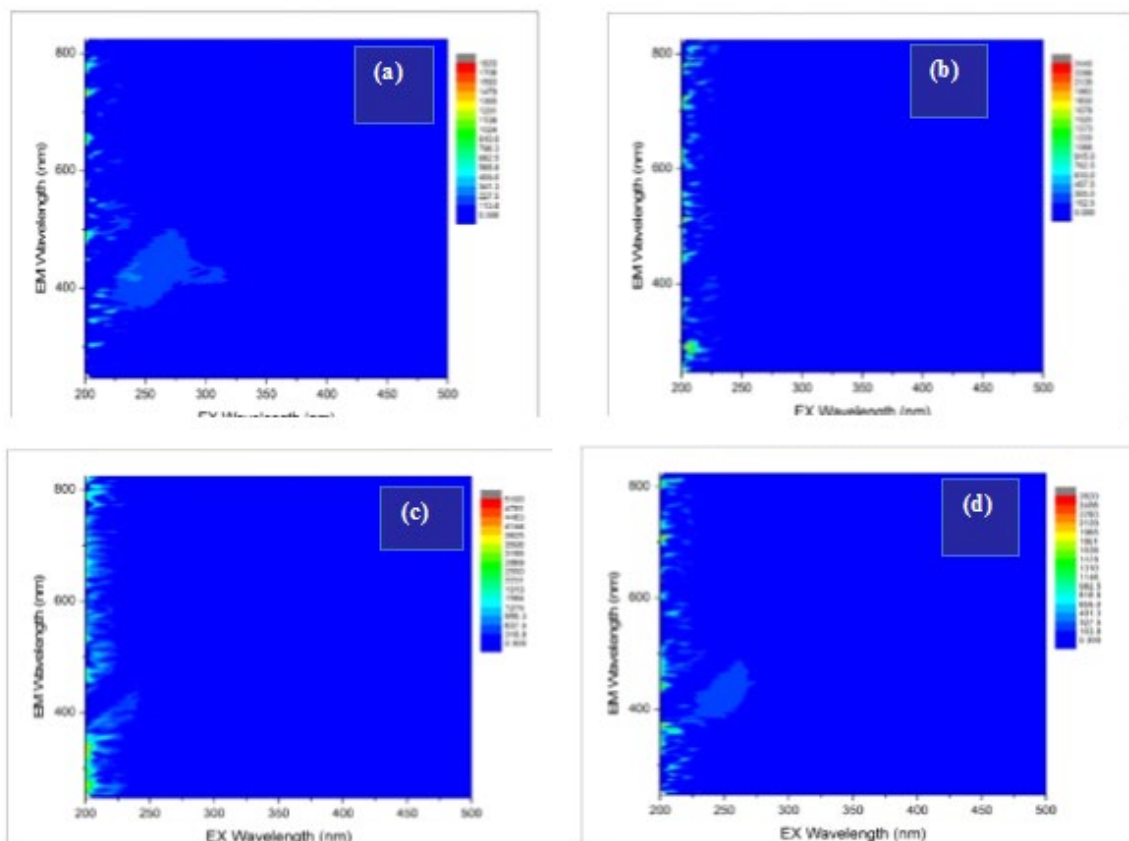
Figure 7-1 FEEM graphs for HA eluents from 1 mg/ℓ (a), 3 mg/ℓ (b), 5 mg/ℓ (d) and 10 mg/ℓ (c)

7.2.4   Ultraviolet-visible (UV-Vis) and specific ultraviolet absorbance (SUVA) analysis

In order to identify the nature of NOM in each sample, both SUVA and UV analysis were carried out. UV_{254} absorbance measures the presence of humic substances, while SUVA values of >2, 2–4, >4 ℓ/mg.m correspond to the HPI, TPI and HPO part of NOM, respectively.

Table 7-3 summarises the UV-Vis results obtained from HA eluents from cartridge 5 at different concentrations. The SUVA calculations were carried out using **equation 3.1** in order to assess the concentrations of the HPI, HPO and TPI fraction of NOM (Xia *et al*., 2014).

Table 7-3 UV-Vis and SUVA values of HA eluents from cartridge 5

PSQ/PS-DVB ratio (1:1) 2 g	UV-Vis (cm^{-1})	SUVA ℓ/mg.m

Cartridge 5 at 1 mg/ℓ	2.57	17
Cartridge 5 at 3 mg/ℓ	0.148	0
Cartridge 5 at 5 mg/ℓ	2.322	11
Cartridge 5 at 10 mg/ℓ	2.886	12

The SUVA provides information on the specification of humic substances versus the non-humic substances of NOM (Nkambule *et al*., 2009a; 2009b). SUVA can also be used as a tool to determine the nature of the organics found in NOM samples with regard to the aromaticity and conjugated C=C bonds (Fabris, 2008; Papageorgiou *et al*., 2016). The SUVA values from **Table 7-3** are relatively high compared to SUVA values obtained from the literature, thus indicating high aromaticity associated with the hydrophobic NOM fraction (Quaranta *et al*., 2012; Papageorgiou *et al*., 2016). The information in **Table 7-3** indicates that the samples are rich in humic substances; these are actually the hydrophobic fraction of NOM since the SUVA value is above 4 4 ℓ/mg.m (Nkambule *et al*., 2011; Quaranta *et al*., 2012).

7.3 EFFICIENCY OF E-PSQ/PS-DVB AS STATIONARY PHASE FOR GEL PERMEATION CHROMATOGRAPHY (SEC/GPC)

Packing the SEC/GPC column was achieved with constant pressure (0–500 sand flow-rate of 0.2 mℓ/min). To test for the efficiency of the column, various performance tests on the packed columns were undertaken.

7.3.1 Packed column performance tests

7.3.1.1 Interactions with acidic compounds

7.3.1.1.1 Activity towards acids

The packed SEC/GPC column was tested against 4-chlorocinnamic acid (**Figure 7-2**). The column was able to elute a peak of the analyte at about 10 minutes. This was achieved using a mobile phase of ratio 30:70 (methanol/aqueous 0.02 M phosphate buffer of pH 2.7) (Claessens, 1999), flow rate of 0.25 mℓ/min, sample volume of 5 μℓ, column temperature of 40 °C, elution time of 15 minutes, and wavelength of 254 nm. When compared with literature data (Sander and Wise, 2003; Vantran *et al*., 2003), the test results imply that it can be used for the acidic analytes such as those forming NOM composition (humic acids, fulvic acids).
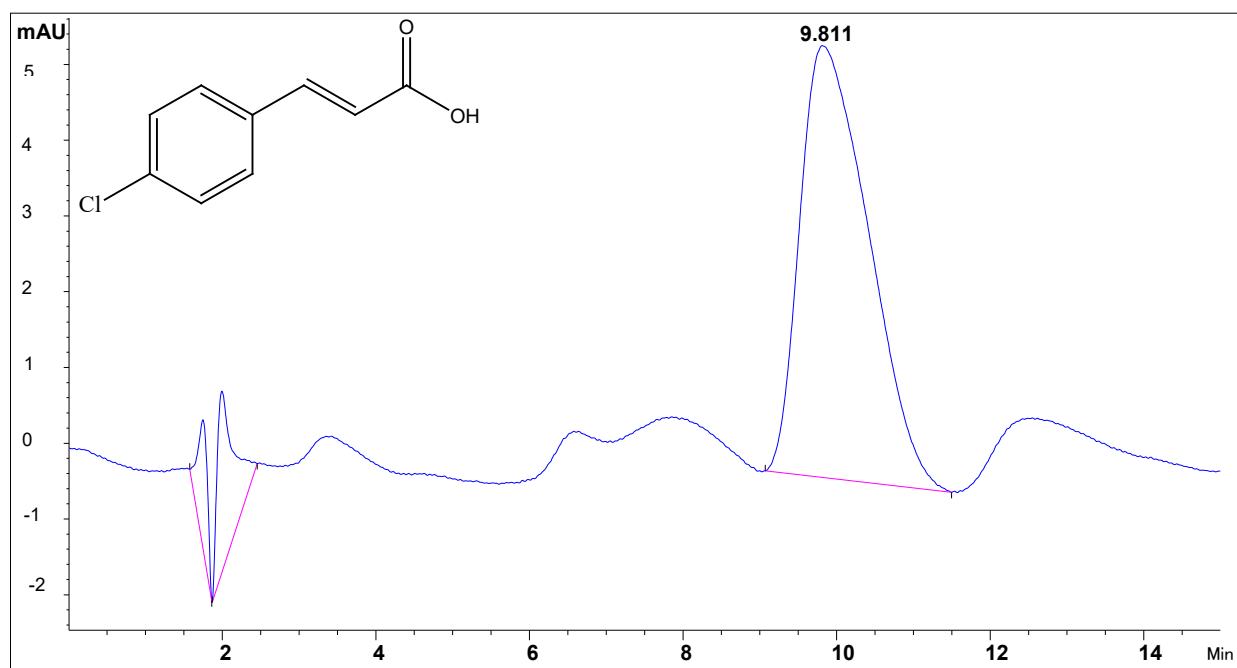
Figure 7-2 Chromatogram of 4-chlorocinnamic acid using E-PSQ/PS-DVB (0.5:0.5; w/w) as stationary phase

7.3.1.1.2 Tanaka test (Acidic ion exchange capacity)

This test measured acidic (H^+) activity of the silanol groups present on the stationary phase (Eureby *et al*., 2007). The concentration used for the analytes was 5 mg/mℓ. The retention factor of protonated silanol (SiO^-) was estimated by the selectivity factor (**equation 7.1**) between phenol and benzyl amine. The benzyl amine was retained in the column and was eluted at around 7 minutes while the phenol was eluted at around 2.5 minutes (**Figure 7-3**). The selectivity factor of the two analytes was found to be 9 (higher than that of C-18 and lower than that of Zr-PBD); this is an acceptable value since the retention factors of commercial columns such as Discovery C-18, Discovery Zr-PBD, ACE phenyl, ACE AQ and Discovery F5 were reported to be 0.0672, 23.288, 0.14, 0.11 and 0.34, respectively (Eureby *et al*., 2007; Sigma-Aldrich, 2017). This high value of the selectivity factor of the two analytes indicates that the column has minimum silanol groups. The compounds were eluted in the column by using a mobile phase of ratio 30:70 (methanol/aqueous 0.02 M phosphate at pH 2.7) (Claessens, 1999), with the flow rate of 0.25 mℓ/min, sample volume of 5 µℓ, column temperature of 40 °C, elution time of 15 minutes, and wavelength of 254 nm.
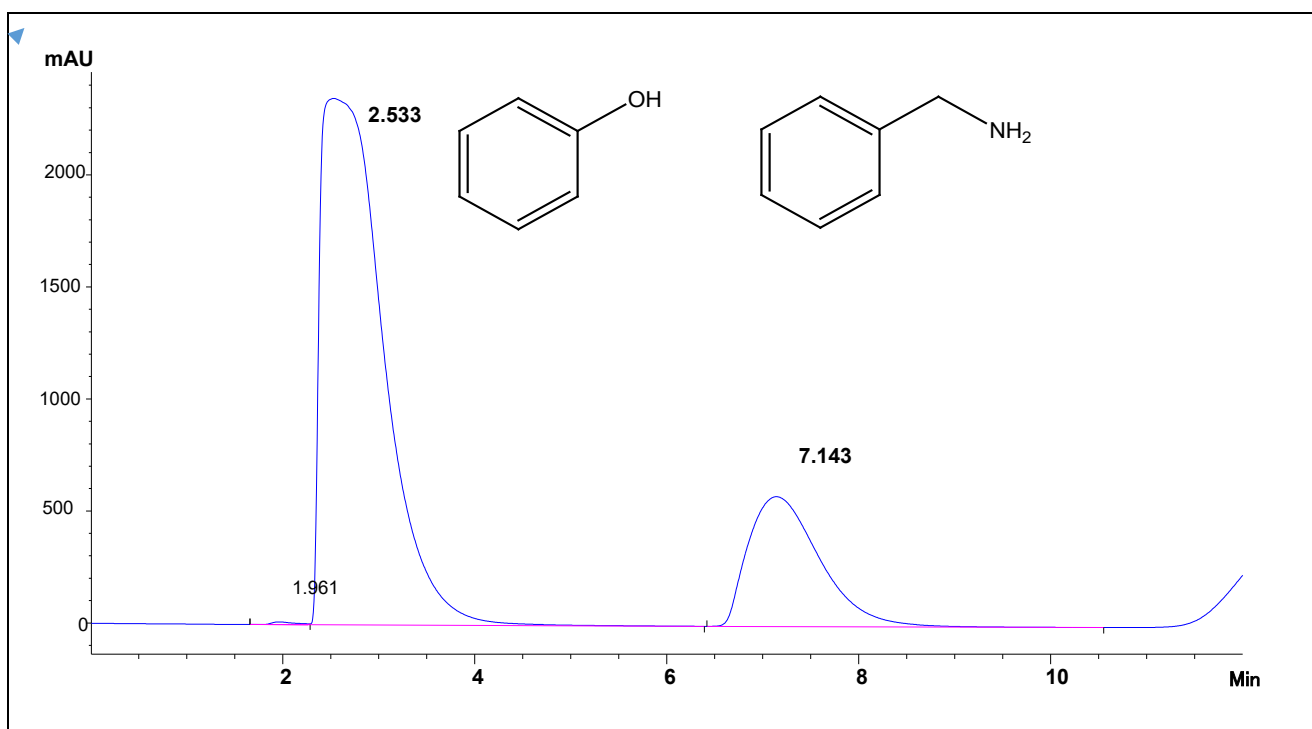
Figure 7-3 Chromatogram of phenol and benzyl amine using E-PSQ/PS-DVB (0.5:0.5; w/w) as stationary phase

7.3.1.2 Hydrophobic interactions

7.3.1.2.1 Hydrophobic retention (HR)

This test reveals the surface area and surface coverage of the stationary phase with the aid of calculating the retention factor pentyl benzene (K_{PB}) (Eureby *et al*., 2007). This parameter was evaluated by eluting pentyl benzene in a column packed with the PS-DVB: E-PSQ. The K_{PB} value was calculated using the **equation 7.1**. The retention factor of analyte was found to be 0.87, different from the literature values for Discovery C-18, Discovery Zr-PBD, ACE phenyl, ACE AQ and Discovery F5 are quoted as 3.19, 0.86, 1.20, 2.30 and 1.70, respectively (Eureby *et al*., 2007, Sigma-Aldrich, 2017). The broad peak that resulted is due to the high concentration (i.e. 5 mg/mℓ) of the analyte. The results obtained show that the strength of the stationary phase is different to that of the commercial columns (**Figure 7-4**), this may be caused by the mixture of two stationary phases (E-PSQ: PS-DVB). The experimental conditions are as follows: Water/methanol (20; 80 v/v) was used as mobile phase (Minakuchi *et al*., 1998; Tanaka *et al*., 2001), flow rate of 0.25 mℓ/min; sample volume of 5 μℓ; column temperature of 40 °C; elution time of 10 minutes; and wavelength of 254 nm.
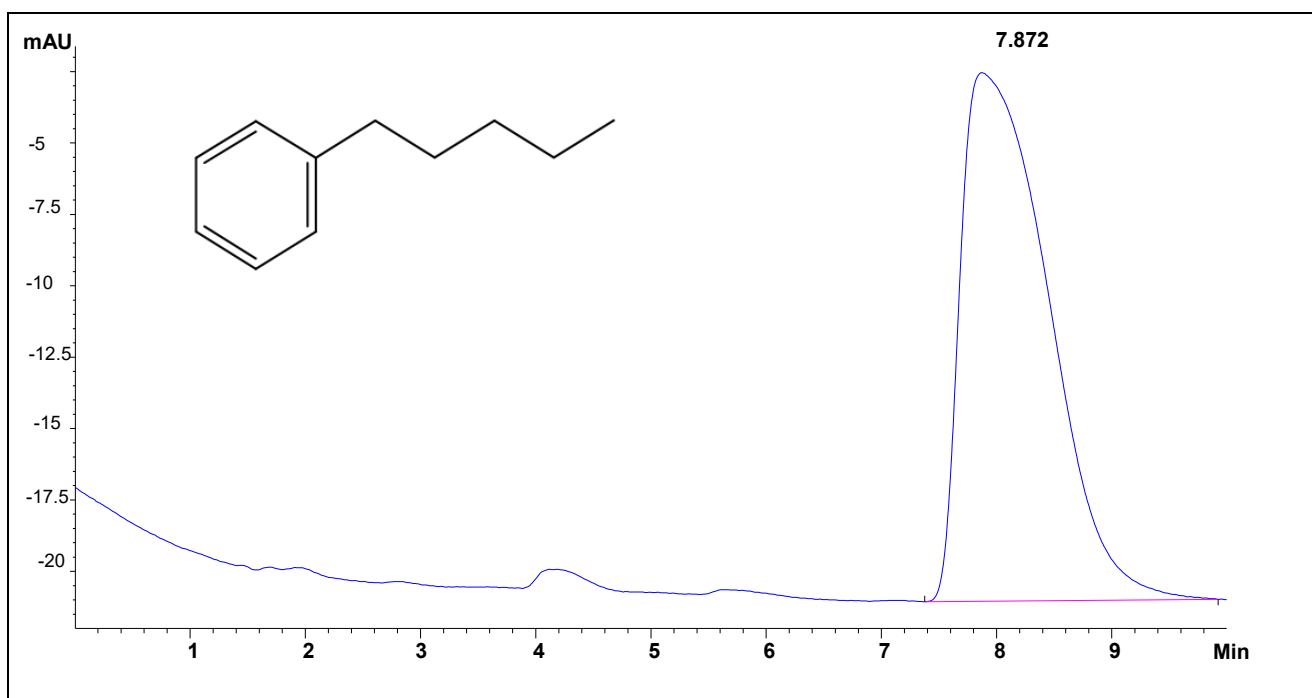
Figure 7-4 Chromatogram of pentyl benzene using E-PSQ/PS-DVB (0.5:0.5; w/w) as stationary phase

7.3.1.2.2 Hydrophobic selectivity (HS)

This test measured the retention factor ratio between the two alkylbenzene analytes (pentylbenzene (PB) and butylbenzene (BB)); the retention factor is calculated using **equation 7.1** $\alpha CH2 = k_{PB}/k_{BB}$ (Eureby *et al*., 2007). This test also measures the surface coverage of the stationary phase as it can separate alkylbenzenes with different chains of alkyl group (Eureby *et al*., 2007). The separation is shown in **Figure 7-6**. The PB and BB were eluted through the column with 80:20 (v/v) methanol/water mobile phase (Claessens, 1999), flow rate of 0.25 mℓ/min, sample volume of 5 µℓ, column temperature of 40 °C, elution time of 10 minutes, and wavelength of 254 cm^{-1} using the DAD detector. The first peak appearing at around 5.6 minutes is associated with the pentyl benzene and the second peak, at around 7.9 minutes, concurs with butyl benzene (**Figure 7-5**). The retention factor was found to be 0.574; however, this value is lower than expected since the values for Discovery C-18, Discovery Zr-PBD, ACE phenyl, ACE AQ and Discovery F5 were found to be higher (1.406, 1.423, 1.26, 1.35 and 1.26, respectively) (Eureby *et al*., 2007; Sigma-Aldrich, 2017). The elution sequence of the two molecules as well as the retention factor ratio obtained is lower than commercial columns, but the peaks on the chromatogram prove that the column can selectively elute molecules based on their densities.
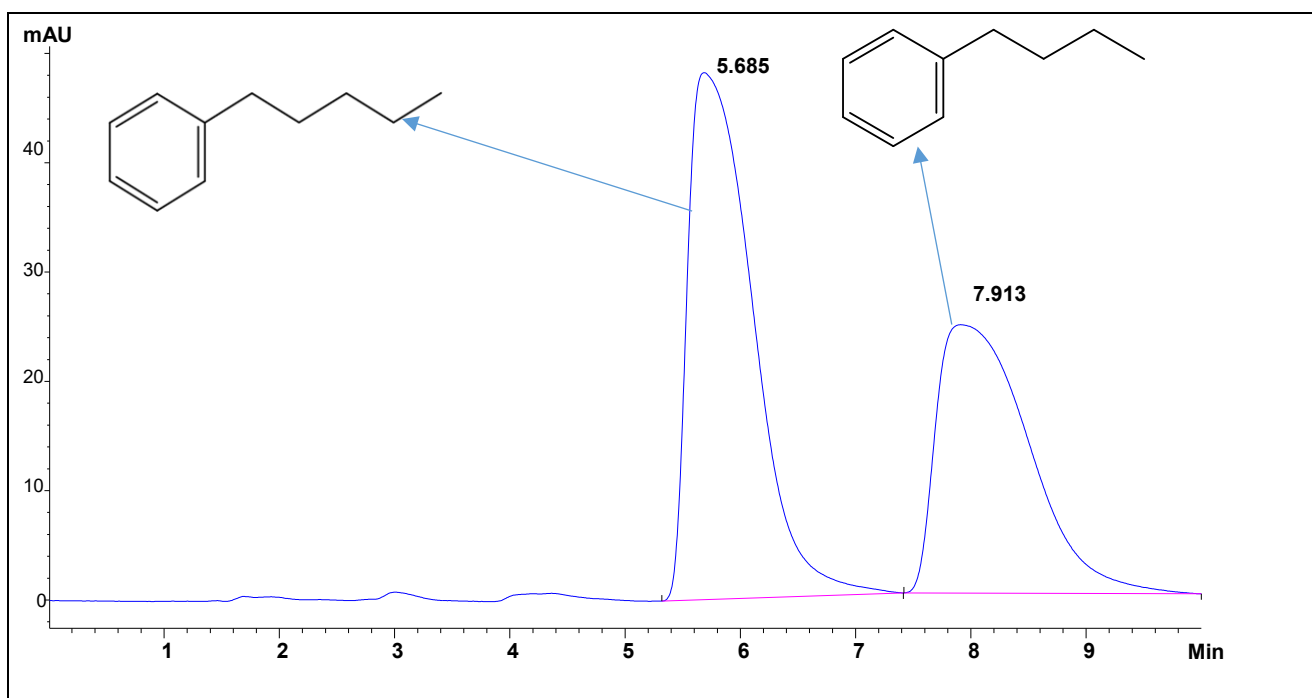
Figure 7-5 Chromatogram of pentyl benzene and butyl benzene

7.3.1.2.3 Steric selectivity (SS)

This test measured retention factor ratio between triphenylene (T) and o-terphenyl (O), (α T/O = k_T/k_O) (Eureby $et\ al$., 2007). Steric selectivity measures the ability of the stationary phase to distinguish between molecules with similar hydrophobicity and structure but different shapes. The steric selectivity was successful since the elution times of o-terphenyl and triphenylene were found to be 6.6 minutes and 10.1 minutes, respectively (**Figure 7-6**). The retention factor ratio value was found to be 0.61, which is slightly lower than the literature values of 1.474, 1.634, 1.00, 1.22 and 2.55 for Discovery C-18, Discovery Zr-PBD, ACE phenyl, ACE AQ and Discovery F5, respectively (Eureby $et\ al$., 2007; Sigma-Aldrich, 2017). The two compounds were eluted through the column using a mobile phase with 80:20 (v/v) methanol/water (Claessens, 1999), flow rate of 0.25 mℓ/min, sample volume of 5 µℓ, column temperature of 40 °C, elution time of 10 minutes, wavelength of 254 and the DAD detector. The chromatogram in **Figure 7-6** shows two peaks which correspond to the two analytes, therefore the packed GPC column can separate the two analytes.
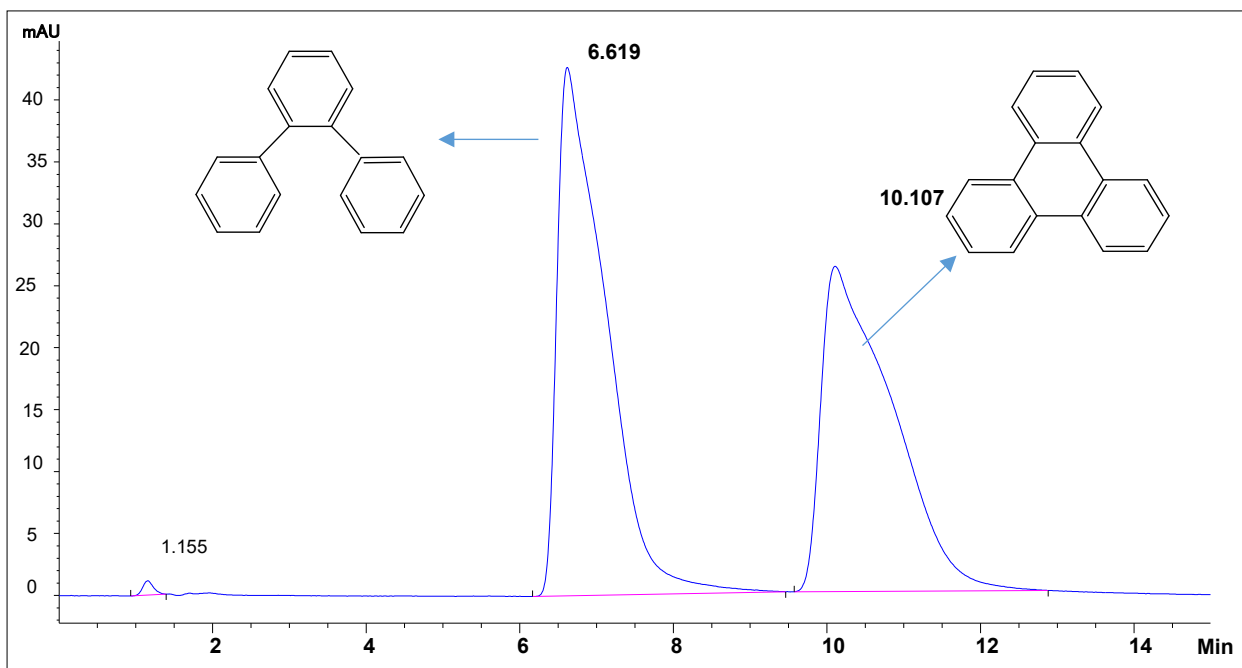
Figure 7-6 Chromatogram of O-terphenyl and Triphenylene

7.3.1.2.4 Hydrogen bonding capacity (HBC)

This technique measured the number of free silanol groups and the degree of end capping by comparing the relative retention of caffeine with respect to phenol and by calculating the retention factor ratio between caffeine (C) and phenol (P) using the equation $\alpha C/P = k_C/k_P$ (Eureby *et al*., 2007). The obtained retention factor ratio of 0.43 is comparable to the values of commercial columns such as Discovery C-18, Discovery Zr-PBD, ACE phenyl, ACE AQ and Discovery F5 which are 0.615, 0.307, 1.14, 0.48 and 0.68, respectively (Eureby *et al*., 2007; Sigma-Aldrich, 2017). The results in **Figure 7-7** show that there are minimum silanol groups and the end-capping on the E-PSQ was successful. Methanol and water (30:70 v/v) were used as mobile phase (Claessens, 1999), flow rate of 0.25 mℓ/min, sample volume of 5 µL, column temperature of 40 °C, elution time of 10 minutes, wavelength of 254 and the DAD detector.
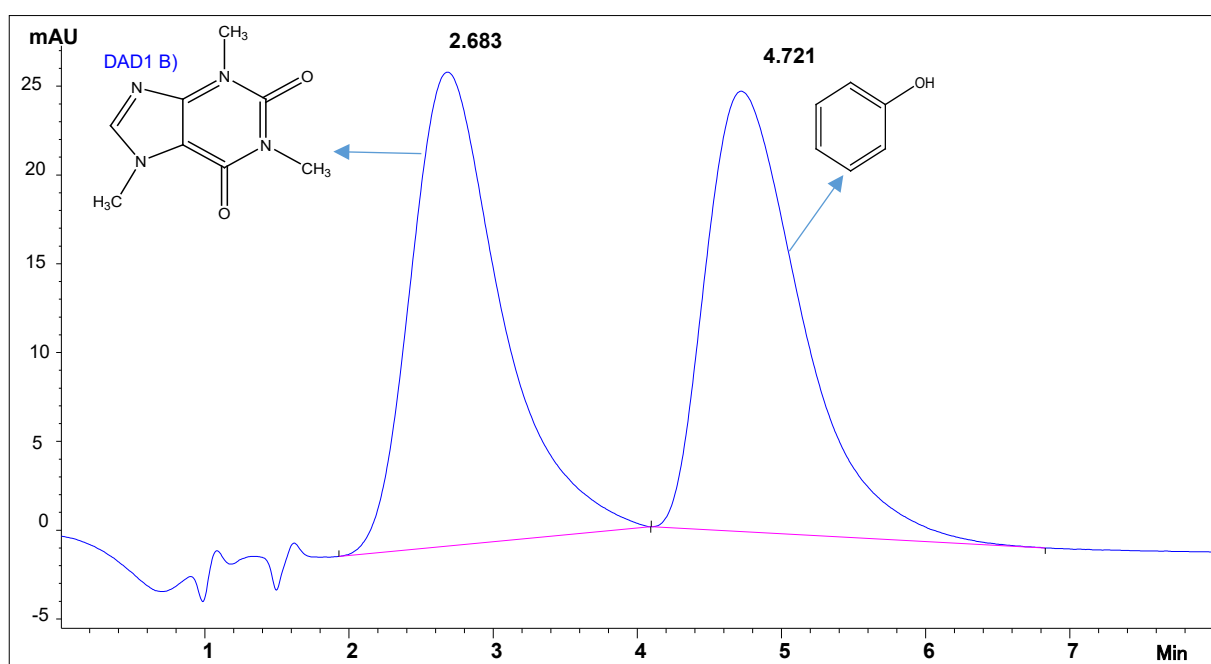
Figure 7-7 Chromatogram of caffeine and phenol

7.3.1.3   Stability at high pHs

The stability of the stationary phase at basic pH ranges using amitriptyline as an analyte (see **Figure 7-8**) was eluted with a mobile phase of 30:70 methanol/aqueous 0.02 M phosphate at pH 7.6 (Claessens, 1999), flow rate of 0.25 mℓ/min, sample volume of 5 µℓ, column temperature of 40°C, elution time of 10 minutes, wavelength of 254 nm and the DAD detector. The values of the capacity factor (**equation 7.2**) and tailing factor (**equation 7.3**) were evaluated. The capacity and tailing factor of amitriptyline was found to be 0.22 and 0.65, respectively, indicating that the column can tolerate high pH values (Sander and Wise, 2003).

$$T_f = \frac{AB}{2AC}$$

[Equation 7.2]
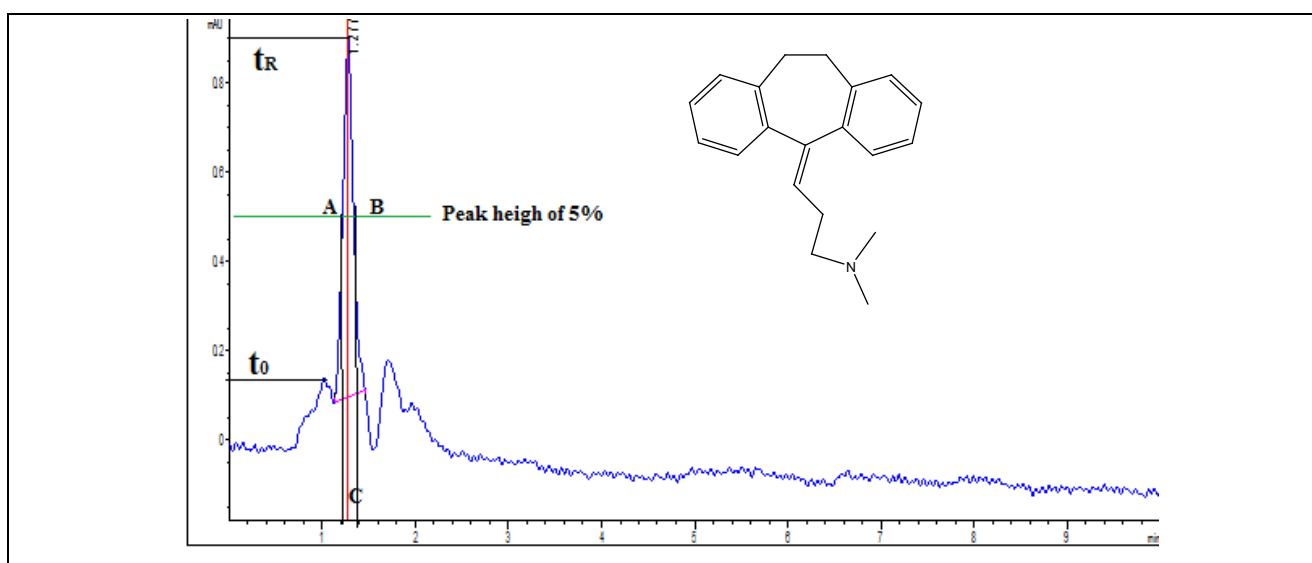
Figure 7-8 Chromatogram of amitriptyline

7.3.1.4   Ion exchange capacity

This parameter was investigated by eluting a mixture of benzyl amine and phenol. This test estimates the total silanol activity by the retention factor of the two analytes at pH 5.6 (Eureby *et al*., 2007). The two compounds were eluted with a mobile phase of 70:30 aqueous 0.02 M phosphate/methanol at pH 7.6, (Claessens, 1999) flow rate of 0.25 mℓ/min, sample volume of 5 µℓ, column temperature of 40 °C, elution time of 10 minutes, wavelength of 254 and the DAD detector. The magnitude of the selectivity factor between benzyl amine and phenol was found to be 4 (**Figure 7-9**) when compared to Discovery C-18, Discovery Zr-PBD, ACE phenyl, ACE AQ and Discovery F5 values of 0.684, 24.309, 0.46, 0.32 and 0.85, respectively. (Eureby *et al*., 2007; Sigma-Aldrich, 2017). These results are not in agreement with results obtained from the commercial column, therefore there might be some silanol activity on the surface of the prepared stationary phase.
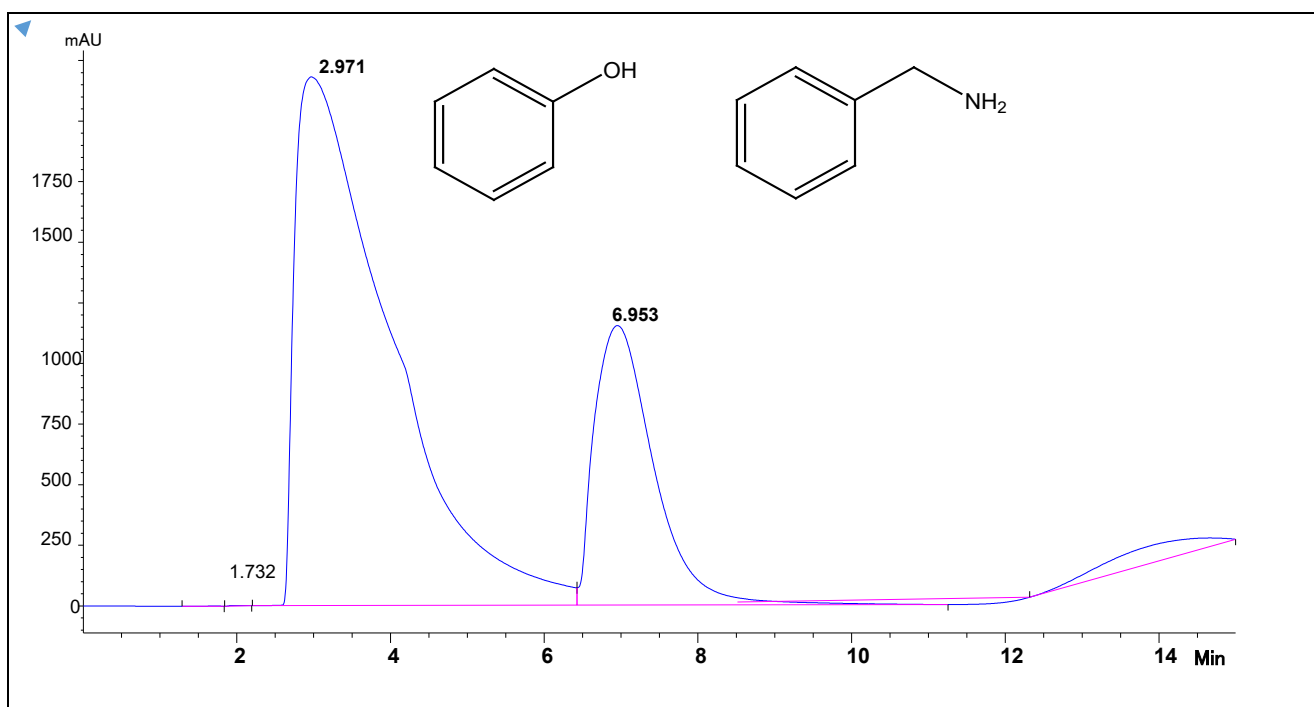
Figure 7-9 Chromatogram of benzyl amine and phenol

7.3.2   Fractionation of prepared and real NOM samples with the packed E-PSQ/PS-DVB GPC column

The packed column was then connected to a HPLC system to fractionate/separate the fulvic acid (FA), HA and real samples according to molecular weight. The SEC/GPC method is a popular method for separation of molecules according to different molecular weights (Fabris, 2008). The molecular weight separation of NOM was achieved by the elution of NOM through a porous stationary phase. Smaller molecules take a longer time to elute because they diffuse through the pores while large molecules do not diffuse through the pores and therefore elute much more quickly (Fabris, 2008). The pure standards of HA of concentrations 1, 3 and 5 mg/ℓ and FA concentrations of 1 and 5 mg/ℓ were eluted separately to test for the reproducibility of the elution time for both FA and HA.

The elution of FA at 1 mg/ℓ (**Figure 7-10 (a)**) and FA at 3 mg/ℓ (**Figure 7-10 (b)**) were found to be 1.286 minutes and 1.281 minutes, respectively; these elution times correspond to those of the humic substances reported in the literature (Pelekani *et al.*, 1999; Wong *et al.*, 2002; Fabris, 2008).
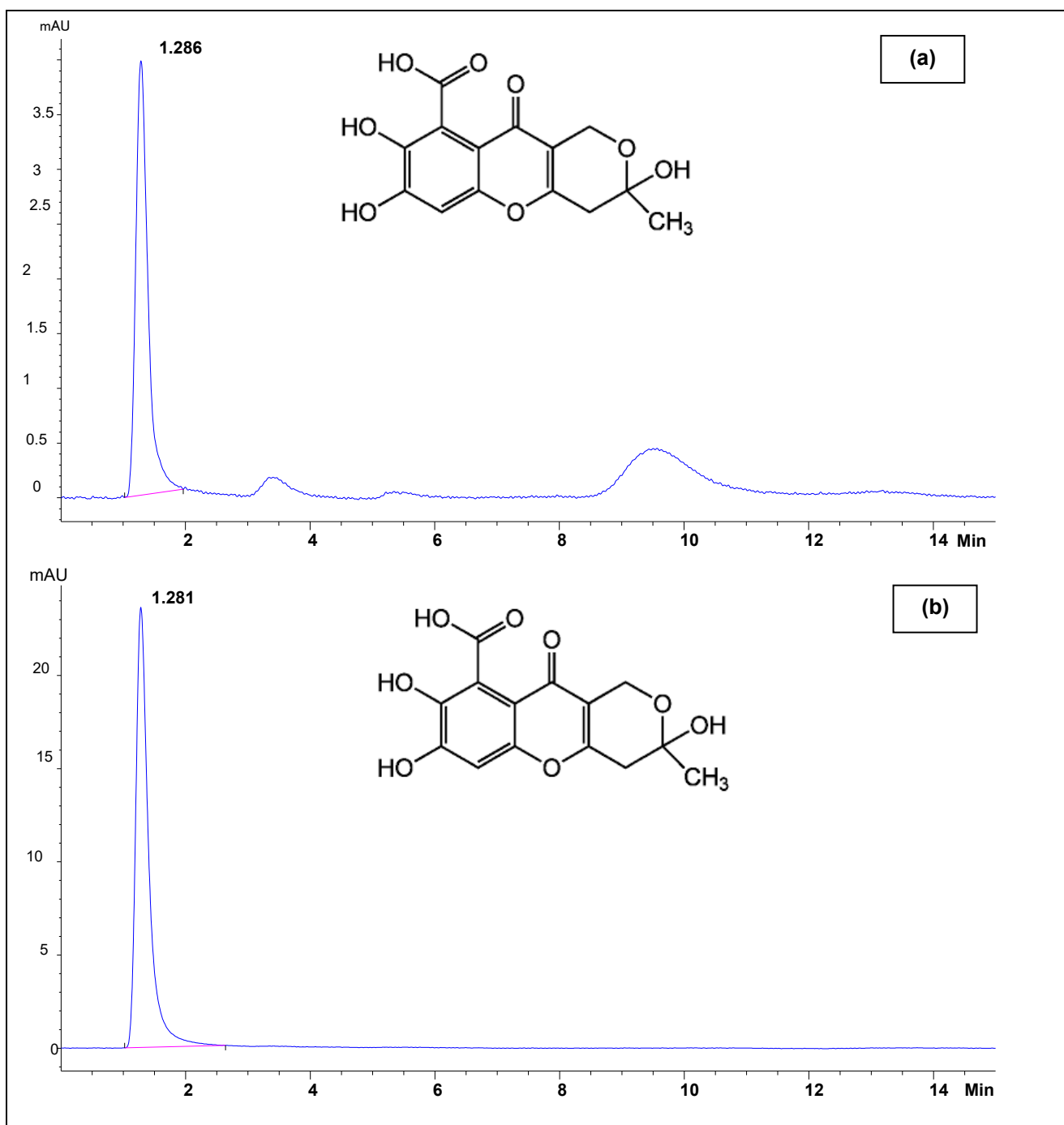
Figure 7-10 Chromatogram of FA at (a) 1 mg/ℓ and (b) 5 mg/ℓ

The separation of HA using the packed column showed a peak at around 1, 5 and 14 minutes for all three concentrations at 1 mg/ℓ (**Figure 7-11 (a)**), HA at 3 mg/ℓ, (**Figure 7-11 (b)**) and HA at 5 mg/ℓ (**Figure 7-11 (c)**). Three peaks were observed because the HA that was used contains 20% residues, most HA peaks were reported to be around 4.91 and 10 minutes depending on the eluent type and the source of HA (Świetlik *et al.,* 2004; Lyubomirova *et al*., 2011). These three peaks were taken as reference peaks for HA.
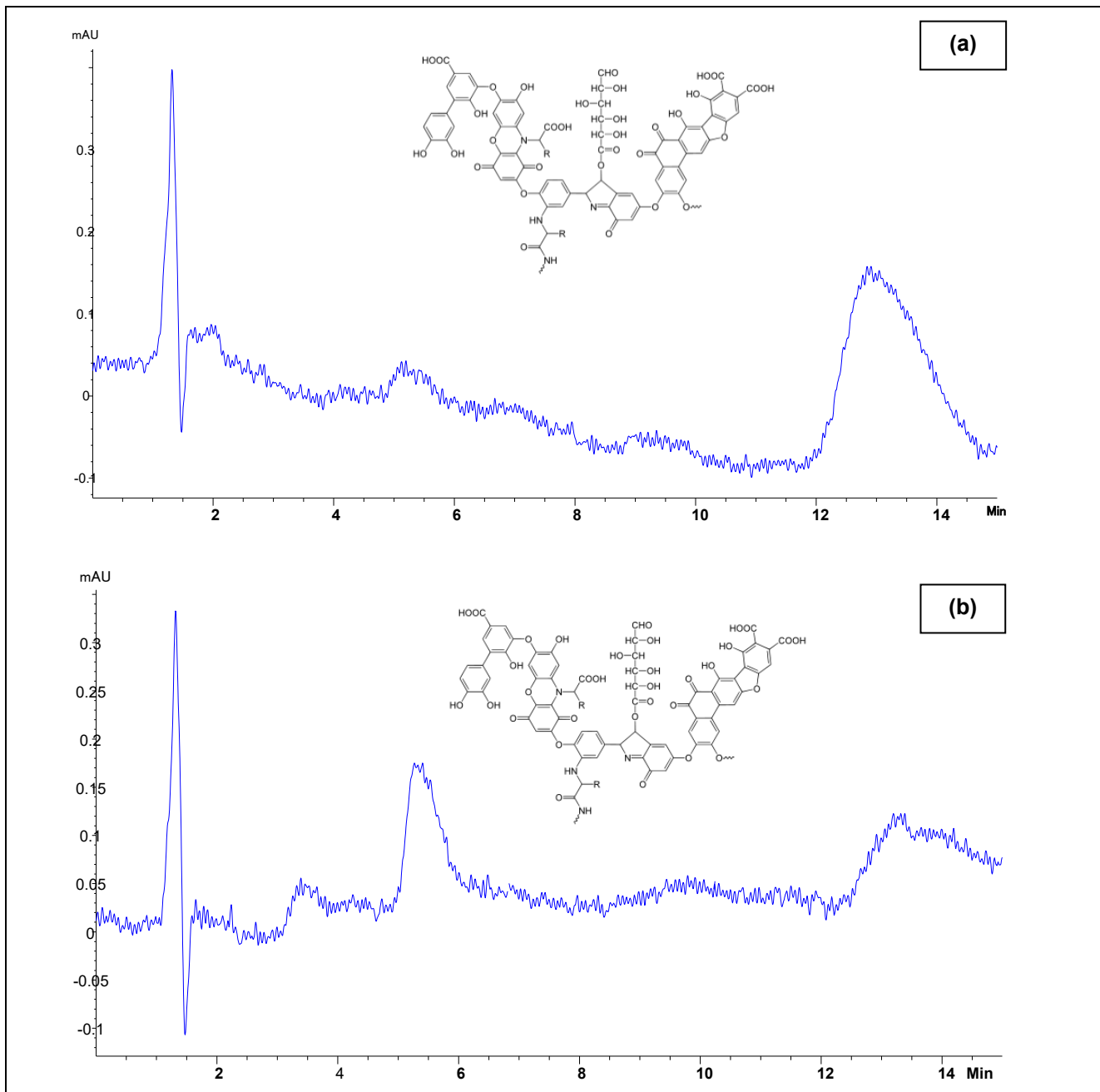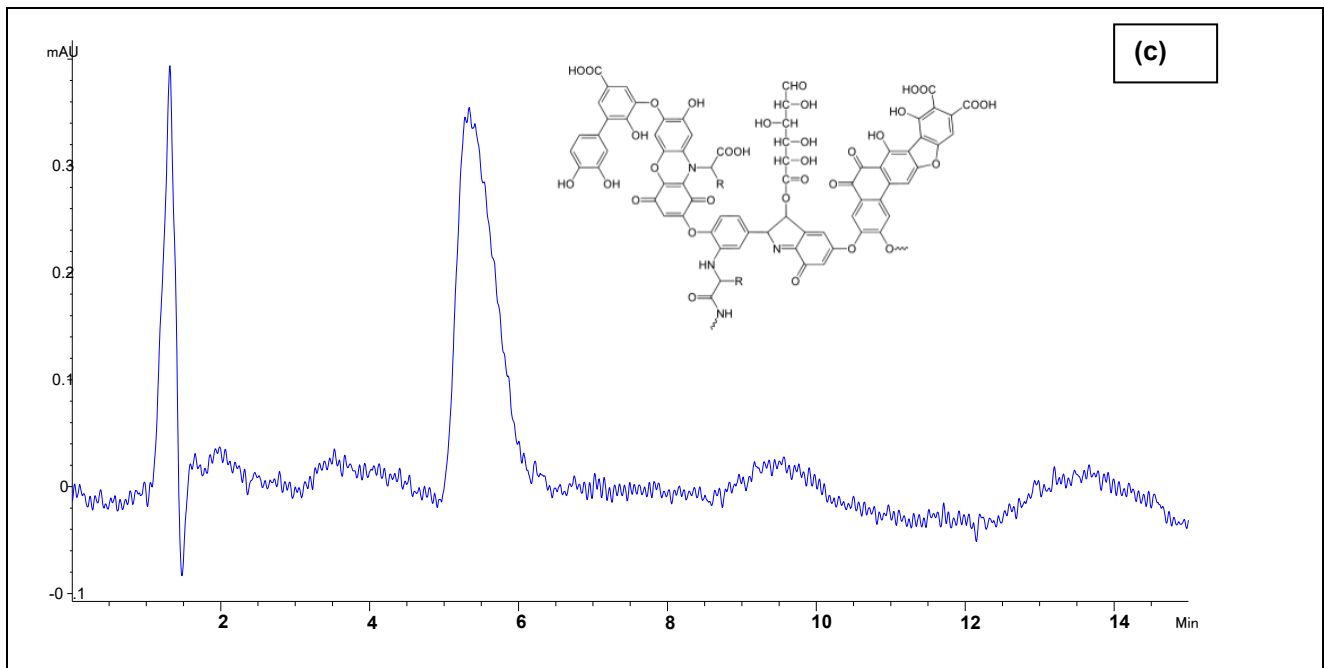
Figure 7-11 Chromatogram of HA samples at (a) 1mg/ℓ, (b) 3mg/ℓ) and (c) 5 mg/ℓ

All real samples were eluted with a mobile phase of 70:30 phosphate buffer:methanol and all other conditions were kept the same for column packing tests. Raw and final water samples (rich with hydrophobic (HPI) part of NOM) from the Olifantspoort (LO) water treatment plant in Limpopo Province (coordinates: 24° 21′1 6.308″ S, 29° 45′ 33.66″ E) were fractionated using the prepared GPC column. It was found that from the final water (TOC: 2.52 mg/ℓ, UV_{254}: 0.12 cm^{-1} and the SUVA value of 4.96 ℓ/mg.m) (**Figure 7-12**the raw water (TOC: 3.17 mg/ℓ, UV_{254}: 0.16 cm^{-1} and the SUVA value of 5.32 ℓ/mg.m) (see **Figure 7-13**) has traces of HA and FA. The peak at around 1.6 minutes corresponds to the peak from the prepared FA standard sample and the peak at around 5.8 minutes corresponds to one of the HA peaks. The results indicate that the current water treatment procedure does not remediate NOM completely. This is evidenced by the increase in the intensity of the HA and FA peak from raw to final samples
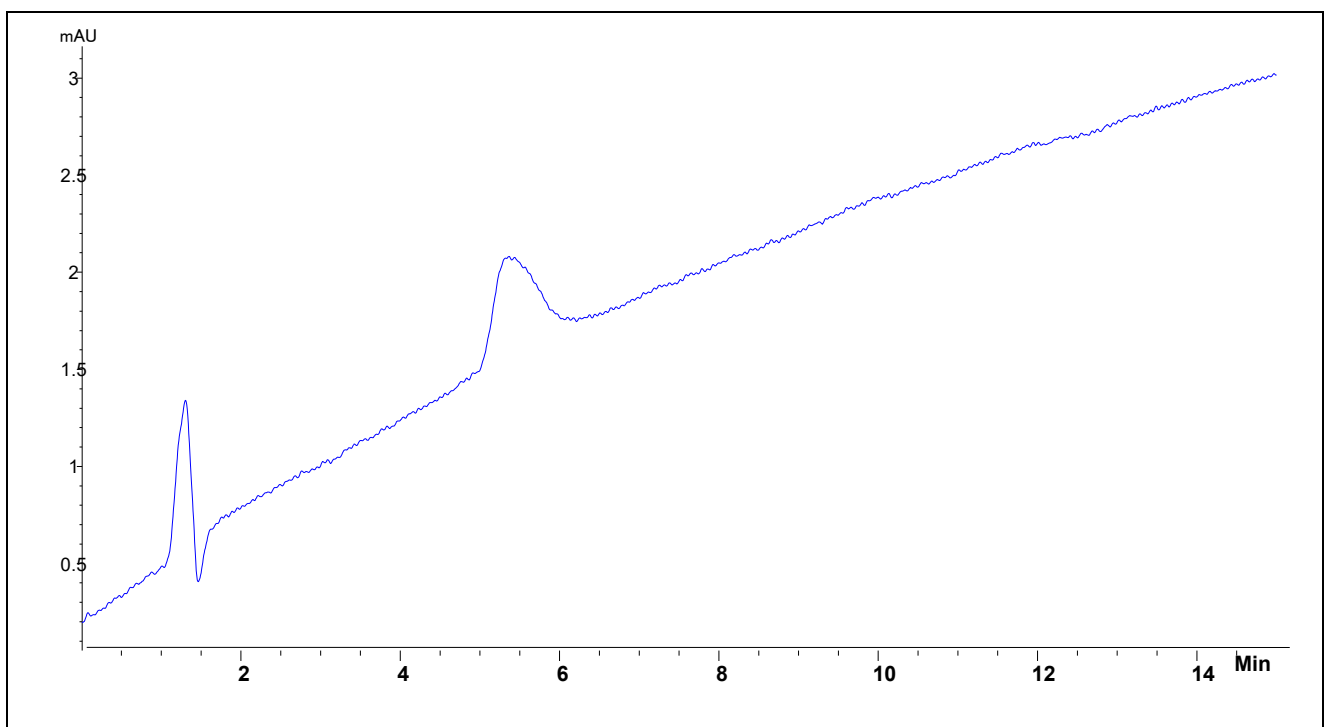
Figure 7-12 Chromatogram of LO final water sample
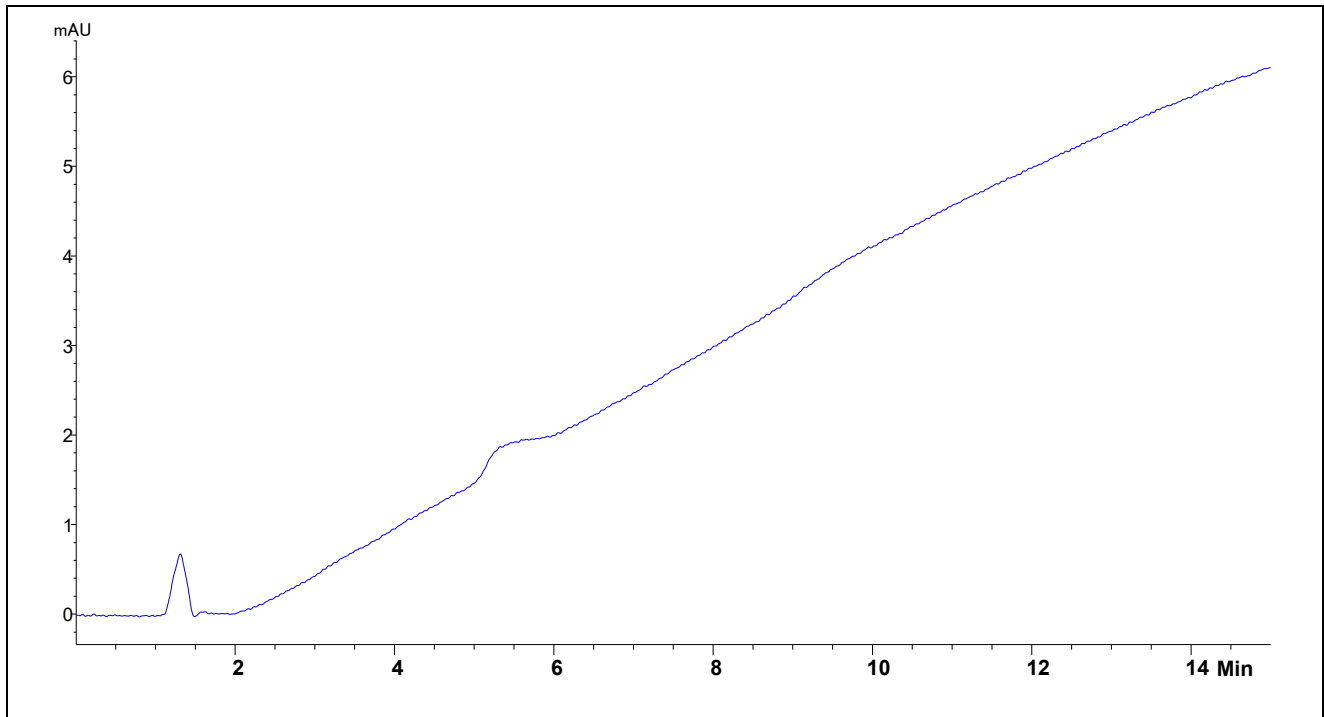
Figure 7-13 Chromatogram of LO water sample

The chromatograms obtained from the water samples of the Umgeni Mtwalume (MT) water treatment plant in Kwa-Zulu Natal (coordinates: 29.6033° S, 30.3847° E) indicate the presence of traces of FA at around 1.6 minutes and HA at around 5.8 minutes for the final samples (TOC: 0.88 mg/ℓ, UV$_{254}$: 0.12 cm^{-1} and SUVA value of 14.18 ℓ/mg.m) (**Figure 7-14**). The raw water samples (TOC: 4.28 mg/ℓ, UV$_{254}$: 0.24 cm^{-1} and SUVA value of 5.93 ℓ/mg.m) (**Figure 7-15**) indicate the presence of FA (1.6 minutes), HA (5.32) minutes and another peak at around 3.32 minutes. The disappearance of the third peak on the final water gave an indication that the current NOM water treatment was partially successful. The high SUVA value of the final water sample indicates deposition of the HPO fraction of the NOM (Nkambule *et al*., 2011).
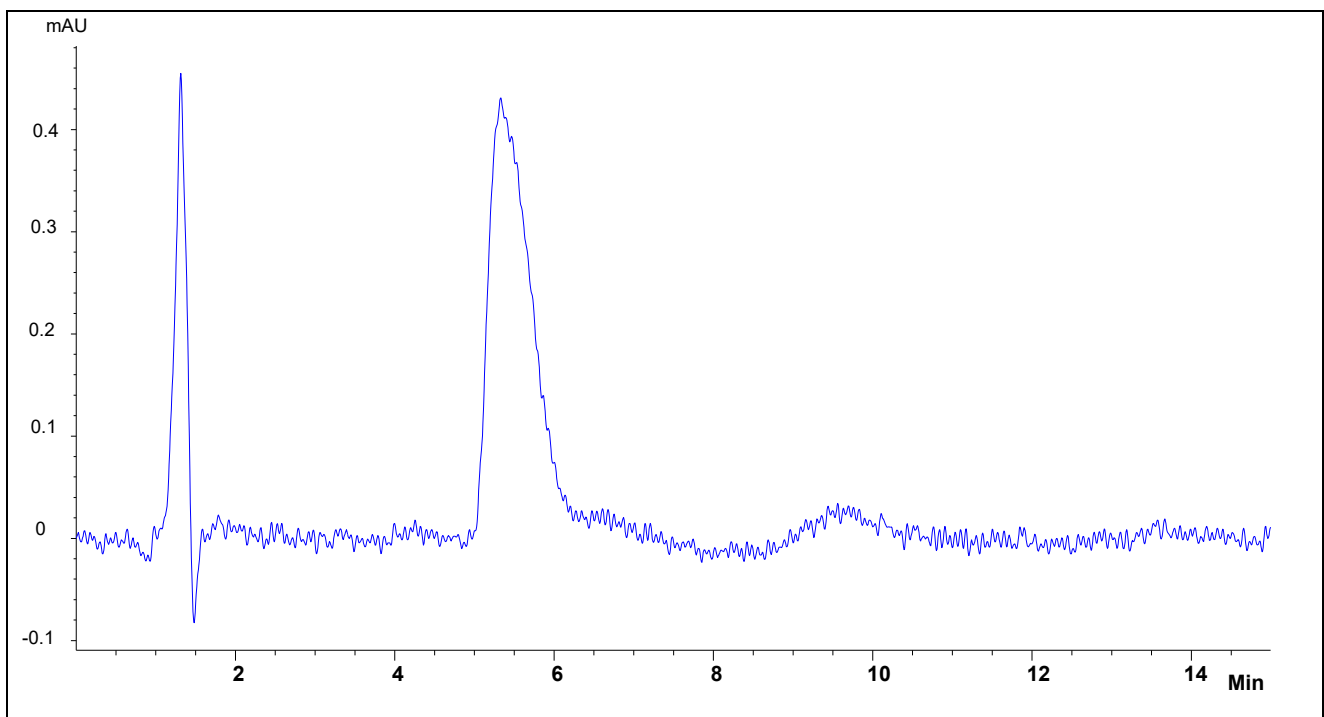
Figure 7-14 Chromatogram of MT final water sample
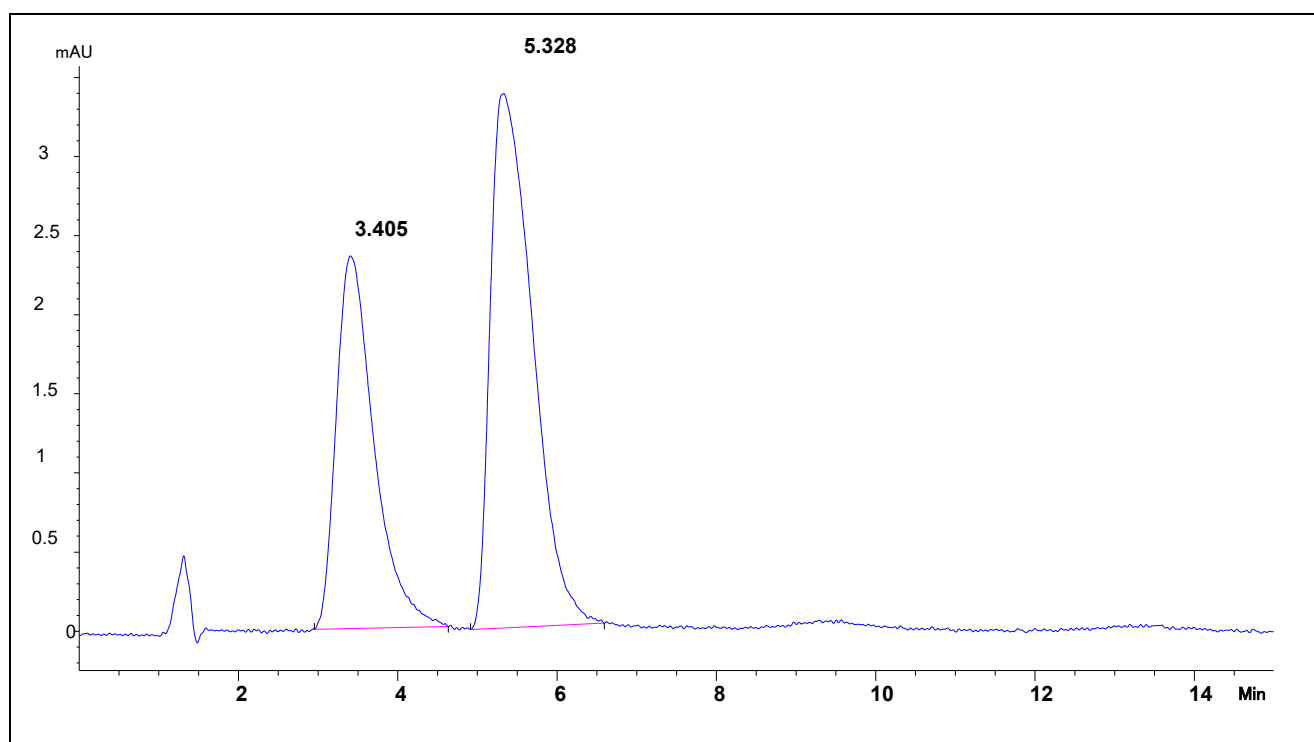
Figure 7-15 Chromatogram of MT raw water sample

The Midvaal (MV) water treatment plant in Gauteng province (Coordinates: 24° 40′S 28°20′E) both showed the presence of HA and FA. The parameters of the MV raw water sample (TOC: 7.84 mg/ℓ, UV_{254}: 0.26 cm^{-1} and SUVA value of 3.42 ℓ/mg.m) are illustrated in **Figure 7-17**. The MV final (TOC: 3.47 mg/ℓ, UV_{254}: 0.25 cm^{-1} and SUVA value of 7.33 ℓ/mg.m) (**Figure 7-16**) was used for the study. The intensity of the peaks corresponding to FA and HA increased from MV raw water to MV final water, which indicates that NOM is accumulated throughout the water treatment process. The raw water is dominated by the TPI fraction of NOM while the final water is dominated by a HPI fraction of NOM (Nkambule *et al*., 2011).
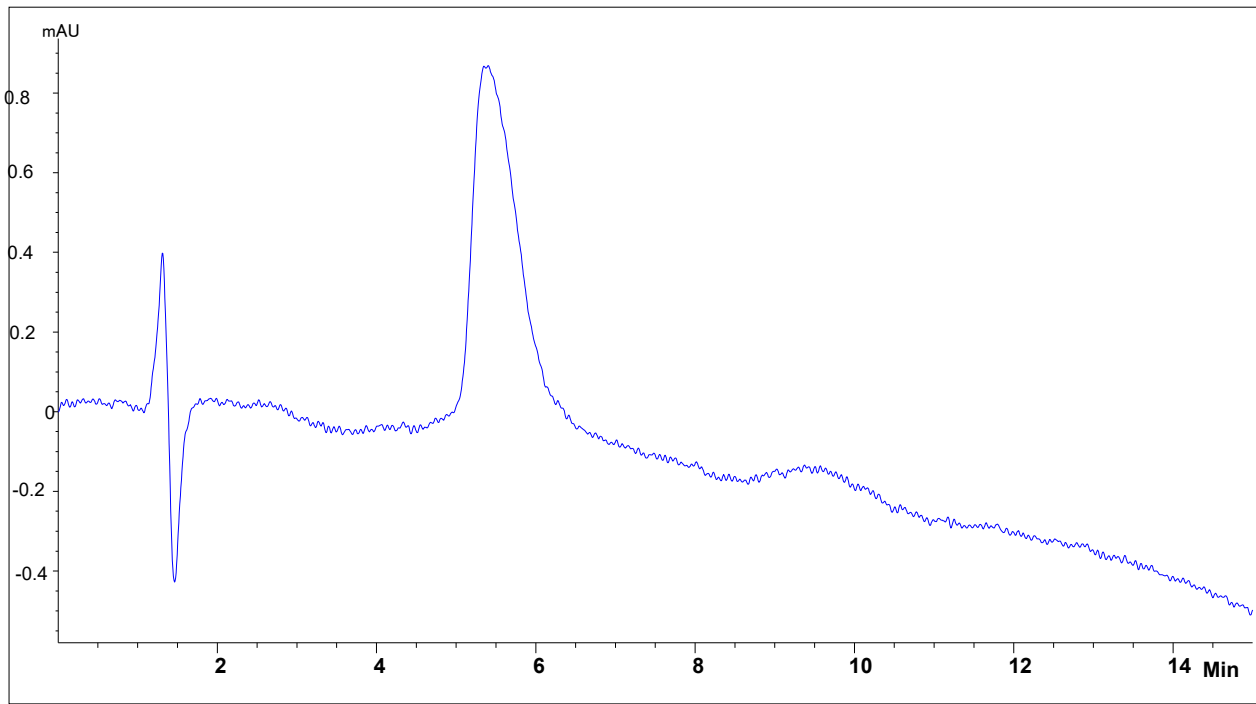
Figure 7-16 Chromatogram of MV final water sample
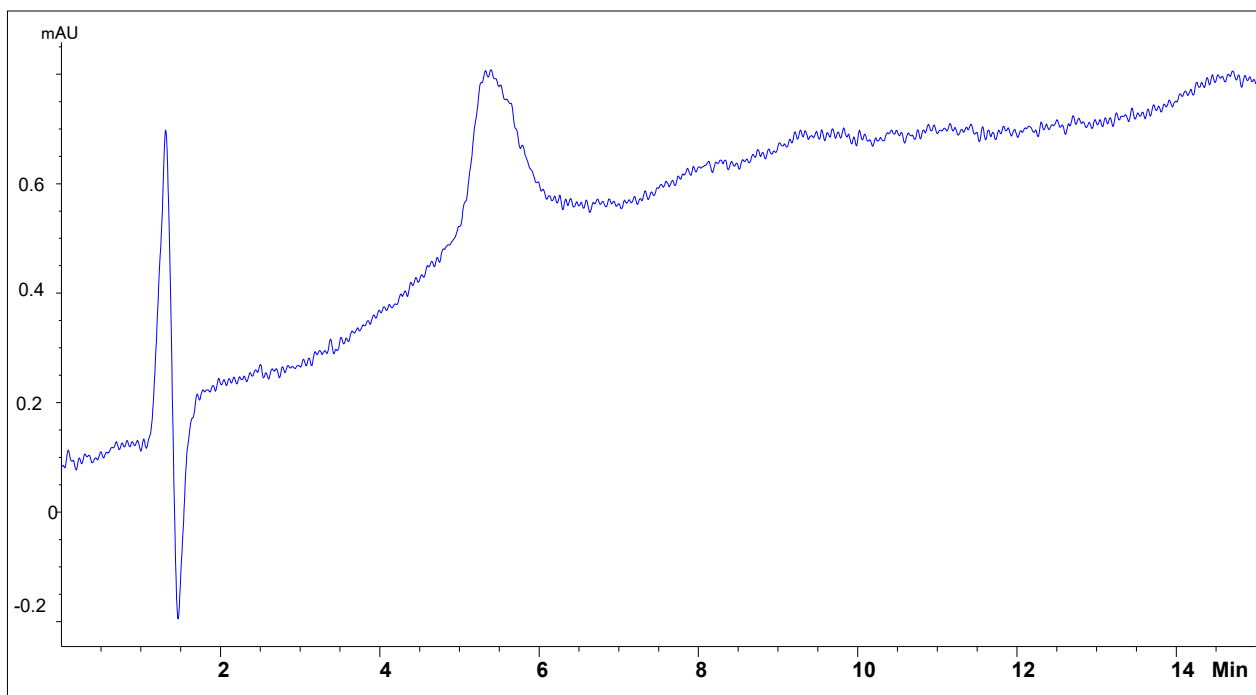
Figure 7-17 Chromatogram of MV raw water sample

The Preekstoel (VP) water treatment plant situated in the Western Cape showed an effective treatment of HA and FA from the final water samples (TOC: 4.35 mg/ℓ, UV$_{254}$: 0.22 cm^{-1} and SUVA value of 5.00 ℓ/mg.m) (**Figure 7-18**) as compared to the raw water samples (TOC: 10.19 mg/ℓ, UV$_{254}$: 0.52 cm^{-1} and SUVA value of 5.25 ℓ/mg.m). The chromatogram showed weak peaks corresponding to HA and FA as compared to the strong peaks in the raw sample **Figure 7-19**.
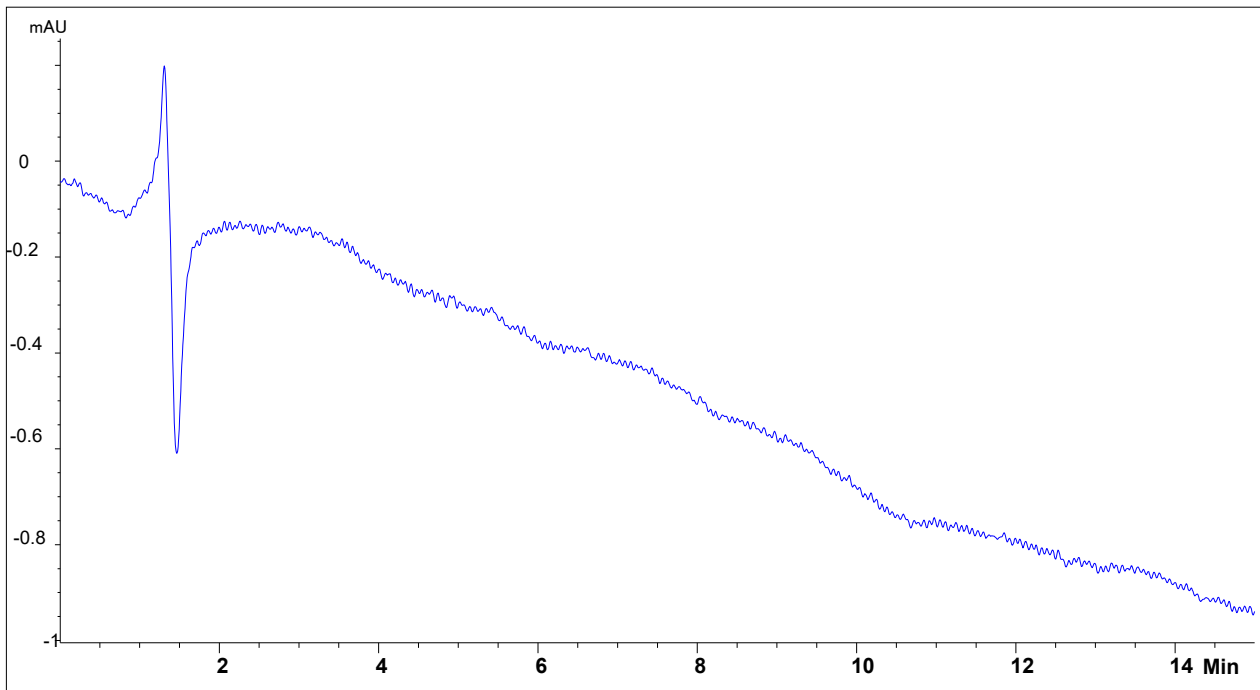
Figure 7-18 Chromatogram of VP final water sample
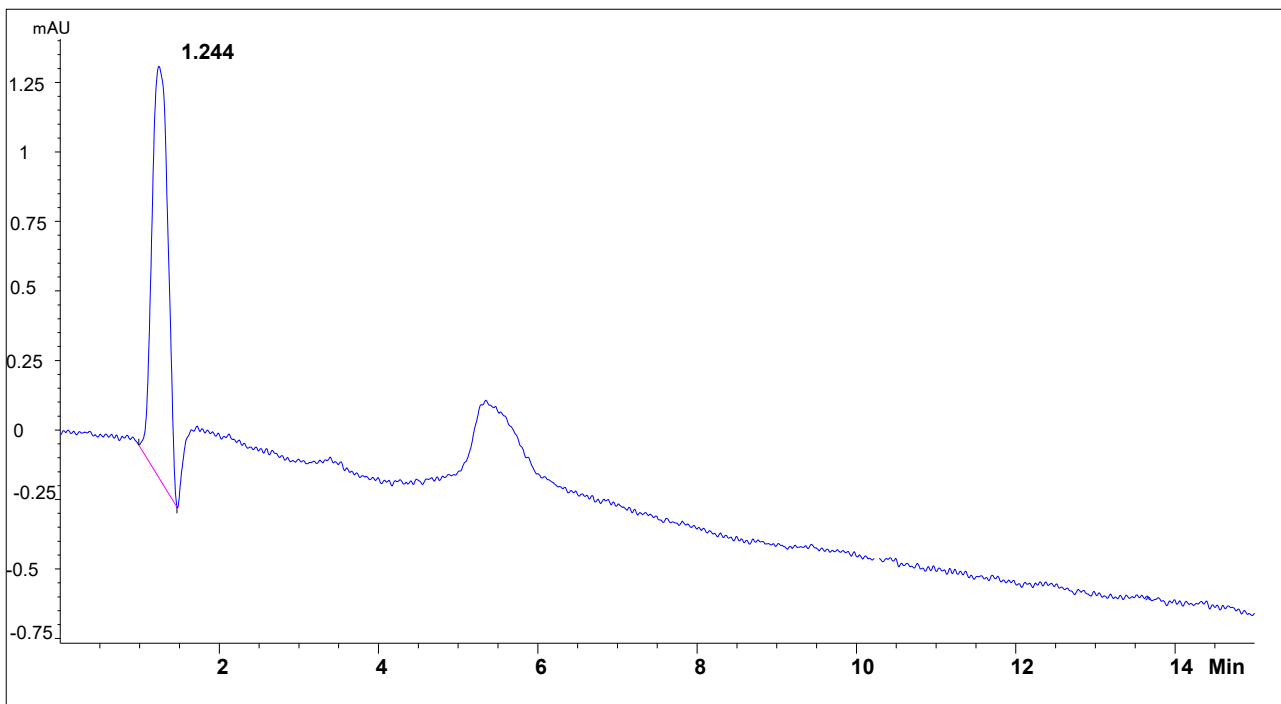
Figure 7-19 Chromatogram of VP raw water sample

7.4 CONCLUSION

The results which were obtained from the test against activity of acid on the column showed that the SEC packed column can elute acidic compounds and other acidic NOM fractions like hydrophilic acid (HpiA) and hydrophobic acid (HpoA). The column packing tests were proficient and, therefore, confirmed suitability of the column for NOM fractionation

The column was able to fractionate the NOM fractions (FA and HA) samples. Fractionation of NOM on Olifantspoort (LO), Mtwalume (MT), Mid-Vaal (MV) and the Preekstoel (VP) raw and final water samples was successful. The overall results show that the SEC packed column can possibly fractionate NOM into its different fractions. The E-PSQ:PS-DVB (1:1 w/w) packed SEC/GPC column was able to separate NOM in all samples according to its different MW fractions. Therefore, the E-PSQ/PS-DVB hybrid SEC/GPC column is indeed the best combination as described in literature.

REFERENCES

ALTAVA, B., BURGUETE, M. I., GARCÍA-VERDUGO, E., LUIS, S. V. & VICENT, M. J. (2001) The use of NIR-FT-Raman spectroscopy for the characterization of polymer-supported reagents and catalysts. *Tetrahedron* 57(41), 8675-8683.

AMY, G. L., COLLINS, M.R., JAMES CUO, C. & KING P.H. (1987) Comparing Gel Permeation Chromatography and Ultrafiltration for the Molecular Weight Characterization of Aquatic Organic Matter. *American Water Works Association Journal* 79(1), 43-49.

ANDREOZZI, R., CAPRIO, V., INSOLA, A. & MAROTTA, R. (1999) Advanced oxidation processes (AOP) for water purification and recovery. *Catalysis Today* 53(1), 51-59.

ASHERY, A.F., RADWAN, K. & GAR AL-ALM RASHED, M.I. (2010) The effect of pH control on turbidity and NOM removal in conventional water treatment. In: *IWTC 15, Alexandria, Egypt.* 28-30 May, 2011 1-16.

AMERICAN WATER WORKS ASSOCIATION. (2011)) *Water Quality and Treatment: A Handbook on Drinking Water*, EDZWALD, J.K. ed. 6th Edition, McGraw Hill, New York.

AXMANOVÁ, Š., KOUTNÝ, J. CUPALOVÁ, J. & RULÍK, M. (2006) Bacterial growth and community composition in fractions of dissolved organic carbon of different molar mass from interstitial water. *Folia Microbiologia*. 51 (5), 439-444.

BAGHOTH, S.A. (2012) 'Characterizing natural organic matter in drinking water treatment processes and trains.' PhD thesis, Delft University of Technology and Academic Board of the UNESCO-IHE Institute of Water Education.

BAGHOTH, S.A., DIGNUM, M., GREFTE, A., KROESBERGEN, J. & AMY, G.L. (2009) Characterization of NOM in a drinking water treatment process train with no disinfectant residual. *Water Science and Technology: Water Supply*. 9(4), 379-386.

BEZUIDENHOUT, N., (2013) 'An Investigation into the Cyanobacteria and Related Cyanotoxins in the Vaalkop Dam and Vaalkop Treatment Plant, Rustenburg', MSc dissertation, Faculty of Science, University of Johannesburg.

BURLEIGH, M.C., MARKOWITZ, M.A., SPECTOR, M.S & GABER B.P. (2002) Porous Polysilsesquioxanes for the Adsorption of Phenols. *Environmental Science and Technology*. 36 (11), 2515-2518.

CAMPBELL, J. (2011) High-throughput assessment of bacterial growth inhibition by optical density measurements. *Current Protocols in Chemical Biology* 3(3), 100-115.

CHAIYASAT, P., CHAIYASAT, A., BOONTUNG, W., PROMDSORN, S. & THIPSIT S. (2011) Preparation and characterization of poly(divinylbenzene) microcapsules containing octadecane. *Materials Sciences and Application* 2(8), 1007-1013.

CHANG, C.Y, HSIEH, Y.H., LIN, Y.M., HU, P.Y, LIU, C.C. & WANG, K.H. (2001) The organic precursors affecting the formation of disinfection by-products with chlorine dioxide. *Chemosphere* 44(5), 1153-1158.

CHEN, J., GU, B., LEBOEUF, E. J., PAN, H. & DAI, S. (2002) Spectroscopic characterization of the structural and functional properties of natural organic matter fractions. *Chemosphere* 48(1), 59-68.

CHEN, J., LEBOEUF, E. J., DAI, S. & GU, B. (2003) Fluorescence spectroscopic studies of natural organic matter fractions. *Chemosphere* 50(5)**,** 639-647.

CHOW, C., FABRIS, R. & DRIKAS, M. (2004) A rapid fractionation technique to characterise natural organic matter for the optimisation of water treatment processes. *Journal of Water Supply: Research and Technology-AQUA* 53(2), 85-92.

CHOW, C. W. K., FABRIS, R., VAN LEEUWEN J., WANG D. & DRIKAS M. (2008) Assessing natural organic matter treatability using high performance size exclusion chromatography. *Environmental Science & Technology* 42(17), 6683-6689

CHOWDHURY, S. (2013) Trihalomethanes in drinking water: Effect of natural organic matter distribution. *Water SA*. 39 (1), 1-8.

CLAESSENS (1999) 'Characterization of stationary phases for reversed-phase liquid chromatography: column testing, classification and chemical stability.' PhD thesis, Department of Chemical Engineering and Chemistry, Eindhoven University of Technology, Netherlands. doi:10.6100/IR518234

COBLE, P.G. (1996) Characterization of marine and terrestrial DOM in seawater using excitation-emission matrix spectroscopy. *Marine Chemistry* 51(4), 325-346.

COVERT, J.S. & MORAN, M.A. (2001) Molecular characterization of estuarine bacterial communities that use high- and low-molecular weight fractions of dissolved organic carbon. *Aquatic Microbial Ecology* 25(2), 127-139.

DENYSSCHEN, J.H. (1990) *Manual on Water Purification Technology*, Division of Water Technology CSIR, South Africa.

DEPARTMENT OF WATER AFFAIRS AND FORESTRY (DWAF) (2000) *Quality of Domestic Water Supplies – Sampling Guide*, Water Research Commission TT 117/99, South Africa.

DLAMINI, S. (2012). 'The profiling and treatability of natural organic matter in South African raw water sources using enhanced coagulation.' MSc dissertation, Faculty of Science, University of Johannesburg.

EDZWALD J.K. & VAN BENSCHOTEN J.E. (2010) Chemical principles, source water composition, and watershed protection. In *Water Quality and Treatment: A Handbook on Drinking Water*. 6th ed. American Water Works Association and McGraw-Hill, New York. 2222-2223.

EUERBY, M. R., PETERSSON, P., CAMPBELL, W. & ROE, W. Chromatographic classification and comparison of commercially available reversed-phase liquid chromatographic columns containing phenyl moieties using principal component analysis. *Journal of Chromatography A*.1154(1-2), 138-151 (2007).

EVANS, C.D., MONTEITH, D.T. & COOPER, D.M. (2005). Long-term increases in surface water dissolved organic carbon: Observations, possible causes and environmental impacts. *Environmental Pollution*. 137 (1), 55-71.

FABRIS, R., CHOW, C. W. K., DRIKAS, M. & EIKEBROKK, B. (2008) Comparison of NOM character in selected Australian and Norwegian drinking waters. *Water Research* 42 (18), 4188-4196.

FAUST, S.D. & ALY, O.M. (1998) *Chemistry of Water Treatment*, 2nd ed., CRC Press LLC, Boca Raton, FL.

FRAM, M.S., FUJII, R., WEISHAAR, J.L., BERGAMASCHI, B.A. & AIKEN G.R. (1999) How DOC composition may explain the poor correlation between specific trihalomethane formation potential and specific UV absorbance. In: *U.S. Geological Survey Toxic Substances Hydrology Program: Proceedings of the Technical Meeting,* March 8-12,1999. 2, 423-430. USGS,Charleston, SC, United States of America.

FRIMMEL F.H., JAHNEL J.B. (2003) Formation of Haloforms in Drinking Water. In: Nikolaou A.D. (eds) Haloforms and Related Compounds in Drinking Water. *The Handbook of Environmental Chemistry (Water Pollution)*. 5/5G, 1-19. Springer, Berlin, Heidelberg.

FUNES, A., DE VICENTE, J., CRUZ-PIZARRO, L. & DE VICENTE, I. (2014). The influence of pH on manganese removal by magnetic microparticles in solution. *Water Research* 53, 110-122.

GALLARD, H. & VON GUNTEN, U. (2002) Chlorination of natural organic matter: kinetics of chlorination and of THM formation. *Water Research* 36(1), 65-74.

GARCIA-DIEGO, C. & CUELLAR, J. (2005). Synthesis of macroporous poly(styrene *co*-divinylbenzene) microparticles using *n*-Heptane as the porogen: Quantitative effects of the DVB concentration and the monomeric fraction on their structural characteristics. *Industrial & Engineering Chemistry Research* 44 (22), 8237-8247.

GOSLAN, E.H. (2003) 'Natural organic matter character and reactivity: Assessing seasonal variation in a moorland water.' EngD thesis, School of Water Sciences, Cranfield University, United Kingdom.

GRINHUT, T., HADAR, Y. & CHEN, Y. (2007) Degradation and transformation of humic substances by saprotrophic fungi: processes and mechanisms. *Fungal Biology Reviews* 21(4), 179-189.

HAARHOFF J., KUBARE, M., MAMBA, B., KRAUSE, R., NKAMBULE, T., MATSEBULA, B. & MENGE J., (2010) NOM characterization and removal at six Southern African water treatment plants. *Drinking Water Engineering Science* 3, 53-61.

HAARHOFF J., MAMBA, B., KRAUSE, R., VAN STADEN, S., NKAMBULE, T., DLAMINI, S. & LOBANGA, K.P. (2013) Natural organic matter in drinking water sources: its characterization and treatability. WRC Report No. 1883/1/12

HASEGAWA, G., KANAMORI, K., NAKANISHI, K. & HANADA, T. (2009) Fabrication of macroporous silicon carbide ceramics by intramolecular carbothermal reduction of phenyl-bridged polysilsesquioxane. *Journal of Materials Chemistry* 19, 7716-7720.

HASSOUNA, M.E.M., BADAWY, M.I., GAD-ALLAH, T.A. & SAID, M.H. (2014) Fate of natural organic matter and THMs formation of raw and conventionally treated water of El-Fayoum Governorate, Egypt. *International Journal of Advanced Research*. 2 (3), 787-794.

HE, J., LI, X., SU, D., JI, H., ZHANG, X. & ZHANG, W. (2016) Super-hydrophobic hexamethyl-disilazane modified ZrO_2-SiO_2 aerogels with excellent thermal stability. *Journal of Materials Chemistry A*. 4, 5632–5638.

HERTKORN, (2006) Molecular level structural analysis of natural organic matter and of humic substances by NMR spectroscopy. Postdoctoral dissertation, Fakultät Wissenschaftszentrum Weihenstephan, Technische Universität München, Germany. https://mediatum.ub.tum.de/doc/606006/606006.pdf

HOSOYA, K. & FRÉCHET, J.M.J. (1993) Reversed-phase chromatographic properties of monodispersed macroporous particles of poly(styrene-divinylbenzene) prepared by a multi-step swelling and polymerization method. *Journal of Liquid Chromatography* 16 (2), 353-365.

HOWE, K.J., HAND, D.W., CRITTENDEN, J.C., TRUSSELL, R.R. & TCHOBANOGLOUS, G. (2012) *Principles of water treatment*. John Wiley and Sons Inc., NJ, United States of America.

HUANG, J., WANG, L., REN, N., LIU, L., SUN, F. & YANG, G. (1997) Disinfection Effect of Chlorine Dioxide on Viruses, Algae and Animal Plankton in Water. *Water Research*, 31(3), 455-460.

HUMBERT H., GALLARD H., SUTY H. & CROUE J.P (2005) Performance of selected anion exchange resins for the treatment of a high DOC content surface water. *Water Research* 39(9), 1699-1708.

HWANG, C.J., SCLIMENTI, M.J. & KRASNER, S.W. (1999) Contribution by NOM fractions to DBP formation in a low humic water. American Chemical Society. Anaheim CA, United States of America, 224-226.

JOHNSTONE, D.W. (2009) 'Drinking water disinfection byproduct formation assessment using natural organic matter fractionation and excitation emission matrices.' PhD thesis, University of Akron, OH, United States of America.

KHODSE, V.B. & BHOSLE, N.B. (2011) Bacterial utilization of size fractionated dissolved organic matter. *Aquatic Microbial Ecology* 64, 299-309.

KIM, H.C. & YU, M.J. (2005) Characterization of natural organic matter in conventional water treatment processes for selection of treatment processes focused on DBPs control. *Water Research* 39(19), 4779-4789.

KLINGENBERG, A. & SEUBERT, A. (1998) Sulfoacylated polystyrene-divinylbenzene copolymers as resins for cation chromatography: Influence of capacity on resin selectivity. *Journal of Chromatography A* 804, 63-68.

KNIGHT, N., WATSON, K., CARSWELL, S., COMINO, E. & SHAW, G. (2011) Temporal and spatial variation of trihalomethanes and haloacetic acids concentration in drinking water: A case study of Queensland, Australia. *Air, Soil and Water Research* 4, 1-17.

KRISTIANA, I., JOLL, C. & HEITZ, A. (2011) Powdered activated carbon coupled with enhanced coagulation for natural organic matter removal and disinfection by-product control: Application in a Western Australian water treatment plant. *Chemosphere* 83 (5), 661-667.

LABANOWSKI, J. & FEUILLADE, G. (2009) Combination of biodegradable organic matter quantification and XAD-fractionation as effective working parameter for the study of biodegradability in environmental and anthropic samples. *Chemosphere* 74(4), 605-611.

LAMSAL, R., WALSH, M. E. & GAGNON, G. A.(2011) A comparison of advanced oxidation processes for the removal of natural organic matter. *Water Research* 45(10), 3263-3269.

LECHEVALLIER, M.W., SCHULTZ, W. & LEE, R.G. (1991) Bacterial nutrients in drinking water. *Applied and Environmental Microbiology* 57(3), 857-862.

LEE, M. K. (2005) 'Application of white-rot fungi for the biodegradation of natural organic matter in wastes. MEng thesis, School of Civil and Chemical Engineering, RMIT University, Melbourne', Australia.

LEENHEER, J.A. (1981) Comprehensive approach to preparative isolation and fractionation of dissolved organic carbon from natural wastewaters. *Environmental Science and Technology* 15(5), 578-587.

LETTERMAN, R.D., AMIRTHARAJAH, A. & O'MELIA, C.R. (1999) Coagulation and flocculation. In: *Water quality and treatment*. 5th ed. American Water Works Association. McGraw-Hill. USA. 6.1-6.5.

LI, T., LIU, H., ZENG, L., YANG, S., LI, Z., ZHANGA, J & ZHOU, X. (2011*)* Macroporous magnetic poly(styrene–divinylbenzene) nanocomposites prepared via magnetite nanoparticles-stabilized high internal phase emulsions. *Journal of Materials Chemistry* 21, 12865-12872.

LISTIARINI, K., TONG, T.J., SUN, D.D. & LECKIE, J.O. (2010) Hybrid coagulation-nanofiltration membrane for removal of bromine and humic acid in water. *Journal of Membrane Science* 365, 154-159.

LOBANGA, K.P., HAARHOFF, J. & VAN STADEN, S.J. (2013) Treatability of South African surface waters by activated carbon. *2012 Water Institute of Southern Africa (WISA) Biennial Conference,* Cape Town, 6-10 May 2012, 39 (3), 379-384.

LOBANGA, HAARHOFF, J. & VAN STADEN, S.J. (2014) Treatability of South African surface waters by enhanced coagulation. *Water SA* 40 (3), 529-534.

LOZOVIK., P.A., MOROZOV, A.K, ZOBKOV, M.B., DUKHOVICHEVA, T.A. & OSPIVA, L.A. (2007) Allochthonous and autochthonous organic matter in surface waters in Karelin. *Water Resources* 34 (2), 204-216.

LU, J., ZHANG, T., MA, J. & CHEN, Z. (2009) Evaluation of disinfection by-products formation during chlorination and chloramination of dissolved natural organic matter fractions isolated from a filtered river water. *Journal of Hazardous Materials* 162 (1), 140-145.

LYUBOMIROVA, V., DJINGOVA, R. & VAN ELTEREN, J. T. (2011) Fractionation of traffic-emitted Ce, La and Zr in road dusts. *Journal of Environmental Monitoring* 13(6), 1823-1830.

MA, J., SHI, L., LI, B., SHEN, D. & XU, J. (2002) Study on pyrolysis of polyphenylsilsesquioxane. *Chinese Journal of Polymer Science* 20(6), 573-577.

MAIGA, D. T., MSAGATI, T. A. M., KILULYA, K. F. & MAMBA, B. B. (2014) Preparation of SPE hybrid mesoporous silica sorbents for the analysis and removal of organic pollutants in water. *Physics and Chemistry of the Earth* 72-75, 83-87.

MAMBA, B.B., Krause, R.W., MATSEBULA, B. & HAARHOFF, J. (2009) Monitoring natural organic matter and disinfection by-products at different stages in two South African water treatment plants. *Water SA* 35(1), 121-127.

MARHABA, T.F., PU, Y. & BENGRAINE, K. (2003) Modified dissolved organic matter fractionation technique for natural water. *Journal of Hazardous Materials* 101(1), 43-53.

MARHABA, T.F. & VAN D. (2000) The variation of mass and disinfection by-product formation potential of dissolved organic matter fractions along a conventional surface water treatment plant. *Journal of Hazardous Materials* 74(3), 133-147.

MATILAINEN, A. (2007) 'Removal of the natural organic matter in the different stages of the drinking water treatment process.' PhD thesis, Tampere University of Technology, Finland.

MATILAINEN, A, GJESSING, E.T., LAHTINEN, T., HED, L., BHATNAGAR, A. & SILLANPÄÄ, M. (2011). An overview of the methods used in the characterisation of natural organic matter (NOM) in relation to drinking water treatment. *Chemosphere* 83 (11), 1431-1442.

MATILAINEN, A., LINDQVIST, N., KORHONEN, S. & TUHKANEN, T. (2002) Removal of NOM in the different stages of the water treatment process. *Environment International* 28(6), 457-465.

MATILAINEN, A. & SILLANPÄÄ, M. (2010) Removal of natural organic matter from drinking water by advanced oxidation processes. *Chemosphere* 80(4), 351-365.

MATILAINEN, A., VEPSÄLÄINEN, M. & SILLANPÄÄ, M. (2010) Natural organic matter removal by coagulation during drinking water treatment: A review. *Advances in Colloid and Interface Science* 159(2), 189-197.

METCALF & EDDY (2003) *Wastewater Engineering:Treatment and Reuse*, 4th ed., McGraw Hill, NY, United States of America.

MINAKUCHI, H., NAKANISHI, K., SOGA, N., ISHIZUKA, N. & TANAKA, N. (1998) Effect of domain size on the performance of octadecylsilylated continuous porous silica columns in reversed-phase liquid chromatography. *Journal of Chromatography A* 797(1-2), 121-131.

MITCH, W.A., SHARP, J.O., TRUSSELL, R.R. VALENTINE, R.L., ALVAREZ-COHEN, L. & SEDLAK, D.L. (2003) N-Nitrosodimethylamine (NDMA) as a drinking water contaminant: A review. *Environmental Engineering Science* 20(5), 389-404.

MYLLYKANGAS, T., NISSINEN, T.K., RANTAKOKKO, P., MARTIKAINEN, P.J. & VARTIAINEN, T. (2002) Molecular size fractions of treated aquatic humus. *Water Research* 36(12), 3045-3053.

NAKANISHI, K. & KANAMORI, K. (2005) Organic–inorganic hybrid poly(silsesquioxane) monoliths with controlled macro- and mesopores. *Journal of Materials Chemistry* 15, 3776-3786

NCUBE, E.J., VOYI, K. & DU PREEZ, H. (2012) Implementing a protocol for selection and prioritisation of organic contaminants in the drinking water value chain: Case study of Rand Water, South Africa. *Water SA* 38(4), 487-504.

NEUE, U.D., VAN TRAN, K., IRANETA, P. C. & ALDEN, B. A. (2003) Characterization of HPLC packings. *Journal of Separation Science* 26(3-4), 174-186.

NISSINEN, T.K., MIETTINEN, I.T., MARTIKAINEN, P.J. & VARTIAINEN, T. (2001) Molecular size distribution of natural organic matter in raw and drinking waters. *Chemosphere* 45(6-7), 865-873.

NKAMBULE, T.I. (2012) Natural organic matter (NOM) in South African waters: characterization of NOM, treatability and method development for effective NOM removal from water. PhD thesis, Faculty of Science, University of Johannesburg, South Africa.

NKAMBULE, T.I., KRAUSE, R.W.M., HAARHOFF, J. & MAMBA, B.B. (2011) Treatability and characterization of natural organic matter (NOM) in South African waters using newly developed methods. *Physics and Chemistry of the Earth* 36(14-15), 1159-1166.

NKAMBULE, T. I., KRAUSE, R. W. M., HAARHOFF, J. & MAMBA, B. B. (2012a) Natural organic matter (NOM) in South African waters: NOM characterisation using combined assessment techniques. *Water SA* 38(5), 697-706.

NKAMBULE, T.I., KUVAREGA, A.T., KRAUSE, R.W.M., HAARHOFF, J. & MAMBA, B.B. (2012b) Synthesis and characterisation of Pd-modified N-doped TiO$_2$ for photocatalytic degradation of natural organic matter (NOM) fractions. *Environmental Science and Pollution Research* 19(9), 4120-4132.

NKAMBULE, T.I., KRAUSE, R.W.M., MAMBA, B.B. & HAARHOFF, J. (2009a) Characterisation of natural organic matter (NOM) and its removal using cyclodextrin polyurethanes. *Water SA* 35(2), 200-203.

NKAMBULE, T.I., KRAUSE, R.W.M., MAMBA, B.B. & HAARHOFF, J. (2009b) Removal of natural organic matter from water using ion-exchange resins and cyclodextrin polyurethanes. *Physics and Chemistry of the Earth* 34(13-16), 812-818.

OBI, C., MOMBA, M., GREEN, E., IGUMBOR, J., SAMIE, A. & MUSIE, E. (2009). Microbiological, physico-chemical and management parameters impinging on the efficiency of small water treatment plants in the Limpopo and Mpumalanga Provinces of South Africa. *Water SA* 33(2), 229-238.

ÖZDEMIR, K. (2014) Characterization of natural organic matter in conventional water treatment processes and evaluation of THM formation with chlorine. *Scientific World Journal* 2014, Article ID 703173.

PĂCURARIU, C., MIHOC, G., POPA, A., MUNTEAN, S. G. & IANOŞ, R. (2013) Adsorption of phenol and p-chlorophenol from aqueous solutions on poly(styrene-co-divinylbenzene) functionalized materials. *Chemical Engineering Journal* 222, 218-227.

PAGE, D.W., VAN LEEUWEN, J.A., SPARK, K.M., DRIKAS, M., WITHERS, N. & MULCAHY, D.E. (2002a) Effect of alum treatment on the trihalomethane formation bacterial regrowth potential of natural and synthetic waters. *Water Research* 36(19), 4884-4892.

PAGE, D.W., VAN LEEUWEN, J.A., SPARK, K.M. & MULCAHY, D.E. (2002b) Pyrolysis characterisation of plant, humus and soil extracts from Australian catchments. *Journal of Analytical and Applied Pyrolysis* 65(2), 269-285.

PARSONS, S.A., JEFFERSON, B., GOSLAN, E.H., JARVIS, P.R. & FEARING, D.A. (2004) Natural organic matter – the relationship between character and treatability. *Water Science and Technology: Water Supply* 4(5-6), 43-48.

PEI, Y. *YU, J., GUO, Z., ZHANG, Y., YANG, M., ZHANG, J. & JUNJI, H.* (2007) Pilot Study on Pre-Ozonation Enhanced Drinking Water Treatment Process. *Ozone: Science & Engineering* 29(5), 317-323.

PELEKANI, C., NEWCOMBE, G., SNOEYINK, V.L., HEPPLEWHITE, C., ASSEMI, S. & BECKETT, R. (1999) Characterization of natural organic matter using high performance size exclusion chromatography. *Environmental Science and Technology* 33(16), 2807-2813.

PAPAGEORGIOU, A., PAPADAKIS, N. & VOUTSA, D. (2016) Fate of natural organic matter at a full-scale Drinking Water Treatment Plant in Greece. *Environmental Science and Pollution Research International* 1841-1851, doi:10.1007/s11356-015-5433-3

PENRU, Y., SIMON, F.X., GUASTALLI, A.R., ESPLUGAS, S., LLORENS, J. & BAIG, S. Characterization of natural organic matter from Mediterranean coastal seawater. *Journal of Water Supply: Research and Technology-AQUA* 62(1), 42-51 (2013).

PIFER, A. D. & FAIREY, J. L. (2012) Improving on SUVA 254 using fluorescence-PARAFAC analysis and asymmetric flow-field flow fractionation for assessing disinfection byproduct formation and control. *Water Research* 46(9), 2927-2936.

PIPER, C., JEFFERSON, B. & JARVIS, P. (2010) 'Development of a rapid fractionation tool for natural organic matter.' MSc dissertation, Centre for Water Sciences. Department of Sustainable Systems. School of Applied Science, Cranfield University, United Kingdom.

QUARANTA, M. L., MENDES, M. D. & MACKAY, A. A. (2012) Similarities in effluent organic matter characteristics from Connecticut wastewater treatment plants. *Water Research* 46(2), 284-294.

RACZYK-STANISLAWIAK, U., SWIETLIK J., DABROWSKA, A., & NAWROCKI, J. (2003) Biodegradability of organic by-products after natural organic matter oxidation with ClO_2 – Case study. *Water Research* 38(4), 1044-1054.

RAO, T. P., PRAVEEN, R. S. & DANIEL, S. (2004) Styrene–divinyl benzene copolymers: Synthesis, characterization, and their role in inorganic trace analysis. *Critical Reviews in Analytical Chemistry* 34(3-4), 177-193.

RITSON, J.P., GRAHAM, N.J.D., TEMPLETON, M.R., CLARK, J.M., GOUGH, R. & FREEMAN, C. (2014). The impact of climate change on the treatability of dissolved organic matter (DOM) in upland water supplies : A UK perspective. *Science of The Total Environment* 473-474, 714-730.

ROE, J.L. (2011) 'Characterising natural organic matter in surface waters and the minimisation of disinfection by-product formation.' PhD thesis, School of Civil Engineering, University of Birmingham, United Kingdom.

ROE, J., BAKER, A. & BRIDGEMAN, J. (2008) Relating organic matter character to trihalomethanes formation potential: a data mining approach. *Water Science and Technology: Water Supply* 8(6), 717-723.

ROSARIO-ORTIZ, F.L., KOZAWA, K., AL-SAMARRAI, H.N., GERRINGER, F.W., GABELICH, C.J. & SUFFET, I.H. (2004) Characterization of the changes in polarity of natural organic matter using solid-phase extraction: introducing the NOM polarity rapid assessment method (NOM-PRAM). *Water Science and Technology: Water Supply* 4(4), 11-18.

ROSARIO-ORTIZ, F.L., SNYDER, S. & SUFFET, I.H. (2007) Characterisation of the polarity of natural organic matter under ambient conditions by the polarity rapid assessment method (PRAM). *Environmental Science and Technology* 41(14), 4895-4900.

SANDER, L. C. & WISE, S. A. (2003) A new standard reference material for column evaluation in reversed-phase liquid. *Journal of Separation Science* 26(3-4) 283-294.

SANTO DOMINGO, J.W., MECKES, M.C., SIMPSON, J.M., SLOSS, B. & REASONER, D.J. (2003) Molecular characterization of bacteria inhabiting the distribution system simulator. *Water Science & Technology* 47(5), 149-154.

SHARP, E.L., PARSONS, S.A. & JEFFERSON, B. (2006) Seasonal variations in natural organic matter and its impact on coagulation in water treatment. *Science of the Total Environment* 363(1-3), 183-194.

SIGMA-ALDRICH. Assessing Column Comparison Studies: Modified-Euerby comparison of discovery Zr-PBD and discovery C18. *Reporter EU*, Volume 10. www.sigmaaldrich.com/technical-documents/articles/reporter-eu/assessing-column-comparison.html , accessed 2017.

SOLARSKA, S., MAY, T., RODDICK, F. A. & LAWRIE, A. C. (2009) Isolation and screening of natural organic matter-degrading fungi. *Chemosphere* 75(6), 751-758.

SOUTH AFRICAN NATIONAL STANDARD (SANS 241-1:2011) *Drinking Water. Part 1: Microbiological, physical, aesthetic and chemical determinands*, Edition 1.

ŚWIETLIK, J., DABROWSKA, A., RACZYK-STANISLAWIAK, U. & NAWROCKI, J. (2004) Reactivity of natural organic matter fractions with chlorine dioxide and ozone. *Water Research* 38(3), 547-558.

ŚWIETLIK, J. & SIKORSKA, E. (2006) Characterization of natural organic matter fractions by high pressure size-exclusion chromatography, specific UV absorbance and total luminescence spectroscopy. *Polish Journal of Environmental Studies* 15(1), 145-153.

SZABÓ, H.M. & TUHKANEN, T. (2007) Deterioration of drinking water sources through leaching of organic matter – development of a method to identify the source of leaching. *International symposium on new directions in urban water management.* 12-14 September 2007, UNESCO, Paris, France.

TANAKA, N., KOBAYASHI, H., NAKANISHI, K., MINAKUCHI, H. & ISHIZUKA, N. (2001) Monolithic LC Columns. *Analytical Chemistry* 73(15), 420A-429A.

TEIXEIRA, M.R. & NUNES, L.M. (2016). The impact of natural organic matter seasonal variations in drinking water quality. *Desalination and Water Treatment* 36(1-3):344-353.

THEBE, T., SWARTZ, C.D., MORRISON, I.R., ENGELBRECHT, W.J. & LOEWENTHAL, R.E. (2000) Characterisation of natural organic matter in South African coloured surface waters. *Water Institute of Southern Africa (WISA) Biennial Conference, Sun City, South Africa, 28 May -1 June 2000*, 1-11.

TIAN, J., LU, J., ZHANG, Y., LI, J., SUN, L. & HU, Z. (2014) Microbial community structures and dynamics in the O3/BAC drinking water treatment process. *International Journal of Environmental Research and Public Health* 11(6), 6281-6290.

TUBIĆ, A., AGBABA, J., DALMACIJA, B., MOLNAR, J., MALETIĆ, S., WATSON, M. & PEROVIĆ, S.U. (2013) Insight into changes during coagulation in NOM reactivity for trihalomethanes and haloacetic acids formation. *Journal of Environmental Management* 118, 153-160.

URBANOWSKA, A. & KABSCH-KORBUTOWICZ, M. (2016) Characteristics of natural organic matter removed from water along with its treatment. *Environment Protection Engineering* 42(2), 183-195.

U.S. Environmental Protection Agency Method 551.1 (1995) Determination of chlorination disinfection byproducts, chlorinated solvents, and halogenated pesticides/herbicides in drinking water by liquid-liquid extraction and gas chromatography with electron-capture detection. U.S. Environmental Protection Agency Cincinnati, OH, United States of America.

UYAK, V., OZDEMIR, K. & TOROZ, I. (2008). Seasonal variations of disinfection by-product precursors profile and their removal through surface water treatment plants. *Science of The Total Environment*, 390(2-3), 417-424.

UYGUNER C.S. & BEKBOLET M. (2005) Implementation of spectroscopic parameters for practical monitoring of natural organic matter. *Desalination* 176(1-3), 47-55.

VAN DER KOOIJ, D. (1992) Assimilable organic carbon as an indicator of bacterial regrowth. *Journal of American Water Works Association* 84 (2), 57-65.

VAN DER WALT, M., KRUGER, M. & VAN DER WALT, C. (2009) *The South African oxidation and disinfection manual*, Water Research Commission.

VAN LEEUWEN, J., DALY, R. & HOLMES, M. (2005) Modeling the treatment of drinking water to maximise dissolved organic matter removal and minimize disinfection by-product formation. *Desalination.* 176(1-3), 81-89.

VUORIO, E., VAHALA, R., RINTALA, J. & LAUKKANEN, R. (1998) The evaluation of drinking water treatment performed with HPSEC. *Environment International* 24(5-6), 617-623.

WEISHAAR, J.L., AIKEN, G.R., BERGAMASCHI, B.A., FRAM, M.S., FUJII, R. & MOPPER, K. (2003) Evaluation of specific ultraviolet absorbance as an indicator of the chemical composition and reactivity of dissolved organic carbon. *Environmental Science and Technology* 37(20), 4702-4708.

WERSHAW, R.L., LEENHEER, J.A. & COX, L. (2005). *Characterization of dissolved and particulate natural organic matter (NOM) in Neversink Reservoir, New York*. US Geological Survey Scientific Investigations Report 2005-5108, USGA, Reston VA, United States of America.

WILEY, R. H. (1975) Crosslinked styrene/divinylbenzene network systems. *Pure and Applied Chemistry* 43(1-2), 57-75.

WILLIAMS, M.M., DOMINGO, J.W.S., MECKES, M.C., KELTY, C.A. & ROCHON, H.S. (2004). Phylogenic diversity of drinking water bacteria in a distribution system simulator. *Journal of Applied Microbiology* 96(5), 954-964.

WONG, S. HANNA, J.V., KING S., CARROLL, T.J., ELDRIDGE, R.J., DIXON, D.R., BOLTO, B.A., HESSE, S., ABBT-BRAUN, G. & FRIMMEL, F.H. (2002) Fractionation of natural organic matter in drinking water and characterization by 13C cross-polarization magic-angle spinning NMR spectroscopy and size exclusion chromatography. *Environmental Science & Technology* 36(16), 3497-3503.

XIA, S. & NI, M. (2014) Preparation of poly(vinylidene fluoride) membranes with graphene oxide addition for natural organic matter removal. *Journal of Membrane Science* 473, 54-62.

YANG, Z., LAN-LAN, Q., PENG-WEI, T. & YOU-XIAN, Z. (2014). Review of N and Metal co-doped TiO_2 for water purification under visible light irradiation. *3rd International Conference on Environment, Chemistry and Biology*, IPCBEE 78 (7), 139-142, IACSIT Press, Singapore.

YEE, L.F., ABDULLAH, M.P., ABDULLAH, A., ISHAK, B. & ZAINAL ABIDIN K.N. (2009) Hydrophobicity characteristics of natural organic matter and the formation of THM. *The Malaysian Journal of Analytical Sciences* 13(1), 94-99.

YOUNG, K.C. (2005) 'Utilization of natural organic matter (NOM) substrates by bacteria.' PhD thesis, University of Notre Dame, IN, United States of America.

YU, Y., YU, J.C., CHAN C.Y., CHE, Y.K., ZHAO, J.C., DING, L., GE, W.K. & WONG, P.K. (2005). Enhancement of adsorption and photocatalytic activity of TiO_2 by using carbon nanotubes for the treatment of azo dye. *Applied Catalysis B: Environmental* 61(1-2),1-11.

YUNOS, M. Z., HARUN, Z., BASRI, H. & ISMAIL, A. F. (2014) Studies on fouling by natural organic matter (NOM) on polysulfone membranes: Effect of polyethylene glycol (PEG). *Desalination* 333(1), 36-44.

ZAMIR, M., ALAM, B., CANTWELL, E., HOFFMAN, R., ANDREWS, R., RAND, J., GAGNON, G., VAN DER MARCK, M., MOFFAT, E. & ANDREWS, S. (2008) Effect of ClO_2 pretreatment on subsequent water treatment processes. *Journal of Environmental Engineering* 134(6), 478-485.

ZHANG, Y., ZHAO, J., JIANG, Z., SHAN, D. & LU, Y. (2014) Biosorption of Fe (II) and Mn (II) ions from aqueous solution by rice husk ash. *Biomed Research International*, 2014. Article ID: 973095

ZHANG, N., JIANG, W., WANG, T., GU, J., ZHONG, S., ZHOU, S., XIE, T. & FU, J. (2015) Facile preparation of magnetic poly(styrene-divinylbenzene) foam and its application as an oil absorbent. *Industrial Engineering and Chemical Research* 54, 11033-11039.

ZHONG, Y., ZHOU, W., ZHANG, P. & ZHU, Y. (2010) Preparation, characterization, and analytical applications of a novel polymer stationary phase with embedded or grafted carbon fibers. *Talanta* 82(4), 1439-1447.

APPENDIX

APPENDIX A: BULK NOM CHARACTERISATION ON THE SAMPLES

Table A 1 Parameters used to study the character of NOM for the Magalies plant (Round 1)

Sample Codes	pH	Conductivity (mS/cm)	Turbidity (NTU)	DOC (mg/ℓ)
MP1-1	8.11±0.37	982±1.54	30.8±005	7.44 ± 0.28
MP1-2	7.25±0.44	1040±2.02	5.42±0.02	5.19 ± 0.03
MP1-3	7.18±0.21	1020±1.55	2.94±0.12	5.25 ± 0.07
MP1-4	7.11±0.18	1043±0.15	0.36±0.03	4.25 ± 0.01
MP1-5	7.05±055	1049±0.21	0.26±0.12	4.59 ± 0.11
MP2-1B	7.95±0.16	990±0.48	39.2±0.00	6.59 ± 0.12
MP2-2	7.77±0.42	977±0.00	0.82±0.22	4.85 ± 0.07
MP2-3	7.97±004	998±0.00	0.67±0.11	4.82 ± 0.06
MP2-4	7.86±0.26	996±0.10	0.44±0.00	4.56 ± 0.09
MP2-5	7.63±0.00	1005±0.01	0.42±0.014	4.52 ± 0.07
MP3-2	7.72±0.08	655±0.08	4.25±0.21	5.24 ± 0.06
MP3-3	7.76±0.01	1003±0.00	0.097±1.00	4.83 ± 0.02
MP3-5	7.63±0.01	1009±0.15	0.57±0.58	4.77 ± 0.07

Table A 2 Parameters used to study the character of NOM for the Magalies plant (Round 2)

Sample Codes	pH	Conductivity (mS/cm)	Turbidity (NTU)	DOC (mg/ℓ)
MP1-1	8.37±0.78	528.0±2.35	24.50±1.55	4.96 ± 0.08
MP1-2	7.63±0.62	577.0±1.82	8.11±1.08	3.83 ± 0.07
MP1-3	7.63±0.60	507.5±1.42	0.02±0.06	3.55 ± 0.26
MP1-4	7.69±0.04	562.2±0.64	0.00±0.00	2.93 ± 0.20
MP1-5	7.32±0.09	567.4±0.03	0.00±0.00	3.08 ± 0.13
MP2/-1B	7.88±0.23	549.5±0.01	41.2±0.15	5.22 ± 0.17
MP2-2	8.04±0.21	531.3±0.02	0.00±0.00	3.99 ± 0.01
MP2-3	8.05±0.71	533.3±0.55	0.00±0.00	4.16 ± 0.01
MP2-5	7.54±0.23	541.4±2.28	0.00±0.00	3.47 ± 0.10
MP3-1	8.27±0.01	530.7±1.77	54.2±0.37	5.36 ± 0.11
MP3-2	7.98±0.01	538.2±0.22	6.35±0.44	4.26 ± 0.10
MP3-3	7.90±0.55	541.5±0.25	0.00±0.00	4.05 ± 0.13
MP3-5	7.67±0.13	545.3±0.11	0.00±0.00	3.81 ± 0.22

Table A 3 Parameters used to study the character of NOM for the Magalies plant (Round 3)

Sample Codes	pH	Conductivity	Turbidity	DOC

		(mS/cm)	(NTU)	(mg/ℓ)
MP1-1	7.63±0.26	559.7±12.01	1.49±0.05	5.94 ± 0.08
MP1-2	7.62±0.81	570.5±2.45	2.03±0.01	5.28 ± 0.02
MP1-3	7.79±0.81	568.2±1.50	0.03±0.01	4.58 ± 0.08
MP1-4	7.84±2.12	579.1±3.52	0.00±0.00	4.35 ± 0.07
MP1-5	7.60±0.05	589.3±2.09	0.00±0.00	4.48± 0.03
MP2-1B	7.93±0.01	579.2±4.1	0.00±0.00	3.96± 0.11
MP2-2	8.59±0.01	568.2±9.21	0.35±0.03	4.44 ± 0.12
MP2-3	8.60±0.65	574.5±2.27	0.02±0.01	4.63 ± 0.08
MP2-5	7.90±0.00	573.1±3.05	0.00±0.00	4.35 ± 0.01
MP3-1	8.23±0.27	588.2±0.12	1.26±0.05	6.06 ± 0.23
MP3-2	8.29±0.89	558.9±0.01	2.46±0.12	4.44 ± 0.02
MP3-3	8.20±0.005	557.6±0.02	0.00±0.00	4.26 ± 0.19
MP3-5	7.81±0.55	574.3±0.00	0.00±0.00	4.06 ± 0.02

Table A 4 Parameters used to study the character of NOM for the Rietvlei plant

Sample code	pH	Conductivity (mS/cm)	Turbidity (NTU)	DOC (mg/ℓ)
RV-1/1	8.58 ±0.03	665.3 ±0.01	13.19 ±0.00	8.25 ± 0.08
RV-1/2	8.33 ±0.01	681.0 ±0.707	10.06 ±0.01	6.22 ± 0.13
RV-1/3	7.94 ±0.00	707.8 ±0.707	0.01 ±0.55	4.83 ± 0.05
RV-1/4	7.96 ±0.028	441.8 ±1.05	0.07 ±0.00	5.59 ± 0.09
RV-1/5	7.84 ±0.084	558.6 ±2.83	0.45 ±0.01	3.67 ± 0.14
RV-2/1	9.04 ±0.07	450.3 ±0.12	5.82 ±0.13	10.12 ± 0.16
RV-2/4	9.30 ±0.02	451.0 ±0.09	0.22 ±0.27	6.62 ± 0.06
RV-2/5	8.99 ±0.03	392.3 ±0.15	0.28 ±0.05	5.16 ± 0.17
RV-3/1	8.13 ±0.035	402.0 ±0.03	2.61 ±0.84	7.42 ± 0.00
RV-3/3	8.06 ±0.005	421.5 ±0.00	0.07 ±0.26	4.32 ± 0.15
RV-3/4	8.11 ±0.015	416.7 ±0.75	0.00 ±0.09	4.73 ± 0.04
RV-3/5	8.05 ±0.005	373.3 ±0.06	0.00 ±0.00	2.87 ± 0.12
RV-4/1	8.08 ±0.00	407.8 ±0.71	3.32 ±0.01	7.53 ± 0.12
RV-4/3	7.62 ±0.0275	425.6 ±0.015	0.00 ±0.01	4.20± 0.13
RV-4/4	7.72 ±0.061	425.6 ±0.20	0.00 ±0.27	4.62± 0.14
RV-4/5	7.44 ±0.50	385.0 ±0.59	0.00 ±0.06	2.97± 0.11
RV-5/1	7.98 ±0.01	427.0 ±0.71	1.07 ±0.11	1.58± 0.06
RV-5/3	7.60 ±0.01	430.0 ±0.35	0.87 ±0.09	1.43± 0.02
RV-5/4	7.63 ±0.04	436.0 ±0.00	0.27 ±0.00	1.37± 0.03
RV-5/5	7.67 ±0.11	384.5 ±2.47	0.46 ±0.01	1.54± 0.04

Table A 5 Parameters used to study the character of NOM for the Ebenezer plant

Sample code	pH	Conductivity (mS/cm)	Turbidity (NTU)	DOC (mg/ℓ)
LE-1/1	7.21±0.005	96.1±0.98	1.87±0.05	2.50 ± 0.05
LE-1/2	9.33±0	77.4±	2.22±0.88	1.62 ± 0.10
LE-1/3	7.95±0.005	72.3±	2.10±0.16	1.52 ± 0.07
LE-1/4	7.20±0.01	86.9±	1.35±0.00	1.23 ± 0.09
LE-1/5	7.19±0.007	209.7±	1.71±0.01	1.23 ± 0.10
LE-2/1	7.25±0.04	39.6±0.1	2.46±0.03	0.21 ± 0.04
LE-2/2	7.22±0.07	48.2±0	1.09±0.12	0.26 ± 0.11
LE-2/3	7.52±0.12	44.3±0.23	1.37±0.01	0.38 ± 0.10
LE-2/4	7.33±0.52	45.0±0.1	0.07±0.00	0.06 ± 0.07
LE-2/5	7.55±0.05	47.9±0.1	0.00±0.00	0.00 ± 0.00
LE-3/1	6.94±0.07	40.7±0.21	3.2±0.35	0.13 ± 0.06
LE-3/2	6.90±0.42	48.4±0.42	2.6±0.01	0.00 ± 0.00
LE-3/3	7.07±0.00	44.4±0.35	9.7±0.74	0.00 ± 0.00
LE-3/4	7.08±0.15	43.5±0.21	0±0.00	0.00 ± 0.00
LE-3/5	7.06±0.36	44.3±0.14	1.3±0.38	0.00 ± 0.00
LE-4/1	7.37±0.19	37.8±0.28	0.81±0.05	0.79± 0.05
LE-4/2	7.49±0.22	45.85±0.35	0.73±0.04	0.92± 0.03
LE-4/3	7.71±0.23	41.3±0.57	0.82±0.21	1.9217± 0.01
LE-4/4	7.57±0.24	40.9±0.00	0.54±0.10	0.18± 0.02
LE-4/5	7.39±0.37	45.4±2.83	0.66±0.08	1.73± 1.01

Table A 6 Parameters used to study the character of NOM for the Olifantspoort plant

Sample code	pH	Conductivity (mS/cm)	Turbidity (NTU)	DOC (mg/ℓ)
LO-1/1	7.75±0.01	600.1±1.00	38.30±0.66	6.69 ± 0.05
LO-1/2	8.27±0.01	601.0±1.00	3.69±0.43	6.39 ± 0.17
LO-1/3	8.15±0.00	606.7±2.08	0.22±0.05	6.03 ± 0.12
LO-1/4	7.62±0.01	616.3±0.58	0.26±0.00	5.67 ± 0.12
LO-2/1	7.88±0.15	588.2±0.15	13.8±0.37	4.49 ± 0.19
LO-2/2	7.91±0.01	625.9±2.45	7.55±1.16	4.03 ± 0.05
LO-2/3	7.83±0.04	645.4±0.05	0.00±0.00	3.81 ± 0.12
LO-2/4	7.41±0.00	638.6±0.19	0.00±0.00	3.46 ± 0.09
LO-3/1	8.24±0.03	1124.5±0.00	15.05±1.11	3.04± 0.09
LO-3/2	8.20±0.00	1097.5±0.70	4.42±0.32	2.57 ± 0.05
LO-3/3	8.13±0.00	1077.5±3.52	0.62±0.27	2.43± 0.04
LO-3/4	7.84±0.00	1089.0±8.48	0.74±0.10	2.26± 0.10

Table A 7 Parameters used to study the character of NOM for the Flag Boshielo plant

Sample code	pH	Conductivity (mS/cm)	Turbidity (NTU)	DOC (mg/ℓ)
LF-1/1	7.61±0.01	512±1.00	10.79±0.29	7.20 ± 0.21
LF-1/2	7.63±0.03	521±1.00	2.91±0.10	6.06 ± 0.05
LF-1/3	7.61±0.01	533±0.58	1.85±0.11	5.83 ± 0.23
LF-1/4	7.43±0.01	537±1.53	0.61±0.05	6.30 ± 0.17
LF-2/1	8.42±0.02	528.0±4.24	6.50±1.00	8.27± 0.45
LF-2/2	8.23±0.55	552.2±2.12	2.4±0.31	6.52± 0.12
LF-2/3	7.93±0.13	545.5±3.53	2.4±1.01	6.69± 0.16
LF-2/4	7.49±0.00	546.2±0.70	2.4±1.13	7.09± 0.13
LF-3/1	7.72±0.05	531.5±2.12	14.37±1.77	11.30± 0.22
LF-3/2	8.75±0.11	549.5±3.54	4.40±0.55	8.53± 0.22
LF-3/3	8.51±0.08	543.0±4.95	3.66±0.25	8.40± 0.31
LF-3/4	7.79±0.41	559.0±5.66	6.06±0.11	8.71± 0.01

Table A 8 Parameters used to study the character of NOM for the Plettenberg Bay plant

Sample code	pH	Conductivity (mS/cm)	Turbidity (NTU)	DOC (mg/ℓ)
P-1/1	6.28±0.16	96.6±5.21	0.01±0.02	4.91± 0.12
P-1/2	5.61±0.07	114.4±0.32	3.45±0.71	0.45± 0.07
P-1/3	6.60±0.23	127.7±2.65	0.14±0.09	0.21± 0.02
P-1/4	6.54±0.32	130.1±3.78	0.00±0.00	0.10± 0.09
P-1/5	6.65±0.16	135.6±9.8	0.05±0.08	0.84± 0.05
P-2/1	5.17±0.00	67.55±3.18	2.68±0.30	21.11± 0.04
P-2/2	4.78±0.01	118.35±1.63	19.02±0.64	1.16± 0.05
P-2/3	4.89±0.01	103.50±0.99	1.54±0.14	1.27± 0.03
P-2/4	5.09±0.06	101.85±1.63	0.58±0.13	1.31± 0.02
P-2/5	9.65±0.13	135.00±0.85	0.49±0.08	1.69± 0.04

Table A 9 Parameters used to study the character of NOM for the Preekstoel (VP) and Hermanus (VH) plants

Sample code	pH	Conductivity (mS/cm)	Turbidity (NTU)	DOC (mg/ℓ)
VP-1/1	2.50±0.02	1732.7±4.20	4.44±4.04	8.50± 0.26
VP-1/2	5.32±0.01	295.0±2.15	13.06±0.56	4.97± 0.05
VP-1/3	2.76±0.01	964.7±0.15	0.00±0.00	3.09± 0.13
VP-1/4	3.55±0.01	403.7±2.18	0.00±0.00	2.45± 0.15
VP-1/5	8.30±0.01	310.7±2.07	0.39±1.52	3.00± 0.05
VP-2/1	6.75±0.21	235.7±4.72	8.15±0.47	6.19± 0.17
VP-2/2	4.71±0.02	251.7±1.5	20.8±1.91	5.90± 0.15

VP-2/3	4.99±0.01	250.3±0.6	2.71±0.12	5.57± 0.09
VP-2/4	5.51±0.06	250.3±0.6	0.24±0.01	4.60± 0.23
VP-2/5	7.15±0.15	549.0±4.6	0.16±0.04	0.44± 0.05
VH-1/1	6.24±0.02	709.0±0.05	8.02±1.00	0.00±0.00
VH-1/4 (Mn)	6.91±0.01	667.5±0.01	0.12±2.65	0.00±0.00
VH-1/4 (Fe)	5.62±0.01	715.7±0.01	1.14±1.53	0.00±0.00
VH-2/1	5.46±0.02	483.3±2.89	12.93±1.55	0.07± 0.01
VH-2/4 (Mn)	5.27±0.07	474.7±2.31	10.23±3.22	0.11± 0.02
VH-2/4 (Fe)	7.86±0.28	540.7±1.00	0.28±0.10	0.24± 0.10

Table A 10 Parameters used to study the character of NOM for the Amanzimtoti (AM), Hazelmere (HL), Umzinto (UM) and Mtwalume (MT) plants

Sample code	pH		Conductivity (mS/cm)	Turbidity (NTU)	DOC (mg/ℓ)
AM-1/1	7.18±0.02		138.4±0.63	6.32±0.15	14.8 ± 0.09
AM-1/2	9.03±0.00		166.3±0.35	9.15±0.18	14.78 ± 0.10
AM-1/3	8.93±0.01		167.7±0.21	0.22±0.07	14.75± 0.11
AM-1/4	8.82±0.22		168.5±0.71	0.00±0.00	14.73± 0.03
AM-1/5	7.68±0.00		236.0±0.00	0.00±0.00	23.8± 0.13
AM-2/1	6.745±0.01		130.65±7.14	9.33±0.00	4.26 ± 0.10
AM-2/2	8.425±0.02		150.1±0.71	6.23±0.57	3.66 ± 0.07
AM-2/3	8.08±0.04		148.65±0.21	1.115±0.01	3.53± 0.06
AM-2/4	7.79±0.13		146.9±0.57	0.30±0.13	3.51± 0.06
AM-2/5	7.65±0.01		210.5±4.95	0.415±0.21	3.328± 0.07
HL-1/1	8.81±0.03		172.3±3.82	8.81±0.03	16.59± 0.07
HL-1/2	8.27±0.01		186.4±1.70	8.22±0.02	18.76± 0.09
HL-1/3	8.47±0.01		189.7±2.83	0.07±0.04	18.46± 0.07
HL-1/4	7.81±0.06		187.4±1.06	0.00±0.00	17.06± 0.04
HL-1/5	7.28±0.18		187.5±0.64	0.00±0.00	17.13 ± 0.12
HL-2/1	6.85±0.11		163.8±0.99	57.95±0.07	4.82 ± 0.17
HL-2/2	8.505±0.05		185.9±0.99	11.27±5.56	3.47 ± 0.09
HL-2/3	8.75±0.01		186.65±1.91	1.37±0.48	3.40 ± 0.08
HL-2/4	8.705±0.02		188.9±0.00	0.33±0.18	3.37 ± 0.02
HL-2/5	8.69±0.01		193.45±1.48	0.63±0.05	3.25 ± 0.0745
UM-1/1 EJ	7.37±0.02		353.5±0.00	3.95±0.20	36.9± 0.14
UM-1/1 U	7.53±0.05		386.0±0.00	0.02±0.01	24.69± 0.09
UM-1/2	8.37±0.03		371.5±7.78	4.02±0.24	29.74± 0.38
UM-1/3	8.35±0.06		374.5±1.42	0.63±0.08	22.49± 0.31
UM-1/4	7.61±0.00		360.5±0.71	0.00±0.00	4.46 ± 0.19
UM-1/5	7.57±005		373.7±4.21	0.00±0.00	3.74 ± 0.05

Sample code	pH		Conductivity	Turbidity	DOC
UM-2/1 EJ	7.63±0.01		314.5±0.71	2.32±0.23	4.46 ± 0.19
UM-2/1 U	6.95±0.00		282.5±0.71	10.325±0.19	6.01 ± 0.25
UM-2/2	7.94±0.02		311±1.41	6.19±0.65	4.56 ± 0.16
UM-2/3	9.04±0.01		271±19.80	3.695±0.59	4.57 ± 0.16
UM-2/4	8.43±0.01		309.5±4.95	0.595±0.35	4.46 ± 0.09
UM-2/5	7.56±0.01		315.5±0.72	0.545±0.28	4.37 ± 0.22
MT-1/1	7.75±0.02		305.5±1.41	26.1±0.11	30.05 ± 0.25
MT-1/2	7.74±0.09		310.0±4.24	22.4±2.24	29.02 ± 0.15
MT-1/3	7.69±0.06		309.5±1.41	3.54±1.66	28.74± 0.11
MT-1/4	7.74±0.05		310.5±2.12	0.00±0.00	28.69± 0.07
MT-1/5	7.55±0.00		305.2±1.41	1.87±1.56	26.52± 0.13
MT-2/1	7.79±0.05		267.0±4.24	13.55±0.45	3.75± 0.13
MT-2/2	8.93±0.03		285.0±4.24	4.62±0.04	1.88± 0.22
MT-2/3	7.86±0.02		269.5±7.78	1.29±0.56	2.91± 0.13
MT-2/4	7.72±0.01		274.0±1.4	0.58±0.04	2.80± 0.11
MT-2/5	7.36±0.04		269.5±4.9	0.82±0.04	2.46± 0.09

Table A 11 Parameters used to study the character of NOM for the Midvaal plant

Sample code	pH	Conductivity (mS/cm)	Turbidity (NTU)	DOC (mg/ℓ)
MV-1/1	9.15±0.83	606.3±2.50	19.01±1.35	5.53 ±0.05
MV-1/2	9.06±0.02	610.3±1.52	17.79±0.01	6.45 ±0.12
MV-1/3	8.98±0.01	665.0±0.15	12.92±0.01	5.48 ±0.12
MV-1/4	8.76±0.05	619.0±0.27	5.33±0.01	5.14 ±0.07
MV-1/5	8.74±0.00	621.7±1.57	4.78±0.00	5.14 ±0.09
MV-1/6	9.09±0.30	621.3±2.77	5.59±0.04	5.10 ±0.08
MV-1/7	8.99±0.07	617.3±0.48	2.82±0.07	5.02 ± 0.08
MV-1/8	8.01±0.14	614.0±0.04	0.41±0.12	4.44 ± 0.06
MV-1/9	7.96±0.00	620.7±0.09	0.44±0.00	4.28 ± 0.04
MV-2/1	9.07±0.01	480±1.53	10.27±0.73	5.31 ± 0.09
MV-2/2	9.05±0.01	491±0.58	5.84±0.78	5.49 ± 0.24
MV-2/3	8.94±0.01	495±1.00	6.65±0.77	5.25 ± 0.02
MV-2/4	8.17±0.01	516±1.53	3.64±0.61	5.13 ± 0.11
MV-2/5	8.57±0.17	494±1.53	10.68±0.28	4.87 ± 0.04
MV-2/6	8.34±0.01	510±1.00	6.20±0.28	4.48 ±0.14
MV-2/7	8.22±0.02	523±1.53	2.07±0.47	4.56 ± 0.01
MV-2/8	7.39±0.01	523±3.05	0.00±0.00	3.87 ± 0.06
MV-2/9	7.32±0.01	531±1.00	0.00±0.00	3.50 ± 0.80
MV-3/1	8.82±0.02	644.0±7.07	11.35±1.35	5.45 ± 0.12
MV-3/2	8.84±0.01	640.0±4.24	13.38±5.26	5.37 ± 0.06
MV-3/3	8.80±0.08	637.5±2.12	9.53±7.74	4.81 ± 0.16
MV-3/4	8.58±0.01	643.3±2.83	15.05±1.31	4.68 ± 0.02
MV-3/5	8.30±0.26	647.2±0.71	9.22±0.93	4.76 ± 0.02

MV-3/6	7.95±0.05	643.3±2.82	10.68±1.02	4.53 ± 0.17
MV-3/7	7.91±0.11	661.5±2.82	2.38±2.21	4.61± 0.08
MV-3/8	7.56±0.10	660.0±7.07	0.01±0.00	3.72 ± 0.05
MV-3/9	7.66±0.19	731.5±5.67	0.00±0.00	3.62 ± 0.03
MV-4/1	8.85±0.71	675.5±7.48	11.50±1.55	8.13 ± 0.28
MV-4/2	8.65±0.78	679±5.36	2.03±1.42	8.16 ± 0.25
MV-4/3	8.65±0.23	643±1.72	3.12±0.64	7.82± 0.22
MV-4/4	8.17±0.21	682±5.15	2.09±0.15	7.67 ± 0.26
MV-4/5	8.54±0.62	690.5±8.49	3.12±0.33	7.26 ± 0.12
MV-4/6	8.28±0.23	682.5±27.58	1.47±1.08	6.92 ± 0.03
MV-4/7	8.35±0.04	662±28.28	1.27±0.06	6.65 ± 0.20
MV-4/8	7.48±0.60	686±32.53	0.39±1.82	5.64 ± 0.19
MV-4/9	7.54±0.09	687±8.28	0.30±0.03	5.83 ± 0.22

APPENDIX B: UV ABSORBANCE

Table B 1 UV values at different wavelengths for Magalies plant (in m^{-1}) (Round 1)

Sample Codes	UV Absorbance			
	214	254	272	300
MP1/1-1	23.87	11.26	10.31	11.44
MP1/1-2	15.75	3.14	2.19	2.08
MP1/1-3	17.63	5.02	4.07	3.99
MP1/1-4	18.82	6.21	5.26	5.75
MP1/1-5	14.69	2.08	1.13	1.33
MP2/1-1B	26.79	14.18	13.23	15.09
MP2/1-2	18.41	5.71	4.84	3.27
MP2/1-3	17.79	5.18	4.23	3.67
MP2/1-4	16.32	3.70	2.76	2.81
MP2/1-5	16.94	4.33	5.51	2.60
MP3/1-2	19.16	6.55	2.42	4.91
MP3/1-3	16.61	3.91	3.05	2.22
MP3/1-5	15.98	3.37	3.38	2.46

Table B 2 UV values at different wavelengths for Magalies plant (in m^{-1}) (Round 2)

Sample Codes	UV Absorbance			
	214	254	272	300
MP1/2-1	25.08	10.04	7.43	4.55
MP1/2-2	22.14	8.27	5.82	3.27
MP1/2-3	29.00	9.67	6.99	4.31
MP1/2-4	29.97	5.57	3.9	1.92

Sample Codes	214	254	272	300
MP1/2-5	31.29	8.00	5.47	3.34
MP2/2-1B	26.39	11.38	8.64	5.83
MP2/2-2	28.66	12.09	9.21	6.26
MP2/2-3	23.44	9.70	7.53	5.07
MP2/2-5	30.61	10.67	8.13	5.82
MP3/2-1	26.24	11.44	8.78	5.44
MP3/2-2	27.72	11.62	8.75	5.64
MP3/2-3	21.87	8.74	6.51	4.09
MP3/2-5	27.43	11.17	8.42	5.83

Table B 3 UV values at different wavelengths for Magalies plant (in m^{-1}) (Round 3)

Sample Codes	UV Absorbance			
	214	254	272	300
MP1/2-1	57.98	10.4	8.37	4.55
MP1/2-2	85.15	8.46	6.55	3.44
MP1/2-3	30.18	7.01	5.41	2.7
MP1/2-4	51.93	6.68	5.07	2.42
MP1/2-5	31.82	5.4	3.7	1.83
MP2/2-1B	30.85	5.53	3.8	1.84
MP2/2-2	26.24	7.2	5.62	2.78
MP2/2-3	26.3	7.01	5.35	2.59
MP2/2-5	27.58	5.43	3.64	1.73
MP3/2-1	178.26	12.09	9.8	5.77
MP3/2-2	26.32	8.5	6.44	3.52
MP3/2-3	25.83	7.98	6.03	3.28
MP3/2-5	22.77	5.32	3.53	1.57

Table B 4 UV values at different wavelengths for Rietvlei plant (in m^{-1})

Sample Codes	UV Absorbance			
	214	254	272	300
RV-1/1	24.21	11.69	10.74	9.24
RV-1/2	32.27	19.66	18.71	21.17
RV-1/3	17.51	4.89	3.95	4.87
RV-1/4	20.26	7.65	6.61	5.34
RV-1/5	18.05	5.44	4.48	3.06
RV-2/1	45.97	23.30	19.57	13.10
RV-2/4	46.59	16.51	13.88	9.42
RV-2/5	42.11	12.09	9.70	6.93
RV-3/1	67.67	23.32	19.40	13.14
RV-3/3	68.32	14.04	11.59	8.10

RV-3/4	68.66	15.72	12.92	8.83
RV-3/5	61.26	10.21	7.96	5.99
RV-4/1	103.1	18.39	15.04	9.38
RV-4/3	94.13	8.12	6.34	3.7
RV-4/4	94.58	9.52	7.5	4.34
RV-4/5	83.45	5.54	3.81	2.2

Table B 5 UV values at different wavelengths for Ebenezer plant (in m^{-1})

Sample Codes	UV Absorbance			
	214	254	272	300
LE-1/1	11.28	6.49	5.42	4.21
LE-1/2	12.00	6.79	5.99	4.72
LE-1/3	9.58	5.58	4.91	3.91
LE-1/4	10.34	5.44	4.83	3.90
LE-1/5	12.38	6.38	5.58	4.74
LE-2/1	19.57	9.19	7.87	6.17
LE-2/2	16.49	8.11	7.14	5.76
LE-2/3	20.77	9.83	8.47	6.58
LE-2/4	13.60	5.82	5.13	4.18
LE-2/5	18.43	7.50	6.18	5.08
LE-3/1	10.86	5.6	4.88	3.76
LE-3/2	14.81	5.23	4.53	3.52
LE-3/3	5.85	1.76	1.4	0.83
LE-3/4	6.15	1.33	0.97	0.51
LE-3/5	6.89	1.89	1.55	1.39

Table B 6 UV values at different wavelengths for Olifantspoort plant (in m^{-1})

Sample Codes	UV Absorbance			
	214	254	272	300
LO -1/1	55.36	14.03	11.70	8.08
LO -1/2	54.35	13.37	11.14	7.70
LO -1/3	54.45	12.58	10.51	7.25
LO -1/5	53.12	10.36	8.06	6.06
LO -2/1	47.36	9.77	7.5	4.24
LO -2/2	49.23	9.06	6.64	6.64
LO -2/3	43.14	5.67	3.79	1.19
LO -2/4	51.18	13.58	11.01	8.84
LO -3/1	59.39	8.67	7.03	4.59
LO -3/2	54.64	5.31	4.07	2.3
LO -3/3	55.48	5.26	4.06	2.28

LO -3/4	54.93	3.69	2.2	1.2

Table B 7 UV values at different wavelengths for Flag Boshielo plant (in m^{-1})

Sample Codes	UV Absorbance			
	214	**254**	**272**	**300**
LF 1-1	26.66	12.51	9.7	5.44
LF 1-3	28.26	11.11	8.41	4.81
LF 1-4	28.93	9.19	7.01	3.68
LF 1-5	32.64	10.82	7.73	4.98
LF 2-1	36.52	18.11	14.7	9.44
LF 2-3	25.41	12.56	9.93	6.99
LF 2-4	24.4	10.14	7.74	4.94
LF 2-5	25.78	10.68	8.01	5.36

Table B 8 UV values at different wavelengths for Midvaal plant (Round 1) (in m^{-1})

Sample codes	UV Absorbance			
	214	**254**	**272**	**300**
MV-1/1	38.32	15.74	13.17	8.50
MV-1/2	41.53	17.82	15.04	10.46
MV-1/3	39.28	16.70	14.26	9.87
MV-1/4	39.36	16.90	14.26	9.98
MV-1/5	38.16	15.65	13.22	9.32
MV-1/6	37.74	14.33	11.85	8.58
MV-1/7	34.27	12.35	10.24	7.18
MV-1/8	39.69	10.84	8.43	6.15
MV-1/9	37.03	9.36	7.28	5.19

Table B 9 UV values at different wavelengths for Midvaal plant (Round 2) (in m^{-1})

Sample Codes	UV Absorbance			
	214	**254**	**272**	**300**
MV-2/1	55.18	19.20	16.35	11.23
MV-2/2	56.54	20.01	16.77	11.52
MV-2/3	55.58	19.23	16.23	11.22
MV-2/4	51.94	17.71	15.01	10.37
MV-2/5	51.68	16.36	13.64	9.48
MV-2/6	46.38	11.65	9.65	6.91
MV-2/7	47.62	12.64	10.50	7.46
MV-2/8	52.13	10.73	8.50	6.34
MV-2/9	51.62	10.48	8.37	6.31

Table B 10 UV values at different wavelengths for Midvaal plant (Round 3) (in m^{-1})

Sample Codes	UV Absorbance			
	214	254	272	300
MV-3/1	144.99	12.48	10.44	6.75
MV-3/2	144.08	11.86	9.89	6.34
MV-3/3	144.78	12.09	10.14	6.46
MV-3/4	142.87	11.13	9.35	5.76
MV-3/5	145.59	11.85	9.9	6.42
MV-3/6	140.68	8.61	7.02	4.59
MV-3/7	143.31	8.39	6.82	4.46
MV-3/8	142.49	5.19	3.6	2.02
MV-3/9	142.27	4.99	3.43	1.88

Table B 11 UV values at different wavelengths for Amanzimtoti (AM), Hazelmere (HL), Umzinto (UM) and Mtwalume (MT) plants (Round 1) (in m^{-1})

Sample Codes	UV Absorbance			
	214	254	272	300
AM-1/1	72.87	23.65	20.34	15.00
AM-1/2	50.67	7.72	6.24	4.00
AM-1/3	50.98	7.83	6.42	3.98
AM-1/4	51.38	7.70	6.22	3.92
AM-1/5	43.46	4.30	2.96	1.66
HL-1/1	45.22	19.55	17.06	12.96
HL-1/2	27.45	5.77	4.24	2.63
HL-1/3	27.09	5.30	3.88	2.29
HL-1/4	24.84	3.41	2.25	1.11
HL-1/5	25.40	3.92	2.77	1.70
UM-1/1 U	19.95	10.42	8.53	5.43
UM-1/1 EJ	50.6	15.25	12.40	7.60
UM-1/2	29.92	10.13	8.14	4.98
UM-1/3	30.79	10.26	8.23	5.11
UM-1/4	25.84	6.40	4.27	2.34
UM-1/5	25.41	6.41	4.25	2.28
MT-1/1	16.11	8.99	7.80	5.68
MT-1/2	27.49	21.21	20.21	18.96
MT-1/3	8.79	3.38	2.69	1.62
MT-1/4	9.00	3.23	2.57	1.55
MT-1/5	7.81	2.41	1.67	1.08

Table B 12 UV values at different wavelengths for Veolia plant (Round 1) (in m^{-1})

Sample Codes	UV Absorbance			
	214	254	272	300
VS-1/1	102.39	55.96	46.88	32.65
VS-1/2	80.44	46.34	41.40	31.92
VS-1/3	39.68	12.91	10.09	6.20
VS-1/4	34.19	9.07	7.16	4.11
VS-1/5	39.85	11.49	8.75	5.81
VB-1/1	3.16	1.92	1.46	1.39
VB-1/4 (Mn)	1.52	0.52	0.40	0.17
VB-1/4 (Fe)	2.80	1.05	0.59	0.35

Table B 13 UV values at different wavelengths for Plettenburg Bay plant (Round 3) (in m^{-1})

Sample Codes	UV Absorbance			
	214	254	272	300
P-1/1	37.19	23.86	20.37	14.47
P-1/2	9.76	6.34	5.50	4.06
P-1/3	8.81	5.77	4.91	3.55
P-1/4	4.14	2.19	1.66	1.02
P-1/5	10.91	6.19	5.10	3.44

APPENDIX C: SUVA VALUES

Table C 1 SUVA values for Magalies WTP 1, 2 and 3 (Round 1)

Sample Codes	SUVA (ℓ/mg.m)
MP1-1	1.51
MP1-2	0.60
MP1-3	0.96
MP1-4	1.46
MP1-5	0.45
MP2-1B	2.15
MP2-2	1.20
MP2-3	1.06
MP2-4	0.81
MP2-5	0.96
MP3-2	1.25
MP3-3	0.83
MP3-5	0.71

Table C 2 SUVA values for Magalies WTP 1, 2 and 3 (Round 2)

Sample Codes	SUVA (ℓ/mg.m)
MP1-1	2.02
MP1-2	2.16
MP1-3	2.72
MP1-4	1.90
MP1-5	2.60
MP2-1B	2.18
MP2-2	3.03
MP2-3	2.33
MP2-5	3.07
MP3-1	2.13
MP3-2	2.73
MP3-3	2.09
MP3-5	2.93

Table C 3 SUVA values for Magalies WTP 1, 2 and 3 (Round 3)

Sample Codes	SUVA (ℓ/mg.m)
MP1-1	1.75
MP1-2	1.60
MP1-3	1.53
MP1-4	1.54
MP1-5	1.20
MP2-1B	1.40
MP2-2	1.62
MP2-3	1.51
MP2-5	1.25
MP3-1	1.99
MP3-2	1.91
MP3-3	1.87
MP3-5	1.31

Table C 4 SUVA values for samples form Rietvlei WTP

Sample Codes	SUVA (ℓ/mg.m)
RV-1/1	1.42

RV-1/2	3.16
RV-1/3	1.01
RV-1/4	1.37
RV-1/5	1.48
RV-2/1	2.30
RV-2/4	2.49
RV-2/5	2.34
RV-3/1	3.14
RV-3/3	3.25
RV-3/4	3.32
RV-3/5	3.56
RV-4/1	2.44
RV-4/3	1.93
RV-4/4	2.06
RV-4/5	1.86
RV-5/1	10.06
RV-5/3	7.62
RV-5/4	7.00
RV-5/5	4.59

Table C 5 SUVA values for samples from Ebenezer WTP

Sample Codes	SUVA (ℓ/mg.m)
LE-1/1	2.51
LE-1/2	4.19
LE-1/3	3.67
LE-1/4	4.42
LE-1/5	5.19
LE-2/1	0.21
LE-2/2	0.20
LE-2/3	0.20
LE-2/4	0.24
LE-2/5	1.28
LE-3/1	5.60
LE-3/2	5.23
LE-3/3	1.76
LE-3/4	1.33
LE-3/5	1.89
LE-4/1	3.89
LE-4/2	3.45

LE-4/3	5.54
LE-4/4	16.50
LE-4/5	116

Table C 6 SUVA values for samples from Olifantspoort WTP

Sample Codes	SUVA (ℓ/mg.m)
LO-1/1	2.10
LO-1/2	2.09
LO-1/3	2.09
LO-1/4	1.83
LO-2/1	2.18
LO-2/2	2.25
LO-2/3	1.49
LO-2/4	3.92
LO-3/1	2.85
LO-3/2	2.07
LO-3/3	2.16
LO-3/4	1.63

Table C 7 SUVA values for samples from Flag Boshielo WTP

Sample code	SUVA (ℓ/mg.m)
LF-1/1	1.74
LF-1/2	1.83
LF-1/3	1.58
LF-1/4	1.72
LF-2/1	2.19
LF-2/2	1.93
LF-2/3	1.51
LF-2/4	1.51
LF-3/1	1.87
LF-3/2	0.93
LF-3/3	0.85
LF-/4	1.11

Table C 8 SUVA values for samples from Midvaal WTP (Round 1)

Sample Codes	SUVA (ℓ/mg.m)

MV-1/1	2.85
MV-1/2	1.62
MV-1/3	1.80
MV-1/4	1.94
MV-1/5	1.81
MV-1/6	1.68
MV-1/7	1.43
MV-1/8	1.38
MV-1/9	1.21

Table C 9 SUVA values for samples from Midvaal WTP (Round 2)

Sample Codes	SUVA (ℓ/mg.m)
MV-2/1	3.61
MV-2/2	3.64
MV-2/3	3.66
MV-2/4	3.45
MV-2/5	3.36
MV-2/6	2.60
MV-2/7	2.77
MV-2/8	2.77
MV-2/9	2.99

Table C 10 SUVA values for samples from Midvaal WTP (Round 3)

Sample Codes	SUVA (ℓ/mg.m)
MV-3/1	2.29
MV-3/2	2.21
MV-3/3	2.51
MV-3/4	2.38
MV-3/5	2.49
MV-3/6	1.90
MV-3/7	1.82
MV-3/8	1.40
MV-3/9	1.38

Table C 11 SUVA values for samples from Midvaal WTP (Round 4)

Sample Codes	SUVA (ℓ/mg.m)
MV-4/1	1.07
MV-4/2	1.01
MV-4/3	1.34
MV-4/4	1.45
MV-4/5	1.27
MV-4/6	1.23
MV-4/7	0.91
MV-4/8	0.004
MV-4/9	0.002

Table C 12 SUVA values for samples from Plettenberg Bay WTP (Rounds 1 and 2)

Sample Codes	SUVA (ℓ/mg.m)
P-1/1	4.56
P-1/2	1.40
P-1/3	2.70
P-1/4	2.93
P-1/5	0.72
P-2/1	48.75
P-2/2	16.77
P-2/3	8.88
P-2/4	6.43
P-2/5	5.06

Table C 13 SUVA values for samples from Preekstoel WTP (Rounds 1 and 2)

Sample Codes	SUVA (ℓ/mg.m)
VP-1/1	6.58
VP-1/2	9.32
VP-1/3	4.18
VP-1/4	3.70
VP-1/5	3.82
VP-2/1	8.91
VP-2/2	461
VP-2/3	1.85
VP-2/4	1.57
VP-2/5	6.73

Table C 14 SUVA values for samples from Amanzimtoti WTP (Rounds 1 and 2)

Sample Codes	SUVA (ℓ/mg.m)
AM-1/1	1.60
AM-1/2	0.52
AM-1/3	0.53
AM-1/4	0.52
AM-1/5	0.18
AM-2/1	2.92
AM-2/2	0.07
AM-2/3	0.01
AM-2/4	0.13
AM-2/5	0.96

Table C 15 SUVA values for samples from Hazelmere WTP (Rounds 1 and 2)

Sample Codes	SUVA (ℓ/mg.m)
HL-1/1	1.18
HL-1/2	0.31
HL-1/3	0.29
HL-1/4	0.20
HL-1/5	0.23
HL-2/1	10.65
HL-2/2	1.74
HL-2/3	1.88
HL-2/4	1.90
HL-2/5	1.40

Table C 16 SUVA values for samples from Umzinto WTP (Rounds 1 and 2)

Sample Codes	SUVA (ℓ/mg.m)
UM-1/1 EJ	0.28
UM-1/1 U	0.62
UM-1/2	0.34
UM-1/3	0.46
UM-1/4	1.43
UM-1/5	1.71
UM-1/1 EJ	1.14
UM-1/1 U	2.59
UM-1/2	0.65

UM-1/3	0.78
UM-1/4	0.65
UM-1/5	0.03

Table C 17 SUVA values for samples from Mtwalume WTP (Rounds 1 and 2)

Sample Codes	SUVA (ℓ/mg.m)
MT-1/1	0.30
MT-1/2	0.73
MT-1/3	0.12
MT-1/4	0.11
MT-1/5	0.09
MT-2/1	3.75
MT-2/2	4.36
MT-2/3	2.03
MT-2/4	2.07
MT-2/5	1.70

Table C 18 SUVA values for samples from Veolia (borehole) WTP (Rounds 1 and 2)

Sample Codes	SUVA (ℓ/mg·m)
VB-1	49.86
VB-4 Mn	2.82
VB-4 Fe	3.21

APPENDIX D: UV SCANS
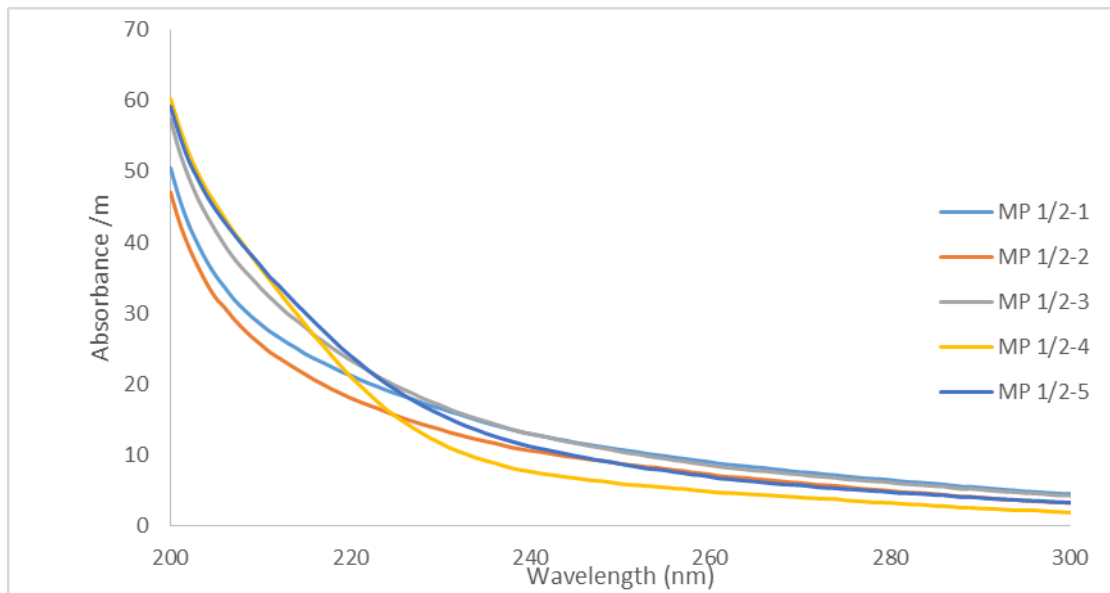
Appendix Figure D 1 UV scan for the Magalies plant 1 water (Round 2)
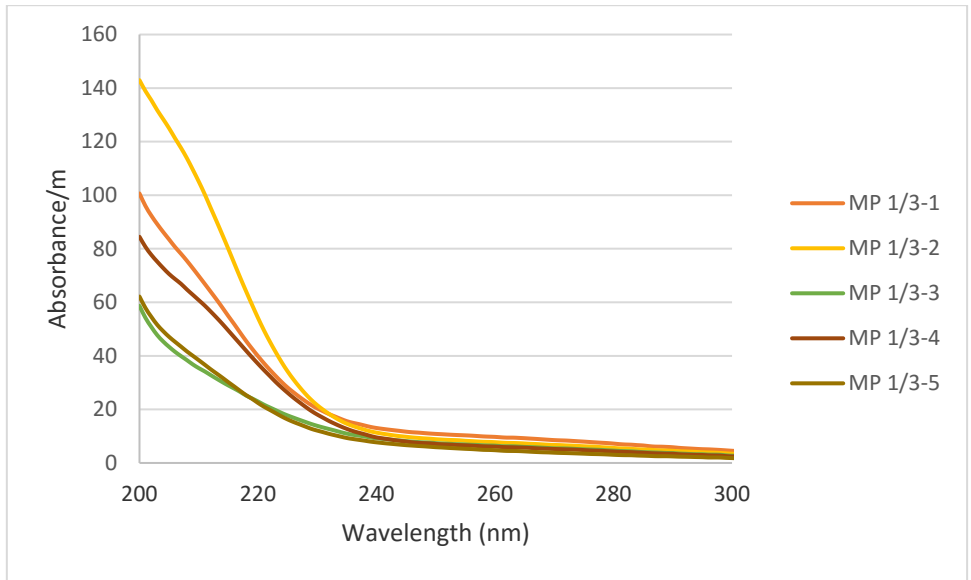
Appendix Figure D 2 UV scan for the Magalies plant 1 water (Round 3)
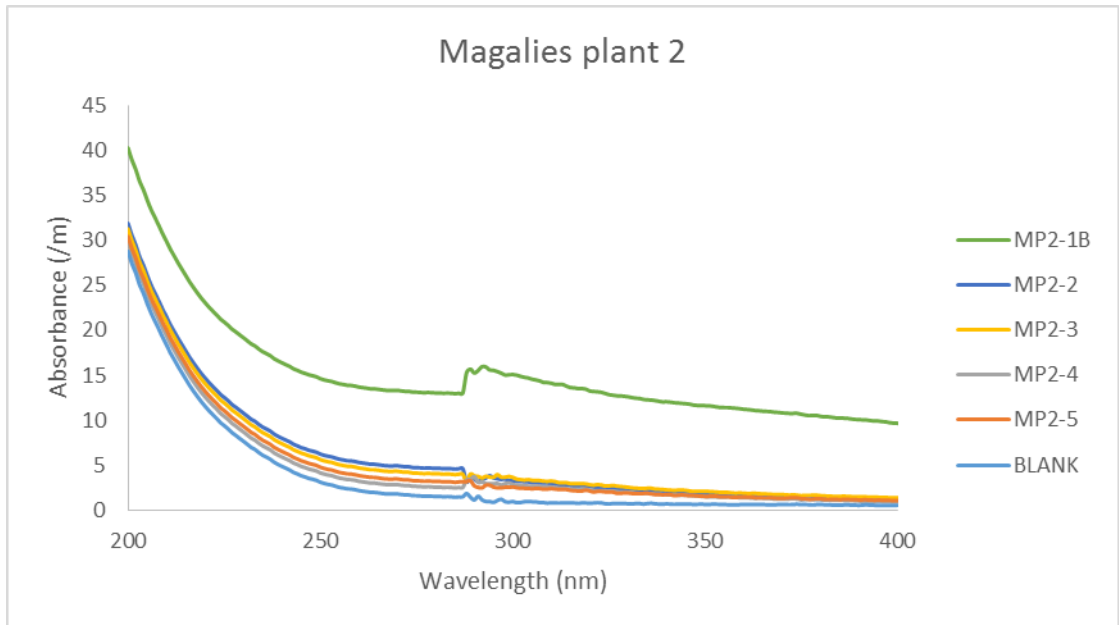
Appendix Figure D 3 UV scan for the Magalies plant 2 water (Round 1)
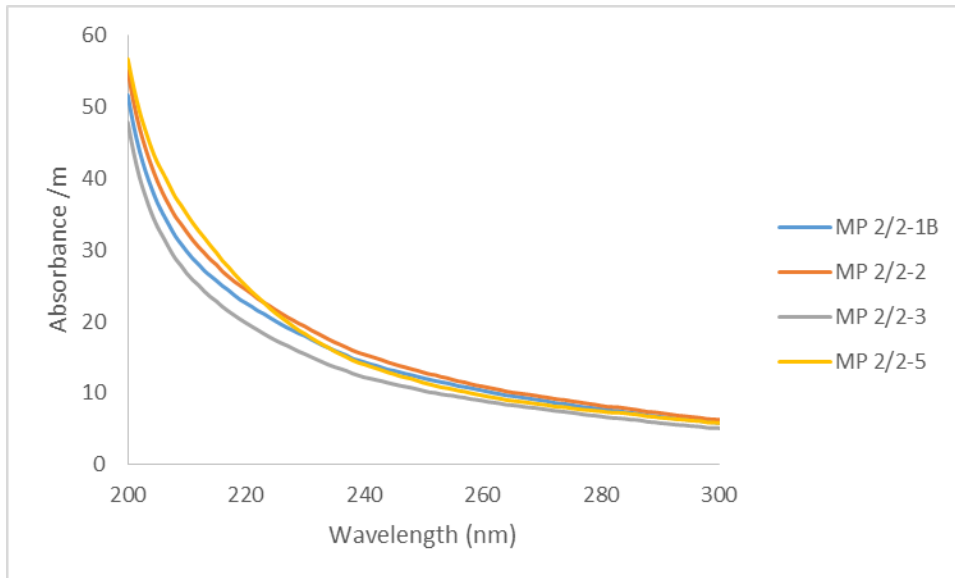
Appendix Figure D 4 UV scan for the Magalies plant 2 water (Round 2)
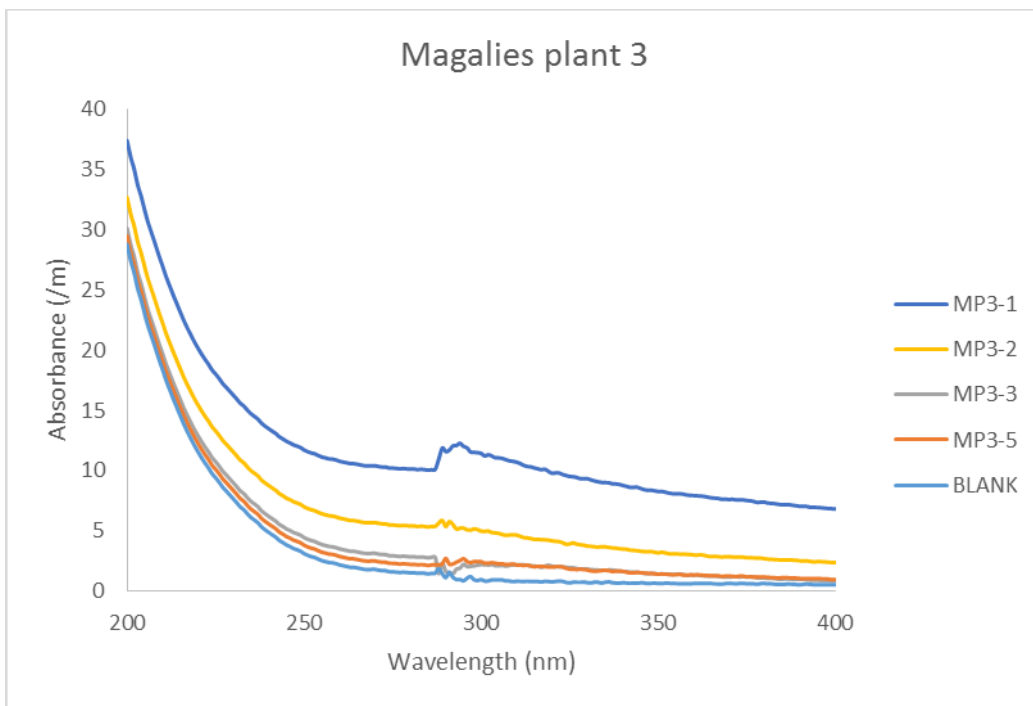
Appendix Figure D 5 UV scan for the Magalies plant 3 water (Round 1)
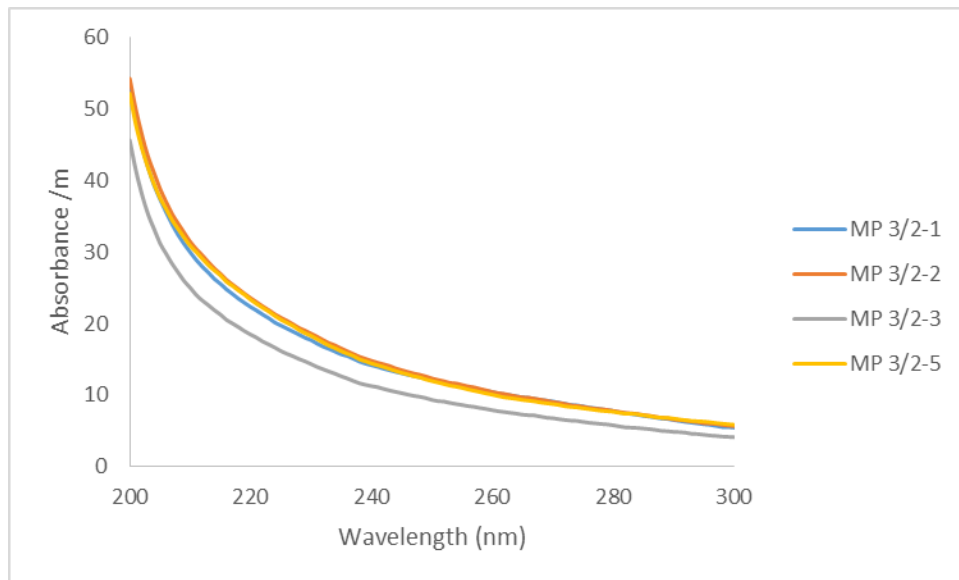
**Appendix Figure D 6** UV scan for the Magalies plant 3 water (Round 2)
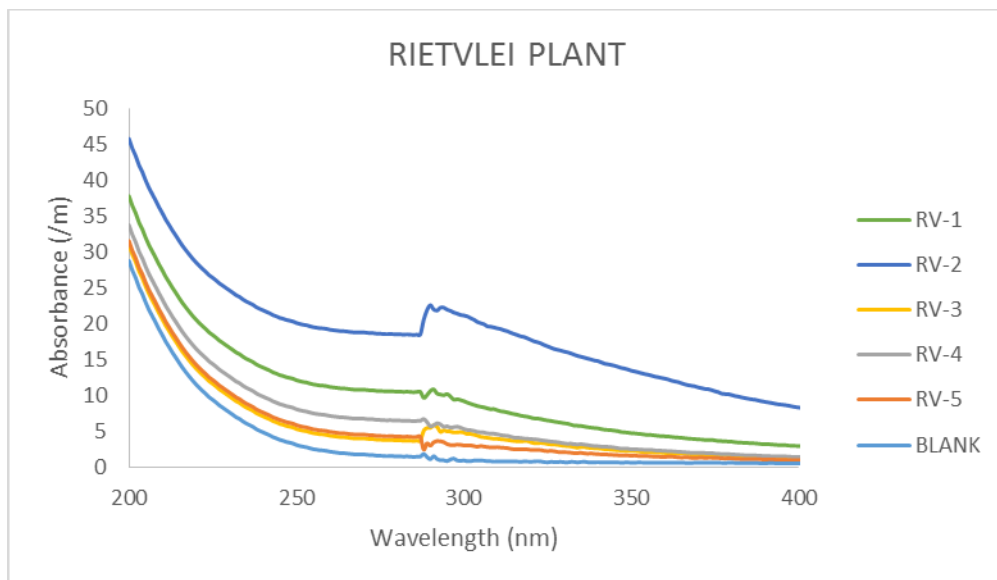
Appendix Figure D 7 UV scan for the Rietvlei plant (Round 1)
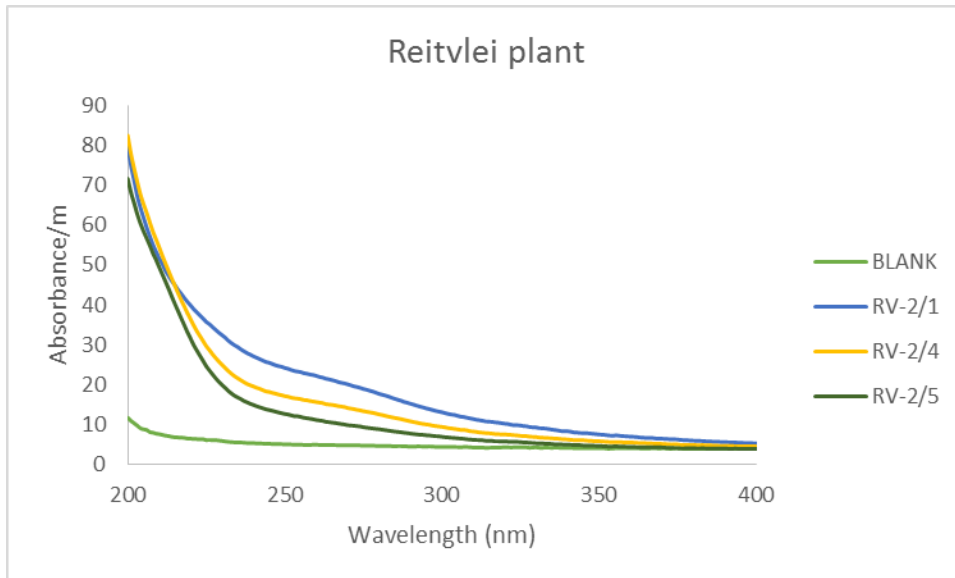
Appendix Figure D 8 UV scan for the Rietvlei plant (Round 2)
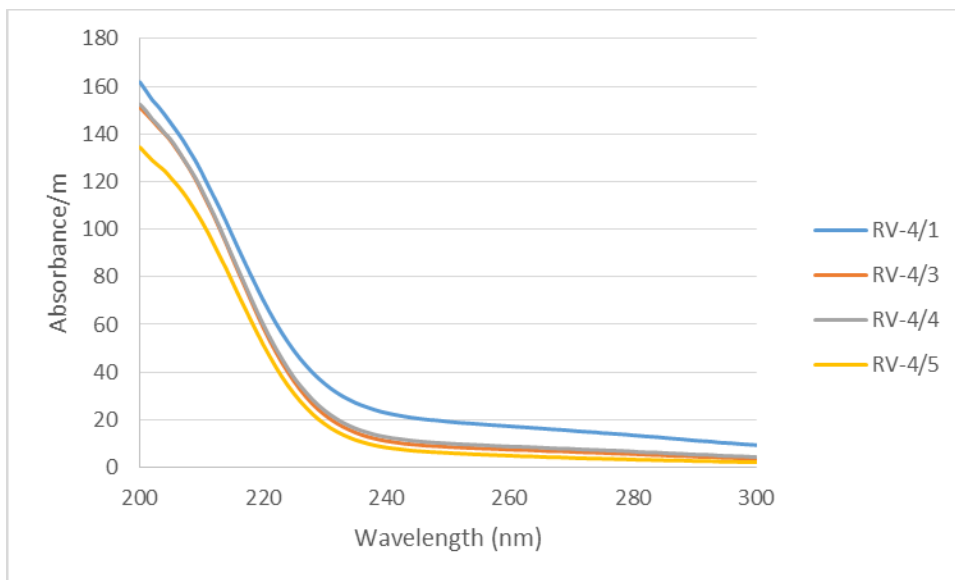
Appendix Figure D 9 UV scan for the Rietvlei plant (Round 4)
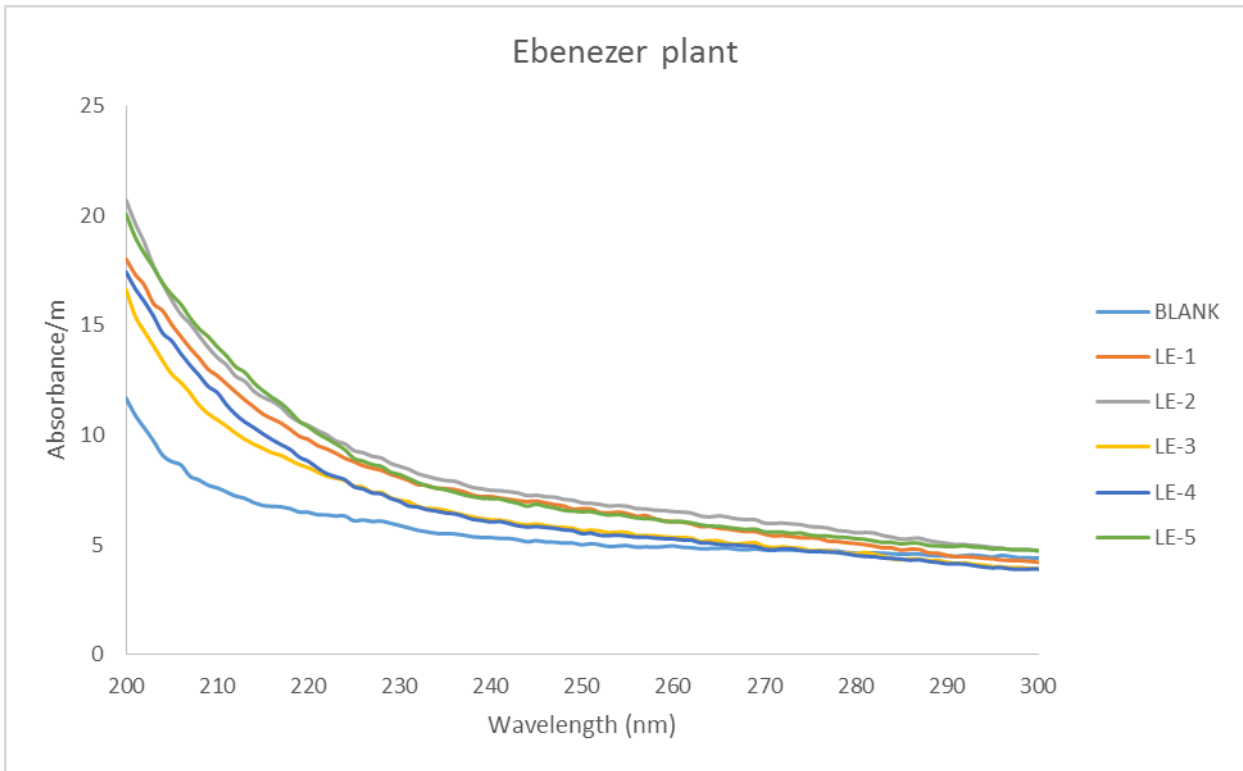
Appendix Figure D 10 UV scan for the Ebenezer plant (Round 1)
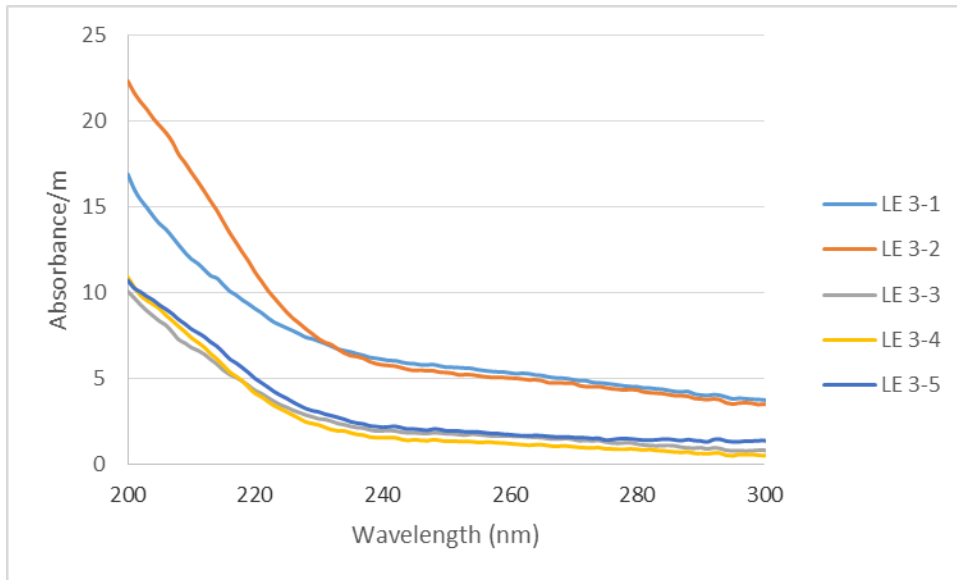
Appendix Figure D 11 UV scan for the Ebenezer plant (Round 3)
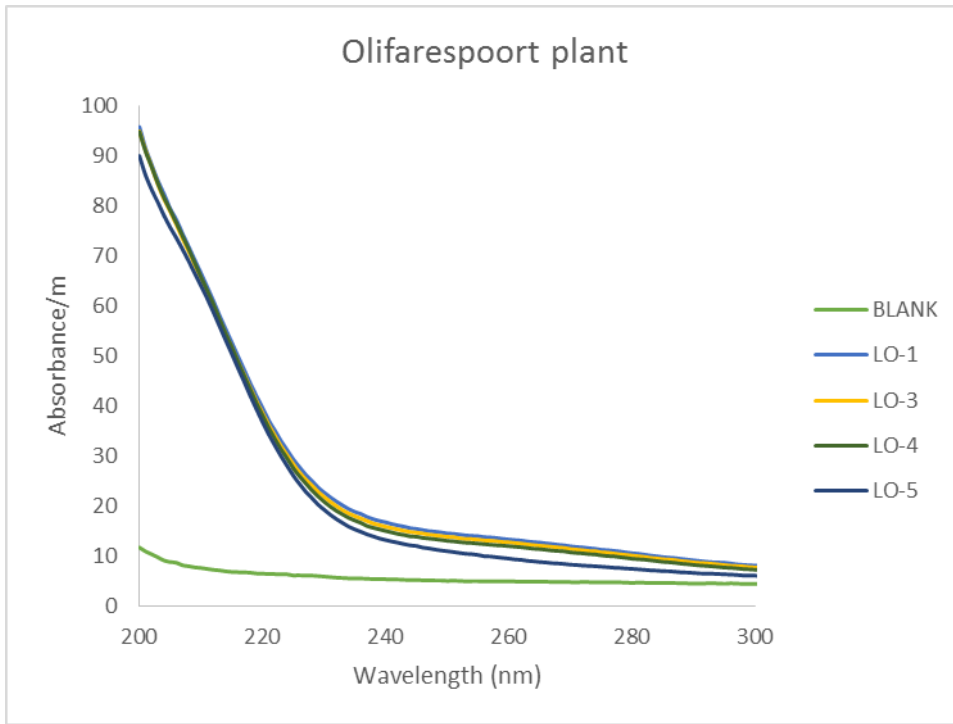
Appendix Figure D 12 UV scan for the Olifantspoort plant (Round 1)
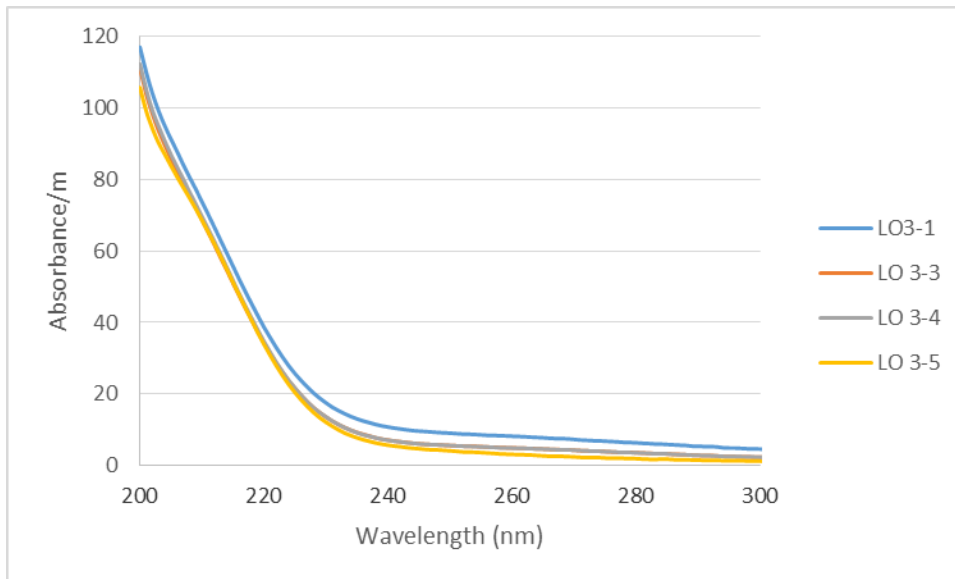
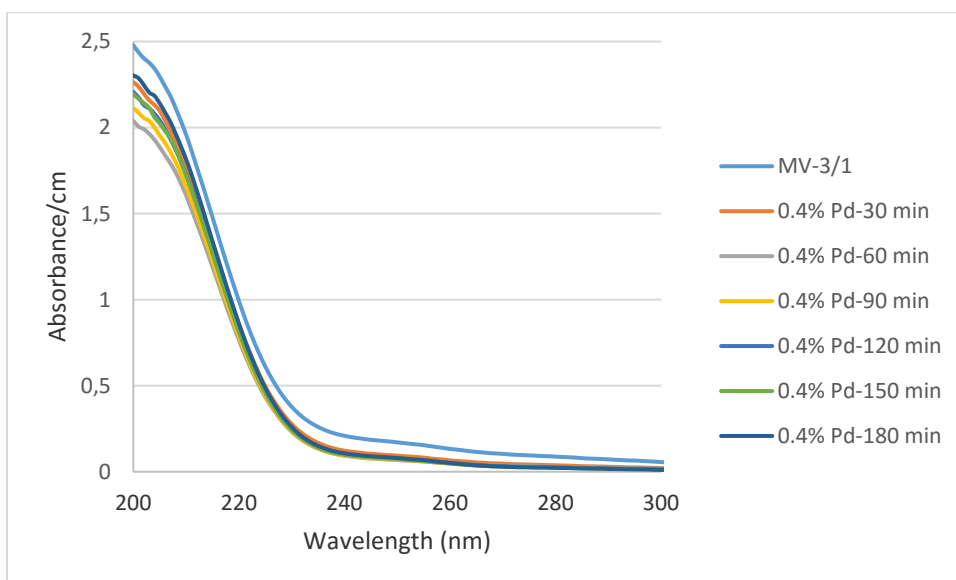**Appendix Figure D 13** UV scan for the Olifantspoort plant (Round 3)
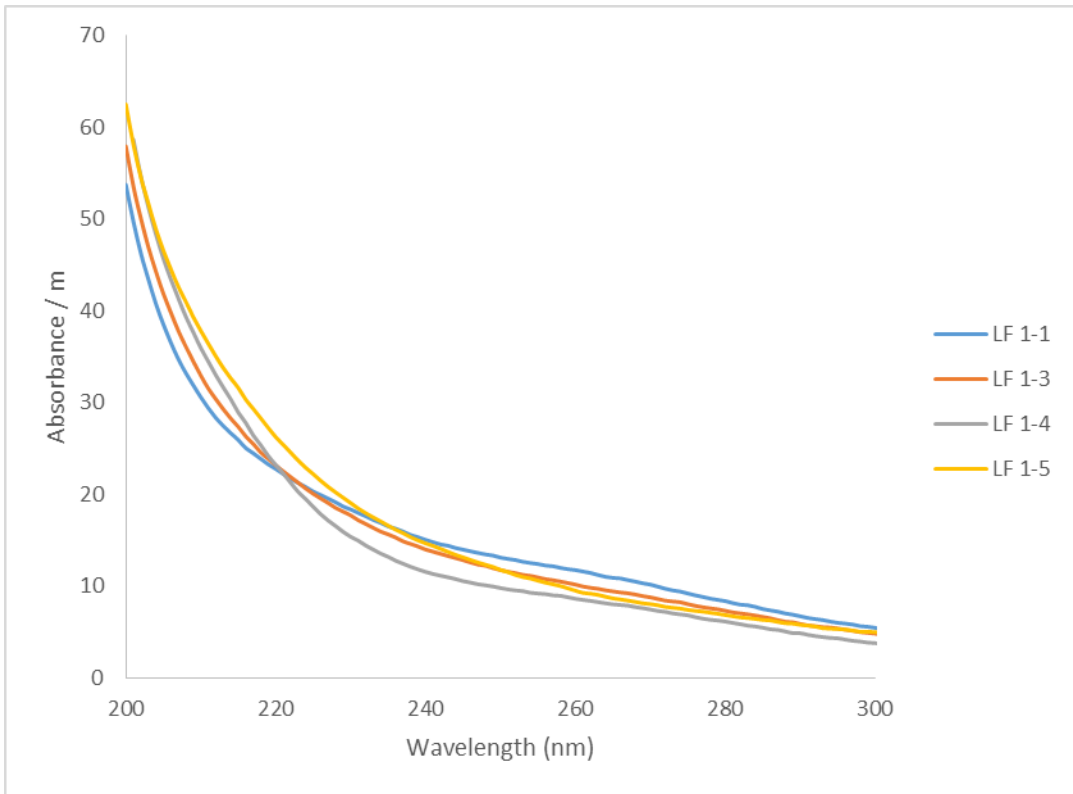
Appendix Figure D 14 UV scan for the Flag Boshielo plant (Round 1)
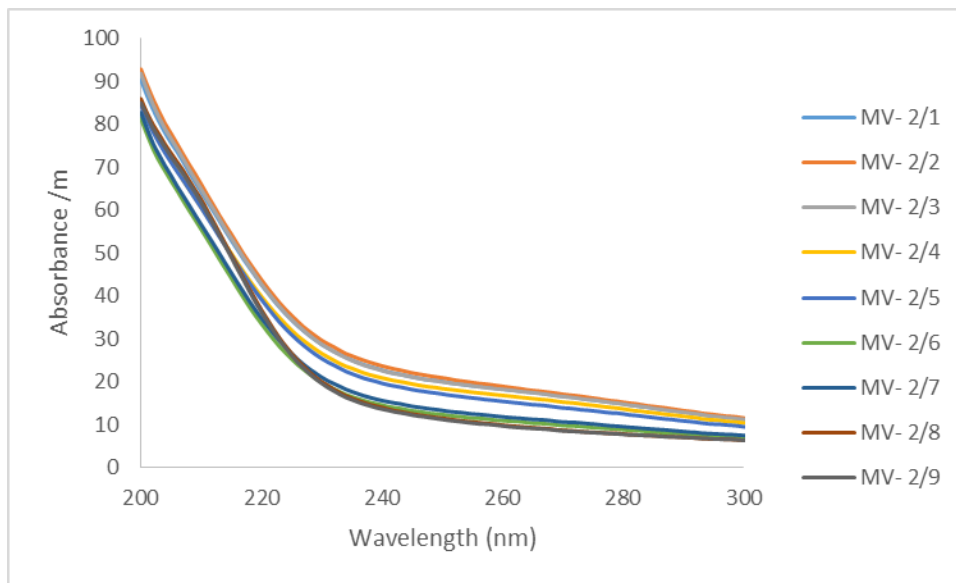
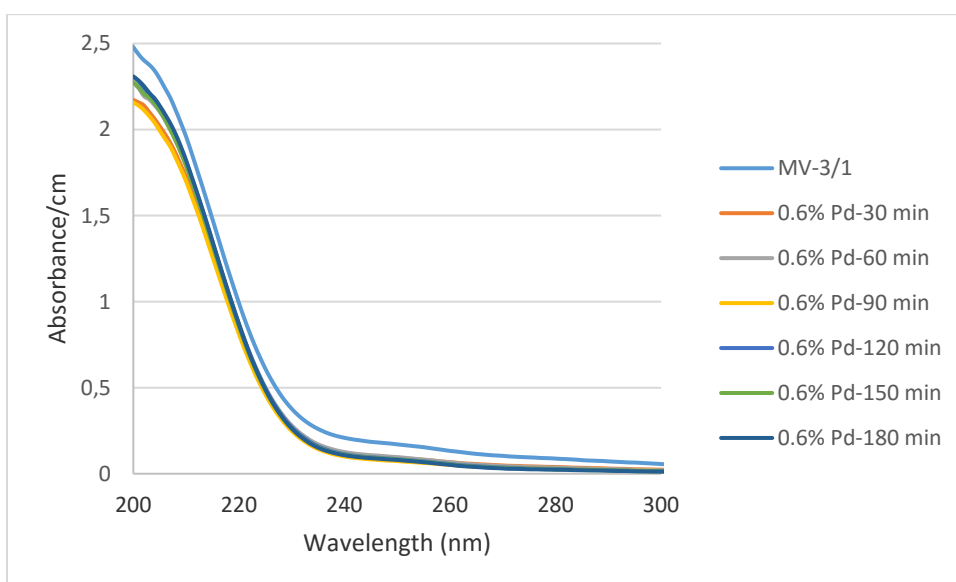**Appendix Figure D 15** UV scan for the Midvaal plant (Round 2)
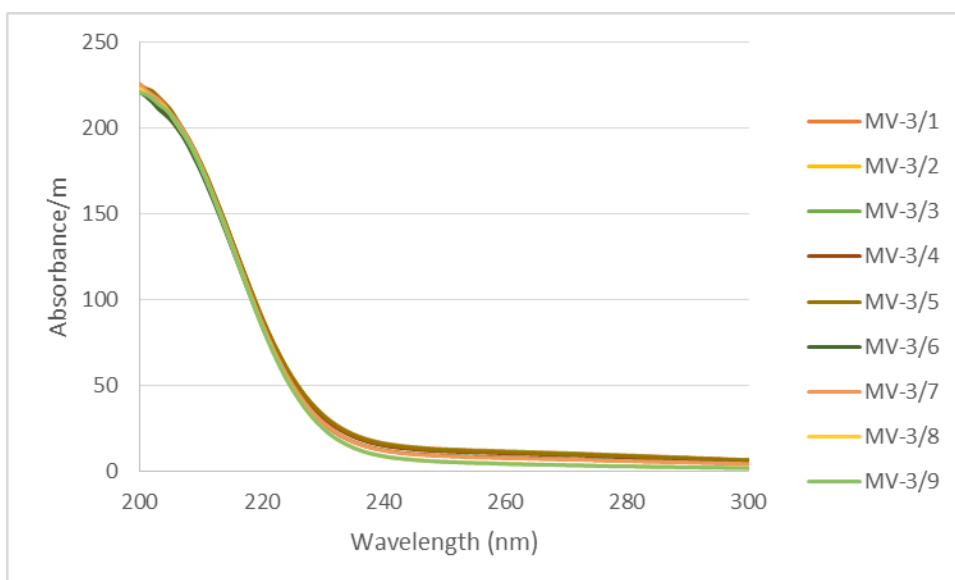
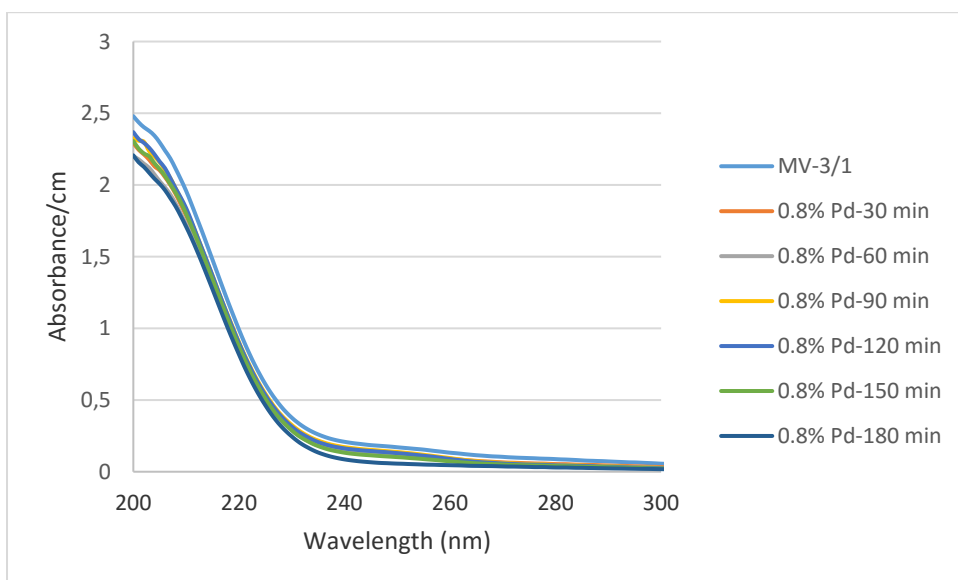**Appendix Figure D 16** UV scan for the Midvaal plant (Round 3)
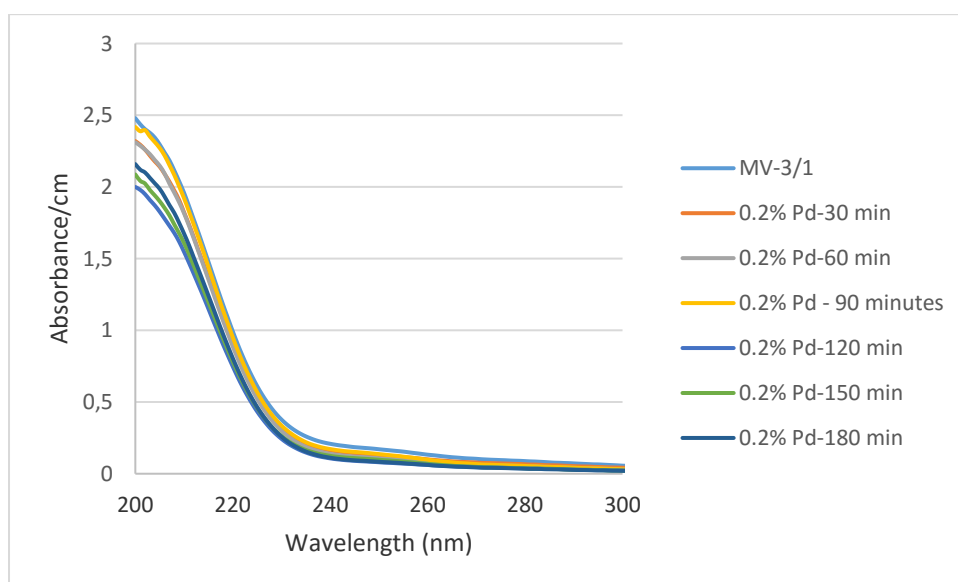
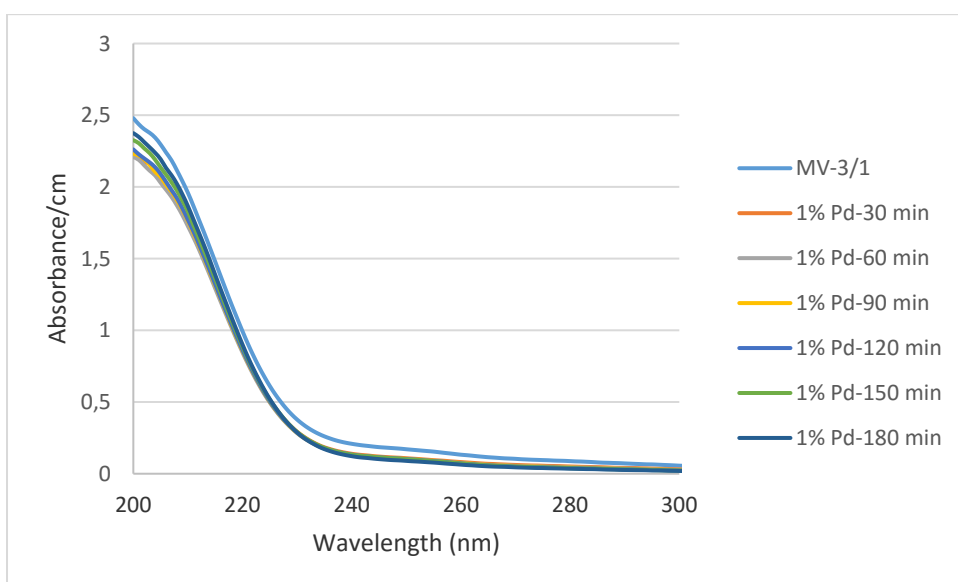**Appendix Figure D 17** UV scan over time of MV1 sample with N, Pd co-doped TiO_2 (0.2% Pd)

Appendix Figure D 18 UV scan over time of MV1 sample with N, Pd co-doped TiO_2 (0.4% Pd)

Appendix Figure D 19 UV scan over time of MV1 sample with N, Pd co-doped TiO_2 (0.6% Pd)

Appendix Figure D 20 UV scan over time of MV1 sample with N, Pd co-doped TiO_2 (0.8% Pd)

Appendix Figure D 21 UV scan over time of MV1 sample with N, Pd co-doped TiO_2 (1% Pd)